NON-STEADY STATE LUBRICATION OF

COUNTERFORMAL CONTACTS

by

MOHAMED AMIN AHMED BEDEWI

Thesis submitted to the University of Leeds

for the Degree of Doctor of Philosophy

INSTITUTE OF TRIBOLOGY

DEPARTMENT OF MECHANICAL ENGINEERING

THE UNIVERSITY OF LEEDS

JULY 1985

ABSTRACT

A theoretical study has been undertaken of the phenomenon of non-steady state lubrication of concentrated point and line contacts. This has been based upon a study of the effect of squeeze-film action in both hydrodynamically and elasto-hydrodynamically lubricated contacts.

The work described in this thesis is in two main sections. The first is concerned with squeeze-film lubrication of lightly loaded point contacts where the surfaces are taken to be rigid. A complete analytical solution is developed considering both piezo-viscous and isoviscous fluids. Formulae representing the relationships between the controlling parameters of hydrodynamic lubrication of point contacts with a pure squeeze action became available.

In the second section general numerical solutions to the non-steady state hydrodynamic and elastohydrodynamic lubrication problems for line contacts are developed. The finite-difference approximation method has been used to solve simultaneously the Reynolds, elasticity and load equations at successive time steps. To avoid convergence difficulties and reduce computing effort a tri-diagonal matrix algorithm has been incorporated. A wide range of line contact lubrication problems is considered. These include the hydrodynamic and elastohydrodynamic lubrication of cylinders with either pure squeeze-film action or under combined 'entraining' and 'squeeze-film' action. Graphical representations of pressure distributions and film shapes are presented in time sequence as the

gap between the two cylinders changes. The variations of the dimensionless minimum film thickness, velocity of approach and peak pressure under various loading conditions are also included. The formation and development of the elastic indentation under constant load with squeeze-film action and with the combined effect of squeeze and entraining action has been ascertained.

It has been established that the squeeze-film action plays an effective role in the enhancement of the smallest value of the minimum film thickness occurring under oscillating loading conditions. This effect is more pronounced in elastohydrodynamic than in hydrodynamic lubrication.

This general analysis of time dependent lubrication problems for both hydrodynamic and elastohydrodynamic conditions permits specific studies to be undertaken of realistic machine components operating under non-steady state conditions.

ACKNOWLEDGEMENTS

I would like to express my sincere thanks to my Supervisors, Professor D. DOWSON and Dr. C.M. TAYLOR for their invaluable guidance, advice and encouragement throughout the course of the research.

I wish to acknowledge, with gratitude, the Ministry of Higher Education of Arab Republic of Egypt for funding the research assistantship which enabled me to perform the work outlined in this thesis.

I am also grateful to my fellow research students and members of staff who have helped with my proof reading.

My thanks to Mrs. S.M. Moore and Mrs. C.M. Goulborn for typing this manuscript.

CONTENTS

NOTATION FOR CHAPTER 2

f_x, f_y, f_z body force components acting on a fluid element in Navier-Stokes equations

F hydrodynamic load carrying capacity

$\bar{F}$ dimensionless hydrodynamic load, $\left(\frac{F}{\eta_o \left(\frac{R^2}{h_o}\right) W}\right)$

$\bar{F}_T$ dimensionless load limiting value, $\left(24\,\pi \left(\frac{1+\delta}{\sqrt{\delta}}\right) \ln 2\right)$

h film thickness

h_o central film thickness

h_{oI} initial film thickness value at time (t_1)

h_{oT} transitional film thickness at the centre of contact

H dimensionless film thickness, $\left(\frac{h}{h_o}\right)$

p piezoviscous pressure

P dimensionless piezoviscous pressure, $\left(\frac{p\, h_o^2}{\eta_o RW}\right)$

q reduced pressure or isoviscous pressure

Q dimensionless isoviscous pressure, $\left(\frac{q\, h_o^2}{\eta_o RW}\right)$

R_x, R_y principal radii of curvature of an ellipsoid in (x) and (y) planes respectively

R Equivalent radius of curvature, $\left(\frac{R_x R_y}{R_x + R_y}\right)$

t time

Δt time of approach, $(t-t_1)$

u, v, w velocity components of the centre of the fluid element in Navier-Stokes equations

u_A, v_A, w_A surface velocity components of the solid (A) in x, y and z directions respectively

u_B, v_B, w_B surface velocity components of the solid (B) in x, y and z directions respectively

W velocity of approach of a moving body towards a plane surface

W_T velocity of approach value at the transitional film thickness (h_{oT})

x,y,z coordinate system defined in the chapter

X,Y dimensionless distances in (x) and (y) directions respectively, $\left(\frac{x}{\sqrt{h_o R_x}}\right)$ $\left(\frac{y}{\sqrt{h_o R_y}}\right)$

η lubricant dynamic viscosity

η_o lubricant viscosity at atmospheric pressure

$\bar{\eta}$ dimensionless viscosity, $\left(\frac{\eta}{\eta_o}\right)$

α pressure viscosity coefficient

δ radius ratio, $\left(\frac{R_y}{R_x}\right)$

$\bar{\omega}$ dimensionless velocity of approach, $\left(\frac{\alpha\ \eta_o RW}{h_o^2}\right)$

ρ lubricant density

Subscripts:

1 initial condition

A solid (A)

B solid (B)

T transitional value of film thickness

o central point or closest point at approach

x,y coordinate system

NOTATION FOR LINE CONTACT

a	amplitude of sinusoidal load
b	half-width of the Hertzian contact, $\left[\frac{8RF}{\pi E'}\right]^{\frac{1}{2}}$
2B	width of rectangular area of uniform pressure
$2\bar{B}$	dimensionless width of rectangular area of uniform pressure, $\left(\frac{2B}{b}\right)$
$2\bar{B}_1$	dimensionless coarse-mesh inter-nodal spacing
$2\bar{B}_2$	dimensionless fine-mesh inter-nodal spacing
d(x)	local relative elastic deflection, $(\delta - C)$
d_o	relative elastic deflection at the centre of contact, $(\delta_o - C)$
$d'(\bar{x})$	relative elastic deflection due to a rectangular area of uniform pressure (p) at a location $(\bar{x})$ from the centre of this area.
D_e	dimensionless damping parameter, $\left(\frac{\omega R}{u}\sqrt{\frac{F_o}{RE'}}\right)$
D_p	dimensionless damping parameter for rigid cylinders, $\left(\omega R\sqrt{\frac{\eta_o}{uF_o}}\right)$
E	elasticity modulus
E'	effective elasticity modulus, $\left[\frac{2}{\frac{1-\sigma_1^2}{E_1}+\frac{1-\sigma_2^2}{E_2}}\right]$
E_1	elasticity modulus of cylinder (1)
E_2	elasticity modulus of cylinder (2)
f(t)	load function, $(1 + a\sin\omega t)$
F	instantaneous normal applied load
F_o	basic load of sinusoidal loading
$\bar{F}$	dimensionless load parameter, $\left(\frac{F}{E'R}\right)$
$\bar{F}$	dimensionless load parameter for rigid cylinders, $\left(\frac{F}{u\eta_o}\right)$

g_e dimensionless entraining parameter, $\left(\frac{\bar{F}_o}{GU}^{3/2}\right)$

G dimensionless material parameter, $(\alpha E')$

h_g rigid geometrical separation between the equivalent cylinder and the plane

h_o' separation in the centre of contact between the rigid cylinder and the plane

h film thickness

h_m minimum film thickness

h_o central film thickness

h^* film thickness at the inlet location

H dimensionless film thickness, $\left(\frac{h}{R}\right)$

H_m dimensionless minimum film thickness, $\left(\frac{h_m}{R}\right)$

H_o dimensionless central film thickness, $\left(\frac{h_o}{R}\right)$

H^* dimensionless film thickness at the inlet location, $\left(\frac{h^*}{R}\right)$

L^* dimensionless length of the inlet region

N total number of nodes

p pressure

P dimensionless pressure, $\left(\frac{P}{E'}\right)$

P dimensionless pressure for rigid cylinders, $\left(\frac{pR}{u\eta_o}\right)$

$\bar{q}$ dimensionless (normal/entraining) velocity parameter for rigid cylinders, $\left(\frac{W}{u}\right)$

R effective radius of curvature, $\left(R = \frac{R_1 R_2}{R_1 + R_2}\right)$

R_1 radius of cylinder (1)

R_2 radius of cylinder (2)

R^* ratio between the dimensionless width of the coarse-mesh on the inlet side and the dimensionless inlet distance (L^*)

s dummy coordinate along the oil film

S(x) local geometrical separation at a position (x), $\left(\frac{x^2}{2R}\right)$

t time

Δt time step

u mean entraining velocity, $\left(\frac{u_1 + u_2}{2}\right)$

u_1 rolling velocity of cylinder (1)

u_2 rolling velocity of cylinder (2)

U dimensionless entraining velocity parameter, $\left(\frac{u\eta_o}{RE'}\right)$

W velocity of approach, $\left(-\frac{\partial h}{\partial t}\right)$

W_d deformation velocity

W_o velocity of approach of the contact centre, $\left(-\frac{\partial h_o}{\partial t}\right)$

$\bar{W}$ dimensionless velocity of approach parameter, $\left(\frac{W\eta_o}{RE'}\right)$

$\bar{W}_o$ dimensionless velocity of approach parameter of the contact centre, $\left(\frac{W_o \eta_o}{RE'}\right)$

x coordinate along the oil film

x_e location of outlet boundary

x_i location of inlet boundary

X dimensionless coordinate along the oil film, $\left(\frac{x}{b}\right)$

X dimensionless coordinate along the oil film for rigid cylinders, $\left(\frac{x}{R}\right)$

X_e dimensionless location of outlet boundary, $\left(\frac{x_e}{b}\right)$

X_i dimensionless location of inlet boundary, $\left(\frac{x_i}{b}\right)$

z, Z	coordinate across the oil film
ω	time base (angular velocity of sinusoidal load)
ϕ	Vogelpohl parameter, $(PH^{3/2})$
σ	Poisson's ratio
σ_1	Poisson's ratio for cylinder (1)
σ_2	Poisson's ratio for cylinder (2)
ρ	lubricant density
ρ_o	density at atmospheric pressure
$\bar{\rho}$	dimensionless density, $\left(\frac{\rho}{\rho_o}\right)$
η	lubricant dynamic viscosity
η_o	lubricant dynamic viscosity at atmospheric pressure
$\bar{\eta}$	dimensionless viscosity, $\left(\frac{\eta}{\eta_o}\right)$
$\delta(x)$	elastic deformation
δ_o	elastic deformation at the centre of contact
$\delta'(\bar{x})$	elastic deformation due to the influence of one rectangular area with uniform pressure (p) at a location $(\bar{x})$ from the centre of this area

CHAPTER 1

INTRODUCTION

1.1 Non-Steady State Elastohydrodynamic Lubrication

The design of machinery requires considerable effort to avoid excessive wear and damage to the interacting surfaces in relative motion. In order to minimise these effects, load bearing surfaces in relative motion such as in bearings and gears, must be separated by an adequate and continuous thin fluid film which serves as a principal load transmitting member. The lubrication mechanism of heavily loaded contacts of low geometrical conformity (counterformal contacts), such as those occurring between the teeth of gears and in rolling element bearings, is commonly referred to as elastohydrodynamic lubrication. The pressures generated in these contacts are considerable and the lubrication process is influenced by two major physical effects. The first is the elastic deformation of the surfaces under the applied load and the second is the large increase in the viscosity of the lubricating fluid.

Elastohydrodynamic lubrication therefore deals with the lubrication of elastic contacts. Hence, the complete solution of the theoretical problem of elastohydrodynamic lubrication requires a simultaneous solution to the equation governing the elastic deformation of the surfaces and the hydrodynamic (Reynolds) equation.

It is possible to divide the elastohydrodynamic lubrication problem into two subdivisions depending upon the operating condition. When the main system parameters are considered independent of time the condition is termed 'steady-state' elasto-hydrodynamic lubrication. When the main system parameters are

assumed to be time-dependent, as would be the case under the influence of time-varying loads and velocities, the condition is known as 'Non-steady state' elastohydrodynamic lubrication.

The theoretical investigation of the 'Non-steady state' elastohydrodynamic lubrication condition is a problem of considerable complexity. In this case the pressure distributions and film shapes are obtained by solving the transient Reynolds' equation coupled with the elasticity equation. In spite of the practical significance of the 'non-steady' state lubrication problem of counterformal contacts it has received relatively little attention in the literature.

1.2 Early Analysis

Before the theories of elastohydrodynamic lubrication had been fully developed, Bowden and Tabor (1954) studied, theoretically and experimentally, the nature of contact between colliding surfaces. This is of general interest in a number of fields involving deformation under impact. For example, it is of importance in the study of the dynamic hardness of metals and in lubrication problems where vibrations in the moving parts may produce rapid changes in the normal forces between the rubbing surfaces. The investigation was concerned with collisions between dry and lubricated spherical and flat surfaces.

Initially they were concerned with the plastic deformation on a dry surface by a hard ball dropped from a measured height. The results showed that when metal surfaces collided the forces

developed between them could be expressed in terms of the elastic and plastic constants of the metals. The time of collision was very short and the pressure developed at the region of contact very high indeed. Even for relatively light impacts these pressures would readily exceed the yield pressure of the materials, resulting in a permanent plastic indentation. This pressure increased with an increase in the velocity of collision.

In order to examine the effect of liquid films interposed between the two surfaces, the flat surfaces were lubricated by a viscous fluid. The electrical conductance method was used to compare the time of impact and the area of metallic contact for both dry and lubricated conditions. The conductance at any instant was recorded on a cathod-ray oscillograph and used as a criterion for the area of contact. The presence of a lubricating layer between the two colliding surfaces had a significant effect upon the impact process. In general as the lubricant film is extruded during the impact process, high rates of flow, rates of shear, and pressures are developed. These pressures would readily cause permanent deformation and damage to the colliding surfaces at relatively small velocities of impact, even though no actual metallic contact took place.

The theoretical analyses showed that the maximum pressure in the centre of contact was proportional to $\sqrt{\frac{1}{\eta_o}}$, thus high viscosity liquid gave a relatively low maximum pressure. The features of the deformation in the case of lubricated and dry impact were different. The shape of the deformation with dry impact was always found to be similar to the ball shape. However, the deformation of the

lubricated impact was approximately conical and, sometimes when using a high viscosity liquid, it was nearly similar to the shape of the hard ball with a depression in the centre. This conical shape was attributed to the very high hydrodynamic pressure generated in the trapped liquid between the two surfaces, which caused plastic deformation of the materials, particularly in the centre of the contact area.

The temperatures produced by the impact were also considered. It was found that if the surfaces were separated by a liquid, the heating due to the plastic deformation of the metal itself was greatly reduced. However, the high rates of shear in the liquid film would produce appreciable viscous heating in the liquid. Hence, it was suggested that even if the speed of rotation of bearing surfaces was low, rapid vibrations or heavy impulsive loading might produce viscous heating which would lead to a serious deterioration in the lubricant.

1.3 Line Contact

1.3.1. Line Contact Lubrication with Squeeze-Film Action

The normal approach problem was first examined theoretically by Christensen (1961), who introduced a solution for the case of two cylinders approaching each other along their line of centres. Firstly, the case of rigid cylinders lubricated with either an isoviscous or a piezoviscous fluid was considered and solved analytically to obtain the pressure distribution and the hydrodynamic load carrying capacity. Later, the case of most

practical interest, pressure dependent viscosity and elastic cylinders, was considered. This complex problem was simplified by introducing an average uniform velocity over the whole contact surface and neglecting the effect of the local deformation velocity. The two governing equations - the transient Reynolds' equation and elasticity equation - were solved simultaneously under the influence of a constant central pressure, in time sequence as the gap between the two cylinders decreased, by using a forward-iterative solution technique. Unfortunately, when the gap between the two cylinders became very thin, the solution technique was not able to ensure satisfactory convergence in this important region. Based upon this theoretical analysis, Christensen concluded:

(i) With constant viscosity and elastic cylinders, under the influence of a constant load, the maximum pressure in the fluid film cannot exceed the Hertzian pressure corresponding to the applied load. With pressure dependent viscosity and elastic cylinders, however, a very high pressure in excess of the maximum Hertzian pressure can be developed in the fluid film.

(ii) Elastic deformation causes a depression or pocket to be formed in the centre of the contact during the early stage of normal approach. As the film thickness is further reduced, the film profile and pressure distribution converge to the Hertzian solutions for dry contact.

(iii) For a given load, the maximum pressure at the contact centre is directly proportional to the material parameter ($G = \alpha E'$).

To check the validity of the suggested theory, an experimental procedure similar to that adopted by Bowden and Tabor was used. A steel ball was dropped on different polished surfaces under different applied loads to enable the effect of the load and the material parameter ($\alpha E'$) upon material deformation to be examined. No direct agreement between the theory and the experiment was found, since the theory was related to cylindrical surfaces. However, the experimental results did exhibit qualitative agreement with the theoretical predictions.

A new development to the normal approach problem for elastic cylinders was presented by Herrebrugh (1970). In this method the transient Reynolds' and elasticity equations were reduced to one single integral equation. The solution of this integral equation was obtained by the method of successive approximations with a semi-numerical procedure. The squeeze film process was assumed to be isothermal and the lubricant to be incompressible. The results were obtained for a constant load assuming a uniform velocity of approach over the surface. The most valuable result to emerge from this analysis was the recognition that the relative velocity of approach must vary along the conjunction and that this may have serious consequences for the solution at small separations.

Lee and Cheng (1973) re-examined the normal approach problem of elastic cylinders lubricated by a piezoviscous fluid by

assuming a constant central pressure, as considered earlier by Christensen. They developed an iterative method in which the transient Reynolds' equation and the elasticity equation were solved numerically by using a combination of the forward iterative technique and the Newton-Raphson method. This iterative procedure overcame the convergence difficulties encountered in the previous numerical analysis, and allowed satisfactory solutions to be obtained during the final stages of approach, when the film thicknesses became relatively small. The analysis included several effects which had not been considered previously, that is to say, the effect of local deformation velocity, the lubricant compressibility and a more realistic representation of lubricant pressure-viscosity coefficients. It was found that the local velocity played an important role during the final stages of normal approach where the ratio of local velocity to central velocity exceeded unity. It caused the lubricant to be entrapped within the contact region. Thus, both the pressure and film profiles did not appear to converge to the Hertzian solution for dry contact. the effect of compressibility of the lubricant was found to be relatively insignificant.

Conway (1973), completed an analysis of the normal approach of a rigid cylindrical roller toward the surface of a thin elastic layer covered with a fluid film whose viscosity was assumed to increase exponentially with pressure. Moreover, the deformation at any point on the surface of the layer was assumed to be directly proportional to the pressure at that point. Through this simple analysis it was shown that the assumption of a uniform velocity of approach could be erroneous.

Wada and Tsukijihara (1978), applied the Lee and Cheng technique to study the elastohydrodynamic squeeze film problem between two cylinders lubricated by grease. By using an interferometric method to measure the separation of a cylinder dropping onto a lubricated optical flat plate, the film profiles between them were observed and photographed by a high speed cine-camera. The experimental results were in good agreement with the theory.

Higginson (1978) produced a simple analytical formula for the variation of film thickness with time for the normal approach of compliant cylinders $\left(h = 4F^{1/4} \left(\frac{R}{E'}\right)^{3/4} \sqrt{\frac{\eta_o}{t}} \right)$ and spheres $\left(h = 2F^{1/6} \left(\frac{R}{E'}\right)^{2/3} \sqrt{\frac{\eta_o}{t}} \right)$ under conditions of isoviscous lubrication. These formulae were derived by using a 'Grubin type' analysis. The contact between the two cylinders was approximated by a flat rigid surface with width equal to the dry Hertzian contact zone under the corresponding static load. The corresponding simple geometry for the contact between two spheres consisted of a circular flat plate with a radius equal to the dry Hertzian contact radius. The formulae were found to provide good agreement between experimental and theoretical results of other authors.

Chandra and Rogers (1983) carried out an intensive two-dimensional analysis of the normal approach, contact and rebound of two cylinders lubricated by an isoviscous fluid. An algorithm with a combined elastohydrodynamic squeeze film model and a solid-solid model was used. In the squeeze film action a direct iterative

procedure was used to solve the time coupled elasticity equation and Reynolds' equation simultaneously. The fluid inertia effects were taken into account, approximately, by a load correction factor. During the final stage of approach, where the minimum film thickness became less than the average asperity height, a solid-solid contact model was introduced. Constant and sinusoidal loading were considered. The pressure and film thickness profiles, particularly under constant load, were found to be similar to previous work in the same field. Unlike the early work of Christensen, the pressure and film profiles did not appear to approach the Hertzian solution. An experiment was set up with sinusoidal loading and the experimental results compared well with the simulated results.

1.3.2. Line Contact Lubrication with Combined 'Entraining' and 'Normal' Motion

Sasaki, Mori and Okino (1962) presented an interesting solution to the isothermal problem for lubricated rigid cylinders subjected to a sinusoidal loading. The solution was developed for a Bingham plastic which, at high speeds, would behave as a Newtonian-lubricant. The pressure curve in the outlet region was allowed to terminate at a point where the positive pressure generated by normal approach exactly cancelled the negative pressure obtained by the action of the wedge-shaped entraining film. This boundary condition was incorrect, since the film rupture condition consistent with the continuity of mass flow was not satisfied.

Vichard (1971) investigated theoretically and experimentally the viscous damping phenomenon associated with

squeeze-film action under both hydrodynamic and elastohydrodynamic conditions for lubricated contacts. The technique used allowed for the dynamic variation of the load, entraining velocity and surface curvature and their effects were investigated. Under elasto-hydrodynamic conditions the Grubin approximations were made for the film shape and pressure distribution. Such an approach has a long history of success in the case of steady rolling in elasto-hydrodynamic lubrication. However, it did not produce solutions which satisfied the elasticity and hydrodynamic equations throughout the entire contact. Further, it did not give the details of the pressure distribution and film profile which characterize the elastohydrodynamic lubrication conditions. It was concluded that the damping phenomenon due to normal motion had a more substantial effect under elastohydrodynamic than under rigid solid lubrication conditions.

Dowson, Markho and Jones (1976), presented a general theoretical analysis of the lubrication of rigid cylindrical solids by an isoviscous lubricant in combined normal motion with rolling and sliding. It was shown that the major bearing performance characteristics could be accounted for by means of a dimensionless parameter (q), $\left(q = \frac{W}{\dot{u}}\sqrt{\frac{R}{2h_o}}\right)$. Results showed that sinusoidal normal motion imposed upon 'entraining' motion could considerably enhance the load carrying capacity of a lubricating film, even if with very small amplitudes of vibration, provided the frequency was sufficiently high. The location of the film rupture boundary was found to have a significant effect upon the pressure according to a comparison with the findings of Sasaki et al. The theoretical predictions were found to be in reasonably good agreement with experiment in a subsequent paper by the same authors.

Steinfuhrer (1980) calculated the elastohydrodynamic film thickness for nominal line contacts subjected to time-varying 'entraining' velocities by an iterative method in which horizontal (wedge) and vertical (squeeze) flows were superimposed.

Wada and Tsukijihara (1981, a,b) examined the elasto-hydrodynamic squeeze film problem of two rotating cylinders lubricated by either a Newtonian fluid or a grease under flooded and starved conditions. The governing equations - the transient hydrodynamic equation and elasticity equation - were solved simultaneously by the Newton-Raphson method. Unfortunately, the solutions were obtained for a constant central pressure, exit film thickness and squeeze to entraining velocity ratio which does not lend itself to ready application to practical problems. It was shown that the approaching velocity decreased with a decrease of the film thickness for a certain rolling velocity and load capacity, and an elastic indentation or entrapment appeared in the film profile for a large approach velocity. Further, a greater load capacity was obtained with a Bingham solid than with a Newtonian fluid and the effect of inlet location on the load capacity was less for the former than for the latter lubricant.

Medley and Dowson (1983) analysed the problem of elastic-isoviscous line contacts subjected to cyclic time-varying loads and entraining velocities. A simplified approach was developed by introducing a plane inclined surface slider bearing model, based upon the notional length of the Hertzian contact zone. The analytical procedure were solved numerically and checked against other elastohydrodynamic analysis based upon the model of an elastic

layer on a rigid parabolic solid. Excellent agreement was obtained. In a specific study of the human ankle joint, the analysis was found to provide a reasonable prediction of the variation of the film thickness during the walking cycle.

Recent studies by Dowson et al (1983), have shown that it is essential to consider the variation of squeeze-film velocity throughout the conjunction under combined entraining and squeeze-film action. This has been illustrated in relation to elasto-hydrodynamic lubrication of piston rings. Dowson (1983) discussed in a comprehensive review and study for both hydrodynamic and elasto-hydrodynamic conditions, the vital role played by the squeeze film action in preserving the lubricating film during cyclic variations of load and speed.

Hai-Tsing et al (1983) studied the elastohydrodynamic lubrication of cam-tappet pairs by using superposition of the entraining and squeeze flows. Wang and Cheng (1981), and Line and Medley (1984) incorporated Vichard's analysis into a model for the lubrication of involute spur gears. Prakash (1984) extended the work of Dowson et al (1976) to include surface roughness effects.

1.4 Point Contact

1.4.1. Point Contact Lubrication with Squeeze-Film Action

Experimental evidence was introduced by Dowson and Jones (1967) for the formation and development of the elastic indentation, expected theoretically, when a steel ball was pushed through an oil

film towards a glass plate. The shape and thickness of the elasto-hydrodynamic film were recorded during normal approach by using an optical interferometric technique with high speed photography. The most important and unexpected result of this work was the trapping of a pool of oil between the two surfaces inside the indentation for a long period and recovery of the ball when the load was removed. This observation contradicted what Christensen concluded about the pressure and film thickness profiles converging to the corresponding Hertzian shapes in the final stages of the impact.

Christensen (1970) gave a numerical solution for spherical bodies in normal approach motion under constant central pressure, considering variation in viscosity with pressure in accordance with the simple exponential relationship. The non-uniform local approach velocity assumption was taken into account. However, a confused concept about its effect on the motion still persisted. The reason for this was that the iteration procedure used failed to obtain converging solutions within the most important region of the normal approach process, when a very small central film thickness was developed. The main conclusions of this analysis were quite similar to those obtained for the normal approach problem with line contact.

Gould (1971) considered the effect of the temperature rise and the effect of the pressure rise on viscosity for the normal approach of a rigid sphere to a plane. It was noted that if the effect of the pressure upon viscosity was important in squeeze film action, the influence of temperature rise would also be significant.

Paul and Cameron (1972) developed a new method for measuring the viscosity of oils at high pressure by using an impact

viscometer. The idea was based upon the measurement of the variation of refractive index, using optical interferometry, over the whole region of a trapped pool of oil during the normal approach of a ball against a lubricated surface. The refractive index was then used to determine the density variation using the Lorentz-Lorentz equation which relates the refractive index to the density. The elastic deformation represented by the film thickness was obtained from the surface contours produced by optical interferometry. The pressure distribution was then determined by the inverse solution of the elastic equation. Finally, the viscosity variation was obtained by solving Reynolds' equation. At low pressures the viscosities were found to provide good agreement with conventional values.

James and Ettles (1978) considered the normal impact problem of an elastic ball on to an elastic surface covered by a thin layer of compressible fluid in which the viscosity was pressure-dependent. The ball was assumed to fall under its own weight and to be retarded by the pressure generated within the oil film. Furthermore, account was taken of the time rate of change of the local elastic deformation. The Reynolds, state and elasticity equations were solved simultaneously using a Newton-Raphson technique. A non-linear mesh was used with points concentrated at the centre of contact. The system was integrated in time using the Rung-Kutta-Merson method. It was shown that the variation of the normal approach velocity through the conjunction could not be ignored. In the region of minimum film thickness it was found that this velocity tended to push the surfaces together, helping to seal in the fluid in a central elastic indentation or pocket.

1.4.2. Point Contact Lubrication with Combined 'Entraining' and 'Normal' Motion

A full thermo-elastohydrodynamic analysis of hypoid gears was performed by Simon (1981). The elasticity, Reynolds and energy equations were solved numerically by the finite difference method using a direct iterative technique. The fluid film pressure profile, the temperature field, the load capacity and the friction factor were determined as functions of the teeth positions throughout the contact cycle, the minimum film thickness, the speed and the supplied oil temperature.

Mostofi (1981) obtained formulae for the variation of the central and minimum film thickness under combined squeeze and rolling for elastohydrodynamic lubrication of point contacts. The hydrodynamic and elasticity equations were solved numerically by using a forward-iterative technique similar to that of Hamrock (1976) for steady running conditions. The oil film profile and pressure distribution were determined for an assumed value of the downward squeeze velocity under the influence of a constant load. it was concluded that if a downward squeeze film velocity was superimposed upon rolling action, the pressures are much higher than those resulting under pure rolling conditions, and a dent in the film shape was formed as the squeeze-rolling speed ratio was increased.

Rahnejat (1984), investigated the vibration characteristics of line and point contacts under hydrodynamic and elastohydrodynamic lubrication conditions. The conjunctions were assumed to be

subjected to a combined 'entraining' and squeeze film action. Under hydrodynamic lubrication conditions, the hydrodynamic load was obtained by a superposition approximation to simplify the analysis, although this approximation is not absolutely accurate. In order to obtain the dynamic response of elastohydrodynamic lubricated contacts, a solution to the generalized Reynolds' equation which included an approximation for the effect of squeeze velocity on minimum film thickness was employed. Finally, the theory was applied to study the elastic and elastohydrodynamic vibration of rolling elements bearings.

Ghosh, Hamrock and Brewe (1984) presented a numerical solution for the hydrodynamic lubrication of point contacts by an isoviscous, incompressible lubricant in combined rolling and normal motion. The features of the theoretical analysis and results were quite similar to those of an earlier analysis reported by Dowson et al for lightly loaded line contacts. Regression formulae describing how dynamic load carrying-capacity and peak pressure vary with the geometrical parameter $\left(\frac{R_y}{R_x}\right)$ and the dimensionless normal velocity parameter (β) were developed. These expressions were;

$$\frac{\text{dynamic load}}{\text{steady state load}} = \left[\left(\frac{R_y}{R_x}\right)^{-0.028} \text{sech}(1.68\beta)\right]^{1/\beta}$$

$$\frac{\text{dynamic peak pressure}}{\text{steady state peak pressure}} = \left[\left(\frac{R_y}{R_x}\right)^{-0.032} \text{sech}(2\beta)\right]^{1/\beta}$$

$$\beta = \frac{W}{u}\sqrt{\frac{R_x}{2h_o}}$$

1.5 Other Conditions

Rohde, Whicker and Browne (1976), developed a unified mathematical analysis for both non-steady soft and hard elasto-hydrodynamic problems. The finite element method was used in the numerical analysis. The model allowed realistic time dependent constraints on load, pressure, or indenter velocity to be used. This technique was applied to the full problem of squeeze film action for a rigid rectangular indenter without inertia approaching an elastic half-space surface lubricated by an isoviscous lubricant. It was found that the results provided good agreement with the findings of previous work in the squeeze film field. That is, the pocket formation within the elastic surface in the early stage of impact was established, the depth of this pocket remained essentially constant without much change until contact occurred.

Subsequently, the same authors (1975) applied the above mentioned technique to study the action of individual tyre tread elements on polished sections of road covered by thin fluid films. The effect of normal approach with slip under constant and time-dependent loading were incorporated.

It was against this background that the present research programme was established. Its objectives were as detailed below.

(a) The first aim was to carry out a theoretical study of squeeze-film lubrication for rigid elliptical solids.

A complete analytical solution and the theoretical relationships between the different parameters affecting the squeeze

motion has been developed considering both piezoviscous and isoviscous fluids in Chapter (2).

(b) The second objective of the work described in this thesis was to present a more effective numerical solution for the non-steady state hydrodynamic and elastohydrodynamic lubrication of line contacts which is capable of achieving the following:

(i) allowing more realistic loading conditions corresponding to practical situations to be considered.

(ii) admitting a wide range of lubrication problems to be considered; that is where there is pure squeeze action, pure entraining action or combined effect of entraining and squeeze film action.

(iii) satisfying simultaneously the governing elastic and hydrodynamic equations and obtaining details of the hydrodynamic pressure distribution and oil film shape at different instants in the squeeze-film process.

The mathematical formulation of this complex problem will be discussed in Chapter (3) and the numerical solution procedure will be detailed in Chapter (4).

The ability of the solution procedure to deal with different types of line contact lubrication problem is then

demonstrated. A theoretical study of the squeeze-film lubrication of elastic cylinders will be introduced in Chapter (5). Theoretical studies of the hydrodynamic and elastohydrodynamic lubrication of cylinders in combined rolling and normal motion will then be presented in Chapter (6) and (7) respectively.

The overall conclusions of the work undertaken will be presented in Chapter (8).

CHAPTER 2

THEORETICAL ANALYSIS OF SQUEEZE

FILM LUBRICATION FOR A POINT CONTACT BETWEEN RIGID ELLIPTICAL SOLIDS

2.1 Introduction

When two lubricated rigid ellipsoids approach each other along the line connecting their geometrical centres under an external force, the lubricant between them is expelled by the squeezing action accompanied by a high pressure generation due to the viscous resistance of the fluid. The pressure distribution and the load supported hydrodynamically depend upon the geometrical characteristics of the contacting surfaces and the physical properties of the lubricant. Contacts lubricated by piezoviscous fluids show a viscosity variation with pressure throughout the pressurized region. This causes higher pressures to be generated than would be the case with an isoviscous lubricant for the same central film thickness and which might reach an infinite value at the centre of the conjunction even though the supported load remains finite.

The main object of the present study was to find the theoretical relationships between the different parameters affecting the squeeze motion, or, the relationships between the central film thickness, the load carrying capacity, the velocity of approach, the fluid properties, e.g., the pressure viscosity coefficient (α) and the principal radii of curvature of the contacting surfaces. The time history of the central film thickness which represents the motion was also to be ascertained.

The complete analytical solution for the above-mentioned problem has been developed considering both piezoviscous and isoviscous fluids

2.2 Geometry

Point contact conditions occur when two unloaded solids (A) and (B), having principal radii of curvature (r_{Ax}, r_{Ay}) and (r_{Bx}, r_{By}) in the vicinity of the point of closest approach make contact at a single point. In general the geometrical separation between these contacting solids, shown in Figure (2.1(a)) can be determined as illustrated in Figure (2.2(a)) by using the following mathematical expression,

$$S = S_{Ax} + S_{Bx} + S_{Ay} + S_{By} \tag{2.1}$$

The case may be represented in hydrodynamic lubrication problems by considering a geometrically equivalent solid of principal radii of curvature (R_x, R_y) adjacent to a plane, as shown in Figure (2.1(b)). The two systems are assumed to be equivalent, since, the total separation at any coordinates (x) and (y), shown in Figure (2.2(a)), is equal to the separation at the same coordinates (x) and (y) in Figure (2.2(b)), providing that both (x) and (y) are small compared with the principal radii of curvature.

From Figure (2.2(b)), the mathematical expression for the separation of the equivalent system can be written as,

$$S = S_x + S_y \tag{2.2}$$

Therefore the two expressions are equivalent when,

$$S_x = S_{Ay} + S_{Bx} \tag{2.3}$$

$$S_y = S_{Ay} + S_{By} \tag{2.4}$$

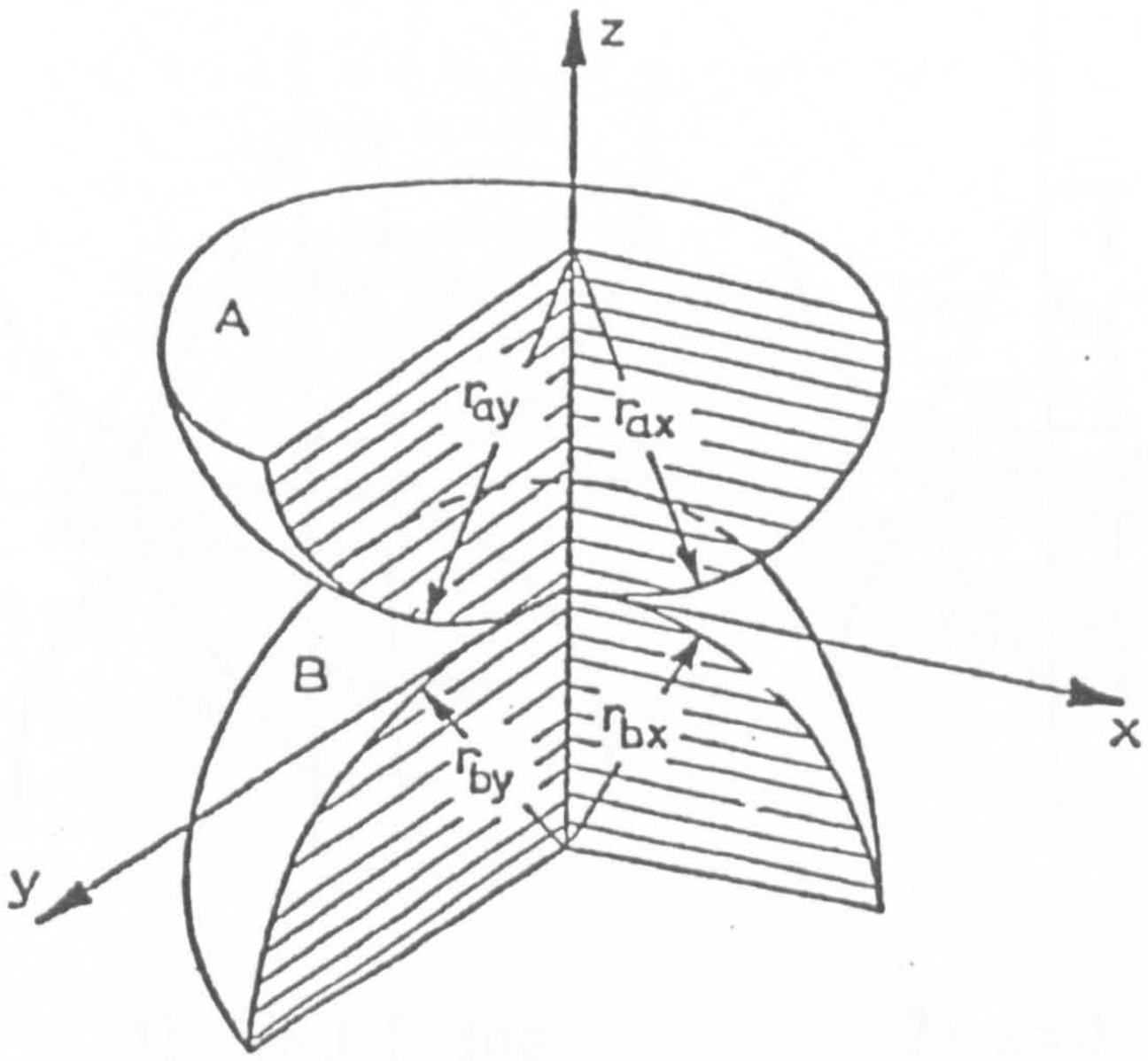

a) Contact Between Two Ellipsoidal Solids

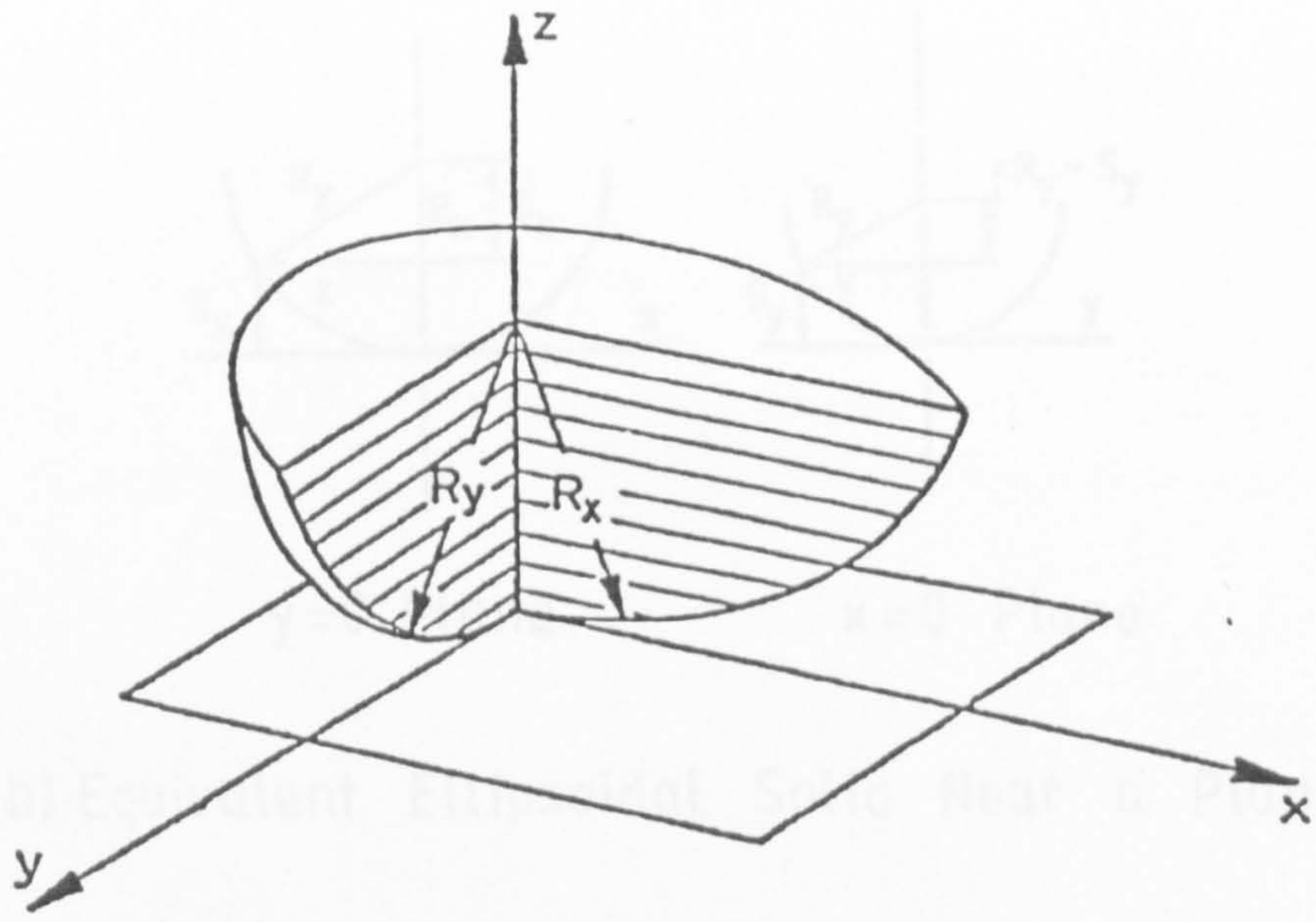

b) Equivalent Geometry

FIGURE (2 - 1) Geometry of Point Contacts

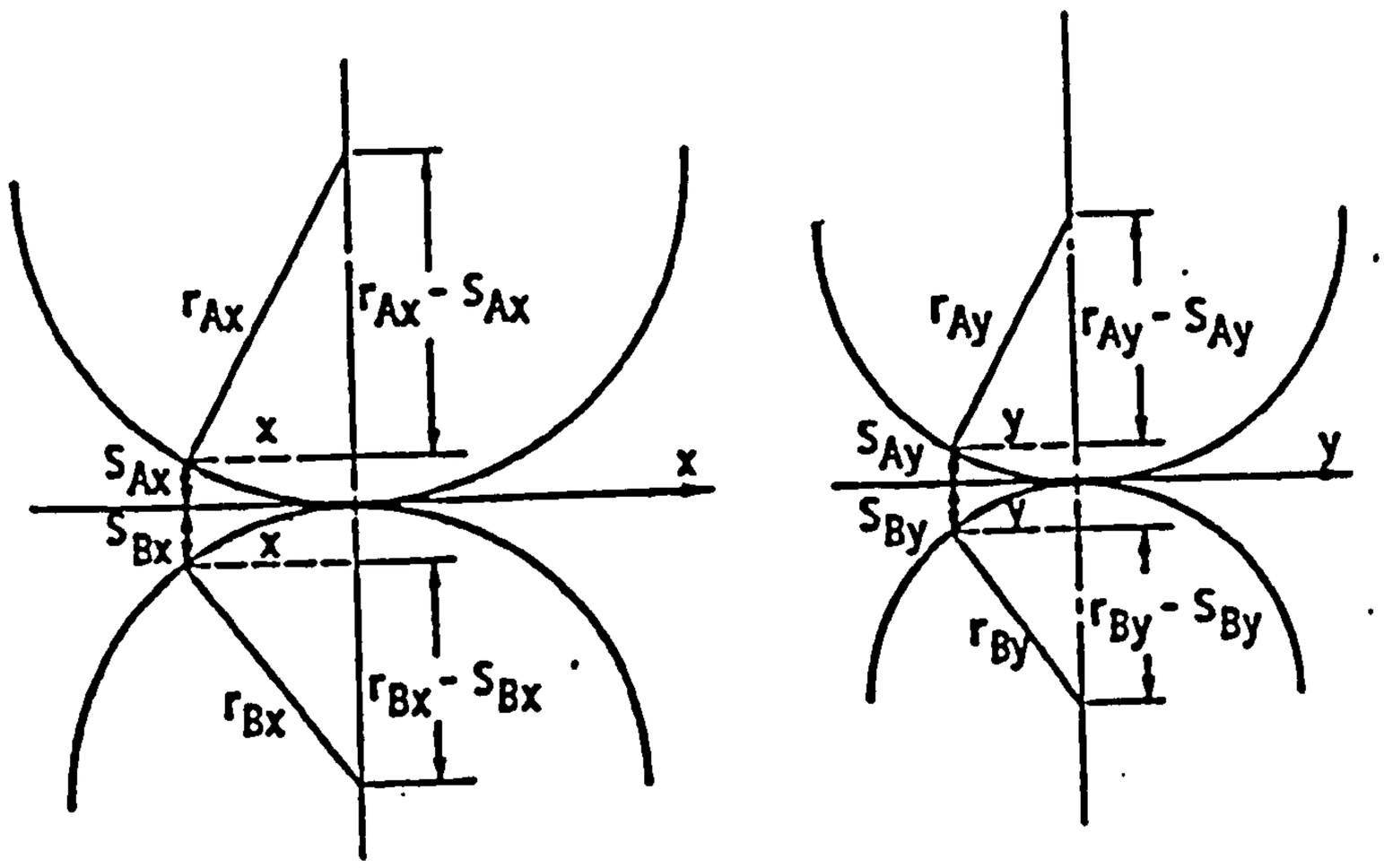

1) y=0 Plane 2) x=0 Plane

a) Two Different Ellipsoidal Solids

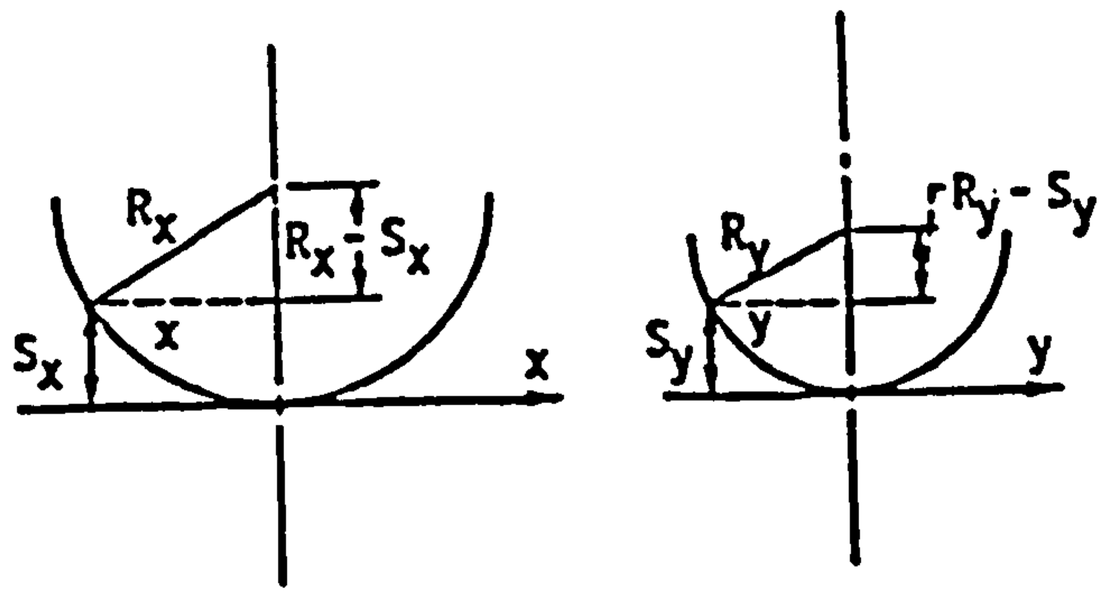

y=0 Plane x=0 Plane

b) Equivalent Ellipsoidal Solid Near a Plane

FIGURE (2 - 2) Equivalent Ellipsoidal Solids

From Figure (2.2 (a-1)) the following can be written,

$$r_{Ax}^2 = x^2 + (r_{Ax}-S_{Ax})^2$$

or
$$x^2 = S_{Ax}\,(2r_{Ax}-S_{Ax}) \qquad (2.5)$$

If the contact region is very small compared with the radius of curvature, $2\,r_{Ax} >> S_{Ax}$ and equation (2.5) can be written as

$$S_{Ax} \cong \frac{x^2}{2r_{Ax}} \qquad (2.6)$$

Likewise,

$$S_{Bx} \cong \frac{x^2}{2r_{Bx}} \qquad (2.7)$$

$$S_{Ay} \cong \frac{y^2}{2r_{Ay}} \qquad (2.8)$$

$$S_{By} \cong \frac{y^2}{2r_{By}} \qquad (2.9)$$

This is the well-known parabolic approximation used for reducing complicated geometries to simpler ones with sufficient accuracy for hydrodynamic lubrication analysis.

Substituting equation (2.6-2.9) into equations (2.3-2.4) gives,

$$\frac{1}{R_x} = \frac{1}{r_{Ax}} + \frac{1}{r_{Bx}} \qquad (2.10)$$

$$\frac{1}{R_y} = \frac{1}{r_{Ay}} + \frac{1}{r_{By}} \qquad (2.11)$$

The radii take positive or negative values depending on whether the solids are convex or concave respectively in the

vicinity of the point of closest approach. The conjunctions between convex solids or a convex solid and a plane are called counterformal, while those between convex and concave solids are called conformal.

If the solids are ellipsoids having semi-axes (a_A, b_A, C_A) and (a_B, b_B, C_B), the equivalent radii of curvature at the point of closest approach are given by,

$$r_{Ax} = \frac{(a_A)^2}{C_A} \quad , \quad r_{Ay} = \frac{(b_A)^2}{C_A}$$

$$r_{Bx} = \frac{(a_B)^2}{C_B} \quad , \quad r_{By} = \frac{(b_B)^2}{C_B} \qquad (2.12)$$

The film thickness between the equivalent ellipsoid and the plane, when the separation in the centre of the contact is (h_o), may be written as,

$$h = h_o + S(x,y) \qquad (2.13)$$

where,

$S(x,y)$ is the local separation at a position (x,y). By writing this local separation according to the parabolic approximation, equation (2.13) takes the following form,

$$h = h_o + \frac{x^2}{2R_x} + \frac{y^2}{2R_y} \qquad (2.14)$$

2.3 Reynolds' Equation

The differential equation which governs the pressure generation and distribution in fluid film lubrication situations is

the Reynolds equation. The derivation of the Reynolds equation is based upon the Navier-Stokes equation, which results from the dynamic equilibrium of an element of fluid, and the continuity equation representing the principle of mass conservation.

The Navier-Stokes equations or the equations of motion for the laminar flow of a Newtonian fluid in Cartesian coordinates have been given by (Bird (1960)) as follows,

$$\rho \frac{Du}{Dt} = \rho f_x - \frac{\partial P}{\partial x} + \frac{2}{3}\frac{\partial}{\partial x}\left[\eta\left(\frac{\partial u}{\partial x} - \frac{\partial v}{\partial y}\right)\right] + \frac{2}{3}\frac{\partial}{\partial x}\left[\eta\left(\frac{\partial u}{\partial x} - \frac{\partial w}{\partial z}\right)\right] + \frac{\partial}{\partial y}\left[\eta\left(\frac{\partial v}{\partial x} + \frac{\partial u}{\partial y}\right)\right] + \frac{\partial}{\partial z}\left[\eta\left(\frac{\partial u}{\partial z} + \frac{\partial w}{\partial x}\right)\right] \quad (2.15)$$

$$\rho \frac{Dv}{Dt} = \rho f_y - \frac{\partial p}{\partial y} + \frac{2}{3}\frac{\partial}{\partial y}\left[\eta\left(\frac{\partial v}{\partial y} - \frac{\partial u}{\partial x}\right)\right] + \frac{2}{3}\frac{\partial}{\partial y}\left[\eta\left(\frac{\partial v}{\partial y} - \frac{\partial w}{\partial z}\right)\right] + \frac{\partial}{\partial x}\left[\eta\left(\frac{\partial u}{\partial y} + \frac{\partial v}{\partial x}\right)\right] + \frac{\partial}{\partial z}\left[\eta\left(\frac{\partial v}{\partial z} + \frac{\partial w}{\partial y}\right)\right] \quad (2.16)$$

$$\rho \frac{Dw}{Dt} = \rho f_z - \frac{\partial p}{\partial z} + \frac{2}{3}\frac{\partial}{\partial z}\left[\eta\left(\frac{\partial w}{\partial z} - \frac{\partial u}{\partial x}\right)\right] + \frac{2}{3}\frac{\partial}{\partial z}\left[\eta\left(\frac{\partial w}{\partial z} - \frac{\partial v}{\partial y}\right)\right] + \frac{\partial}{\partial y}\left[\eta\left(\frac{\partial w}{\partial y} + \frac{\partial v}{\partial z}\right)\right] + \frac{\partial}{\partial x}\left[\eta\left(\frac{\partial w}{\partial x} + \frac{\partial u}{\partial z}\right)\right] \quad (2.17)$$

where,

$$\frac{D}{Dt} = \frac{\partial}{\partial t} + u\frac{\partial}{\partial x} + v\frac{\partial}{\partial y} + w\frac{\partial}{\partial z} \quad (2.18)$$

The left hand side terms of these equations (2.15-2.17) represent the inertia effects and the right hand side terms contain the body forces, pressure gradient and viscous effects respectively.

In order to derive the Reynolds' equation from the Navier-Stokes and continuity equations, the following assumptions are introduced.

(1) The effect of inertia terms is neglected with respect to the pressure and viscous forces. Thus,

$$\frac{Du}{Dt} = \frac{Dv}{Dt} = \frac{Dw}{Dt} = 0$$

(2) No body forces act on the fluid, namely, the gravity forces and any force transmitted through the bulk of the fluid itself like magnetic, electric forces ... etc., are neglected. Thus,

$$f_x = f_y = f_z = 0$$

(3) No viscosity and density variations occur across the film thickness. Thus,

$$\frac{\partial \eta}{\partial z} = \frac{\partial \rho}{\partial z} = 0$$

(4) The 'No-slip' condition applies at the fluid-solid interface. Thus,

$$z = o \ , \ u = u_A \ , \ v = v_A \ , \ w = w_A$$
$$z = h \ , \ u = u_B \ , \ v = v_B \ , \ w = w_B$$

(5) The effects due to the curvature of the fluid film are neglected because the film thickness is very small compared with its dimensions in the (x) and (y) directions.

(6) All the velocity gradients are negligible compared with the velocity gradients $\left(\frac{\partial u}{\partial z}\right)$ and $\left(\frac{\partial w}{\partial z}\right)$

Considering these assumptions the Navier-Stokes equations reduce to,

$$\frac{\partial p}{\partial x} = \eta \frac{\partial^2 u}{\partial z^2} \qquad (2.19)$$

$$\frac{\partial p}{\partial y} = \eta \frac{\partial^2 v}{\partial z^2} \tag{2.20}$$

$$\frac{\partial p}{\partial z} = 0 \tag{2.21}$$

and the continuity equation is,

$$\frac{\partial \rho}{\partial t} + \frac{\partial}{\partial x}(\rho u) + \frac{\partial}{\partial y}(\rho v) + \frac{\partial}{\partial z}(\rho w) = 0 \tag{2.22}$$

Integrating equations (2.19) and (2.20) twice, across the film thickness, with respect to (z) and taking into account the boundary conditions for the velocities according to assumption (3). The following are obtained,

$$u = -z\left(\frac{h-z}{2\eta}\right)\frac{\partial p}{\partial x} + u_B\left(\frac{h-z}{h}\right) + u_A\frac{z}{h} \tag{2.23}$$

$$v = -z\left(\frac{h-z}{2\eta}\right)\frac{\partial p}{\partial y} + v_B\left(\frac{h-z}{h}\right) + v_A\frac{z}{h} \tag{2.24}$$

Substituting these velocity expressions into the continuity equation (2.22) and integrating across the film thickness as follows,

$$\int_o^h \left[\frac{\partial \rho}{\partial t} + \frac{\partial}{\partial x}(\rho u) + \frac{\partial}{\partial y}(\rho v) + \frac{\partial}{\partial z}(\rho w)\right] dz = 0 \tag{2.25}$$

and applying the following rule,

$$\int_o^h \frac{\partial}{\partial x}\left[f(x,y,z)\right] dz = \frac{\partial}{\partial x}\int_o^h f(x,y,z)\,dz - f(x,y,h)\frac{\partial h}{\partial x}$$

Equation (2.25) becomes,

$$h\frac{\partial \rho}{\partial t} + \frac{\partial}{\partial x}\left(\rho\int_o^h u\,dz\right) - u_A\frac{\partial h}{\partial x} + \frac{\partial}{\partial y}\left(\rho\int_o^h v\,dz\right) - \rho v_A\frac{\partial h}{\partial y}$$

$$- \rho(w_A - w_B) = 0 \tag{2.26}$$

Finally, the general equation of fluid film lubrication developed by Reynolds (1886) takes the form

$$\frac{\partial}{\partial x}\left(\frac{\partial h^3}{12\eta}\frac{\partial p}{\partial x}\right) + \frac{\partial}{\partial y}\left(\frac{\rho h^3}{12\eta}\frac{\partial p}{\partial y}\right) = u\frac{\partial}{\partial x}(\rho h) + v\frac{\partial}{\partial y}(\rho h) + \frac{\partial}{\partial t}(\rho h) \qquad (2.27)$$

where,

$$u = \frac{u_A + u_B}{2} \quad , \quad v = \frac{v_A + v_B}{2}$$

For the normal approach problem considered, the fluid was assumed to be incompressible and the approaching solids were represented by rigid ellipsoids. Hence, the Reynolds equation (2.27) becomes,

$$\frac{\partial}{\partial x}\left(\frac{h^3}{\eta}\frac{\partial p}{\partial x}\right) + \frac{\partial}{\partial y}\left(\frac{h^3}{\eta}\frac{\partial p}{\partial y}\right) = -12W \qquad (2.28)$$

where,

$u = o$, $v = o$, ρ = constant

and the velocity of approach $W = -\frac{\partial h}{\partial t}$

2.4 Pressure-Viscosity Relationship

In many engineering situations extreme pressures may occur, especially in heavily loaded lubricated contacts. The very high pressure markedly affects the viscosity of the fluid. A widely used relationship, proposed by Barus, for the effect of pressure on viscosity in the isothermal case, particularly for lubricating oils, is

$$\eta = \eta_o \; e^{\alpha p} \qquad (2.29)$$

where (α) is known as the pressure-viscosity coefficient and depends on temperature only and (η_o) is a reference viscosity at atmospheric pressure for the specific lubricant. Equation (2.29) is valid only for a moderate pressure range.

2.5 The Reduced Pressure (q)

When introducing the viscosity relationship (2.29) into Reynolds equation (2.28), the latter becomes

$$\frac{\partial}{\partial x}\left[\frac{h^3}{e^{\alpha p}}\frac{\partial p}{\partial x}\right] + \frac{\partial}{\partial y}\left[\frac{h^3}{e^{\alpha p}}\frac{\partial p}{\partial x}\right] = -12\,\eta_o\,W \qquad (2.30)$$

It is no longer a simple task to integrate Reynolds equation in this configuration, therefore, a new parameter (q) is introduced, known as the reduced pressure, which is,

$$q = \frac{1}{\alpha}\left(1 - e^{-\alpha p}\right) \qquad (2.31)$$

By replacing (p) by (q), according to this relation, in Reynolds equation (2.30), we obtain

$$\frac{\partial}{\partial x}\left[h^3\frac{\partial q}{\partial x}\right] + \frac{\partial}{\partial y}\left[h^3\frac{\partial q}{\partial y}\right] = -12\,\eta_o\,W \qquad (2.32)$$

which represents the Reynolds equation for an isoviscous lubricant of viscosity (η_o). Thus, the isoviscous pressure or reduced pressure (q) solution can be converted into a piezoviscous solution by the substitution,

$$p = -\frac{1}{\alpha}\ln\left(1 - \alpha q\right) \qquad (2.33)$$

It should be noted from equation (2.33) that the pressure (p), for a piezoviscous fluid, tends to infinity when (q) approaches the value $(\frac{1}{\alpha})$, although the load remains finite. However, this does not occur in practice.

2.6 Generalization of the Problem

(i) Dimensionless Parameters

It is convenient to transform the normalized variables rather than to work with the physical variables of the problem themselves. Non-dimensional variables are introduced by writing,

$$H = \frac{h}{h_o} \quad , \quad X = \frac{x}{\sqrt{R_x h_o}} \quad , \quad Y = \frac{y}{\sqrt{R_y h_o}}$$

$$\bar{\eta} = \frac{\eta}{\eta_o} \quad , \quad P = \frac{p h_o^2}{\eta_o RW} \quad , \quad Q = \frac{q h_o^2}{\eta_o RW}$$

$$\bar{\omega} = \frac{\alpha \eta_o RW}{h_o^2} \quad , \quad \bar{F} = \frac{F}{\eta \left(\frac{R^2}{h_o}\right) W} \quad , \quad \delta = \frac{R_y}{R_x}$$

(ii) Normalized Film Thickness Equation

By dividing both sides of equation (2.14) by (h_o) and rearranging, it can be shown that,

$$\frac{h}{h_o} = 1 + \frac{x^2}{2 R_x h_o} + \frac{y^2}{2 R_y h_o}$$

Introducing the previous dimensionless variables into this equation, the normalized film thickness can be written as,

$$H = 1 + \frac{X^2 + Y^2}{2} \tag{2.34}$$

(iii) Normalized Reynolds' Equation

Reynolds' equation (2.32) may be expressed in terms of the previous dimensionless parameters as follows,

$$\frac{\partial}{\sqrt{R_x h_o}\,\partial X}\left(h_o^3 H^3 \frac{\eta_o RW}{h_o^2\sqrt{R_x h_o}}\frac{\partial Q}{\partial X}\right) + \frac{\partial}{\sqrt{R_y h_o}\,\partial Y}\left(h_o^3 H^3 \frac{\eta_o RW}{h_o^2\sqrt{R_y h_o}}\frac{\partial Q}{\partial Y}\right)$$

$$= -12\,\eta_o W$$

or, for an incompressible fluid,

$$\frac{\partial}{\partial X}\left(H^3 \frac{\partial Q}{\partial X}\right) + \frac{1}{\delta}\frac{\partial}{\partial Y}\left(H^3 \frac{\partial Q}{\partial Y}\right) = -12\left(\frac{1+\delta}{\delta}\right) \tag{2.35}$$

2.7 Boundary Conditions

Due to the symmetry of the contact surface around the (z) axis, the pressure and film thickness profiles are symmetrical with respect to it.

The boundary conditions required to solve the Reynolds' equation (2.35) are that the pressure is zero at the edges of the calculation zone, which has infinite dimensions as shown in Figure (2.3), that is,

$$\begin{aligned} Q &= 0 \quad \text{at} \quad X = \pm\infty \quad \text{for all Y values} \\ Q &= 0 \quad \text{at} \quad Y = \pm\infty \quad \text{for all X values} \end{aligned} \tag{2.36}$$

2.8 Analytical Solution

At this stage all the main governing equations have been presented. The first requirement, therefore, was to develop a basic

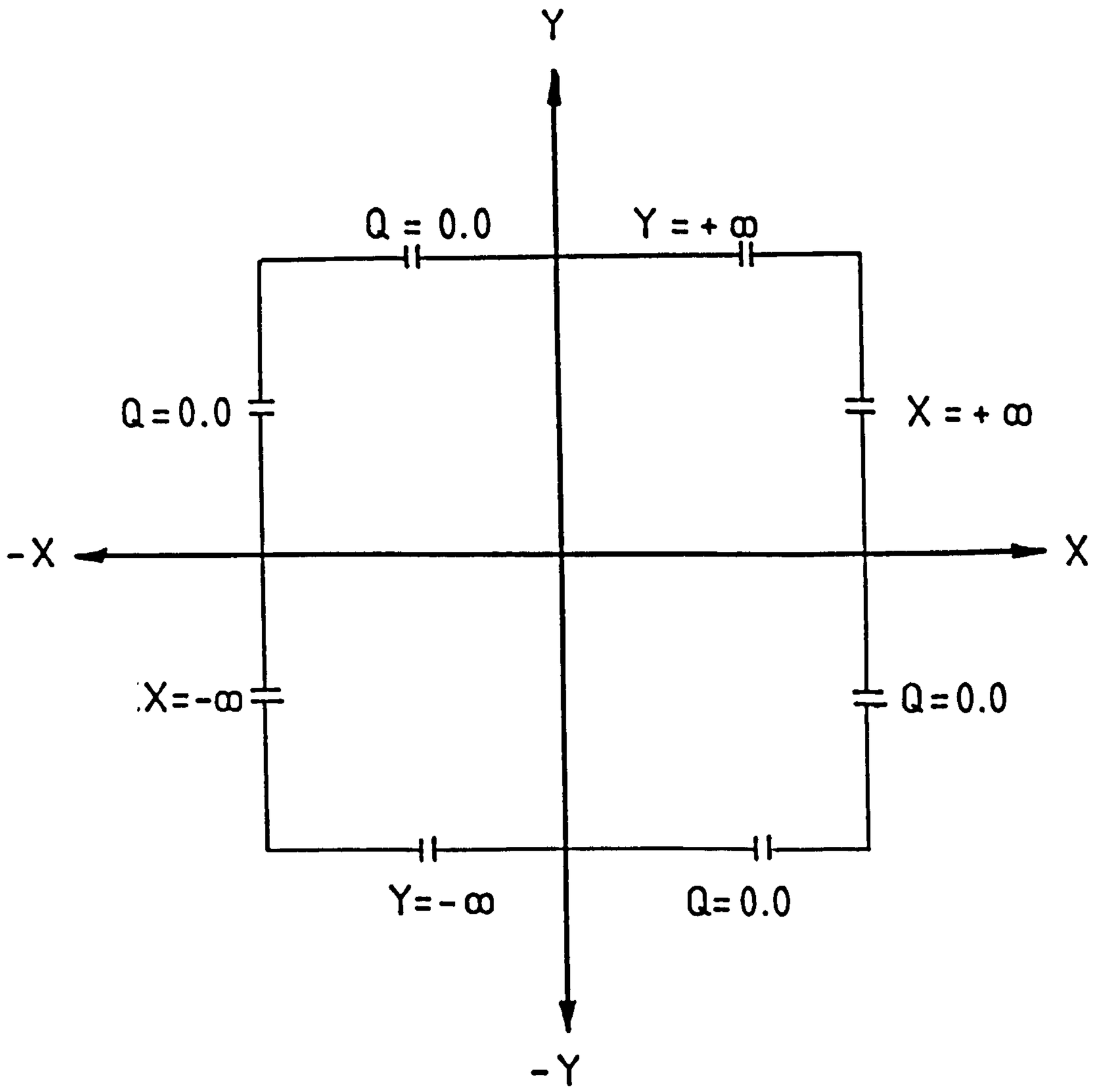

FIGURE (2-3) The Calculation Zone and the Boundary Conditions

solution to the problem of the lubrication of rigid ellipsoidal solids with an isoviscous, incompressible fluid. Namely, the pressure distribution, normal applied load, velocity of approach and the variation of the central film thickness with time had to be determined. A solution to this problem was achieved by solving the second-order differential equation (2.35) with the specific film thickness equation (2.34) and the boundary conditions (2.36).

The second requirement was to determine the general solution to the same problem, taking into account the variation of viscosity with pressure according to the Barus formula (2.29), by converting the isoviscous pressure obtained to the corresponding piezoviscous pressure through the reduced pressure relationship (2.33).

2.8.1. Constant Viscosity, Rigid Solids

(a) Pressure Distribution

An expression for the dimensionless pressure (Q) may be obtained from the complete solution of the second-order differential equation (2.35). This solution consists of two parts: firstly, the solution of the equation without the right hand side, which is called the homogeneous solution, denoted by (Q_h), a function of (X) and (Y), and satisfies the specific boundary conditions (2.36),

$$\frac{\partial}{\partial X}\left(H^3 \frac{\partial Q_h}{\partial X}\right) + \frac{1}{\delta} \frac{\partial}{\partial Y}\left(H^3 \frac{\partial Q_h}{\partial Y}\right) = 0 \qquad (2.37)$$

and, secondly, the solution of the complete equation including both sides, which is called the particular solution and denoted by (Q_p),

$$\frac{\partial}{\partial X}\left(H^3 \frac{\partial Q_p}{\partial X}\right) + \frac{1}{\delta}\frac{\partial}{\partial Y}\left(H^3 \frac{\partial Q_p}{\partial Y}\right) = -12\left(1 + \frac{1}{\delta}\right) \qquad (2.38)$$

In accordance with (Kapitza (1955)), it was found that the particular solution (Q_p) of equation (2.38) is inversely proportional to (H^2), and is

$$Q_p = \frac{K}{H^2} \qquad (2.39)$$

where (K) is a constant which is found by the direct substitution of expression (2.39) into equation (2.38) as given below:

The partial differentiation of expression (2.39) twice with respect to (X) and twice with respect to (Y) leads to

$$\frac{\partial}{\partial X}\left(H^3 \frac{\partial Q_p}{\partial X}\right) = -2K \frac{\partial 2_H}{\partial X^2}$$

$$\frac{\partial}{\partial Y}\left(H^3 \frac{\partial Q_p}{\partial Y}\right) = -2K \frac{\partial 2_H}{\partial Y^2} \qquad (2.40)$$

and the partial differentiation of the dimensionless film thickness equation (2.34) yields.

$$\frac{\partial^2 H}{\partial X^2} = 1$$

$$\frac{\partial^2 H}{\partial Y^2} = 1 \qquad (2.41)$$

Substituting these expressions from equations (2.41) into equation (2.40) gives

$$\frac{\partial}{\partial X}\left(H^3 \frac{\partial Q_p}{\partial X}\right) = -2K$$

$$\frac{\partial}{\partial Y}\left(H^3 \frac{\partial Q_p}{\partial Y}\right) = -2K \qquad (2.42)$$

Inserting the relationships of equation (2.42) into equation (2.38), the value of the constant (K) is determined as,

$$K = 6$$

Hence, the particular solution, equation (2.39), becomes,

$$Q_p = \frac{6}{H^2} \qquad (2.43)$$

The complete solution of equation (2.35) is therefore,

$$Q = Q_p + Q_h$$

or,

$$Q = \frac{6}{H^2} + f(X,Y) \qquad (2.44)$$

If the boundary conditions are to be satisfied it is necessary to determine the function f(X,Y) and for this purpose equation (2.37) must be solved. No analytical solution of equation (2.37) was found, but there are two suggested solutions: the first is the trivial solution which consideres f(X,Y) to be zero, and, the second which considers f(X,Y) to be a constant function over the main load carrying region. Consequently,

$$Q = \frac{6}{H^2} + C \qquad (2.45)$$

In order to determine the constant (C), the boundary conditions of (2.36) were applied, thus,

$$C = 0$$

Then, the pressure distribution over the whole field becomes,

$$Q = \frac{6}{H^2} \tag{2.46}$$

It should be noted that the effect of the shape of the boundaries on the pressure distribution is ignored when the extension of the oil film boundary is sufficiently large compared with the main load carrying region. This may be confirmed by considering a rigid spherical solid and matching the final resulting equation with the general equation (2.46).

(b) Hydrodynamic Load Carrying Capacity

Having produced the isoviscous pressure distribution, the corresponding hydrodynamic load carrying capacity (F) can be expressed as,

$$F = \int_{-\infty}^{+\infty} \int_{-\infty}^{+\infty} q \, dx \, dy \tag{2.47}$$

By making use of the dimensionless groups, it follows,

$$F = \frac{\eta_o RW}{h_o^2} (R_x h_o)^{\frac{1}{2}} (R_y h_o)^{\frac{1}{2}} \int_{-\infty}^{+\infty} \int_{-\infty}^{+\infty} Q \, dX \, dY$$

or,

$$F \frac{h_o}{\eta_o RW} = \sqrt{R_x R_y} \int_{-\infty}^{+\infty} \int_{-\infty}^{+\infty} Q \, dX \, dY$$

But,

$$\sqrt{R_x R_y} = R \left(\frac{1+\delta}{\delta}\right), \quad \bar{F} = F \frac{h_o}{\eta_o R^2 W}$$

Thus, the dimensionless hydrodynamic load carrying capacity is,

$$\bar{F} = \frac{1+\delta}{\sqrt{\delta}} \int_{-\infty}^{+\infty} \int_{-\infty}^{+\infty} Q \, dX \, dY \tag{2.48}$$

Because of the symmetry of the film thickness shape and pressure distribution about the (Z) axis in the (X), (Y) coordinate system, equation (2.48) may be written in alternative form,

$$\bar{F} = \frac{1+\delta}{\sqrt{\delta}} \int_{o}^{\bar{R}_1} \int_{o}^{2\pi} Q \, \bar{R} \, d\theta \, d\, \bar{R} \tag{2.49}$$

or,

$$\bar{F} = 2\pi \frac{1+\delta}{\sqrt{\delta}} \int_{o}^{\bar{R}_1} Q \, \bar{R} \, d\bar{R} \tag{2.50}$$

where, $\bar{R}^2 = X^2 + Y^2$ and $H = 1 + \frac{\bar{R}^2}{2}$

Hence, $dH = \bar{R} d\bar{R}$

and,

$$\bar{F} = 2\pi \frac{1+\delta}{\sqrt{\delta}} \int_{1}^{H_1} Q \, dH \tag{2.51}$$

Substituting the expression for pressure, equation (2.46). Therefore,

$$\bar{F} = 2\pi \frac{1+\delta}{\sqrt{\delta}} \int_1^{H_1} \frac{6}{H^2} \, dH \tag{2.52}$$

Finally, the dimensionless hydrodynamic load carrying capacity in an elliptical contact lubricated by an isoviscous fluid is obtained by,

$$\bar{F} = 12\pi \frac{1+\delta}{\sqrt{\delta}} \left(1 - \frac{1}{H_1}\right) \tag{2.53}$$

If (H_1) approaches (∞) (or $H_1 >> 1$)

$$\bar{F} = 12\pi \frac{1+\delta}{\sqrt{\delta}} \tag{2.54}$$

It should be noted that equation (2.54) reduces to the well-known equation for spheres derived by James and Ettles (1978) when the radius ratio ($\delta = 1$), that is,

$$\bar{F} = 24\pi \tag{2.54(a))}$$

The limiting case of line contact ($\delta = \infty$) can not be obtained directly from equation (2.54). However, an expression for this particular condition may be determined by solving equation (2.47) for an ellipsoidal solid with finite width (L) in the direction (y) as follows,

$$F = \int_{-\frac{L}{2}}^{\frac{L}{2}} \int_{-\infty}^{+\infty} q \; dx \, dy$$

or,

$$F = 6\eta_o WR \int_{-\frac{L}{2}}^{\frac{L}{2}} \int_{-\infty}^{+\infty} \frac{dx \, dy}{\left(h_o + \frac{x^2}{2R_x} + \frac{y^2}{2R_y}\right)^2}$$

By integrating with respect to (x), thus,

$$F = \frac{3\pi\eta_o \quad RW}{\sqrt{\frac{1}{2R_x}}\left(\frac{1}{2R_x}\right)^{3/2}} \int_{-\frac{L}{2}}^{\frac{L}{2}} \frac{dy}{\left(2R_y h_o + y^2\right)^{3/2}}$$

Finally, the general expression of the hydrodynamic load carrying capacity for an ellipsoidal solid with finite width (L) is,

$$F = \frac{3\pi\eta_o \quad RW}{h_o \sqrt{\frac{1}{2\ R_x}}} \left[\frac{L}{\left(h_o + \frac{L^2}{8R_y}\right)^{\frac{1}{2}}}\right] \qquad (2.54(b))$$

As the width (L) becomes infinite, equation (2.54(b)) takes the same form as equation (2.54). When the principal radius of curvature (R_y) tends to infinite (∞), i.e., the case of cylindrical solid, equation (2.54(b)) reduces to,

$$\frac{F}{L} = \frac{3\sqrt{2}\pi\eta_o R^2 W}{h_o^{3/2}} \qquad (2.54(c))$$

which represents the hydrodynamic load carrying capacity per unit width of a cylindrical body approaching a lubricated plane.

(c) Velocity of Approach

Consider an ellipsoidal solid, sinking under a constant load (F) onto a smooth surface covered by a thin, isoviscous fluid. In the absence of inertia forces, the velocity of approach (W), at a central fluid film thickness (h_o), can be determined by rewriting equation (2.54) in terms of the physical quantities of the problem as,

$$F = \frac{12\pi\ \eta_o\ WR^2}{h_o} \left(\frac{1+\delta}{\sqrt{\delta}}\right) \tag{2.55}$$

Therefore, the velocity of approach (W) is,

$$W = \frac{F\ h_o}{12\pi\ \eta_o\ R^2} \left(\frac{\sqrt{\delta}}{1+\delta}\right) \tag{2.56}$$

(d) Time of Approach

The time of approach is the time taken to reduce the central film thickness (h_o) between the rigid ellipsoid and the lubricated surface by a given amount. When the velocity of approach (W) is replaced by $\left(-\frac{\partial\ h_o}{\partial t}\right)$, equation (2.56) can be rearranged and written in the form,

$$-\frac{dh_o}{h_o} = \frac{1}{12\pi\ \eta_o\ R^2} \left(\frac{\sqrt{\delta}}{1+\delta}\right) F\ dt \tag{2.57}$$

If the load (F) is assumed to be constant with respect to time and the initial central film thickness is (h_{o1}) at a specific time (t_1), equation (2.57) can be integrated to give the central film thickness (h_o) at any instant (t) throughout the approaching process.

Thus,

$$\int_{h_{o1}}^{h_o} -\frac{dh_o}{h_o} = \frac{F}{12\pi\ \eta_o\ R^2} \frac{\sqrt{\delta}}{(1+\delta)} \int_{t_1}^{t} dt$$

Then,

$$\Delta t = (t-t_1) = \frac{12\pi\ \eta_o\ R^2}{F} \frac{1+\delta}{\sqrt{\delta}} \ln \frac{h_{o1}}{h_o}$$

Otherwise,

$$h_o = h_{ol} \; e^{\left[\frac{F}{2\pi \eta_o R^2} \frac{\sqrt{\delta}}{(1+\delta)} (t_1-t)\right]} \qquad (2.58)$$

2.8.2. Variable Viscosity, Rigid Solids

(a) Pressure Distribution

Having obtained the isoviscous, or reduced, pressure (q), an expression for the piezoviscous pressure (p) was determined by making use of equation (2.33) which relates the isoviscous pressure (q) to the piezoviscous pressure (p). Hence,

$$p = \frac{-1}{\alpha} \ln \left(1 - \frac{\alpha \eta_o RW}{h_o^2} Q\right) \qquad (2.59)$$

or, in dimensionless form,

$$P = \frac{-1}{\bar{\omega}} \ln \; (1 - \bar{\omega} . Q) \qquad (2.60)$$

Substituting the value of the dimensionless isoviscous pressure (Q) from equation (2.46) yields (P) the corresponding dimensionless piezoviscous pressure,

$$P = - \frac{1}{\bar{\omega}} \ln \left(1 - \frac{6\bar{\omega}}{H^2}\right) \qquad (2.61)$$

Where ($\bar{\omega}$) is the dimensionless velocity of approach or piezoviscous factor.

An interesting feature of equation (2.61) is that the pressure approaches an infinite value at the centre of the contact,

where the film thickness equals unity, when the dimensionless velocity of approach ($\bar{\omega}$) has the value $\left(\frac{1}{6}\right)$. As fully explained later, the minimum film thickness at which the pressure attains an infinite value, at a specific applied load, is called the transitional film thickness (h_{oT}).

(b) Hydrodynamic Load Carrying Capacity

The domain of the pressure integration required to obtain the dimensionless hydrodynamic load carrying capacity ($\bar{F}$) in this case is similar to the integration domain for the isoviscous condition. Owing to this similarity, the piezoviscous load carrying capacity can be calculated by replacing the isoviscous pressure (Q) by the piezoviscous pressure (P) in equation (2.51), which leads to,

$$\bar{F} = 2\pi \frac{1+\delta}{\sqrt{\delta}} \int_1^{H_1} P \, dH \qquad (2.62)$$

From equation (2.61) and (2.62) we can write,

$$\bar{F} = \frac{-2\pi}{\bar{\omega}} \frac{1+\delta}{\sqrt{\delta}} \int_1^{H_1} \ln\left(1 - \frac{6\bar{\omega}}{H^2}\right) dH \qquad (2.63)$$

Now, the form of this integral was determined as follows,

$$I = \int_1^{H_1} \ln\left(1 - \frac{6\bar{\omega}}{H^2}\right) dH$$

$$= \int_1^{H_1} \ln\left(\frac{H^2 - 6\bar{\omega}}{H^2}\right) dH$$

$$= \int_1^{H_1} \left[\ln (H^2 - 6\bar{\omega}) - \ln H^2 \right] dH$$

$$= \left[H \ln (H^2 - 6\bar{\omega}) - 2H + \sqrt{6\bar{\omega}} \ln \left(\frac{H + \sqrt{6\bar{\omega}}}{H - \sqrt{6\bar{\omega}}} \right) \right.$$

$$\left. -2H \ln H + 2H \right]_1^{H_1}$$

$$I = \left[H \{ \ln (H^2 - 6\bar{\omega}) - \ln H^2 \} + \sqrt{6\bar{\omega}} \ln \left(\frac{H + \sqrt{6\bar{\omega}}}{H - \sqrt{6\bar{\omega}}} \right) \right]_1^{H_1}$$

$$= \left[H \ln \left(1 - \frac{6\bar{\omega}}{H^2} \right) + \sqrt{6\bar{\omega}} \ln \left(\frac{H + \sqrt{6\bar{\omega}}}{H - \sqrt{6\bar{\omega}}} \right) \right]_1^{H_1}$$

As (H_1) approaches (∞) (or $H_1 >> 1$),

$$I = - \left[\ln (1 - 6\bar{\omega}) + \sqrt{6\bar{\omega}} \ln \left(\frac{1 + \sqrt{6\bar{\omega}}}{1 - \sqrt{6\bar{\omega}}} \right) \right]$$

Hence, the dimensionless piezoviscous load is,

$$\bar{F} = \frac{2\pi}{\bar{\omega}} \frac{1+\delta}{\sqrt{\delta}} \left[(1+\sqrt{6\bar{\omega}}) \ln (1+\sqrt{6\bar{\omega}}) + (1-\sqrt{6\bar{\omega}}) \ln (1-\sqrt{6\bar{\omega}}) \right] \quad (2.64)$$

It was noted earlier that under some circumstances an infinite pressure is predicted at the contact centre of the conjunction, when the dimensionless velocity of approach $(\bar{\omega})$ has the value $\left(\frac{1}{6}\right)$. It can be shown that the corresponding dimensionless load carrying capacity $(\bar{F})$ remains constant at a specific limiting value $(\bar{F}_T)$ throughout the rest of the squeeze process if the pressures remain finite. This limiting load $(\bar{F}_T)$ was obtained by calculating the limit of equation (2.64) when the quanity $(\bar{\omega})$ tends to $\left(\frac{1}{6}\right)$. Therefore,

$$\bar{F}_T = 12\pi\left(\frac{1+\delta}{\sqrt{\delta}}\right) \quad \left[2 \ln 2 + 0\right]$$

or,

$$\bar{F}_T = 24\pi \left(\frac{1+\delta}{\sqrt{\delta}}\right) \ln 2$$

$$\cong 52.26 \left(\frac{1+\delta}{\sqrt{\delta}}\right) \tag{2.65}$$

Equation (2.64) represents the general condition of squeeze-film lubrication for ellipsoids with a piezoviscous fluid. As the dimensionless velocity ($\bar{\omega}$), the important characteristic in this case, tends to zero, the isoviscous condition is obtained, that is, equation (2.64) turns to the simple equation (2.54). This was established by taking the limit of equation (2.64) using the L'Hopital rule of the limits.

Rearranging equation (2.64), thus

$$\bar{F} = 2\pi \left(\frac{1+\delta}{\sqrt{\delta}}\right) \lim_{\bar{\omega} \to 0} \left[\frac{(1+\sqrt{6\bar{\omega}}) \ln (1+\sqrt{6\bar{\omega}}) + (1-\sqrt{6\bar{\omega}}) \ln (1 -\sqrt{6\bar{\omega}})}{\bar{\omega}}\right]$$

Differentiating separately the nominator and the denominator of the indeterminate quantity in the brackets with respect to ($\bar{\omega}$) and repeating the same process with the result yields,

$$\bar{F} = 2\pi \left(\frac{1+\delta}{\sqrt{\delta}}\right) \lim_{\bar{\omega} \to 0} \frac{6}{2} \quad \left[\frac{1}{1+\sqrt{6\bar{\omega}}} + \frac{1}{1-\sqrt{6\bar{\omega}}}\right]$$

or,

$$\bar{F} = 2\pi \left(\frac{1+\delta}{\sqrt{\delta}}\right)[6]$$

$$= 12\pi \left(\frac{1+\delta}{\sqrt{\delta}}\right)$$

which is the simple equation (2.54) for the isoviscous condition.

(c) Transitional Film Thickness

It was stated before that two important conditions must be satisfied at the transitional film thickness (h_{oT}). The first, is that the pressure at the point of closest approach is infinite where the dimensionless velocity of approach has the value $\left(\frac{1}{6}\right)$. The second is that the dimensionless load ($\bar{F}$) is constant and has the limiting value ($\bar{F}_T$) of equation (2.65). These two conditions in mathematical form are,

$$\bar{\omega} = \frac{1}{6} = \frac{\eta_o WR\alpha}{h_o^2} \tag{2.66}$$

and,

$$\bar{F} = \frac{F\, h_o}{\eta_o R^2 W} = 24\pi \left(\frac{1+\delta}{\sqrt{\delta}}\right) \ln 2 \tag{2.67}$$

Eliminating the approach velocity (W) between equation (2.66) and (2.67) gives,

$$h_{oT} = \frac{F.\alpha}{4\pi R \ln 2} \frac{\sqrt{\delta}}{1+\delta} \tag{2.68}$$

which represents the transitional film thickness equation.

Substituting the resulting central film thickness value (h_{oT}) into equtions (2.66) yields,

$$W_T = \frac{h_{oT}^2}{6\eta_o R\alpha} \tag{2.69}$$

where (W_T) is the velocity of approach at the transitional film thickness (h_{oT}).

(d) Velocity of Approach

The velocity of approach for an ellipsoid moving towards a plane in a piezoviscous fluid when the dimensionless velocity of approach ($\bar{\omega}$) is less than its limiting value $\left(\frac{1}{6}\right)$ may be evaluated from the dimensionless load equation (2.64) in the following way.

The quantity in the brackets in equation (2.64) may be written for convenience as,

$$\bar{D} = \frac{1}{\bar{\omega}} \left[(1 + \sqrt{6\bar{\omega}}) \ln (1 + \sqrt{6\bar{\omega}}) + (1 - \sqrt{6\bar{\omega}}) \ln (1 - \sqrt{6\bar{\omega}})\right]$$

Using the algebraic expansion of the logarithmic quantity of $\ln (1 + \sqrt{6\bar{\omega}})$ and $\ln (1 - \sqrt{6\bar{\omega}})$, one may write.

$$\bar{D} = \frac{1}{\bar{\omega}} \left[\left\{1 + (6\bar{\omega})^{\frac{1}{2}}\right\}\left\{(6\bar{\omega})^{\frac{1}{2}} - \frac{(6\bar{\omega})}{2} + \frac{(6\bar{\omega})^{3/2}}{3} - \frac{(6\bar{\omega})^{2}}{4} + \frac{(6\bar{\omega})^{5/2}}{5} - \frac{(6\bar{\omega})^{3}}{6} + \cdots\cdots\right\} + \left\{1 - (6\bar{\omega})^{\frac{1}{2}}\right\}\left\{-(6\bar{\omega})^{\frac{1}{2}} - \frac{(6\bar{\omega})}{2} - \frac{(6\bar{\omega})^{3/2}}{3} - \frac{(6\bar{\omega})^{2}}{4} - \frac{(6\bar{\omega})^{5/2}}{5} - \frac{(6\bar{\omega})^{3}}{6} - \cdots\right\}\right]$$

Re-arranging,

$$\bar{D} = \frac{1}{\bar{\omega}} \left[-(6\bar{\omega}) - \frac{(6\bar{\omega})^{2}}{2} - \frac{(6\bar{\omega})^{3}}{3} - \frac{(6\bar{\omega})^{4}}{4} + 2(6\bar{\omega}) + \frac{2}{3}(6\bar{\omega})^{2} + \frac{2}{5}(6\bar{\omega})^{3} + \frac{2}{7}(6\bar{\omega})^{4}\right]$$

or,

$$\bar{D} = \left[6 + 6\bar{\omega} + \frac{72}{5}\bar{\omega}^2 + \frac{324}{7}\bar{\omega}^3 + \ldots.\right] \qquad (2.70)$$

Now the dimensionless load equation (2.64) takes the form.

$$\bar{F} = 2\pi\left(\frac{1+\delta}{\sqrt{\delta}}\right)\left[6 + 6\bar{\omega} + \frac{72}{5}\bar{\omega}^2 + \frac{324}{7}\bar{\omega}^3 + \ldots..\right] \qquad (2.71)$$

Then, as $(\bar{\omega})$ tends to zero this equation reduces to the isoviscous results. That is it yields the dimensionless isoviscous load equation (2.54).

Writing expression (2.71) in terms of the physical quantity of the problem and neglecting the cubic and higher terms of $(\bar{\omega})$. Thus,

$$\frac{F\,h_o}{\eta_o R^2 W} = 2\pi\left(\frac{1+\delta}{\sqrt{\delta}}\right)\left[6 + 6\,\frac{\alpha\,\eta_o\,RW}{h_o^2} + \ldots..\right]$$

Re-arranging,

$$\frac{\alpha\,\eta_o R}{h_o^2}W^2 + W - \frac{F\,h_o}{12\pi\eta_o R^2}\,\frac{\sqrt{\delta}}{(1+\delta)} = 0 \qquad (2.72)$$

Equation (2.72) is a quadratic equation in (W), which has the following positive root,

$$W = \frac{h_o^2}{2\alpha\eta_o R}\left[-1 + \sqrt{1 + \frac{\alpha\,F\sqrt{\delta}}{3\pi h_o R(1+\delta)}}\right] \qquad (2.73)$$

Expanding the quantity of the square root leads to,

$$W = \frac{h_o^2}{\alpha\,\eta_o R}\left[\frac{1}{4}\left\{\frac{\alpha\,F\,\sqrt{\delta}}{3\pi h_o R(1+\delta)}\right\} - \frac{1}{16}\left\{\frac{\alpha\,F\,\sqrt{\delta}}{3\pi h_o R(1+\delta)}\right\}^2 + \frac{1}{32}\left\{\frac{\alpha\,F\,\sqrt{\delta}}{3\pi h_o R(1+\delta)}\right\}^3 - \ldots..\right] \qquad (2.74)$$

Neglecting the cubic term, therefore,

$$W = \frac{h_o^2}{\alpha \eta_o R}\left[\frac{\bar{A}}{h_o} - \frac{A^2}{h_o^2}\right] \qquad (2.75)$$

where,

$$A = \frac{\alpha F \sqrt{\delta}}{12\pi R(1+\delta)}$$

The first term in equation (2.75) gives the isoviscous velocity of approach. Inclusion of the second term enables the velocity of approach with a piezoviscous fluid to be determined.

(e) Time of Approach

In this case the squeeze process, with a constant load, may be divided into two distinct stages. Firstly, the initial stage of approach where the dimensionless velocity ($\bar{\omega}$) is less than its limiting value $\left(\frac{1}{6}\right)$ and secondly, the final stage where the central pressure tends to infinity and the dimensionless approach velocity has the limiting value $\left(\frac{1}{6}\right)$.

(i) The Initial Stage ($h_{ol} > h_o > h_oT$)

The important feature of this stage is that the aspects of the motion are related to the applied load. Hence, the time of approach was calculated by replacing the velocity of approach (W) by $\left(-\frac{\partial h_o}{\partial t}\right)$ in equation (2.76). Thus,

$$-\frac{\partial h_o}{\partial t} = \left(\frac{A}{\alpha \eta_o R}\right) h_o - \frac{A^2}{\alpha \eta_o R} \qquad (2.76)$$

If the initial central film thickness was (h_{ol}) at a specific time (t_1), equation (2.76) can be integrated to give the new position at a central film thickness (h_o) at any instant (t) as,

$$\int_{t_1}^{t} dt = \int_{h_{ol}}^{h_o} -\frac{\alpha\eta_o R}{A} \frac{dh_o}{(h_o - A)} \tag{2.77}$$

and,

$$t - t_1 = \frac{\alpha\eta_o R}{A} \ln\left[\frac{h_{ol} - A}{h_o - A}\right]$$

or,

$$\Delta t = \frac{\alpha\eta_o R}{A} \ln\left(\frac{h_{ol} - A}{h_o - A}\right) \tag{2.78}$$

Also,

$$h_o = A + (h_{ol} - A)\, e^{-\frac{A}{\alpha\eta_o R}\Delta t} \tag{2.79}$$

Where,

$$A = \frac{\alpha F \sqrt{\delta}}{12\pi R(1+\delta)}$$

Equation (2.79) describes the motion of an ellipsoid towards a plane covered by a piezoviscous fluid throughout the initial stage of the approaching process. The isoviscous case can be deduced by substituting the value of the constant (A) and considering the coefficient (α) to be zero.

ii - The Final Stage ($h_o < h_{oT}$)

The squeeze film action continues, beyond the point at which the pressure becomes infinite at the centre of contact only and remains finite everywhere. It is however, independent of the applied load and the relationship (2.66) for the velocity of approach holds throughout the subsequent squeeze action. Replacing the approach velocity (W) by $\left[-\frac{\partial h_o}{\partial t}\right]$ and integrating between different positions (h_{o1}) and (h_o) at times (t_1) and (t) respectively, gives,

$$\int_{t_1}^{t} dt = 6\eta_o R\alpha \int_{h_{o1}}^{h_o} -\frac{dh_o}{h_o^2} \qquad (2.80)$$

Thus,

$$\Delta t = 6\eta_o R\alpha \left[\frac{1}{h_o} - \frac{1}{h_{o1}}\right] \qquad (2.81)$$

or,

$$h_o = \frac{1}{\left[\frac{\Delta t}{6\eta_o R\alpha} + \frac{1}{h_{o1}}\right]} \qquad (2.82)$$

2.9 Discussion of Results

Typical results are presented as a series of curves for the dimensionless load ($\bar{F}$), the transitional film thickness (h_{oT}) and the time history of the central film thickness (h_o) as an ellipsoid approaches a flat surface for a given constant load and specific radius ratio (δ).

2.9.1 The Dimensionless Hydrodynamic Load ($\bar{F}$)

The dimensionless load ($\bar{F}$) is recorded as a function of radius ratio (δ) for different values of the dimensionless velocity of approach ($\bar{\omega}$) in Figure (2.4). The values of the dimensionless velocity of approach range from zero, which corresponds to the isoviscous case, to the piezoviscous condition representing the limiting value $\left(\frac{1}{6}\right)$. It is suggested from this figure that the dimensionless load ($\bar{F}$) for all the values of the dimensionless velocity ($\bar{\omega}$) has the same trend, that is, for a constant value of ($\bar{\omega}$), the dimensionless load ($\bar{F}$) first decreases with the increase of (δ) until it reaches a minimum value at (δ=1), i.e. a sphere and starts to increase again with an increase of (δ). Moreover, at a constant value of (δ) the dimensionless load ($\bar{F}$) increases with an increase of ($\bar{\omega}$). Also Figure (2.5) displays the variation of the non-dimensional load ($\bar{F}$) with the non-dimensional approach velocity ($\bar{\omega}$). Results are shown for three values of the radius ratio (δ) which were chosen to correspond to typical geometries. It is apparent from this figure that the limiting value of the dimensionless load ($\bar{F}_T$) at a value of ($\bar{\omega}$) of $\left(\frac{1}{6}\right)$ increases with an increase of (δ) according to equation (2.65).

2.9.2 The Transitional Film Thickness (h_{oT})

Figure (2.6) shows the variation of the non-dimensional transitional film thickness (h_{oT} R/F.α) with the radius ratio (δ). The dimensionless transitional film thickness increases with the increase of (δ) until it reaches the maximum value at (δ=1) and decreases afterwards with a further increase in (δ). Hence, the

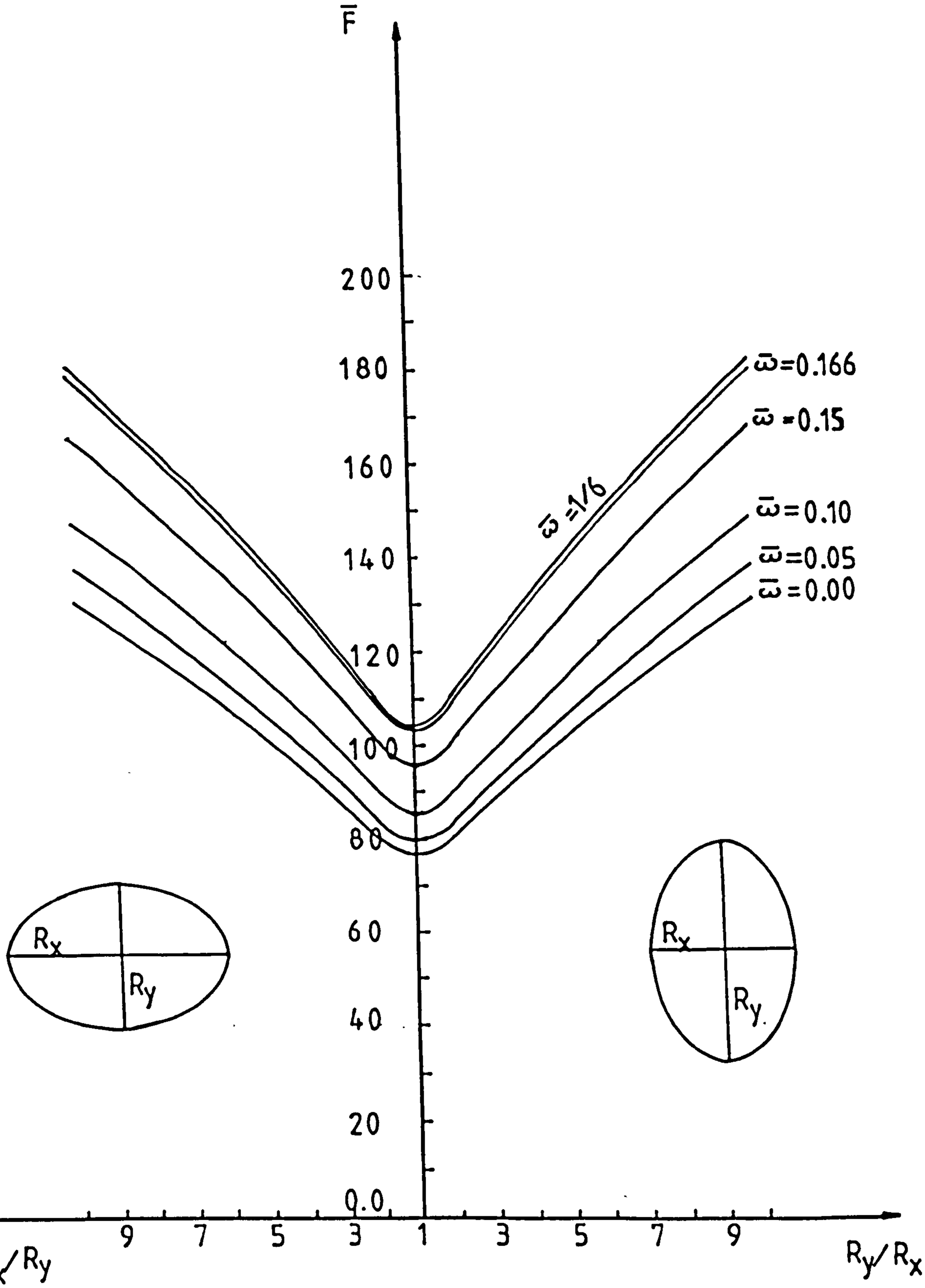

FIGURE (2 - 4) Variation of Dimensionless Load with the Radius Ratio for Various Values of $\bar{\omega} = 0.00, 0.05, 0.10, 0.15, 0.166, 1/6$

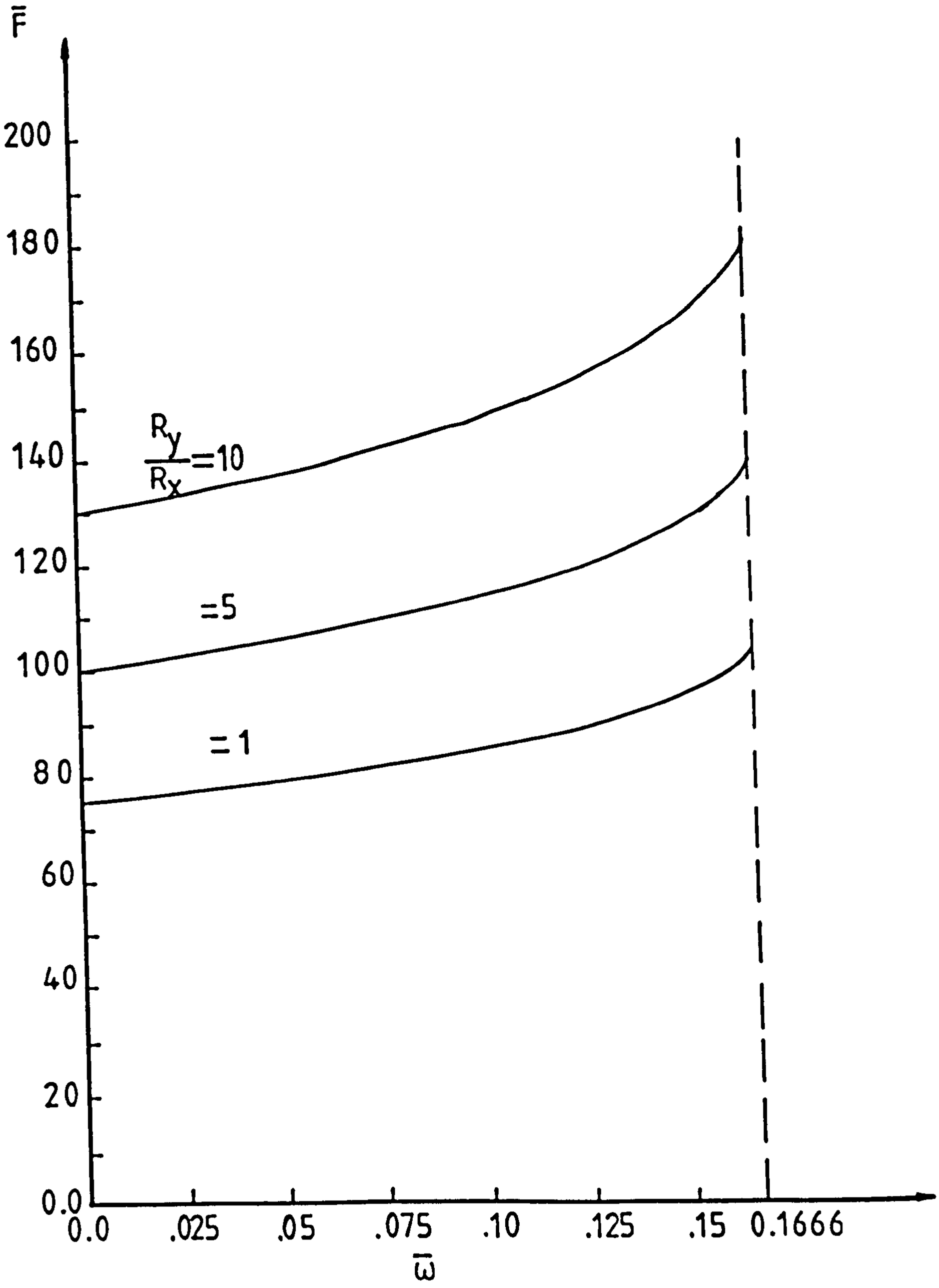

FIGURE (2 - 5) Variation of the Dimensionless Load with the Dimensionless Approach Velocity ($\bar{\omega}$) for Various Values of the Radius Ratio δ = 1 , 5 , 10

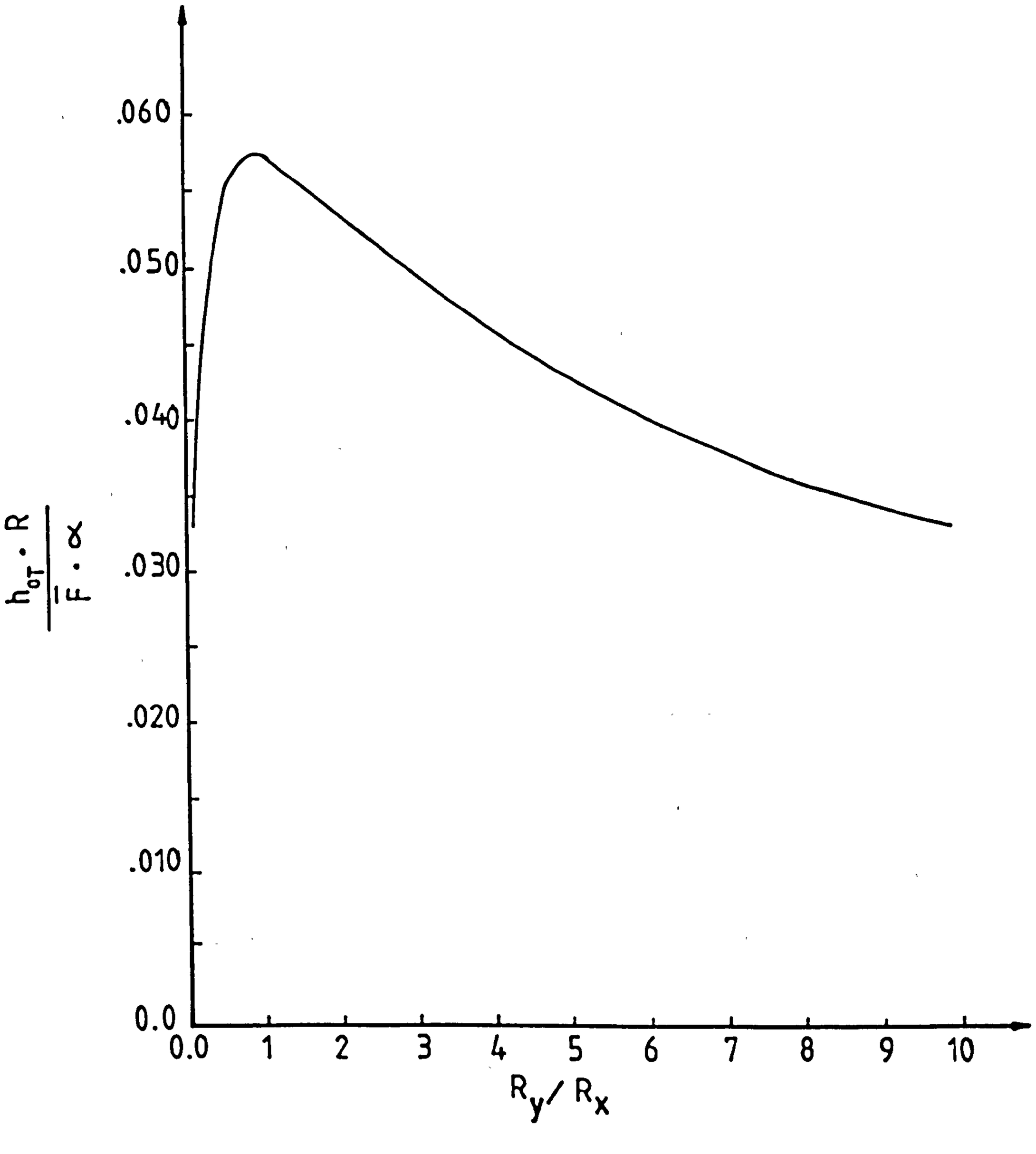

FIGURE (2 - 6) Variation of the Transitional Film Thickness with the Radius Ratio (R_y / R_x)

load independent process would be expected to occur earlier at a higher film thickness (h_o) when the ellipsoidal body approaches the spherical shape (δ=1).

2.9.3 Central Film Thickness

A time history of the central film thickness (h_o) when considering both isoviscous and piezoviscous lubrication is recorded for particular cases in Figures (2.7) to (2.15). To give an indication of the variation of the central film thickness with time, the present theory has been applied to a specific example of an ellipsoid of equivalent radius (0.005 m) and radius ratio (31). These specifications have been especially chosen to match approximately the practical case of the contact geometry between a ball and the inner-race of a real standard single-row, radial, deep-groove ball bearing with the following dimensions (Hamrock and Dowson (1981)):

Inner-race diameter, d_i	0.052291	m
Outer-race diameter, d_o	0.077706	m
Ball diameter, d	0.012700	m
Number of balls in complete bearing, n	9	
Inner-groove radius, r_i	0.006604	m
Outer-groove radius, r_o	0.006604	m
Contact angle, β	0	
rms surface finish of balls, f_b	0.0625×10^{-6}	m
rms surface finish of races, f_r	0.175×10^{-6}	m

A bearing of this kind might well experience the following operating conditions:

Radial load, F_r	8900	N
Inner-ring angular velocity, ω_i	400	rad/s
Outer-ring angular velocity, ω_o	0	
Lubricant viscosity at atmospheric pressure and effective operating temperature of bearing, η_o	0.04	Ns/m^2
Viscosity-Pressure coefficient, α	2.3×10^{-8}	m^2/N
Modulus of elasticity for both balls and rings, E	2×10^{11}	N/m^2
Poisson's ratio for both balls and rings, σ	0.3	

The essential features of the geometry of the inner conjunction can be ascertained as follows:

Pitch diameter, $d_e = \frac{1}{2}(d_o+d_i)$	0.065	m
Diametral clearance, $P_d = d_o - d_i - 2d$	1.5×10^{-5}	m
Race conformity, $f_i = f_o = \frac{r}{d}$	0.52	
Equivalent radius, $R_{x,i} = d\,(d_e - d)/2d$	0.00511	m
Equivalent radius, $R_{y,i} = f_i\, d/(2f_i-1)$	0.165	m
Equivalent radius, $R = \frac{R_{x,i} \times R_{y,i}}{R_{x,i} + R_{y,i}}$	4.956×10^{-3}	m
Radius ratio, $\delta = R_{y,i}/R_{x,i}$	32	
The load carried by the most heavily loaded ball in the bearing, F	4513	N

For the sake of comparison another two cases of an ellipsoid of

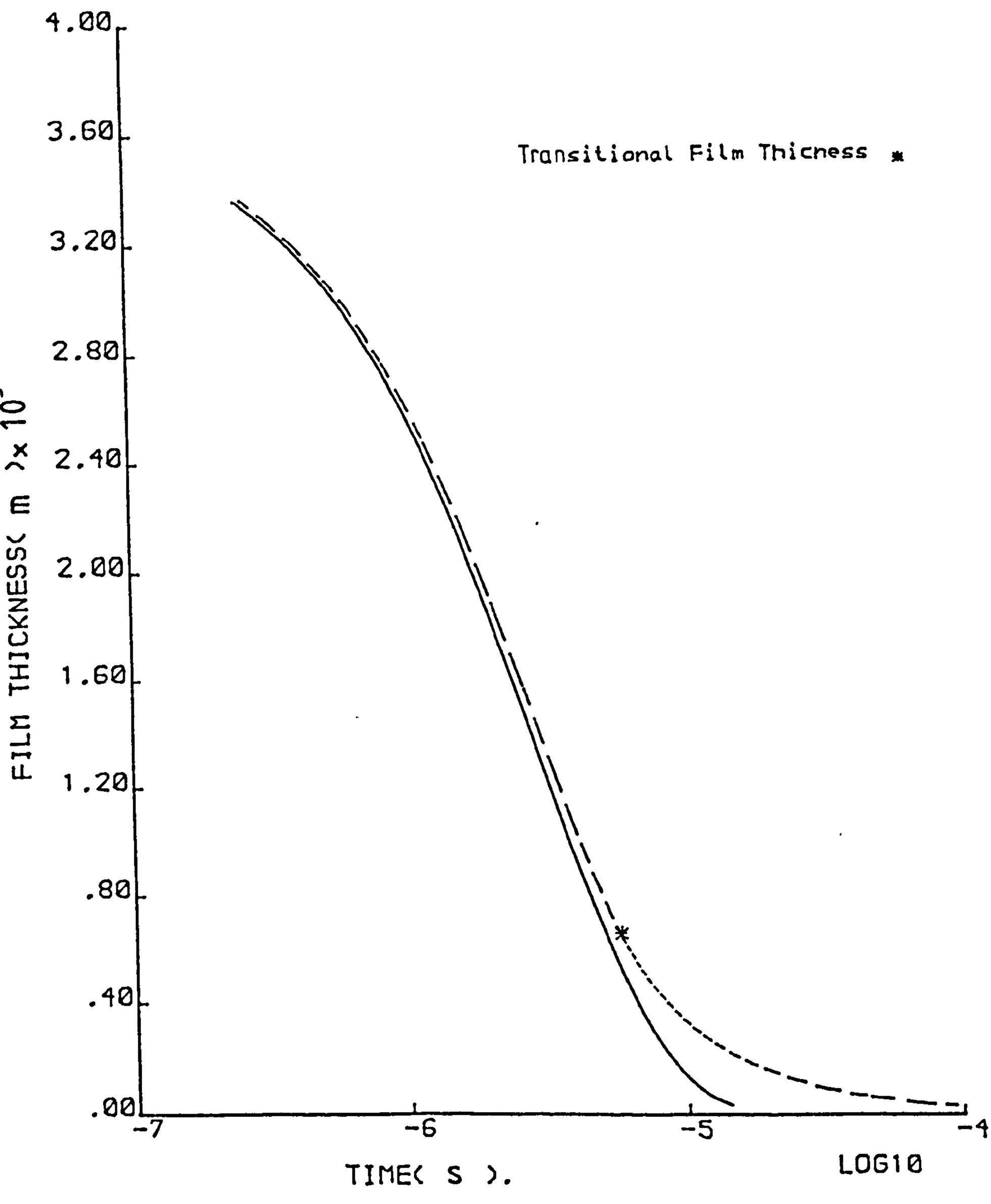

FIGURE(2 - 7) Film Thickness History for an Ellipsoid of Equivalent Radius(0.005 m) and Radius Ratio(1) Approaching a Plane Surface in the Presence of Isoviscous(———) and Piezoviscous(— — —) Fluids Under a Load of (25 N)

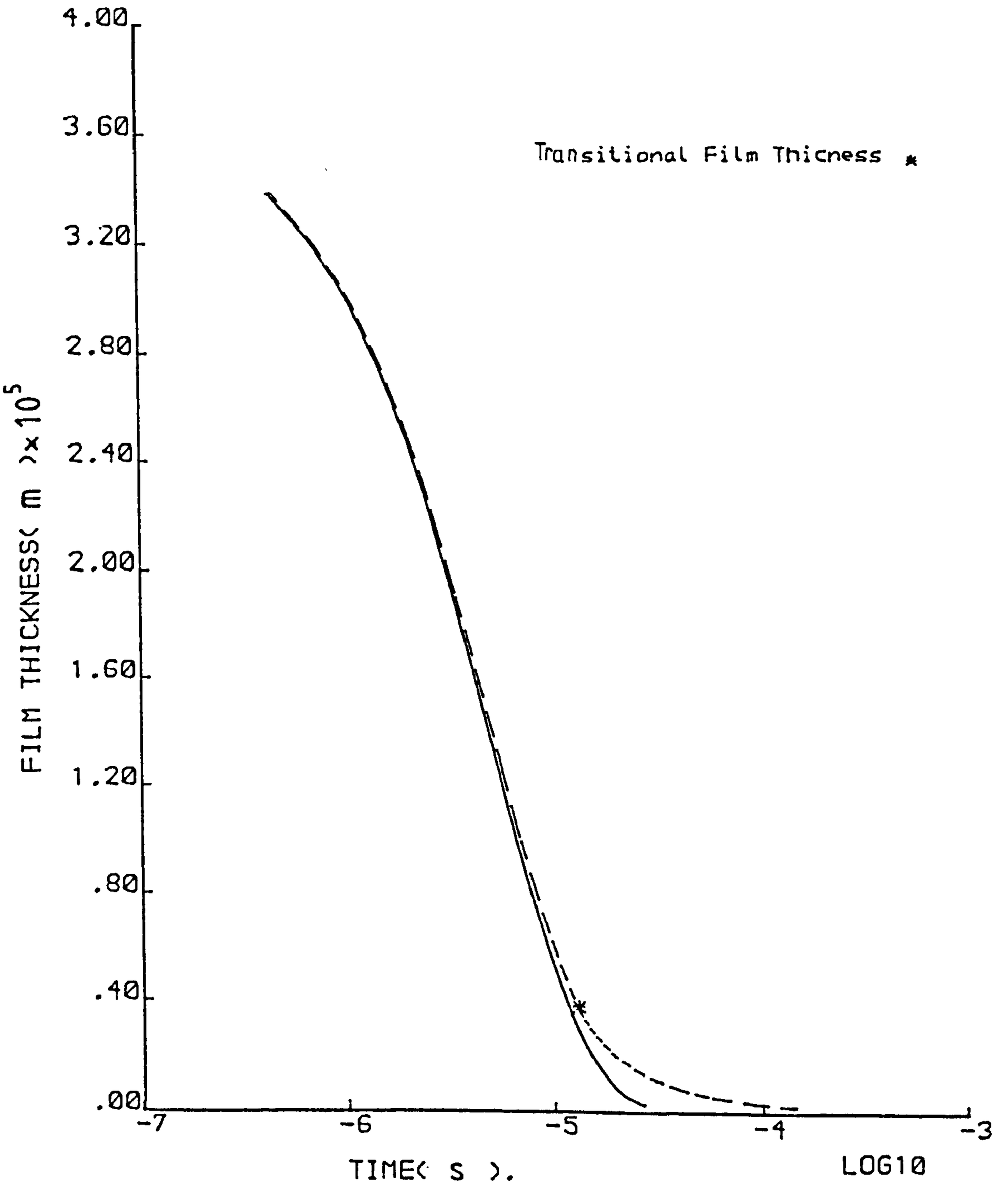

FIGURE(2 - 8) Film Thickness History For an Ellipsoid of Equivalent Radius(0.005 m) and Radius Ratio(10) Approaching a Plane Surface in the Presence of Isoviscous(————) and Piezoviscous(— — —) Fluids Under a Load of (25 N)

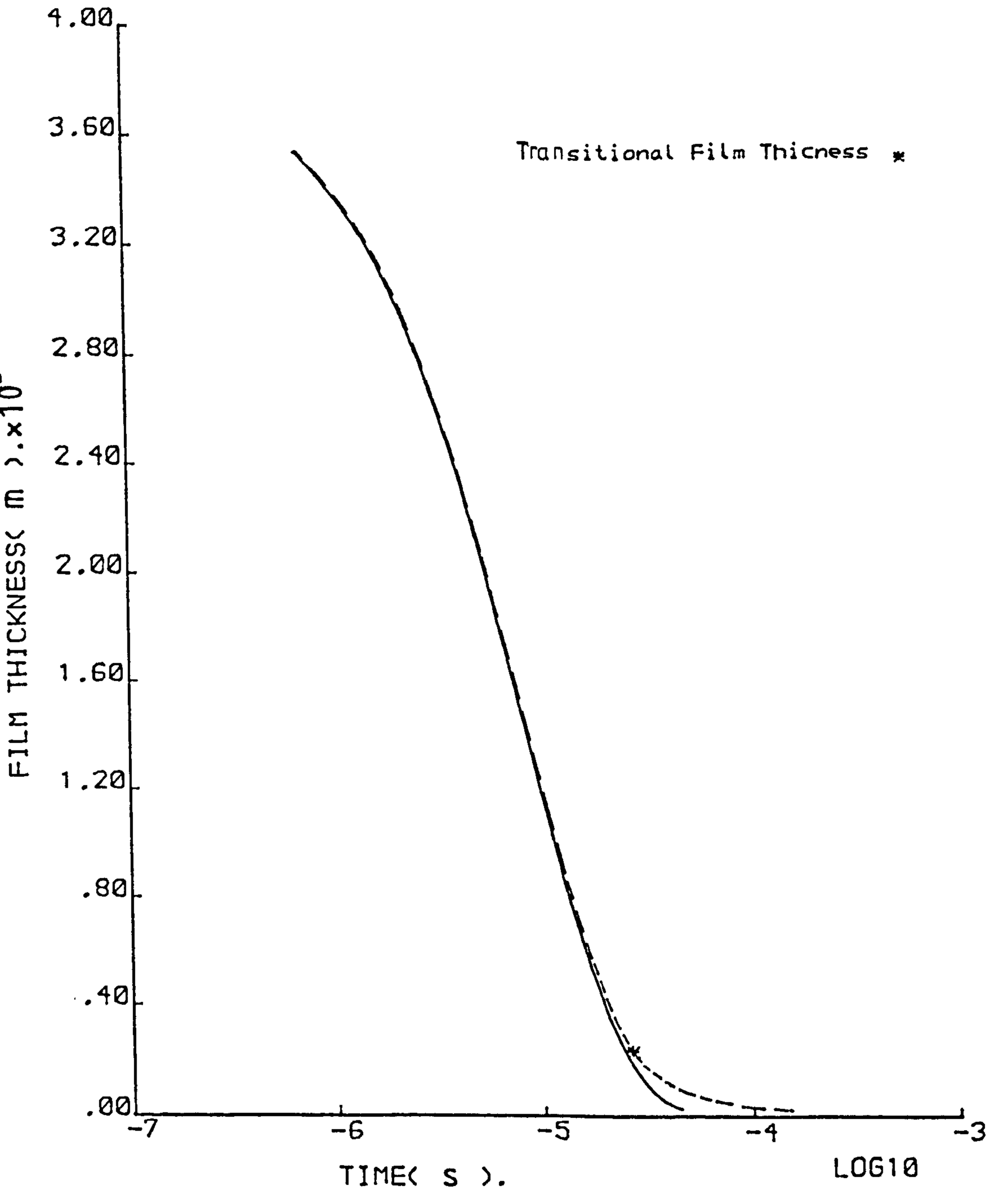

FIGURE(2 - 9) Film Thickness History For an Ellipsoid of Equivalent Radius(0.005 m) and Radius Ratio(31) Approaching a Plane Surface in the Presence of Isoviscous(————) and Piezoviscous(— — —) Fluids Under a Load of (25 N.)

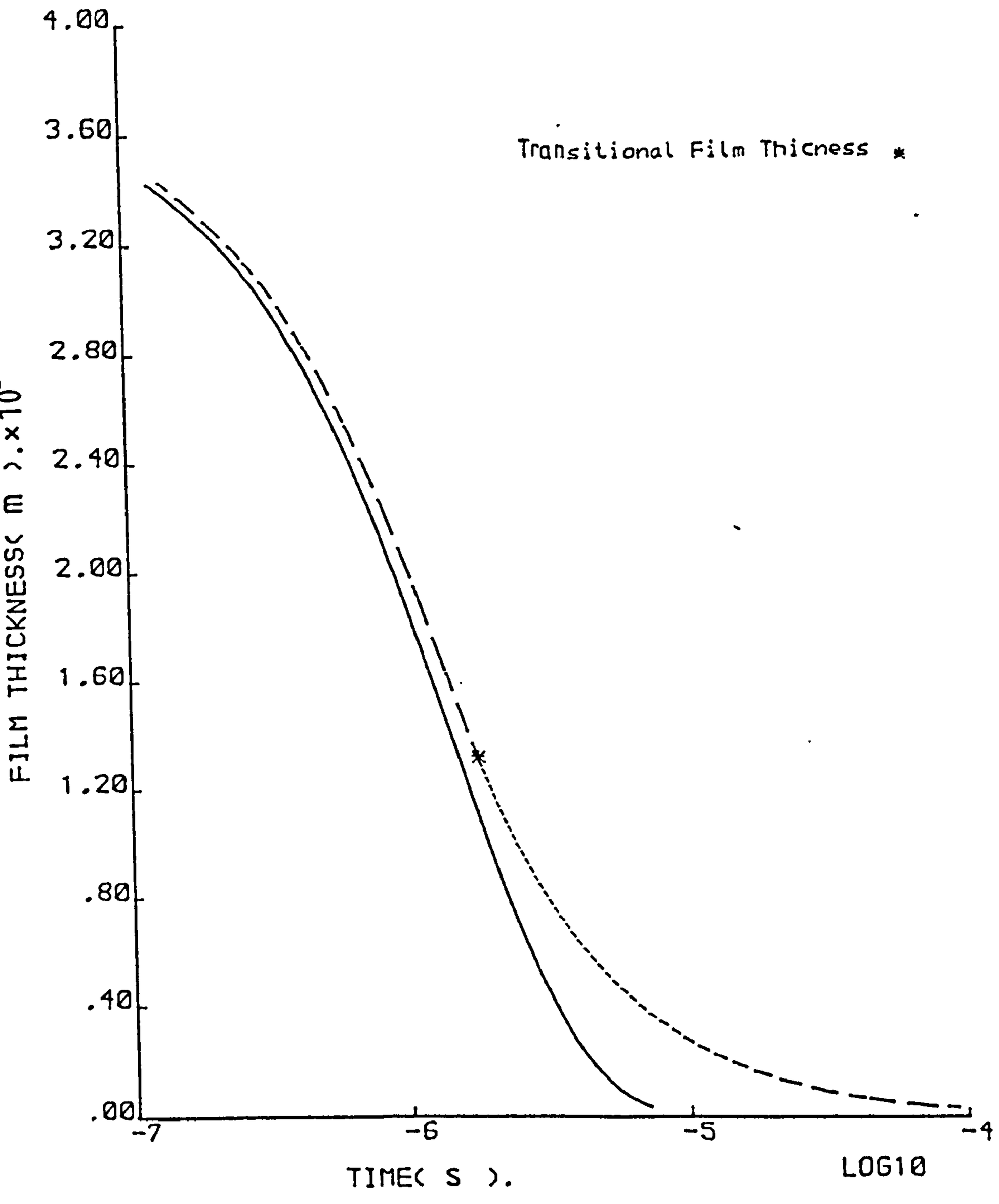

FIGURE(2 -10) Film Thickness History For an Ellipsoid of Equivalent Radius(0.005 m) and Radius Ratio(1) Approaching a Plane Surface in the Presence of Isoviscous(————) and Piezoviscous(— — —) Fluids Under a Load of (50 N)

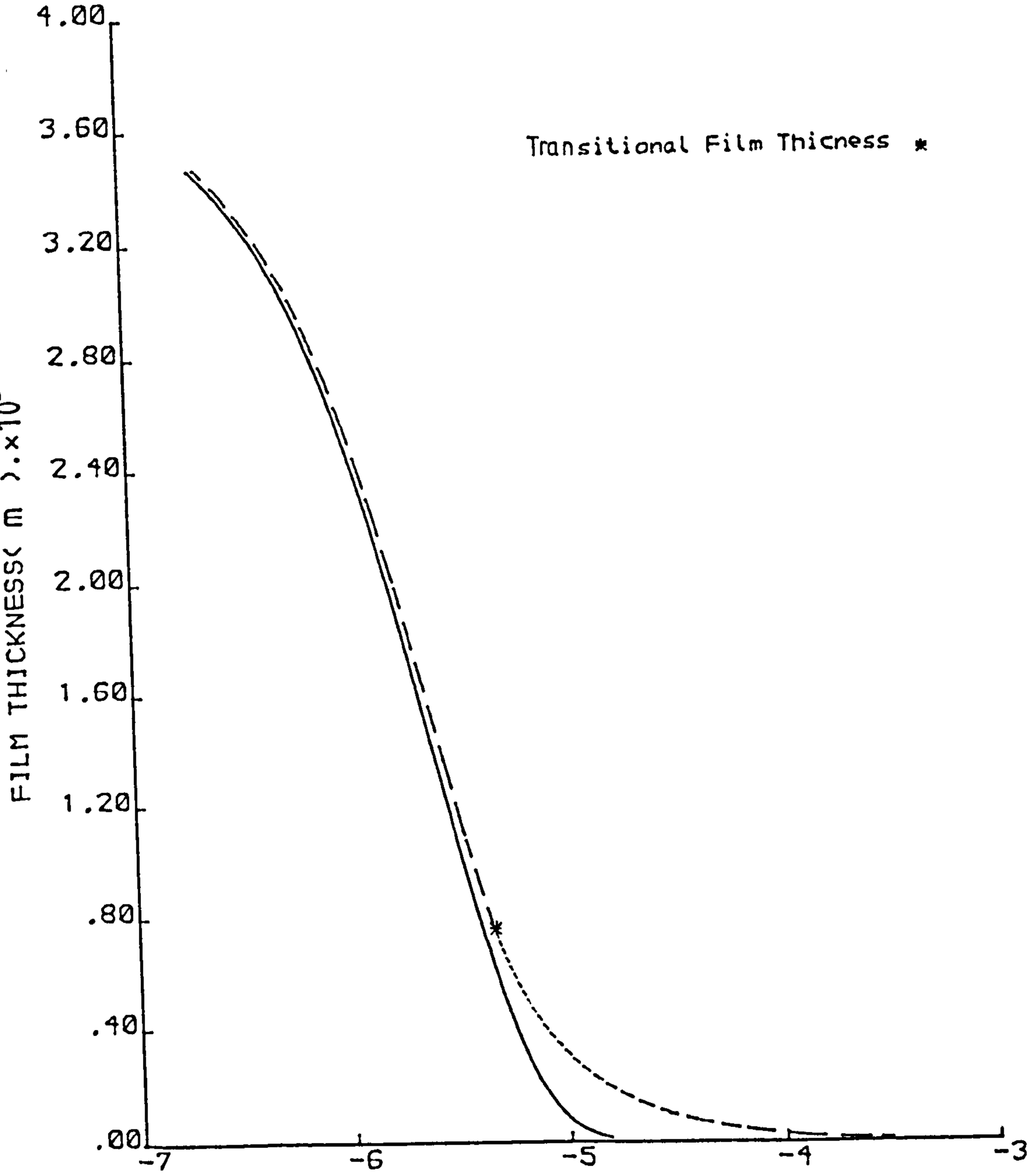

FIGURE(2 -11) Film Thickness History For an Ellipsoid of Equivalent Radius(0.005 m) and Radius Ratio(10) Approaching a Plane Surface in the Presence of Isoviscous(————) and Piezoviscous(— — —) Fluids Under a Load of (50 N)

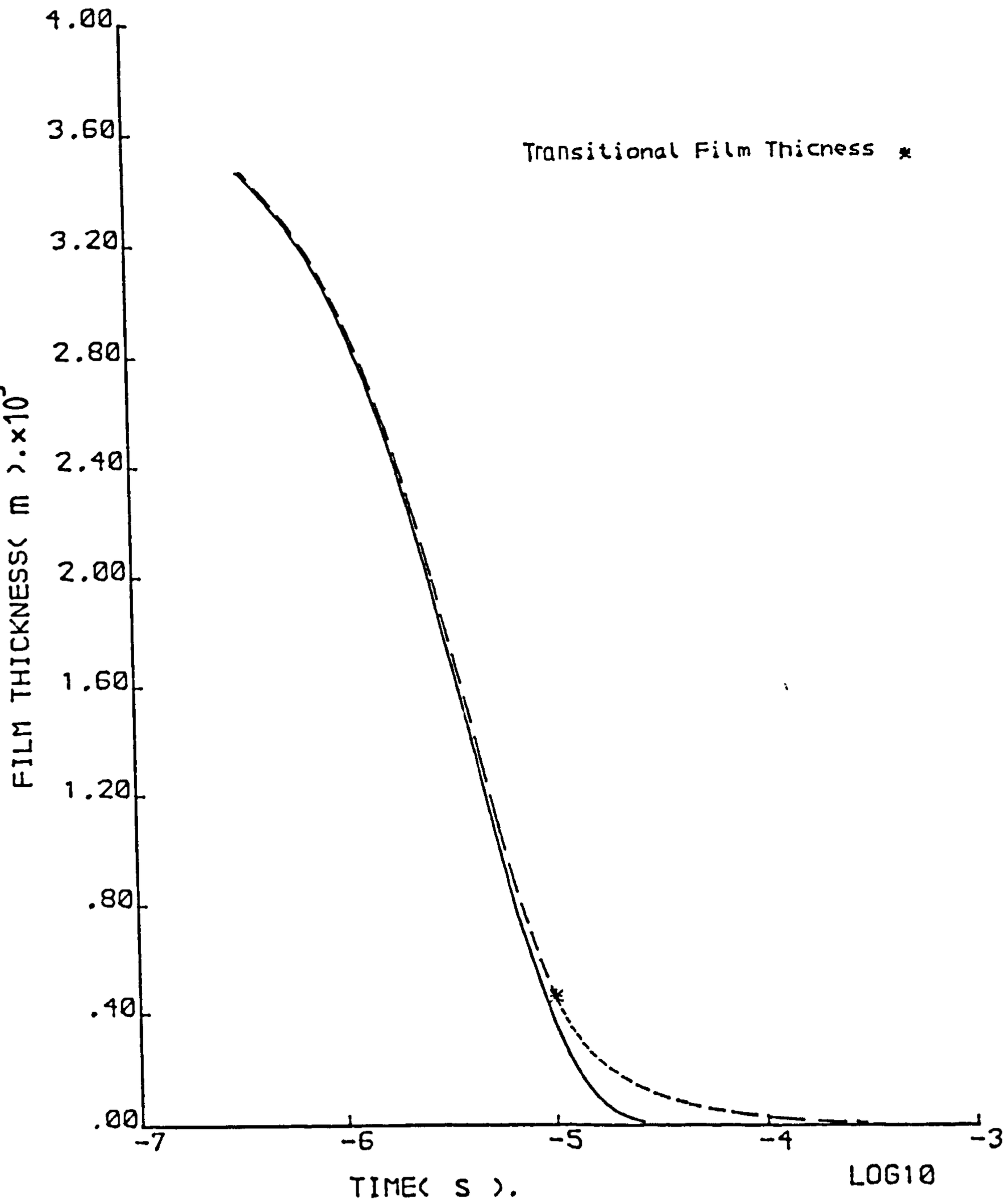

FIGURE(2 -12) Film Thickness History for an Ellipsoid of Equivalent Radius(0.005 m) and Radius Ratio(31) Approaching a Plane Surface in the Presence of Isoviscous(————) and Piezoviscous(— — —) Fluids Under a Load of (50 N)

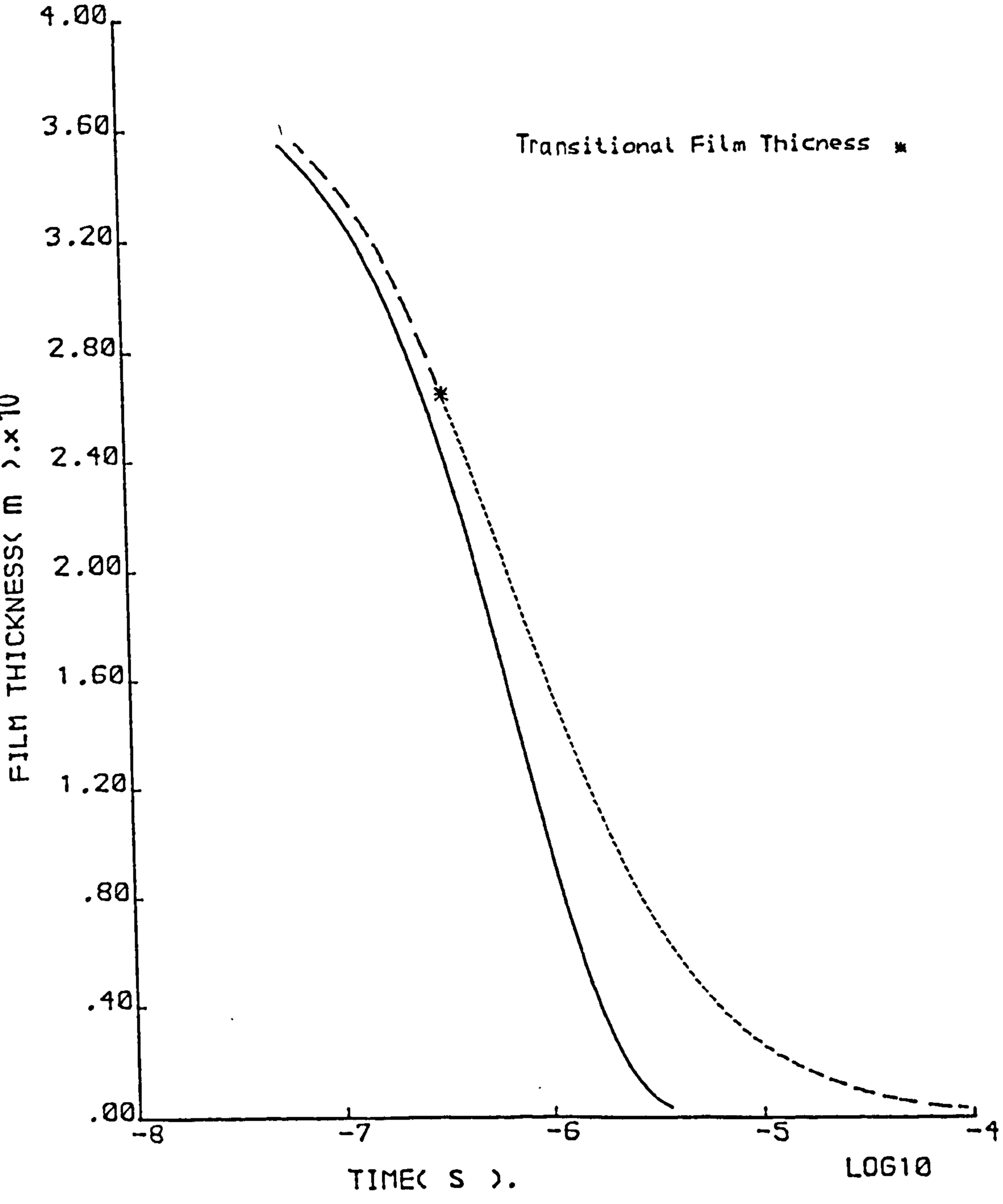

FIGURE(2 - 13) Film Thickness History For an Ellipsoid of Equivalent Radius(0.005 m) and Radius Ratio(1) Approaching a Plane Surface in the Presence of Isoviscous(————) and Piezoviscous(— — —) Fluids Under a Load of (100 N.)

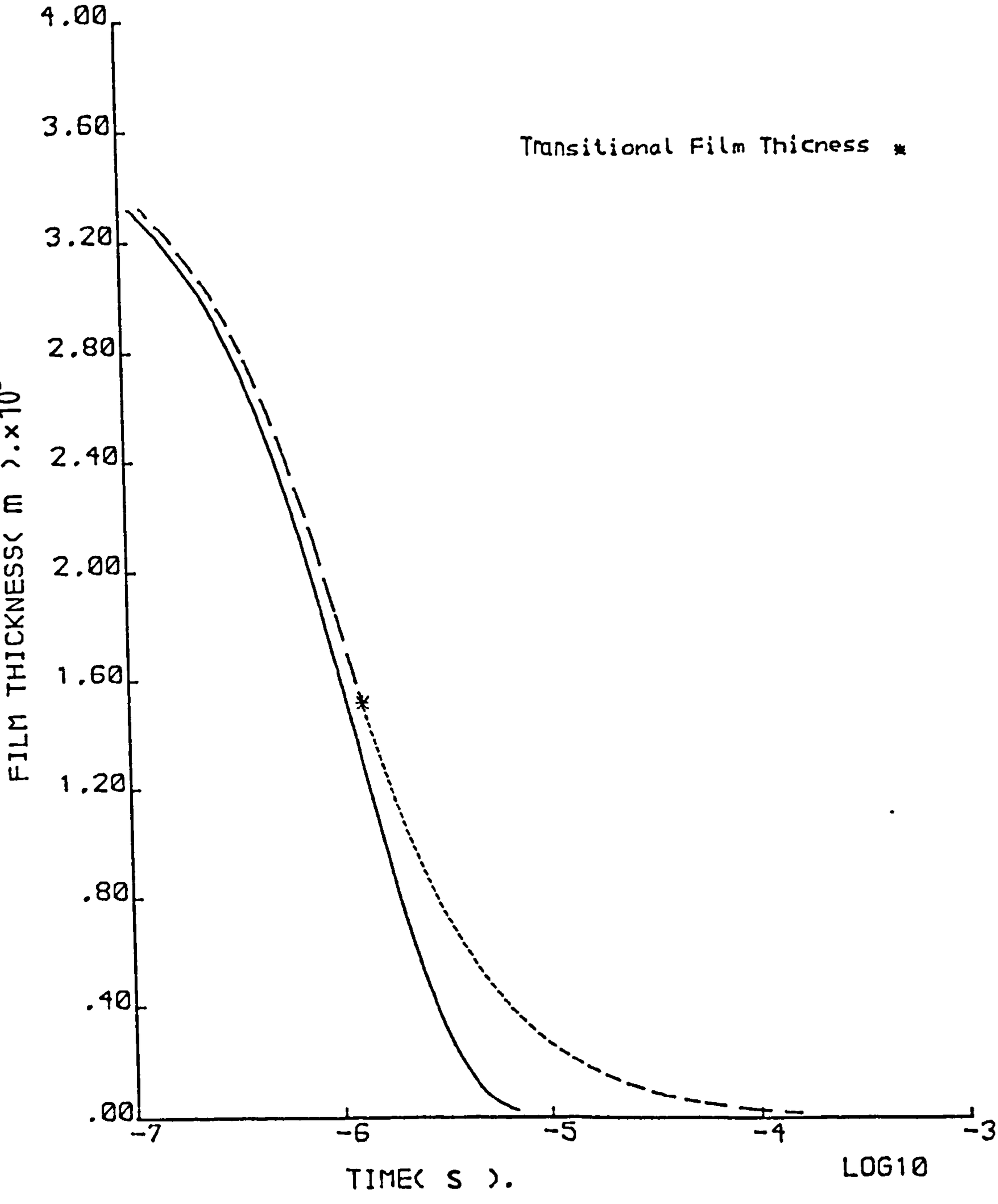

FIGURE(2 - 14) Film Thickness History For an Ellipsoid of Equivalent Radius(0.005 m) and Radius Ratio(10) Approaching a Plane Surface in the Presence of Isoviscous(————) and Piezoviscous(— — —) Fluids Under a Load of (100 N.)

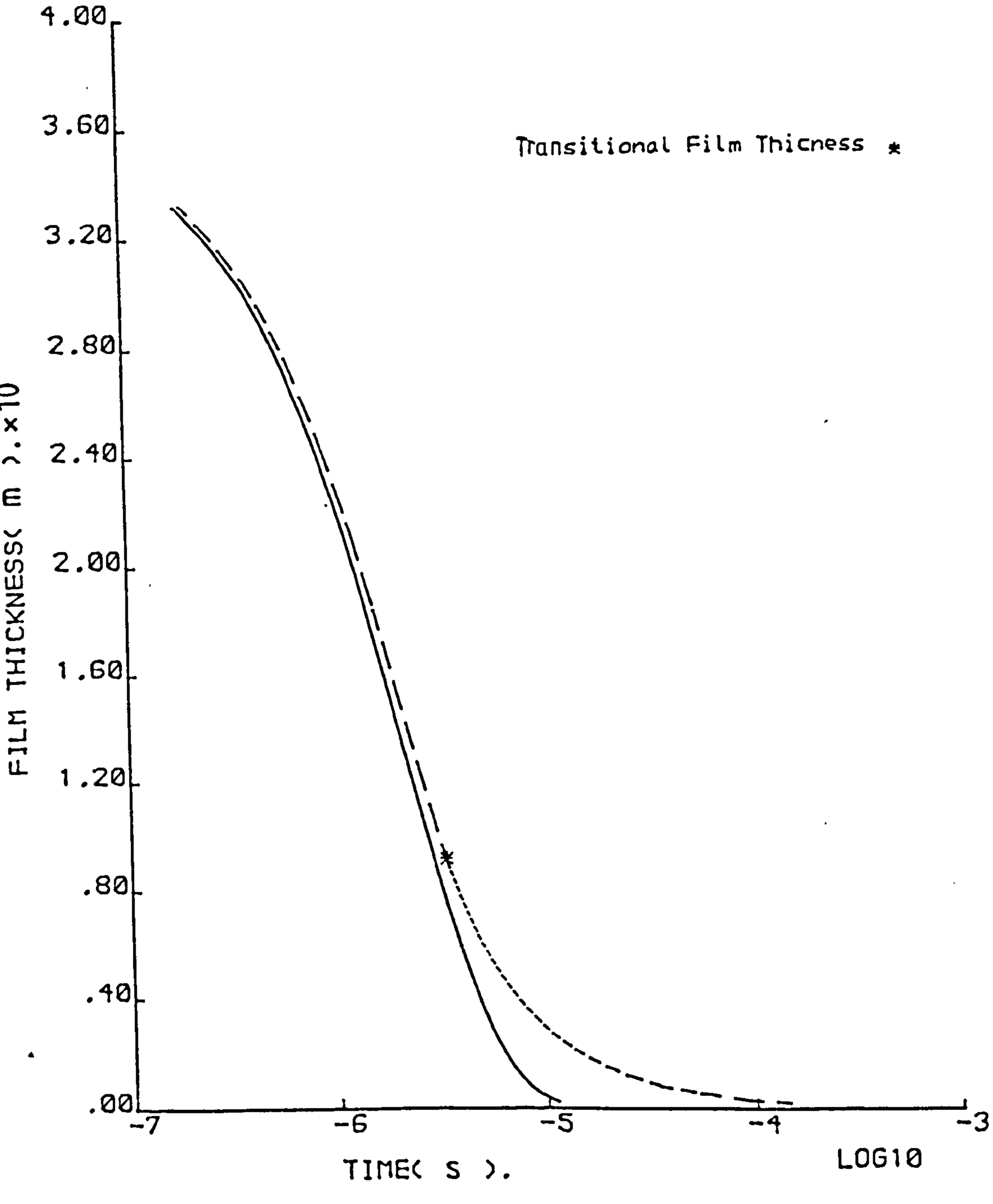

FIGURE(2 - 15) Film Thickness History For an Ellipsoid of Equivalent Radius(0.005 m) and Radius Ratio(31) Approaching a Plane Surface in the Presence of Isoviscous(————) and Piezoviscous(— — —) Fluids Under a Load of (100 N.)

radius ratio (10) and a sphere with the same equivalent radius (0.005 m) have been considered. All the data used are given in Table (2.1). The same operating conditions outlined for the ball bearing problem have been considered but for a range of loads varying from (25N) to (100 N).

Obviously, the attempt of the moving body to displace the viscous fluid covering the plane surface, during the normal approaching process, reduces the central film thickness (h_o) continuously. This fact is clear from all the figures, which show that the central film thickness (h_o) decreases with the passage of time and its decay seems to take an approximate exponential form.

At large values of (h_o), the isoviscous and piezoviscous solutions coincide and then start to deviate from each other as the central film thickness (h_o) decreases. This deviation is smaller during the initial stage of approach and becomes more pronounced in the final stages of squeeze film motion. As the applied load (F) decreases and the radius ratio (δ) increases the deviation in the initial stage decreases.

Also, it can be seen that the motion of the solid body through the isoviscous fluid is faster than that through the piezoviscous fluid. This can be noticed from (Table 2.2) and may be attributed to the larger viscous resistance of the piezoviscous fluid due to the tremendous increase of viscosity with pressure. The time taken for the same amount of reduction (Δh_o) in the film thickness, increases with an increase of (δ) at the same applied load (F) when they start from the same position (h_{o1}). A numerical example is given in Table (2.2) for an applied load (25 N) to illustrate this fact.

Table (2.1) Data used for Figure (2.7) to (2.15)

Load (F) (N)	Radius Ratio (δ) (R_x/R_y)	Equivalent Radius (R) (m)
25	1 10 31	0.005
50	1 10 31	0.005
100	1 10 31	0.005

Table (2.2) Effect of the Radius Ratio (δ) and Lubrication Condition on the Time of Approach for Load (F = 25N)

$h_{ol}^{+} \times 10^4$	$\Delta h_o^{++} \times 10^4$	$\Delta t_{(iso)} \times 10^5$ (s)			$\Delta t_{(piezo)} \times 10^5$ (s)		
		$\delta = 1$	$\delta = 10$	$\delta = 31$	$\delta = 1$	$\delta = 10$	$\delta = 31$
0.33	0.31	0.80	1.40	2.36	1.28	1.74	2.58

Table (2.3) Effect of the Load (F) on the Time of Approach for ($\delta = 10$)

δ	$h_{ol} \times 10^4$	$\Delta h_o \times 10^4$	$\Delta t_{(iso)} \times 10^5$ (s)			$\Delta t_{(piezo)} \times 10^5$ (s)		
			F=25 (N)	F=50 (N)	F=100 (N)	F=25 (N)	F=50 (N)	F=100 (N)
10	0.33	0.31	1.40	0.70	0.35	1.74	1.44	1.16

+ Starting film thickness

+ Change in film thickness

+

Similarly, increasing the load for the same radius ratio (δ) accelerates the motion for both isoviscous and piezoviscous conditions as shown in Figures (2.8), (2.11)and (2.14) for (δ=10) and given in Table (2.3).

Now consider the real example mentioned earlier. In order to generate an appreciation of the physics of the developed analysis, the time taken by a ball as it traverses the loaded region has been calculated as (1.95×10^{-2} s) using the bearing kinematics. Then, the minimum film thickness between the ball and the inner-race, under pure rolling conditions, has been calculated using the formula developed by Brewe et al (1979) for isoviscous lubrication and the formula developed by Dowson et al (1983) for the piezo-viscous lubrication. Furthermore, the time of approach (Δt) between a ball and the inner-race, to reduce the film thickness from an initial value of (5 μm) to a value equal to that for the pure rolling condition, has been determined by using the present analysis for both isoviscous and piezoviscous regime. As shown in Table (2.4), the time taken by a ball as it traverses the loaded region, in the real bearing, is greater by three orders of magnitude than the time of approach, for both the small load of (25 N) and the heavy load of (4513 N). That is to say that the squeeze-film time is much shorter than the transit time for the ball passing through the loaded region. It therefore appears that pure squeeze-film lubrication alone is not sufficient to ensure that a satisfactory lubricating film will completely separate the ball and the inner-race of the bearing at all times.

Table (2.4) Comparison Between the Transit Time for a Ball as it Traverses the Loaded Region and the Time of Approach Between a Ball and the Inner-Race of a Real Bearing (Rigid solids)

(from $h_{o(initial)} = 5 \times 10^{-6}$ (m) to $h_{o(final)}$ = minimum film for the pure rolling condition)

Parameter Calculated	Load of (25 N)	Load of (4513 N)
Minimum film thickness for pure rolling (h_o) in the presence of an isoviscous fluid, (m)	1.88×10^{-7}	5.77×10^{-12}
Limiting minimum film thickness for pure rolling (h_o) in the presence of a piezoviscous fluid, (m)	9.04×10^{-7}	9.04×10^{-7}
Transitional film thickness (h_{oT}), (m)	2.27×10^{-6}	410×10^{-6}
Time of approach (Δt) for pure squeezing action in the presence of an isoviscous fluid, (s)	2.85×10^{-5}	6.58×10^{-7}
Time of approach (Δt) for pure squeezing action in the presence of a piezoviscous fluid, (s)	2.64×10^{-5}	2.48×10^{-5}
Transit time for a ball as it traverses the loaded region in the real bearing, (s)	1.95×10^{-2}	1.95×10^{-2}

2.10 Concluding Remarks

The results presented in this chapter provide an analysis of the hydrodynamic lubrication of a rigid ellipsoid approaching a plane surface. Although the equations derived, particularly for piezoviscous conditions, involved some mathematical approximations, the theory described all the aspects of hydrodynamic lubrication with a pure squeeze action. The analysis presented is, of course, limited practically to small loads since elastic deformation of the solids has been neglected. The development of a theory which is applicable under more practical situations with heavy loads is presented later in this thesis. Nevertheless, it is instructive to consider first the simple condition of a rigid ellipsoid approaching a plane since an analytical solution has been obtained and the effect of changing various parameters can readily be investigated.

The results showed that:

1. Inclusion of the effect of pressure on viscosity enhances the dimensionless hydrodynamic load ($\bar{F}$). The load supported by an ellipsoidal solid is always greater than that supported by a sphere at the same central film thickness.

2. The hydrodynamic lubrication behaviour under piezoviscous conditions is characterized by the dimensionless velocity of approach ($\bar{\omega}$). Once ($\bar{\omega}$) attains its limiting value of $\left(\frac{1}{6}\right)$, an infinite pressure can be obtained at a finite film thickness, called the transitional film thickness $\left(h_{oT} = \frac{F.\alpha}{4\pi R \ln 2} \frac{\sqrt{\delta}}{(1+\delta)}\right)$, by the application of a finite load. Also, the dimensionless load ($\bar{F}$) has the limiting value of $\left(\bar{F}_T = 24\pi \frac{(1+\delta)}{\sqrt{\delta}} \ln 2\right)$.

3. The squeeze process under piezoviscous conditions with a constant applied load (F) may be divided into two distinct stages. Firstly, the initial stage where the dimensionless velocity ($\bar{\omega}$) is less than its limiting value of $\left(\frac{1}{6}\right)$ and secondly the final stage where the central pressure tends to infinity and the motion becomes independent of the applied load (F).

4. The general expressions derived for an ellipsoid and a plane reduce to the typical expressions of a sphere and a plane when the radius ratio ($\delta = 1$). However, the expressions do not approach the solutions of the infinitely long cylinder and a plane except in the case of alternative expressions for an ellipsoidal solid with finite width (L) in the (y) direction. This cannot be done because of the cumbersome calculations of the resulting integrals in the rectangular coordinate system.

5. Pure squeeze-film lubrication alone is not sufficient to provide a continuous film of lubricant to separate the ball and the inner-race in the ball bearing example considered.

CHAPTER 3

MATHEMATICAL FORMULATION OF THE ELASTOHYDRODYNAMIC LUBRICATION ANALYSIS OF TWO ROTATING CYLINDERS IN NORMAL APPROACH

3.1 Introduction

The analysis of the fluid film lubrication of machine elements such as rolling element bearings, gears and cams and tappets reveals that their lubricated contacts involve a normal motion (squeeze effect) during operation. However, conventional elastohydrodynamic lubrication theory has treated the vast majority of line contact lubrication problems either by considering steady-state conditions, i.e., pure rolling, sliding and rolling with sliding, or the non-steady state condition of pure squeeze film action.

Many investigations have drawn attention to the vital role played by the squeeze film action in preserving the lubricating film, in many cases when the entraining velocity, which is responsible for hydrodynamic film formation in steady-state conditions, falls to zero at some stage in the cycle, as in synovial joints and reciprocating mechanisms. Nevertheless, the effect of superimposing a normal motion upon a steady state 'entraining' action has received little attention. The lubrication of lightly loaded cylinders under combined entraining and normal motion has been studied analytically and experimentally, e.g., (Dowson, et al (1976)) and (Vichard (1971). These authors dealt with rigid cylinders neglecting the elastic deformation of the bearing surfaces. This hypothesis is not reasonable in the practical lubrication situations of heavily loaded contacts where the condition is quite severe because of the high pressure generated. This high pressure can lead to substantial local elastic deformation of the elastic solids bounding the conjunction and a marked effect upon the viscosity of liquid lubricants.

In this chapter a complete mathematical formulation of the elastohydrodynamic lubrication problem of line contacts is presented taking into account the effect of squeeze film action on the lubrication behaviour and the influence of pressure on the physical properties of the lubricant.

3.2 Geometry

Considering the pair of infinitely long cylinders shown in Figure (3.1(a)), the geometry of the contact in the important region near to the centre of conjunction can be replaced, as has been demonstrated in Chapter (2), by an equivalent cylinder of radius (R) near a plane as shown in Figure (3.1(b)). The rigid geometrical separation (h_g) between the equivalent cylinder and the plane, when the separation in the centre of the contact is (h'_o), may be written as,

$$h_g = h'_o + S(x) \tag{3.1}$$

where,

S(x) is the local separation at a position (x). For this particular problem, this local separation may be determined by using equation (2.6) and (2.7) with equation (2.12) as,

$$S(x) = \frac{x^2}{2R} \tag{3.2}$$

Hence equation (3.1) takes the following form,

$$h_g = h'_o + \frac{x^2}{2R} \tag{3.3}$$

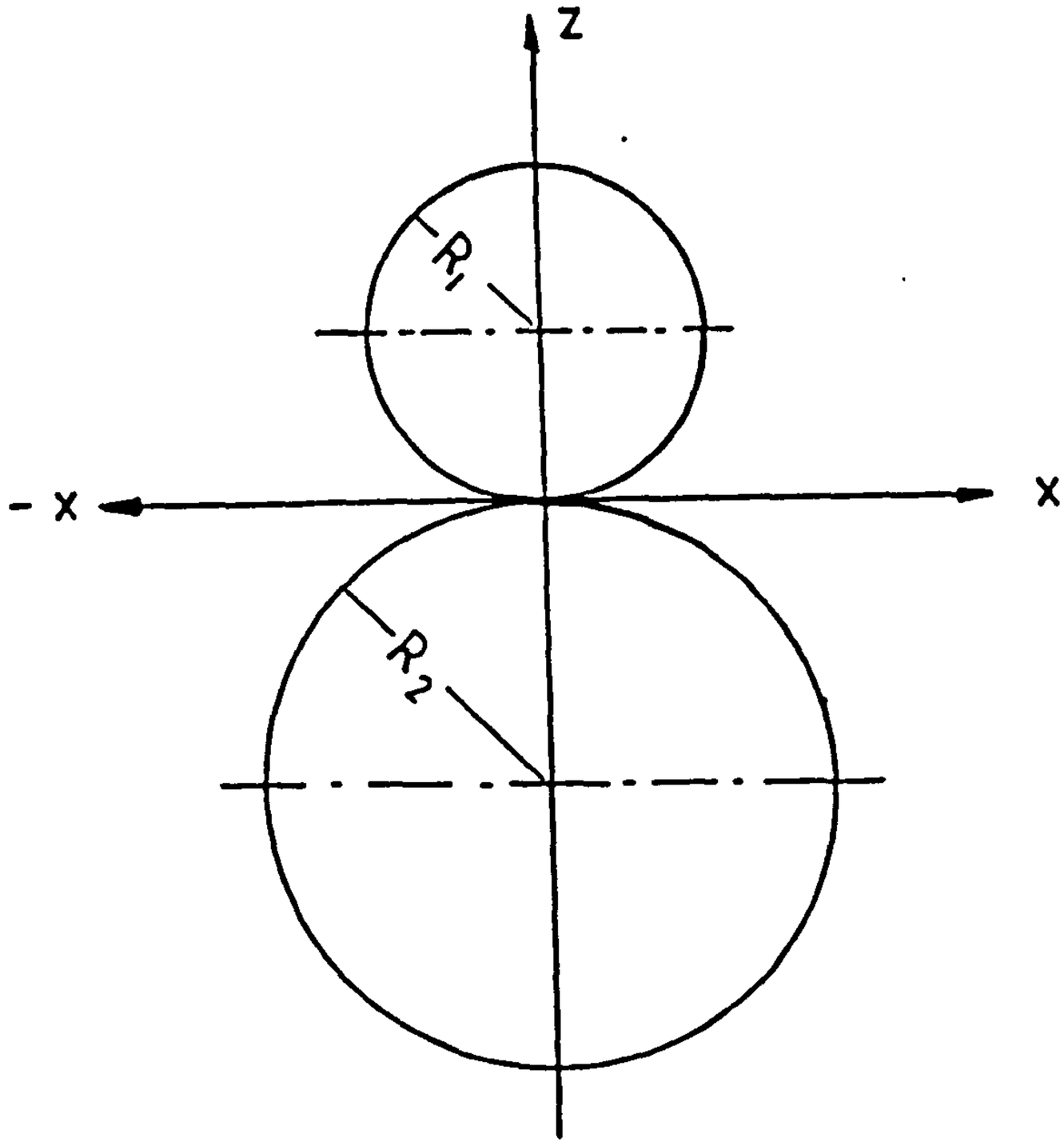

(a) Contact Between Two Undeformed Cylinders

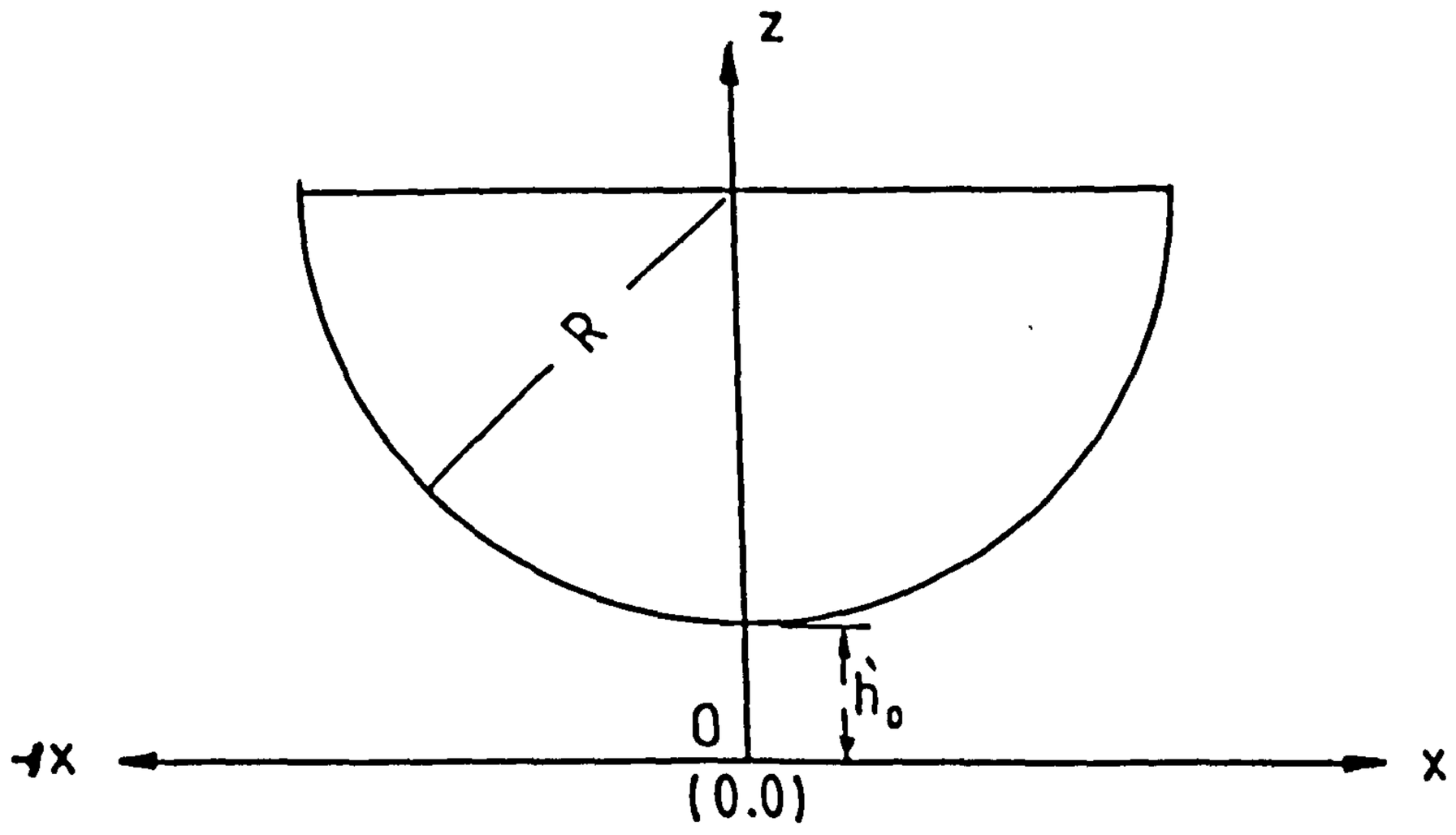

(b) Equivalent Cylindrical Solid Near a Plane

FIGURE (3 - 1) Geometry of Line Contacts

3.3 Elasticity Equation

In practice, bearing surfaces subjected to heavy loads are deformed elastically. In typical conditions for a nominal line contact, the contact region is very small compared with the radius and length of the cylinders. Hence the displacement is a state of plane strain uniform along the length, except near the ends. Furthermore tangential displacements can be neglected because they do not have significant effects on the lubricated contact. The normal displacement produced by the pressure generated in the fluid film is calculated for a semi-infinite plane and then added to the rigid geometrical separation of the equivalent cylinder.

Considering Figure (3.2(a)) and the corresponding coordinate system, the elastic deformation at a point (g) at a distance (x) from the origin on the surface of a semi-infinite solid subjected to a strip of non-uniform pressure p(s) between ($s=s_1$) and ($s=-s_1$) can be written as (see Dowson and Higginson (1977));

$$\delta(x) = -\frac{(1-\sigma^2)}{\pi E}\int_{-s_1}^{s} p(s)\ln(x-s)^2\,ds + C \qquad (3.4)$$

where,

(E) and (σ) are the modulus of elasticity and Poisson's ratio of the solid respectively. The constant (C) is eliminated by including it in the central film thickness (h_o). Thus the displacement is not an absolute, but a relative quantity.

In order to remove the singularity from the integral of equation (3.4) at (s=x) and to calculate the elastic deformation at

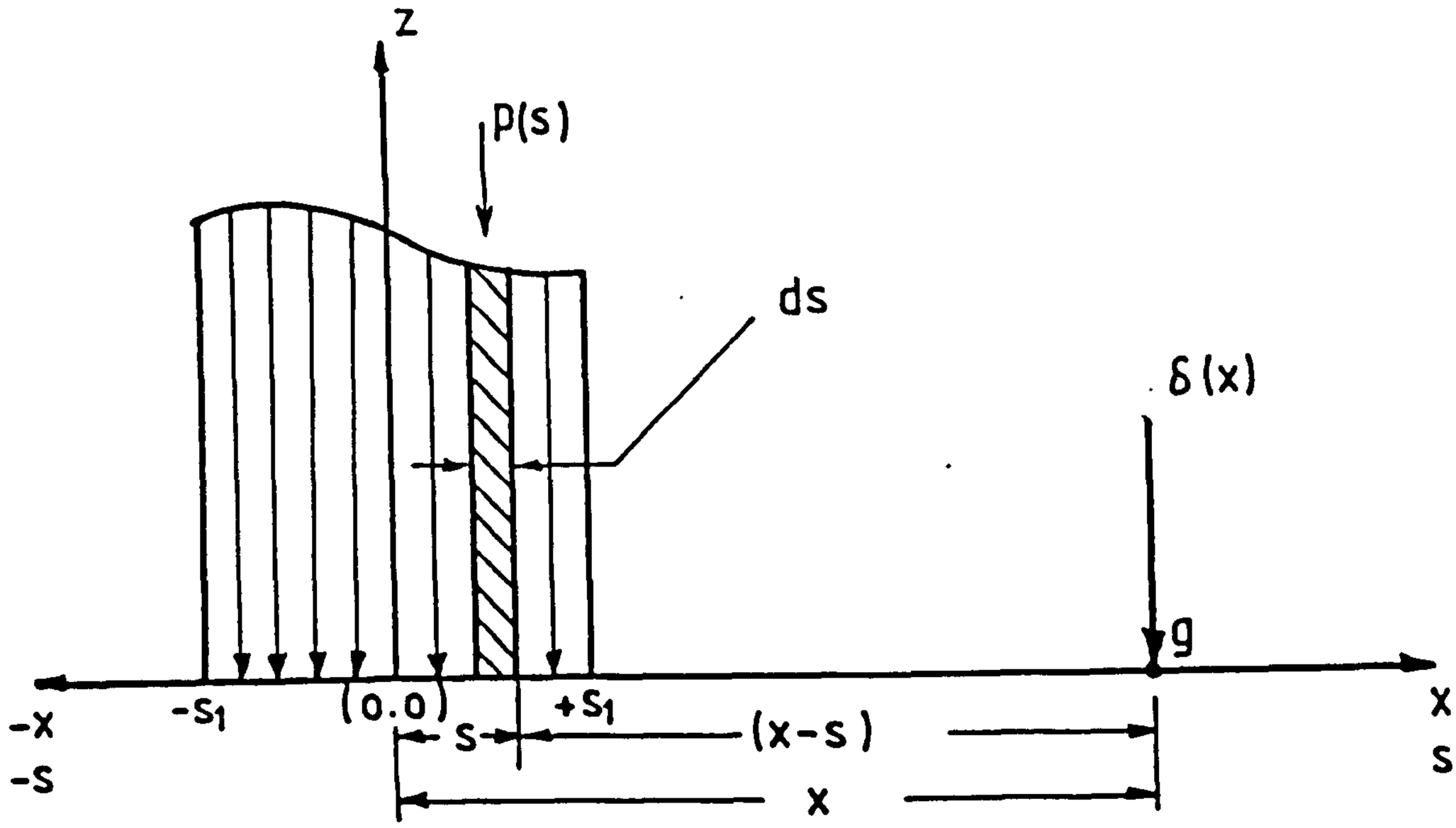

(a) Analysis of the Surface Deformation of a Semi-infinite Solid Subjected to a Non-uniform Pressure Over a Rectangular Area

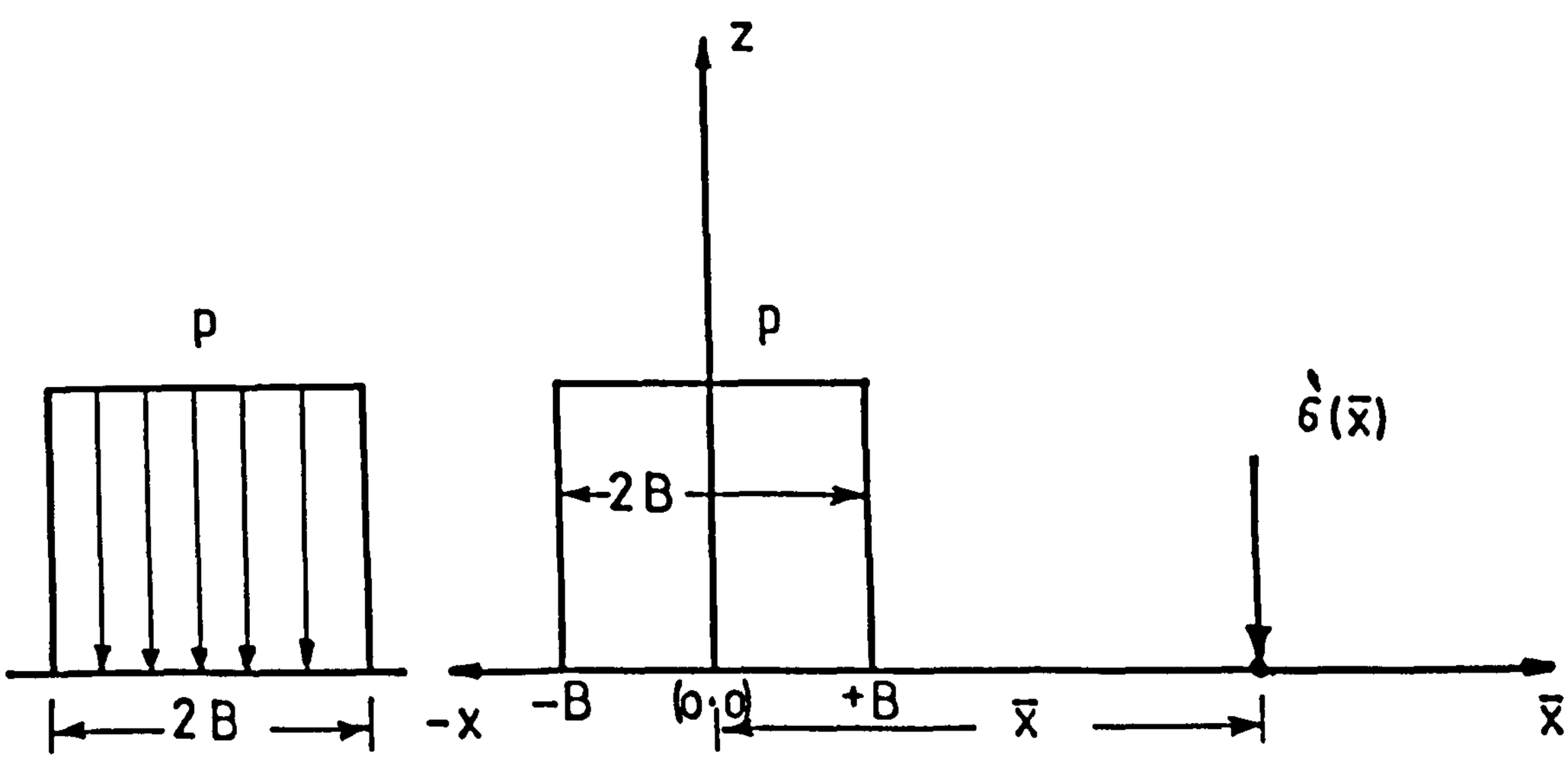

(b) Analysis of the Surface Deformation of a Semi-infinite Solid Subjected to a Uniform Pressure Over a Rectangular Area

FIGURE(3-2) Analysis of the Surface Deformation of a Semi-infinite Solid

any location in the contact field, the method developed by Hamrock and Dowson (1976a) was used. In this method the contact region was divided into a number of rectangular areas of uniform pressure (p). The elastic deformation due to the influence of one element of these rectangular areas at a location ($\bar{x}$) from the centre of the element as shown in Figure (3.2(b)) is,

$$\delta'(\bar{x}) = -\frac{2p}{\pi E}\int_{-B}^{+B} \ln(\bar{x}-s)^2\, ds + \text{constant} \qquad (3.5)$$

or,

$$\delta'(\bar{x}) = \frac{2p}{\pi E}\left[(\bar{x}-B)\ln(\bar{x}-B)^2 - (\bar{x}+B)\ln(\bar{x}+B)^2 + 4B\right] + \text{constant} \qquad (3.6)$$

The total elastic deformation at any location in the calculation field may then be determined by summing the contributions of the various rectangular areas of uniform pressure over the whole region.

3.4 Film Thickness Equation

The instantaneous film thickness (h) between two lubricated cylinders is the sum of the rigid geometrical separation (h_g) and the elastic deformation (δ) of the two cylinders.

$$h = h_o' + \frac{x^2}{2R_1} + \frac{x^2}{2R_2} + \delta_1(x) + \delta_2(x) \qquad (3.7)$$

Otherwise,

$$h = h_o' + \frac{x^2}{2R_1} + \frac{x^2}{2R_2} - \frac{(1-\sigma_1^2)}{\pi E_1}\int_{-\infty}^{+\infty} p(s)\ln(x-s)^2\, ds$$

$$- \frac{(1-\sigma_2^2)}{\pi E_2} \int_{-\infty}^{+\infty} p(s) \ln (x-s)^2 \, ds + C_1 + C_2 \qquad (3.8)$$

According to the equivalent system shown in Figure (3.3), the film shape can be written in terms of the local relative deflection (d(x)) as,

$$h = h_o' + \frac{x^2}{2R} - d(x) + C \qquad (3.9)$$

or,

$$h = h_o' + \frac{x^2}{2R} - \frac{2}{\pi E'} \int_{-\infty}^{+\infty} p(s) \ln (x-s)^2 \, ds + C \qquad (3.10)$$

where,

(E') is the effective elastic modulus $\left[\frac{2}{\left(\frac{1-\sigma_1^2}{E_1}\right) + \left(\frac{1-\sigma_2^2}{E_2}\right)}\right]$

using equation (3.10), the film thickness at the centre of the conjunction, is,

$$h_o = h_o' - \frac{2}{\pi E'} \int_{-\infty}^{+\infty} p(s) \ln (s)^2 \, ds + C \qquad (3.11)$$

Eliminating the constant of integration (C) between equation (3.10) and (3.11) yields,

$$h = h_o + \frac{x^2}{2R} - \frac{2}{\pi E'} \int_{-\infty}^{+\infty} p(s) \ln \left(\frac{x-s}{s}\right)^2 \, ds \qquad (3.12)$$

or, the general film shape can be written simply as,

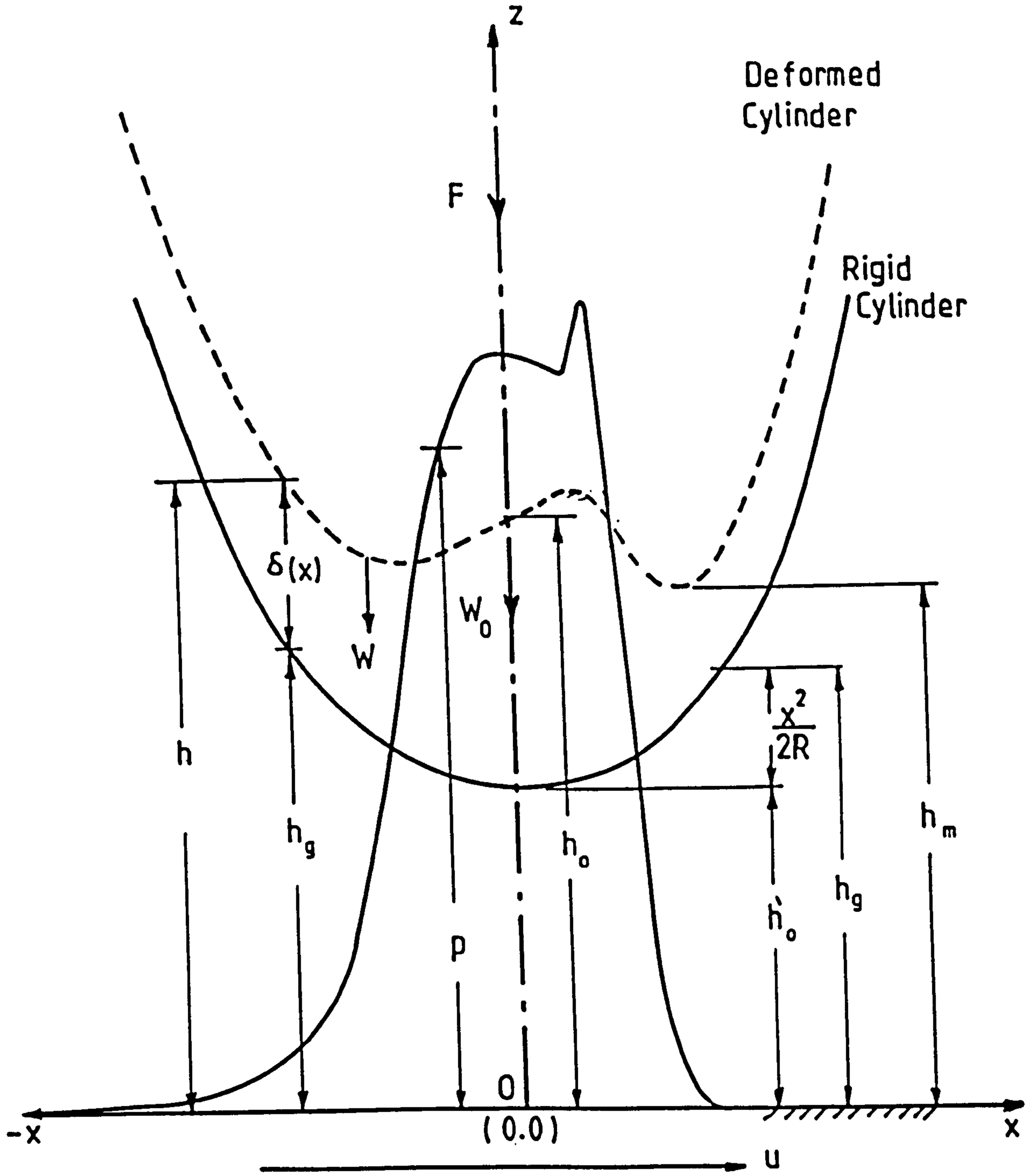

FIGURE(3 - 3) Pressure Distribution and Film Shape for a Line Contact Under Combined Squeeze Film and Rolling Action.

$$h = h_o + \frac{x^2}{2R} + (d_o - d(x)) \qquad (3.13)$$

where,

(d_o) is the relative deflection $(\delta_o - C)$ at the centre of the contact and $d(x)$ is the relative deflection $(\delta - C)$ at the location (x).

3.5 Hydrodynamic Equation

The variation of lubricant pressure in a lubricated conjunction is determined by the Reynolds' equation (2.27), which was derived and fully presented in Chapter (2). For the line contact problem under consideration side-leakage effects are neglected. Therefore equation (2.27) may be reduced to yield the transient one-dimensional Reynolds' equation governing pressure generation and its variation used in the present study.

The governing equation for pressure distribution is,

$$\frac{\partial}{\partial x}\left[\frac{\rho h^3}{\eta}\frac{\partial p}{\partial x}\right] = 12u\frac{\partial}{\partial x}(\rho h) + 12\frac{\partial}{\partial t}(\rho h) \qquad (3.14)$$

Because of the presence of the term $\left[\frac{\partial}{\partial t}(\rho h)\right]$ a coupling exists between the time and space coordinates which greatly adds to the computational difficulties. A simple alternative form which leads to a great advantage of the direct interaction of the velocity of approach of the contact centre (W_o) and the applied load (F) in the calculations can be obtained by using the relation,

$$\frac{\partial}{\partial t}(\rho h) = \frac{\partial h_o}{\partial t}\frac{\partial}{\partial h_o}(\rho h) \qquad (3.15)$$

or,

$$\frac{\partial}{\partial t}(\rho h) = -W_o \frac{\partial}{\partial h_o}(\rho h) \qquad (3.16)$$

where,

$$W_o = -\frac{\partial h_o}{\partial t} \qquad (3.17)$$

considering the relationship (3.16), the Reynolds' equation (3.14) becomes,

$$\frac{\partial}{\partial x}\left[\frac{\rho h^3}{\eta}\frac{\partial p}{\partial x}\right] = 12u\frac{\partial}{\partial x}(\rho h) - 12 W_o \frac{\partial}{\partial h_o}(\rho h) \qquad (3.18)$$

where the mean entraining velocity (u) is given by,

$$u = \frac{u_1 + u_2}{2}$$

and (W_o) is the approach velocity of the contact centre $\left(-\frac{\partial h_o}{\partial t}\right)$.

3.6 Load Equation

If the mass of the cylinder is neglected the instantaneous normal applied load per unit width (F) acting on the cylinder is the integral of the pressure distribution generated throughout the fluid film,

$$F = \int_{-\infty}^{+\infty} p\,dx \qquad (3.19)$$

3.7 Velocity of Approach $\left(W = -\frac{\partial h}{\partial t}\right)$

Figure (3.4) details the normal motion of a rigid cylindrical body approaching an elastic semi-infinite lubricated

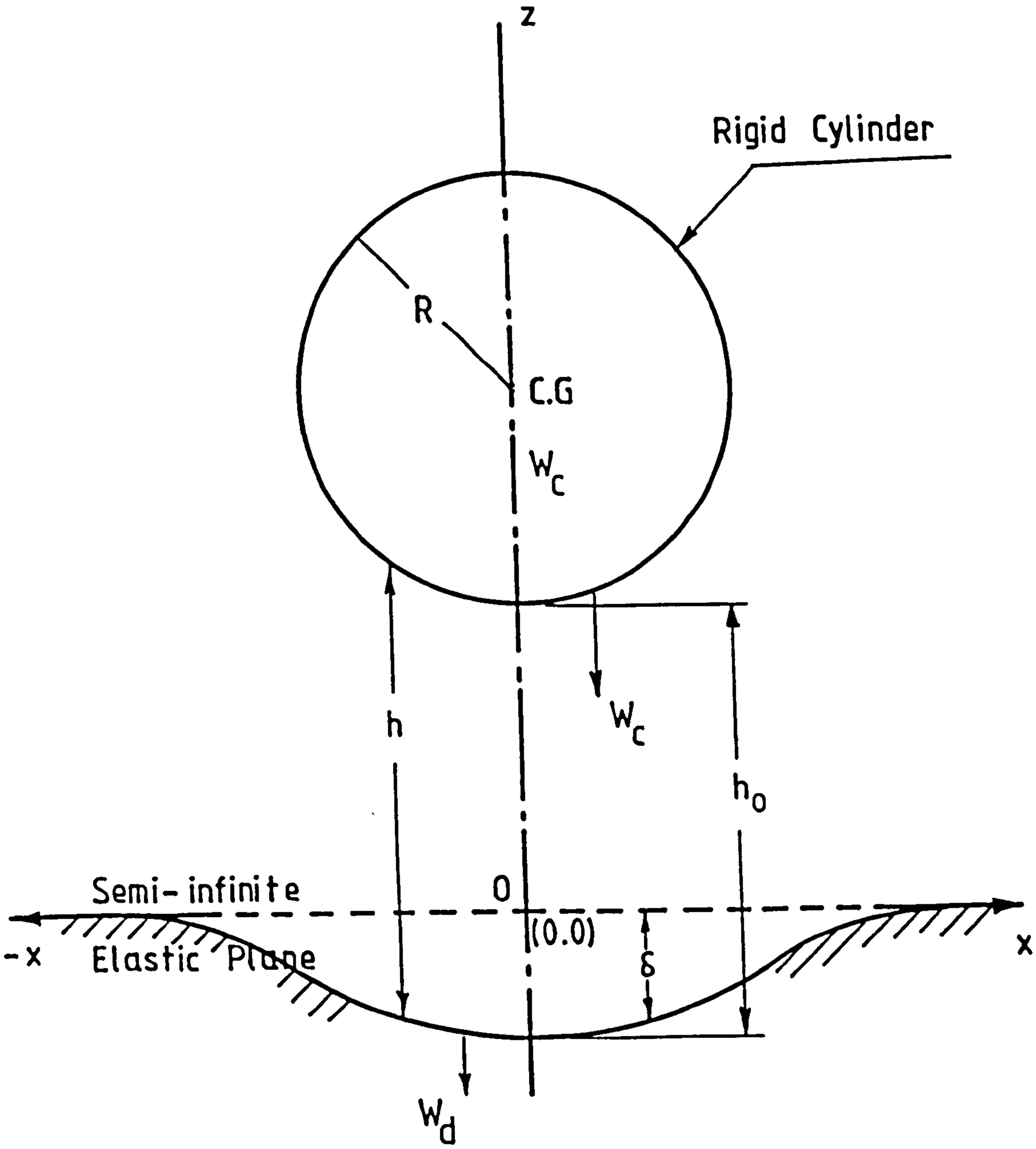

FIGURE (3 - 4) Normal Approach of a Rigid Cylinder Towards a Lubricated Semi-infinite Elastic Plane

plane. For convenience, although the presentation is given in terms of a rigid cylinder approaching an elastic plane, for the sake of simplicity, it is realized that the theory is valid for the inverse case of an elastic cylinder with the same modulus of elasticity approaching a rigid plane. The relative velocity (W) between the body and plane surfaces is a resultant of two components: the first is the absolute velocity of the gravitational centre of the body and the second is the velocity of the plane surface due to elastic deformation. In accordance with the usual assumptions made in lubrication theory, it is the relative position and motion of the surfaces that are of importance.

Differentiating the film thickness equation (3.13) with respect to time (t) gives,

$$\frac{\partial h}{\partial t} = \frac{\partial h_o}{\partial t} + \frac{\partial}{\partial t} (d_o - d(x)) \qquad (3.20)$$

Let,

$$W = - \frac{\partial h}{\partial t}, \; W_o = - \frac{\partial h_o}{\partial t} \text{ and } W_d = \frac{\partial}{\partial t} (d_o - d(x))$$

Now, equation (3.20) becomes,

$$- W = - W_o + W_d \qquad (3.21)$$

It is thus seen that the relative velocity of approach (W) consists of two terms. The first, the approach velocity of the centre of the contact is a function of time alone, while the second term is the deformation velocity (W_d) which is a function of time (t) and location (x). If, however, this latter variation is small within the important contact region, the approach velocity distribution can be assumed to be uniform along the surface.

is it?

So $\dot{d}_o = \dot{d}(x)$

3.8 Pressure - Viscosity Relationship

The Roelands (1966) formula describing the variation of viscosity with pressure, for isothermal conditions, has been used in the present analysis. This is,

$$\bar{\eta} = \frac{\eta}{\eta_o} = \left[\frac{\eta_\infty}{\eta_o}\right]^{\left[1 - \left(1 + \frac{p}{c}\right)^{0.67}\right]} \qquad (3.22)$$

where,

$$\eta_\infty = 6.31 \times 10^{-5} \quad \text{pas}$$

$$c = 1.96 \times 10^{8} \quad \text{pa}$$

This formula was introduced by Roelands after extensive investigations of the effect of pressure on the viscosity of lubricants. It gives more reliable results than can be obtained by the (Barus (1893)) formula, particularly at high pressures.

3.9 Pressure - Density Relationship

In elastohydrodynamic lubrication very high pressures exist, and the liquid can no longer be considered as an incompressible medium. From Dowson and Higginson (1977) the density function for mineral oil may be written as,

$$\bar{\rho} = \frac{\rho}{\rho_o} = 1 + \frac{0.58p}{1+1.68p} \qquad (3.23)$$

where (p) is the gauge pressure in GPa. It may be noted that the variation of density with pressure is almost linear at low pressures, but the rate of increase falls away at high pressures.

Also, for mineral oils the maximum increase expected in density is around thirty three percent.

3.10 Generalization of the Problem

i) Dimensionless Parameters

It is convenient to use dimensionless variables so that results may be discussed in more general terms. The equations presented before can be normalized by introducing the following non-dimensional parameters,

$$H = \frac{h}{R}, \quad X = \frac{x}{b}, \qquad \bar{\eta} = \frac{\eta}{\eta_o}$$

$$\bar{\rho} = \frac{\rho}{\rho_o}, \quad P = \frac{p}{E'}, \qquad U = \frac{u\eta_o}{RE'}$$

$$\bar{F} = \frac{F}{RE'}$$

where,

(U) and ($\bar{F}$) are the speed and load parameters respectively.

ii) Normalized Film Thickness Equation

The non-dimensional film thickness shape can be written as,

$$H = H_o + \left(\frac{b}{R}\right)^2 \frac{X^2}{2} + \frac{1}{R}\left[d_o - d(X)\right] \qquad (3.24)$$

Likewise, the normalized form of equation (3.6), which represents the deformation resulting from the influence of one element of the

rectangular areas of uniform pressure at a location ($\bar{X}$) from the element centre, can be expressed as,

$$\delta'(\bar{X}) = \frac{2Pb}{\pi}\left[(\bar{X}-\bar{B})\ \ln\ (\bar{X}-\bar{B})^2 - (\bar{X}+\bar{B})\ \ln\ (\bar{X}+\bar{B})^2 + 4\bar{B}\ (1-\ln\ b)\right] + \text{constant} \tag{3.25}$$

iii) Normalized Reynolds' Equation

Inserting the previous dimensionless parameters into equation (3.18), the normalized, transient, one-dimensional Reynolds' equation is,

$$\frac{\partial}{X}\left[\frac{\bar{\rho}\bar{H}^3}{\bar{\eta}}\ \frac{\partial P}{\partial X}\right] = 12U\ \left(\frac{b}{R}\right)\ \frac{\partial}{\partial X}\left(\bar{\rho}\bar{H}\right) - 12\left(\frac{b}{R}\right)^2\ \frac{\eta_o W_o}{E' R}\ \frac{\partial}{\partial H_o}\ (\bar{\rho}\bar{H}) \tag{3.26}$$

(iv) Normalized Load Equation

The dimensionless load equation is,

$$\frac{F}{E' b} = \int_{-\infty}^{+\infty} P dX \tag{3.27}$$

3.11 Phi (ϕ) Solution

The numerical solution suggested later, particularly with the relaxation method, becomes more accurate and efficient when the pressure distribution (P) of the Reynolds' equation (3.26) exhibits small gradients over the calculation field. In order to produce a

much gentler curve, the Vogelpohl parameter (ϕ) adopted by Hamrock (1976) was used, where,

$$\phi = PH^{3/2} \tag{3.28}$$

The dimensionless pressure (P) is smaller at large values of film thickness (H) and large when the film thickness is small. Hence, the parameter (ϕ) varies more gradually than the real variable (P) over the calculation field.

Partially differentiating equation (3.28) with respect to (X), the following is obtained,

$$\frac{\partial \phi}{\partial X} = H^{3/2} \frac{\partial P}{\partial X} + \frac{3}{2}\sqrt{H}\, P \frac{\partial H}{\partial X}$$

Arranging,

$$H^3 \frac{\partial P}{\partial X} = H^{3/2} \frac{\partial \phi}{\partial X} - \frac{3}{2}\sqrt{H} \frac{\partial H}{\partial X} \phi \tag{3.29}$$

Substituting equation (3.29) into equation (3.26) gives,

$$H^{3/2} \frac{\partial}{\partial X}\left[\frac{\bar{\rho}}{\bar{\eta}} \frac{\partial \phi}{\partial X}\right] - \frac{3}{2} \phi \frac{\partial}{\partial X}\left[\frac{\bar{\rho}\sqrt{H}}{\bar{\eta}} \frac{\partial H}{\partial X}\right]$$

$$= 12U\left(\frac{b}{R}\right) \frac{\partial}{\partial X}(\bar{\rho}H) - 12\left(\frac{b}{R}\right)^2 \frac{W_o \eta_o}{E' R} \frac{\partial}{\partial H_o}(\bar{\rho}H) \tag{3.30}$$

Equation (3.30) is solved numerically to obtain the distribution of the parameter (ϕ). The actual dimensionless pressure (P) can then be determined by the substitution of the corresponding film thickness distribution (H) in the relationship (3.28).

3.12 Boundary Conditions

The gap configuration between a cylindrical body and plane

surface is such that the lubricant supplied to the conjunction passes into a converging portion, building up pressure, followed by a diverging portion before ambient pressure is achieved. This implies that in the absence of cavitation or film rupture the pressure drops below the ambient pressure. In the vast majority of cases the liquid is unable to sustain these sub-ambient pressure which leads to disruption of the lubricating film by cavitation. The usual form of cavitation in lubricating films is the ventilation of air from the surrounding atmosphere whenever sub-ambient pressures occur. Moreover, gas cavities may arise from the liberation of dissolved gases contained in the oil as the liquid pressure falls below the saturation pressure. This phenomenon has received considerable attention, (Dowson and Taylor (1979)). Experimental measurements indicate that the lubricant pressure falls to ambient or the saturation pressure of the dissolved air soon after leaving the convergent region and the film is seen to be composed of alternate fingers of liquid and air. The saturation pressure of the air dissolved in the lubricant will be very close to atmospheric pressure.

The boundary conditions usually applied to Reynolds' equation are (P=0) around the boundary. However, whenever cavitation occurs in the fluid film the Reynolds boundary conditions ($P = \frac{\partial P}{\partial X} = 0$) are introduced to satisfy the flow continuity condition at the inception of the cavitation region, namely that the pressure gradient normal to the cavitation boundary must be zero.

Generally the type of the problem specifies the required boundary conditions. Therefore, in the present study the following alternative conditions were considered.

i) Boundary Conditions for the Pure Normal Approach Problem

No cavitation is expected and the pressure and film thickness distribution are symmetric around the contact centre. The boundary conditions are,

$$\left.\begin{aligned} P = \phi = 0 \quad &\text{at} \quad X = +\infty \\ P = \phi = 0 \quad &\text{at} \quad X = -\infty \end{aligned}\right\} \tag{3.31}$$

It should be noted that a separation condition is not considered because the present analysis deals with positive externally applied loads only.

ii) Boundary Conditions for Combined Rolling and Normal Motion

Cavitation is normally expected in this case in the outlet region. Hence, the location of the outlet boundary cannot be specified initially, but emerges from the application of the Reynolds' boundary condition $\left(P(X_e) = \left(\frac{\partial P}{\partial X}\right)_{X=X_e} = 0 \right)$. The location of the inlet boundary (X_{in}) has little influence on the pressure distribution and may be chosen at a position far enough from the centre of contact to avoid starvation effects. That is,

$$\left.\begin{aligned} P = \phi = 0 \quad &\text{at} \quad X = X_{in} = -\infty \\ \left.\begin{aligned} P &= \frac{\partial P}{\partial X} = 0 \\ \phi &= \frac{\partial \phi}{\partial X} = 0 \end{aligned}\right\} \quad &\text{at} \quad X = X_e \end{aligned}\right\} \tag{3.32}$$

3.13 Concluding Remarks

In this chapter the equations governing an analysis of the effect of normal motion on the behaviour of isothermal elastohydrodynamic lubrication of line contacts has been formulated. From a theoretical viewpoint the generalized equations concerned with the problem have been introduced, these being; the Reynolds' equation taking into account transient effects; the elasticity equation to calculate the surface deformation; the film thickness equation and the load equation. The corresponding boundary conditions for different types of problem have been discussed and the possibility of cavitation has been recognized by the adoption of the Reynolds' boundary condition.

CHAPTER 4

A NUMERICAL PROCEDURE FOR THE ANALYSIS OF A NON-STEADY ELASTOHYDRODYNAMIC LINE CONTACT

4.1 Introduction

In the elastohydrodynamic lubrication regime, it is necessary to obtain a solution satisfying the Reynolds and elasticity equations simultaneously. The equations constituting this particular type of lubrication problem represents a non-linear integral-differential system which is very complicated and a full analytical solution has not yet been found. Furthermore, the inclusion of the squeeze effect in the analysis of the lubrication behaviour entails the solution of the elastohydrodynamic system of equations at time intervals which add tremendous difficulties to the problem.

A procedure for the numerical solution of the complete isothermal transient elastohydrodynamic lubrication problem of line contacts, under the application of constant and variable loads, is presented in this chapter. This procedure calls for the simultaneous solution of the elasticity, Reynolds and load equations at successive time steps. In the elasticity analysis the conjunction is divided into irregular areas with uniform pressure. In the numerical analysis of the Reynolds' equation an under-relaxation of the resulting pressure in each iteration process is used to aid the convergence.

This method is simple and efficient, but is only effective for cases of moderate loads. As the load increases and the film thickness decreases, the convergence rate becomes progressively worse.

4.2 Elastic Deformation Calculation

The next task is to calculate the elastic deformation that occurs within the surrounding solids due to the action of the high pressure generated through the fluid film. In the present analysis it is convenient to consider the deformation of an equivalent elastic half-space subjected to the assumed pressure distribution.

The contact zone, shown in Figure (4.1), is divided into irregular rectangular areas. The pressure (P) applied over each area is assumed uniform. According to equation (3.25) the relative elastic deformation at a point ($\bar{X}$) due to a rectangular area of uniform pressure (P) and width ($2\bar{B}$) can be written as,

$$d'(\bar{X}) = \frac{2b}{\pi} \quad PD \tag{4.1}$$

where,

$$D = \left[(\bar{X}-\bar{B}) \ln (\bar{X}-\bar{B})^2 - (\bar{X}+\bar{B}) \ln (\bar{X}+\bar{B})^2 + 4\bar{B} (1-\ln b)\right]$$

By taking into account the coordinate system shown in Figure (4.1), the total relative elastic deformation at a point (X) due to the contributions of the various rectangular areas of uniform pressure in the contact zone can be evaluated numerically as follows,

$$d_i(X) = \frac{2b}{\pi} \sum_{j=1,2,3}^{N} P_j D_j \tag{4.2}$$

where,

$$D_j = \left[(\bar{X}-\bar{B}) \ln (\bar{X}-\bar{B})^2 - (\bar{X}+\bar{B}) \ln (\bar{X}+\bar{B})^2 + 4\bar{B} (1 - \ln b)\right]$$

and,

$$\bar{X} = \left| X_i - X_j \right|$$

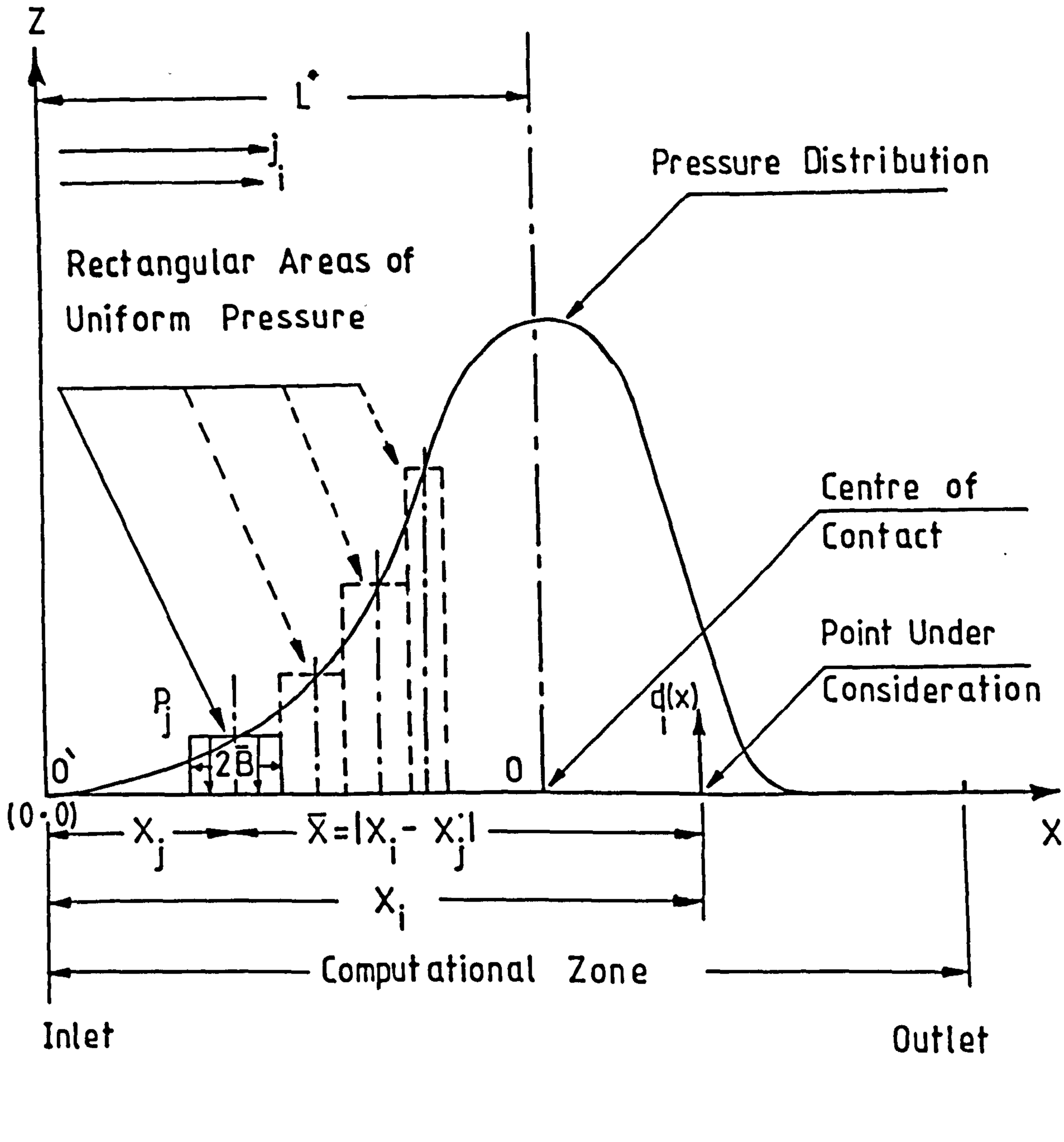

FIGURE(4-1) Numerical Calculations of The Elastic Deformation

An adequate prediction of the relative elastic deformation d(X) depends on the suitable representation of the normal pressure distribution by rectangular blocks of uniform pressure (P).

In order to check the accuracy of this method a Hertzian contact stress distribution, related to a specific load (F), was assumed. In this condition the semi-infinite elastic plane is deformed as shown in Figure (4.2). The difference (Δd) between the maximum deflection (δ_o) at the contact centre and the deflection (δ) at the edge of the Hertzian contact area was determined numerically. An excellent agreement, as shown in Table (4.1), was obtained when the results for different loads were compared with the following analytical formula,

$$\Delta d = R \left[1 - \sqrt{1 - \left[\frac{b}{R}\right]^2}\right] \qquad (4.3)$$

Or, by using the parabolic approximation,

$$\Delta d \cong \frac{b^2}{2R} \qquad (4.4)$$

where

$$\Delta d = d_o - d$$

$$= \delta_o - \delta$$

and (b) is the semiwidth of the Hertzian contact zone, $\sqrt{\frac{8FR}{\pi E'}}$

4.3 Film Thickness Calculation

By making use of equation (3.24) with the coordinate system developed in Figure (4.1), the film thickness equation can be written as,

$$H = H_o + \left[\frac{b}{R}\right]^2 \frac{(X-L^*)}{2} + \frac{1}{R}(d_o - d(X)) \qquad (4.5)$$

Table (4.1) Accuracy of the Elastic Deformation Calculations

$E' = 2.3 \times 10^{11}$ N/m^2 $\sigma = 0.3$

$R = 0.01$ m

Load (F) N/m	Hertzian semi-width (b) m	Computed (Δd) m	$\Delta d = R\left[1-\sqrt{1-\left(\frac{b}{R}\right)^2}\right]$ m	error %	$\Delta d = \frac{b^2}{2R}$ m	error %
0.5×10^5	0.7439×10^{-4}	0.2768×19^{-6}	0.277×10^{-6}	0.07	0.2767×10^{-6}	0.04
10^5	0.1052×10^{-3}	0.5536×10^{-6}	0.554×10^{-6}	0.07	0.5534×10^{-6}	0.05
2×10^5	0.1488×10^{-3}	0.1107×10^{-5}	0.1107×10^{-5}	0.0	0.11065×10^{-5}	0.05
3×10^5	0.1822×10^{-3}	0.1661×10^{-5}	0.1661×10^{-5}	0.0	0.1660×10^{-5}	0.06

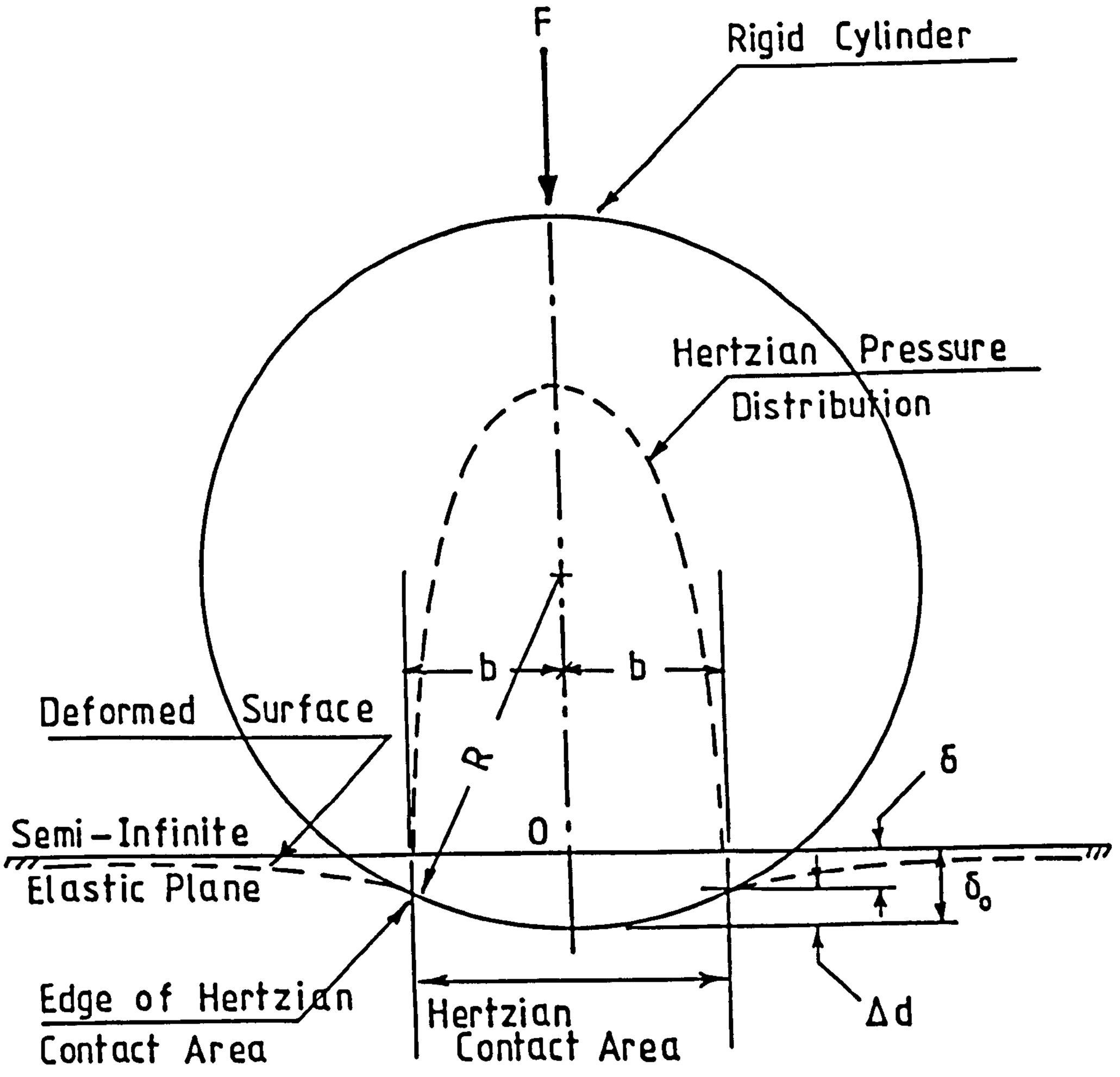

FIGURE(4-2) Elastic Deformation of Semi-Infinite Elastic Solid in the Dry Contact Condition

where,

(L^*) is the dimensionless length of the inlet region.

As described in the previous chapter the terms (d_o) and (d(X)) represent the relative elastic deformations at the contact centre (o) and a point (X) in the calculation field respectively. These terms can be determined numerically via equation (4.2).

4.4 Finite-Difference Representation for an Irregular Mesh

An approximate solution to the non-steady state differential equation (3.26) can be found by using the finite-difference approximation method. The solution region is divided into small rectangular areas which are considered to be interconnected at specific joints which are called nodes or nodal points (mesh points). Since the actual variation of the field variable inside the contact region is not known, the finite-difference method assumes that the variation of the field variable over a small range can be approximated by a simple function. This approximating function is defined in terms of the values of the field variable at the nodes. Accordingly, each derivative of the partial differential equation at a node (j) can be replaced by expressions in terms of the field variable at the same node and the surrounding nodes (j+1) and (j-1). This process clearly gives (N) algebraic equations for (N) unknowns in the field variable. By solving the field equations, the nodal values of the field variable can be determined.

In the present analysis, the approximating function is assumed to be a second order polynomial and the distribution of the

nodes over the whole region is irregular, as shown in Figure (4.3). All of the basic equations required for the finite-difference approximation are developed with the dummy field variable (ψ) in Appendix (A2). For convenience, these equations are summarized in the following,

$$\left(\frac{\partial\psi}{\partial X}\right)_{j-1} \frac{\psi_j(\alpha_1+\alpha_2)^2 - \psi_{j-1}\,\alpha_2\,(2\alpha_1+\alpha_2) - \psi_{j+1}\,\alpha_1^2}{\alpha_1\alpha_2\,(\alpha_1+\alpha_2)} \tag{4.6}$$

$$\left(\frac{\partial\psi}{\partial X}\right)_{j} = \frac{\psi_{j+1}\,\alpha_1^2 - \psi_j\,(\alpha_1^2-\alpha_2^2) - \psi_{j-1}\,\alpha_2^2}{\alpha_1\,\alpha_2(\alpha_1+\alpha_2)} \tag{4.7}$$

$$\left(\frac{\partial\psi}{\partial X}\right)_{j+1} \frac{\psi_{j+1}\,(\alpha_1^2+2\alpha_1\,\alpha_2) - \psi_j\,(\alpha_1+\alpha_2)^2 + \psi_{j-1}\,\alpha_2^2}{\alpha_1\alpha_2(\alpha_1+\alpha_2)} \tag{4.8}$$

$$\left(\frac{\partial\psi^2}{\partial X^2}\right)_{j-1} = \left(\frac{\partial\psi^2}{\partial X^2}\right)_{j} = \left(\frac{\partial\psi^2}{\partial X^2}\right)_{j+1} = \frac{\left[\psi_{j+1}^2\,\alpha_1 - \psi_j\,(\alpha_1+\alpha_2) + \psi_{j-1}\alpha_2\right]}{\alpha_1\alpha_2(\alpha_1+\alpha_2)} \tag{4.9}$$

Having obtained these basic equations with the dummy variable (ψ), we can now proceed to develop the various terms in equation (3.26) by making use of the finite-difference approximations. The following equation is written at time step (m) for the node (j),

$$H_j^{3/2}\left[\frac{\partial}{\partial X}\left(\frac{\bar{\rho}}{\bar{\eta}}\frac{\partial\phi}{\partial X}\right)\right]_j - \frac{3}{2}\phi_j\left[\frac{\partial}{\partial X}\left(\frac{\bar{\rho}\sqrt{H}}{\bar{\eta}}\frac{\partial H}{\partial X}\right)\right]_j = 12U\left(\frac{b}{R}\right)\left[\frac{\partial}{\partial X}(\bar{\rho}H)\right]_j - 12\left(\frac{b}{R}\right)^2\frac{\eta_o\,W_o}{E'R}\left[\frac{\partial}{\partial H_o}(\bar{\rho}H)\right]_{j,m} \tag{4.10}$$

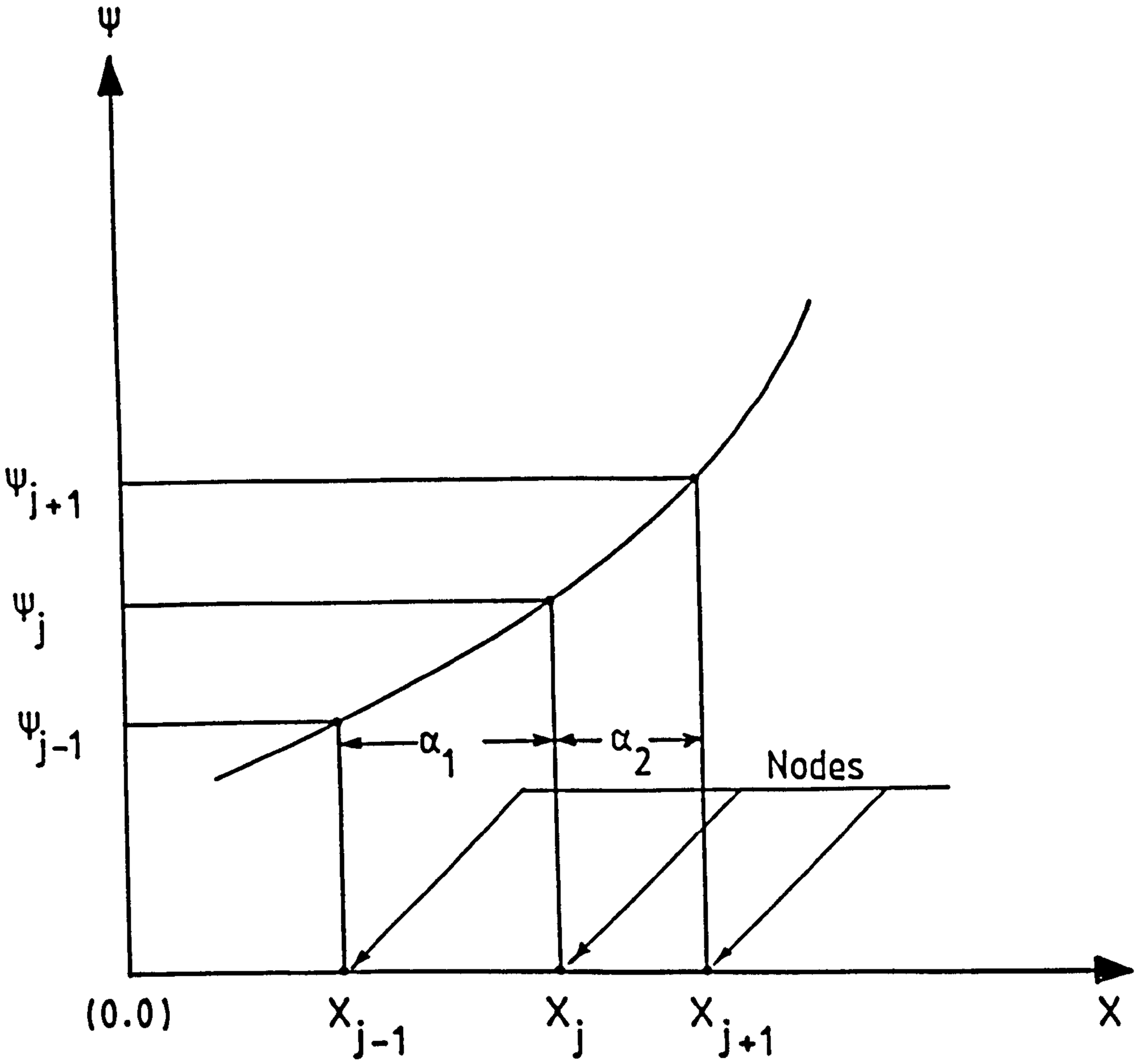

FIGURE (4 - 3) Second Order Polynomial and Corresponding Points Representing (Ψ) as a Function of (X)

From equation (4.7) the first term on the left hand side of equation (4.10) can be expressed as,

$$H_j^{3/2}\left[\frac{\partial}{\partial X}\left(\frac{\bar{\rho}}{\bar{\eta}}\frac{\partial\phi}{\partial X}\right)\right]_j = \frac{H_j^{3/2}}{\alpha_1\alpha_2(\alpha_1+\alpha_2)}\left[\frac{\bar{\rho}_{j+1}}{\bar{\eta}_{j+1}}\left(\frac{\partial\phi}{\partial X}\right)_{j+1}\alpha_1^2 - \frac{\bar{\rho}_j}{\bar{\eta}_j}\left(\frac{\partial\phi}{\partial X}\right)_j(\alpha_1^2-\alpha_2^2) - \frac{\bar{\rho}_{j-1}}{\bar{\eta}_{j-1}}\left(\frac{\partial\phi}{\partial X}\right)_{j-1}\alpha_2^2\right] \quad (4.11)$$

From equation (4.6), (4.7) and (4.8) we get,

$$\left(\frac{\partial\phi}{\partial X}\right)_{j+1} = \frac{\phi_{j+1}(\alpha_1^2+2\alpha_1\alpha_2) - \phi_j(\alpha_1+\alpha_2)^2 + \phi_{j-1}\alpha_2^2}{\alpha_1\alpha_2(\alpha_1+\alpha_2)} \quad (4.12)$$

$$\left(\frac{\partial\phi}{\partial X}\right)_j = \frac{\phi_{j+1}\alpha_1^2 - \phi_j(\alpha_1^2-\alpha_2^2) - \phi_{j-1}\alpha_2^2}{\alpha_1\alpha_2(\alpha_1+\alpha_2)} \quad (4.13)$$

and,

$$\left(\frac{\partial\phi}{\partial X}\right)_{j-1} = \frac{-\phi_{j+1}\alpha_1^2 + \phi_j(\alpha_1+\alpha_2)^2 - \phi_{j-1}\alpha_2(2\alpha_1+\alpha_2)}{\alpha_1\alpha_2(\alpha_1+\alpha_2)} \quad (4.14)$$

substituting equations (4.12), (4.13) and (4.14) into equation (4.11) gives,

$$H_j^{3/2}\left[\frac{\partial}{\partial X}\left(\frac{\bar{\rho}}{\bar{\eta}}\frac{\partial\phi}{\partial X}\right)\right]_j = \frac{H_j^{3/2}}{[\alpha_1\alpha_2(\alpha_1+\alpha_2)]^2}\Bigg\{$$

$$\frac{\rho_{j+1}}{\bar{\eta}_{j+1}}\left[\phi_{j+1}(\alpha_1^2+2\alpha_1\alpha_2) - \phi_j(\alpha_1+\alpha_2)^2 + \phi_{j-1}\alpha_2^2\right]\alpha_1^2$$

$$-\frac{\bar{\rho}_j}{\bar{\eta}_j}\left[\phi_{j+1}\alpha_1^2 - \phi_j(\alpha_1^2-\alpha_2^2) - \phi_{j-1}\alpha_2^2\right](\alpha_1^2-\alpha_2^2)$$

$$- \frac{\bar{\rho}_{j-1}}{\bar{\eta}_{j-1}} \left[- \phi_{j+1}\alpha_1^2 + \phi_j (\alpha_1 + \alpha_2)^2 - \phi_{j-1} \alpha_2 (2\alpha_1 + \alpha_2) \right] \alpha_2^2 \Bigg\} \quad (4.15)$$

Likewise, the second term on the left hand side of equation (4.10) can be expressed as

$$\frac{3}{2} \phi_j \left[\frac{\partial}{\partial X} \left(\frac{\bar{\rho}\sqrt{H}}{\bar{\eta}} \frac{\partial H}{\partial X} \right) \right]_j = \frac{3/2 \ \phi_j}{[\alpha_1\alpha_2 (\alpha_1 + \alpha_2)]^2} \Bigg\{$$

$$\frac{\bar{\rho}_{j+1} \sqrt{H_{j+1}}}{\bar{\eta}_{j+1}} \left[H_{j+1} (\alpha_1^2 + 2 \alpha_1\alpha_2) - H_j (\alpha_1 + \alpha_2)^2 + H_{j-1}\alpha_2^2 \right] \alpha_1^2$$

$$- \frac{\bar{\rho}_j \sqrt{H_j}}{\bar{\eta}_j} \left[H_{j+1} \alpha_1^2 - H_j (\alpha_1^2 - \alpha_2^2) - H_{j-1} \alpha_2^2 \right] (\alpha_1^2 - \alpha_2^2)$$

$$- \frac{\bar{\rho}_{j-1} \sqrt{H_{j-1}}}{\bar{\eta}_{j-1}} \left[H_j(\alpha_1+\alpha_2)^2 - H_{j-1}\alpha_2(2\alpha_1+\alpha_2) - H_{j+1}\alpha_1^2 \right] \alpha_2^2 \Bigg\} \quad (4.16)$$

And the first term on the right hand side of equation (4.10) becomes,

$$12U \left(\frac{b}{R} \right) \left[\frac{\partial}{\partial X} (\bar{\rho}H) \right]_j = \frac{12U \left(\frac{b}{R} \right)}{\alpha_1\alpha_2 (\alpha_1 + \alpha_2)} \left[(\bar{\rho}H)_{j+1} \alpha_1^2 \right.$$

$$\left. - (\bar{\rho}H)_j (\alpha_1^2 - \alpha_2^2) - (\bar{\rho}H)_{j-1} \alpha_2^2 \right] \quad (4.17)$$

The second term on the right hand side of equation (4.10) which represents the effect of the squeeze action $\left[\frac{\partial}{\partial H_o} (\bar{\rho}H) \right]_{j,m}$ can be approximated in the time domain at a time step (m) by the Lagrangian three point quadrature as,

$$12 \left(\frac{b}{R} \right)^2 \frac{\eta_o W_o}{E'R} \left[\frac{\partial}{\partial H_o} (\bar{\rho}H) \right]_m = 12 \left(\frac{b}{R} \right)^2 \frac{\eta_o W_o}{E'R} \left[\right.$$

$$H_m \left(\bar{\omega}_{m-2}\,\bar{\rho}_{m-2} + \bar{\omega}_{m-1}\,\bar{\rho}_{m-1} + \bar{\omega}_m\,\bar{\rho}_m\right) + \bar{\rho}_m \left(\bar{\omega}_{m-2}\,H_{m-2} + \bar{\omega}_{m-1}\,H_{m-1} + \bar{\omega}_m\,H_m\right)\Big] \qquad (4.18)$$

where,

$$\bar{\omega}_{m-2} = \frac{Ho_m - Ho_{m-1}}{(Ho_{m-2} - Ho_{m-1})(Ho_{m-2} - Ho_m)}$$

$$, \qquad \bar{\omega}_{m-1} = \frac{(Ho_m - Ho_{m-2})}{(Ho_{m-1} - Ho_{m-2})(Ho_{m-1} - Ho_m)}$$

and,

$$\bar{\omega}_{m-1} = \frac{(Ho_m - Ho_{m-1}) + (Ho_m - Ho_{m-2})}{(Ho_m - Ho_{m-1})(Ho_m - Ho_{m-2})}$$

The terms subscripted (m-2) and (m-1) on the right hand side of equation (4.18) were determined in the previous time steps (m-2) and (m-1). Therefore, they are considered constants over the time step (m).

Substituting equations (4.15), (4.16), (4.17) and (4.18) into equation (4.10) while collecting terms gives,

$$A_j\,\phi_{j+1} + B_j\,\phi_j + C_j\,\phi_{j-1} + D_j\,W_o = E_j \qquad (4.19)$$

where,

$$A_j = \frac{H_j^{3/2}}{[\alpha_1\alpha_2(\alpha_1+\alpha_2)]^2}\left[\frac{\bar{\rho}_{j+1}}{\bar{\eta}_{j+1}}(\alpha_1^2+2\alpha_1\alpha_2)\alpha_1^2 - \frac{\bar{\rho}_j}{\bar{\eta}_j}\alpha_1^2(\alpha_1^2-\alpha_2^2) + \frac{\bar{\rho}_{j-1}}{\bar{\eta}_{j-1}}\alpha_1^2\alpha_2^2\right]$$

$$B_j = \frac{H_j^{3/2}}{[\alpha_1\alpha_2(\alpha_1+\alpha_2)]^2}\left\{-\frac{\bar{\rho}_{j+1}}{\bar{\eta}_{j+1}}(\alpha_1+\alpha_2)^2\alpha_1^2 + \frac{\bar{\rho}_j}{\bar{\eta}_j}(\alpha_1^2-\alpha_2^2)^2 - \frac{\bar{\rho}_{j-1}}{\bar{\eta}_{j-1}}(\alpha_1+\alpha_2)^2\alpha_2^2\right\} - \frac{3/2}{[\alpha_1\alpha_2(\alpha_1+\alpha_2)]^2}\left\{\right.$$

$$\frac{\bar{\rho}_{j+1}\ \sqrt{H_{j+1}}}{\bar{\eta}_{j+1}}\left[H_{j+1}\ (\alpha_1^2+2\alpha_1\alpha_2) - H_j\ (\alpha_1+\alpha_2)^2 + H_{j-1}\ \alpha_2^2\right]\alpha_1^2$$

$$-\frac{\bar{\rho}_j\ \sqrt{H_j}}{\bar{\eta}_j}\left[H_{j+1}\ \alpha_1^2 - H_j\ (\alpha_1^2-\alpha_2^2) - H_{j-1}\ \alpha_2^2\right](\alpha_1^2-\alpha_2^2)$$

$$-\frac{\bar{\rho}_{j-1}\ \sqrt{H_{j-1}}}{\bar{\eta}_{j-1}}\left[H_j\ (\alpha_1+\alpha_2)^2 - H_{j-1}\ \alpha_2\ (2\alpha_1+\alpha_2) - H_{j+1}\ \alpha_1^2\right]\alpha_2^2\Bigg\}$$

$$C_j = \frac{H_j^{3/2}}{[\alpha_1\alpha_2(\alpha_1+\alpha_2)]^2}\left[\frac{\bar{\rho}_{j+1}}{\bar{\eta}_{j+1}}\alpha_2^2\alpha_1^2 + \frac{\bar{\rho}_j}{\bar{\eta}_j}\alpha_2^2\ (\alpha_1^2-\alpha_2^2) + \frac{\bar{\rho}_{j-1}}{\bar{\eta}_{j-1}}\alpha_2^3\ (2\alpha_1+\alpha_2)\right]$$

$$D_j = 12\left(\frac{b}{R}\right)^2\frac{\eta_o}{E'R}\left[H_m\ (\bar{\omega}_{m-2}\ \bar{\rho}_{m-2} + \bar{\omega}_{m-1}\ \bar{\rho}_{m-1} + \bar{\omega}_m\ \bar{\rho}_m)\right.$$

$$\left. + \bar{\rho}_m\ (\bar{\omega}_{m-2}\ H_{m-2} + \bar{\omega}_{m-1}\ H_{m-1} + \bar{\omega}_m\ H_m)\right]$$

$$E_j = \frac{12U\left(\frac{b}{R}\right)}{\alpha_1\alpha_2(\alpha_1+\alpha_2)}\left[(\bar{\rho}H)_{j+1}\ \alpha_1^2 - (\bar{\rho}H)_j\ (\alpha_1^2-\alpha_2^2) - (\bar{\rho}H)_{j-1}\ \alpha_2^2\right]$$

4.5 Mesh Structure

The variable mesh nodal structure shown in Figure (4.4) has been used in all of the calculations. This nodal structure was chosen to satisfy the conflicting requirements of a large integration zone with a proper inter-nodal spacing to avoid starvation effects and reduce truncation errors. Moreover, it reduces the number of nodes in the field compared with the number required for a similar accuracy in the case of a uniform mesh, hence the computing time is reduced.

The grid spacing of the coordinate (X) was varied depending on the anticipated pressure distribution. In the vicinity of the

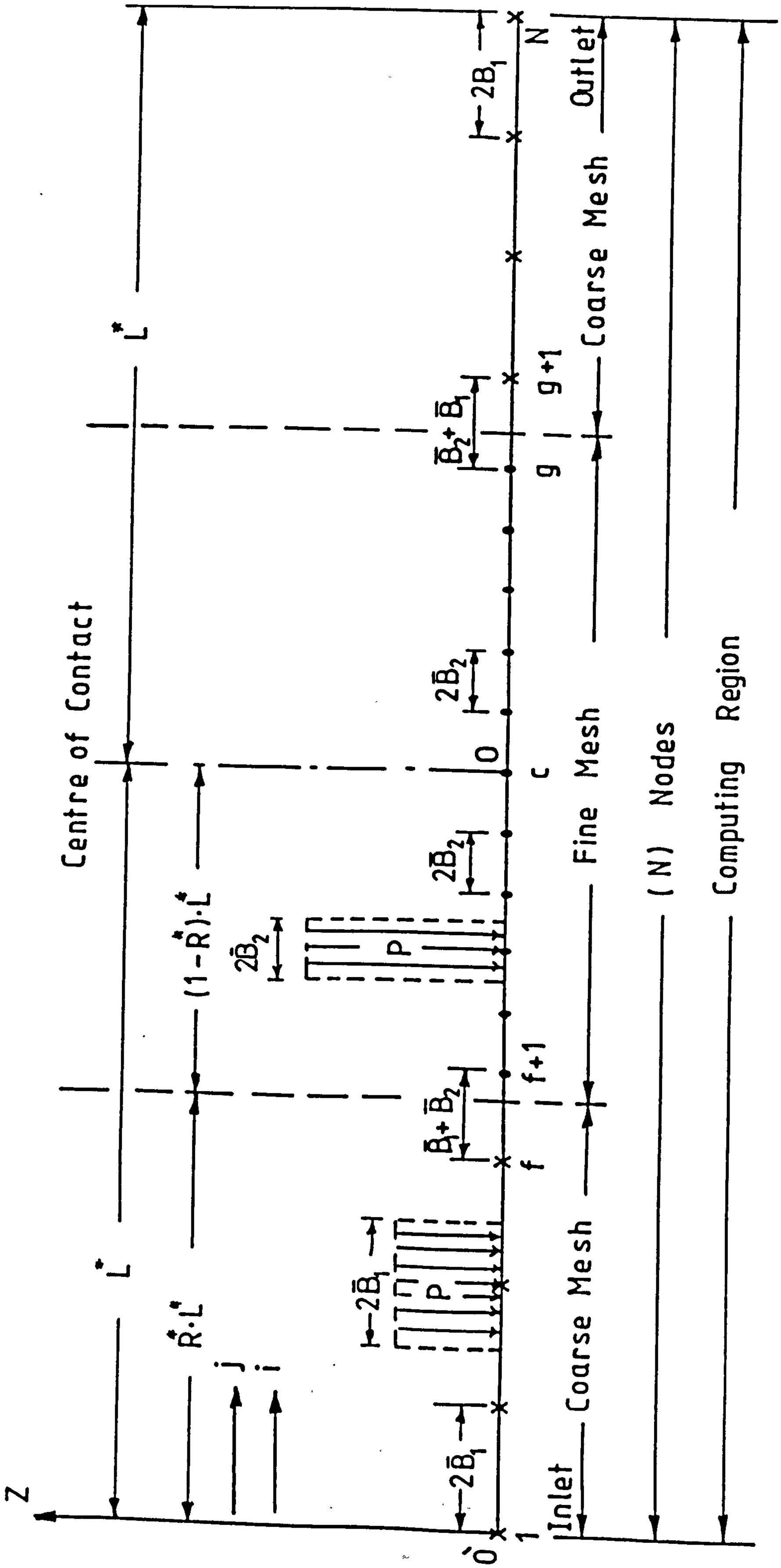

FIGURE(4-4)

Variable Nodal Structure Used for Numerical Calculations

centre of the conjunction, the pressure gradient was far steeper and a pressure spike was expected, thus a fine mesh spacing ($2\bar{B}_2$) was adopted. On the other hand, a larger mesh spacing ($2\bar{B}_1$) was used over the rest of the computation zone where the pressure variation was less abrupt.

For each value of the central film thickness (H_o) during the approach a corresponding inlet boundary location (L^*) was specified to ensure an accurate result. A good prediction for the dimensionless distance (L^*) corresponding to a specific central film thickness (H_o) can be determined from the following equation,

$$L^* = \left(\frac{R}{b}\right) \sqrt{2H_o \left[\frac{H^*}{H_o} - 1\right]} \qquad (4.20)$$

where,

the ratio $\left(\frac{H^*}{H_o}\right)$ is assumed known and has a value greater than (50).

From Figure (4.4) the following notation can be noted:

(L^*) dimensionless inlet distance

(f) number of nodes in the coarse-mesh region on the inlet side.

(c) central node number.

(N) total number of nodes within the computing field.

(c-f) number of nodes in the fine - mesh region on the inlet side including the central node.

(R^*) ratio between the dimensionless width of the coarse-mesh on the inlet side and the dimensionless inlet distance (L^*).

$(2\bar{B}_1)$ coarse-mesh inter-nodal spacing $\left(\frac{2\bar{R}^* L^*}{2f - 1}\right)$

$(2\bar{B}_2)$ fine-mesh inter-nodal spacing $\left(\frac{2(1-R^*)L^*}{2(c-f)-1}\right)$

4.6 Load Equation

The Reynolds' equation was solved throughout this problem keeping the central film thickness (H_o) constant at a prescribed value at a given time, though allowing for the effects of elastic deformation on the overall film shape. Each solution obtained corresponded to a specific external normal applied load (F). As stated in equation (3.19), this load was equal to the integral of the pressure distribution resulting in the fluid film. That is,

$$\frac{F}{bE'} = \int_o^{2L^*} P \, dX \qquad (4.21)$$

In order to determine the central approach velocity (W_o), equation (4.21) must be expressed in numerical form and used with the system of (N) algebraic equations developed by the finite difference representation of the Reynolds' equation. This can be done by applying the trapezoidal rule, with the concept of the variable mesh nodal structure shown in Figure (4.4), to express the pressure integral term as,

$$\frac{F}{bE'} = \delta_1 \sum_{j=2}^{f-1} P_j + \delta_3 P_f + \delta_4 P_{f+1}$$

$$+ \delta_2 \sum_{j=f+2}^{g-1} P_j + \delta_4 P_g + \delta_3 P_{g+1}$$

$$+ \delta_1 \sum_{j=g+2}^{N-1} P_j \qquad (4.22)$$

or, in terms of the parameter (ϕ) this becomes,

$$\frac{F}{bE'} = \delta_1 \sum_{j=2}^{f-1} (\phi H^{-3/2})_j + \delta_3 (\phi H^{-3/2})_f + \delta_4 (\phi H^{-3/2})_{f+1}$$

$$+ \delta_2 \sum_{j=f+2}^{g-1} (\phi H^{-3/2})_j + \delta_4 (\phi H^{-3/2})_g + \delta_3 (\phi H^{-3/2})_{g+1}$$

$$+ \delta_1 \sum_{j=g+2}^{N-1} (\phi H^{-3/2})_j \qquad (4.23)$$

where,

$$\delta_1 = 2\bar{B}_1 \quad , \quad \delta_2 = 2\bar{B}_2$$

$$\delta_3 \quad \frac{(3\bar{B}_1 + \bar{B}_2)}{2} \qquad \delta_4 \quad \frac{(\bar{B}_1 + 3\bar{B}_2)}{2}$$

(f) number of the node on the coarse-mesh (on the inlet side) located near the boundary between the coarse and the fine mesh.

(g) number of the node on the fine mesh (on the outlet side) located near the boundary between the fine and the coarse mesh.

4.7 Time Step Solution

Initially, at (t=0), the central film thickness (H_o) must be specified. This corresponds to some assumed starting situation in squeeze-film lubrication or to the instant at which there is a

sudden variation of a fixed load (F). Keeping the central film thickness (H_o) constant, a complete solution is obtained and the central approach velocity (W_o) is determined. Then, a solution for (H_o) may be marched out in time using the simplest Euler's integration scheme which sets,

$$H_o\ (t+\Delta t) = H_o(t) - W_o(t).\Delta t \qquad (4.24)$$

where,

(Δt) is the time step.

Euler's method has inherent accuracy $O(\Delta t)$, thus, by a suitable choice of the time step (Δt), the numerical results can be made to lie arbitrarily close to those determined by analytical solutions.

4.8 Matrix Solution

The discretized forms of the Reynolds' equation (4.19) and the load equation (4.23) with the corresponding boundary conditions give (N-1) algebraic equations for (N-2) unknowns (ϕ_2), (ϕ_3), (ϕ_4), ..., (ϕ_{N-1}) and the central approach velocity (W_o). This represents a matrix equation (4.25), in which the matrix [M] is tridiagonal. The leading diagonal consists mainly of the coefficients (B_j) and the neighbouring diagonals contain the coefficients (C_j) and (A_j). The last column consists of the central approaching velocity coefficients (D_j). The last row contains the load equation coefficients of the variable (ϕ_j). Thus, multiplying

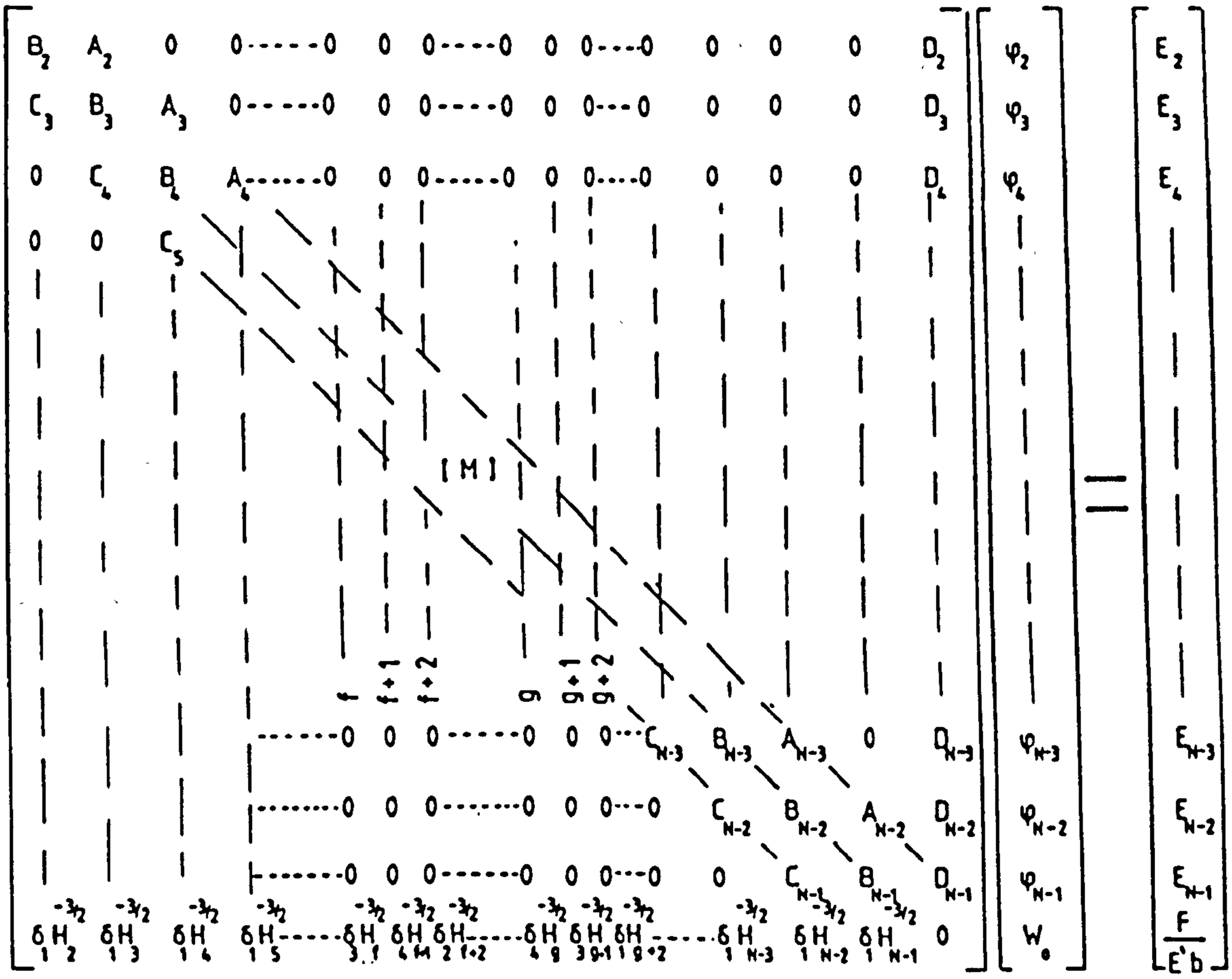

(4-25)

the right-hand side vector by (M^{-1}) gives the (ϕ_j) values (j = 2,3,4 ..... N-1) and the value of the central approaching velocity (W_o).

At small central film thickness (H_o) the scheme failed to converge when starting with zero initial pressure at each grid point, but convergence was achieved by using previously found converged solutions at slightly greater central film thickness (H_o). This problem with the convergence is associated with the well-known pressure spike (see Dowson and Higginson (1977)) which develops near the outlet of heavily loaded lubricated contacts. This gives very large pressure gradients, which are always difficult to deal with.

For combined squeeze and rolling problems the Reynolds' boundary condition ($P = \frac{dP}{dX} = 0$) at the outlet boundary was applied. In this case the location of the outlet boundary is unknown. In order to determine this location, a converged solution was first obtained with an outlet boundary (X_e^{old}) further downstream than expected as shown in Figure (4.5(a)). This produced a pressure distribution which went negative before reaching the outlet boundary. The new outlet boundary (X_e^{new}) was chosen to be at the position of the minimum of the pressure curve obtained. The problem was then re-solved with the boundary condition ($P(X_e^{new}) = 0$). The new pressure distribution was typically as shown in Figure (4.5(b)). This process of changing the outlet boundary according to the position of the pressure curve minimum was repeated until eventually the pressure distribution shown in Figure (4.5(c)) was obtained where ($P = \frac{dP}{dX} = 0$) at ($X = X_e$). This technique of applying the Reynolds' boundary conditions by moving the outlet boundary was introduced by Rohde and Oh (1975).

It should be noted that the Gauss-Seidel iterative method was adopted initially for the solution of the system of simultaneous linear equations (4.25), but considerable difficulty arose with respect to the computational effort and convergence of the process. It was first thought that these difficulties were associated with the direct solution technique (Phi(ϕ) solution). Therefore, the Newton-Raphson technique was investigated with a view to improving the convergence of the process. Nevertheless, no satisfactory progress was achieved. Eventually, it was recognized that the Gauss-Seidel iterative method was the real difficulty. Hence, a matrix method was used to solve the system of simultaneous equations

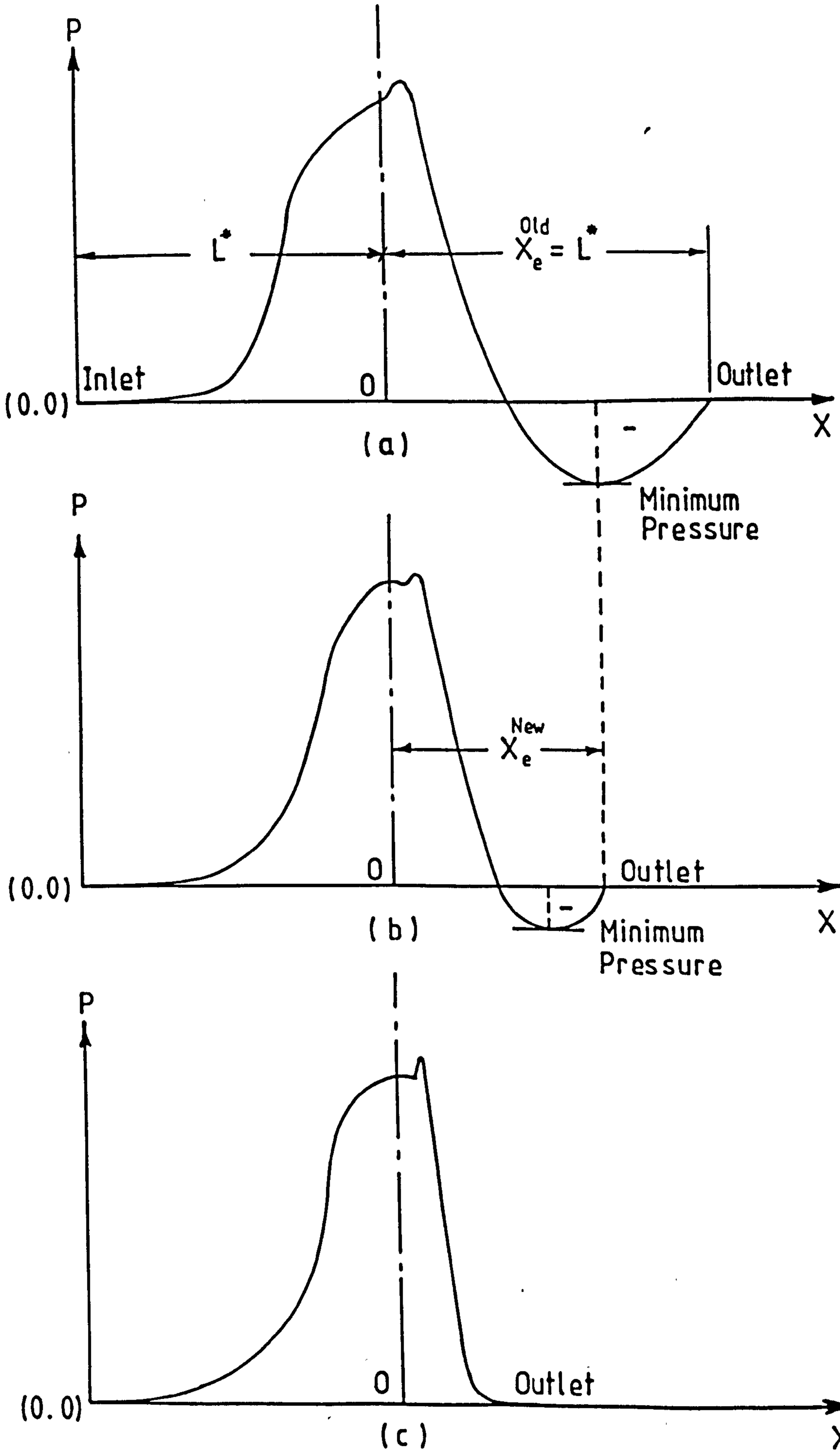

FIGURE (4-5) Locating the Outlet Position

(4.25) and found to be quicker and more accurate (a time reduction of (1/30) was achieved). The only deficiency of the matrix solution method was that it required more computer fast storage space.

4.9 Outline of Numerical Solution

A direct iterative technique was used to solve the elasticity and Reynolds' equations simultaneously at successive time steps. At each time step (m) the central film thickness (H_o) was kept constant. Then the calculations were performed under the application of a fixed instantaneous load (F) to obtain the value of the central velocity of approach (W_o) and the corresponding pressure and film thickness distributions.

The general solution scheme was as follows,

(i) Initially the starting central film thickness (H_o) must be specified at a relatively high value to prime the calculations.

(ii) At the first step an approximate pressure distribution was used as an initial guess of the pressure. From the second time step onwards, the initial guess of the pressure was the previous pressure distribution.

(iii) Using the initial guess of the pressure distribution the dimensionless film thickness (H), density ($\bar{\rho}$) and viscosity ($\bar{\eta}$) were calculated. Then the various coefficients (A_j, B_j, C_j, D_j, E_j) of the finite-difference equation (4.19) were determined, from these values, at all the grid points.

(iv) Once the coefficients of the matrix equation (4.25) were prepared, the centre velocity of approach (W_o) and the values of the variable (ϕ) for every point within the mesh were determined.

(v) Now the new pressure distribution (P) was calculated from the (ϕ) distribution and checked for convergence from the previous guessed pressure. The pressure was taken to have converged to a solution at iteration (n) when,

$$\frac{\sum_{j=2}^{N-1} \left| P_{j,n} - P_{j,n-1} \right|}{\sum_{j=2}^{N-1} P_{j,n}} \leq \varepsilon \qquad (4.26)$$

where (ε) was the allowable tolerance whose value depended on the case investigated.

(vi) If it did not converge, modified values of (P) were calculated by under-relaxation, producing new values of (P) as follows,

$$P_{new} = \frac{P_{new} + (\lambda-1)\, P_{old}}{\lambda} \qquad (4.27)$$

where (λ) was a relaxation factor whose value was usually greater than (1). This factor helped the process of convergence by damping out the oscillations. However, if (λ) was too large, overdamping occurred causing full convergence to be delayed. Having this modified pressure

(P) distribution the above procedures (iii), (iv) and (v) were repeated until the converged solution was obtained.

(vii) If converged, the solution moved to the next time step where,

$$H_o\ (t+\Delta t) = H_o(t) - W_o(t).\Delta t$$

4.10 Flow Chart

The flow chart shown in Figure (4.6) outlines the numerical solution on the digital computer of the elasticity, Reynolds and load equations developed in this analysis. There are essentially two loops within the main program: the first is the pressure loop where the new values of ($\phi_{j,n+1}$) result in new values of pressure ($P_{j,n+1}$), which in turn result in new values of the dimensionless film thickness (H_j), viscosity ($\bar{\eta}_j$) and density ($\bar{\rho}_j$). The second is the 'time stepping' loop where new values of the load ($F(t+\Delta t)$) and central film thickness ($H_o(t+\Delta t)$) are calculated from the previous values, at time (t), of the central velocity of approach ($W_o(t)$) and the central film thickness ($H_o(t)$).

The FORTRAN listings of the main and assisting subroutines are given in the Appendix (A1). The computer used was the Amdahl (580) of the University of Leeds. The amount of C.P.U. time consumed per run depended on the severity of the elastohydrodynamic conditions. Another cost factor was the accuracy required for a solution.

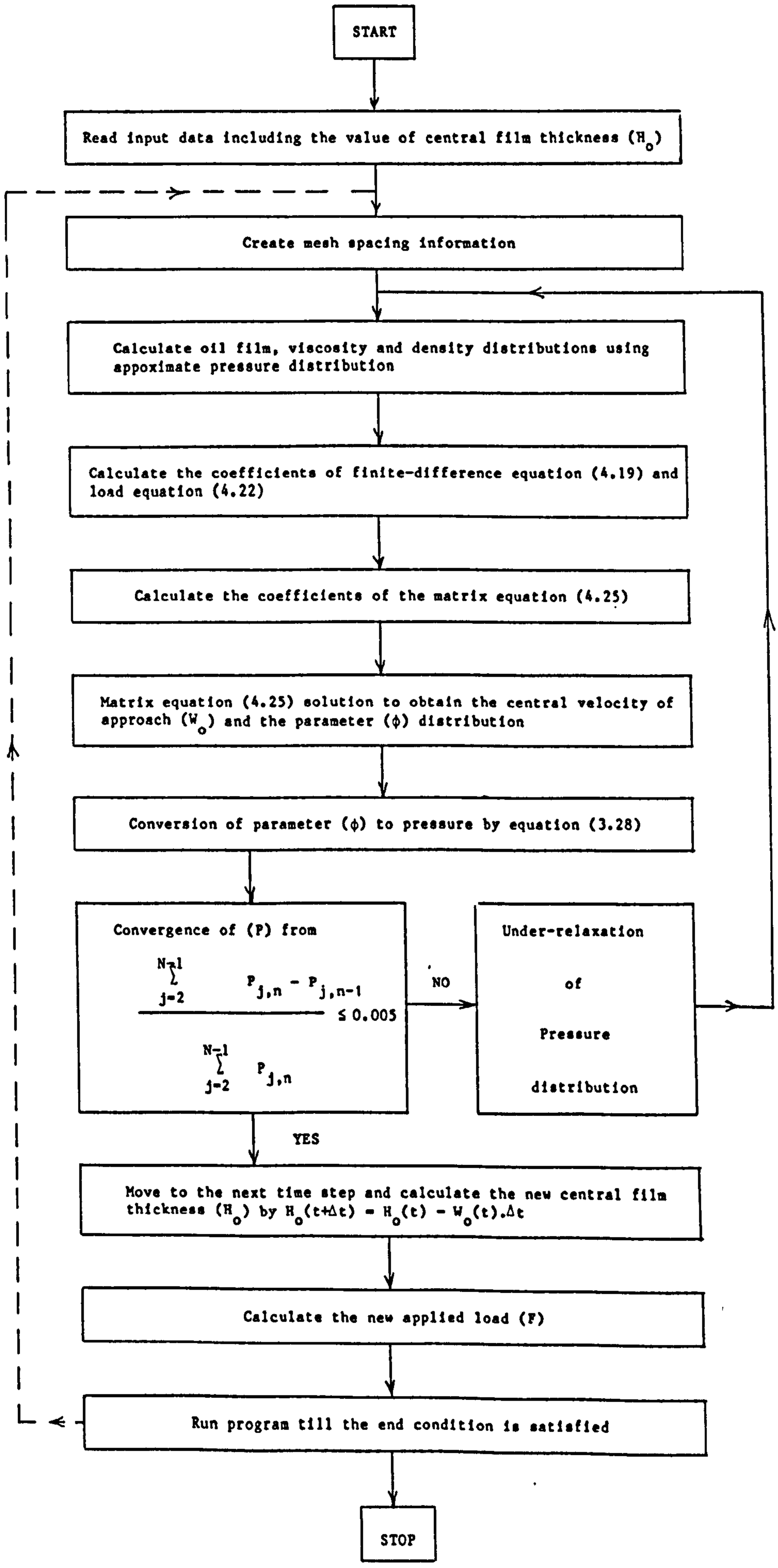

Figure (4.6) Flow Diagram

4.11 Concluding Remarks

In this chapter a procedure for the solution of the complete, isothermal, transient, elastohydrodynamic lubrication problem of line contacts subjected to constant or variable external normal load (F) has been presented. This procedure calls for the simultaneous solution of the elasticity, Reynolds and load equations at successive time steps. In the elasticity analysis the conjunction was divided into irregular areas with uniform pressures. In the numerical analysis of the Reynolds equation an under-relaxation of the resulting pressure was used to aid the process of convergence. The possibility of cavitation was recognized, especially as the rolling effect is considered, by the adoption of the Reynolds boundary condition in the divergent region and the location of the outlet boundary was determined by moving the exit position. A tridiagonal matrix algorithm was used to solve the finite-difference and load equations to obtain the central velocity of approach (W_o) and the pressure distribution (P). The outlines of the numerical procedure and the corresponding flow chart have been presented.

CHAPTER 5

A THEORETICAL STUDY OF THE SQUEEZE FILM LUBRICATION OF ELASTIC CYLINDERS

5.1 Introduction

Squeeze film action occurs frequently in many machine components such as meshing gear teeth, journal bearings, cams and followers etc. The problem of an elastohydrodynamic squeeze film between lubricated cylinders has been treated extensively by Christensen (1961), Herrebrugh (1970), Lee and Cheng (1973), and Wada and Tsukijihara (1978). Excluding the solution of Herrebrugh for elastic cylinders lubricated by an isoviscous fluid, all the other solutions assume constant central pressure (P_o) during the normal approach process, although its correspondence to any practical physical situation is somewhat questionable. A more advanced analysis has been recently developed by Chandra and Rogers (1983), who introduced a squeeze film model which used a two dimensional analysis to obtain the pressure distribution in both the circumferential and axial directions. Moreover, it took into account the effect of fluid inertia terms, considered constant and variable externally applied loads and employed a solid-solid model during the final stage of approach when the solids came into contact.

The present analysis makes the following advances over the former elastohydrodynamic models and solutions schemes:

(a) It is a real transient analysis in which the full time histories of the system parameters are determined;

(b) Any specified loading can be accommodated;

(c) It utilizes an elaborate direct - iteration solution technique capable of handling different types of elastohydrodynamic lubrication problems, for example where there is an entraining action.

In this chapter computed solutions are presented for squeeze film lubrication of elastic cylinders. These results were evaluated for both isoviscous and piezoviscous lubrication conditions. Graphical representations of pressure distributions and film shapes are presented together at successive reductions of the central film thickness (H_o). The variation of the dimensionless minimum film thickness (H_m), velocity of approach ($\bar{W}$) and central pressure (P_o) are included. The results of this work for the isoviscous lubrication case have been compared with those developed by Herrebrugh and good agreement was found. Furthermore, the bifurcation phenomenon that has been observed by Herrebrugh was confirmed.

The central pressure results obtained for constant load in the presence of a piezoviscous fluid are compared with the results of Lee and Cheng. A reasonable agreement was obtained.

5.2 Dimensionless Parameters

The variables resulting from the elastohydrodynamic squeeze film lubrication theory are,

(R) effective radius of curvature, $\left(R = \frac{R_1 R_2}{R_1 + R_2} \right)$ (m)

(h) film thickness (m)

(E') effective elastic modulus, $\left[\frac{2}{\frac{1-\sigma_1^2}{E_1}+\frac{1-\sigma_2^2}{E_2}}\right]$ (N/m^2)

($P_{iv,as}$) asymptotic isoviscous pressure obtained from Roelands (1966), $\left[\simeq \frac{1}{\alpha}\right]$ (N/m2)

(W) velocity of approach (m/s)

(η_o) lubricant viscosity at atmospheric pressure ($N.s/m^2$)

(F) normal applied load (N/m)

The effect of compressibility was not considered in the present study, but it was included in the general elastohydrodynamic theory presented in Chapter (3).

From the seven variables mentioned above the following four dimensionless groups can be written:

(1) Dimensionless film thickness

$$H = \frac{h}{R}$$

(2) Dimensionless load parameter

$$\bar{F} = \frac{F}{E'R}$$

(3) Dimensionless velocity of approach parameter

$$\bar{W} = \frac{\eta_o W}{E'R}$$

(4) Dimensionless material parameter

$$G = \alpha E'$$

It can be shown that the general solution of the elastohydrodynamic squeeze film problem depends on three

dimensionless groups only. These new dimensionless groups consist mainly of the power products of the above mentioned dimensionless parameters. That is,

$$\pi_1 = \frac{24}{\pi} \bar{W} \left(\frac{1}{H_o}\right)^{5/2} \tag{5.1}$$

$$\pi_2 = \frac{1}{12} \frac{H_o^{3/2} \bar{F}}{\bar{W}} \tag{5.2}$$

$$\pi_3 = 12 \frac{G\bar{W}}{H_o^2} \tag{5.3}$$

where,

(H_o) is the dimensionless central film thickness $\left(\frac{h_o}{R}\right)$.

Several interesting forms of functional relations can be obtained by utilizing (π_1), (π_2) and (π_3) via the rules of dimensionless analysis. The first possibility is to construct alternative dimensionless groups in such a way that the dimensionless central film thickness (H_o) and the dimensionless velocity of approach parameter $(\bar{W})$ are separated. Thus,

$$\frac{2}{\pi}\left(\pi_1\pi_2\right)^{-1} = \phi\left[\frac{1}{3\pi\sqrt{2\pi}}\left(\pi_1^{-3/2}\ \pi_2^{-5/2}\right), \frac{\pi_3}{\sqrt{2}}\left(\frac{\pi_2}{\pi_1}\right)^{1/2}\right]$$

or,

$$\frac{H_o}{\bar{F}} = \phi\left[\frac{\bar{W}}{\bar{F}^{5/2}}, \frac{G}{2}\left(\pi\bar{F}\right)^{1/2}\right] \tag{5.4}$$

It is seen that in the isoviscous case $\left[\frac{G}{2}\left(\pi\bar{F}\right)^{1/2} = 0\right]$ the two-dimensional functional relation (5.4) reduces to a simple relationship between two dimensionless groups.

A further set of power products (π_1), (π_2) and (π_3) is the following, in which the dimensionless load ($\bar{F}$) and the dimensionless central film thickness (H_o) are separated,

$$\left(\frac{24}{\pi}\ \frac{1}{\pi_1}\right)^{2/5} = \phi\left[\left[12\left(\frac{\pi}{24}\right)^{3/5}\ \pi_2\,\pi_1^{3/5}\right],\ \frac{\pi_3}{\sqrt{2}}\left(\frac{\pi_2}{\pi_1}\right)^{1/2}\right]$$

or,

$$\frac{H_o}{\bar{W}^{2/5}} = \phi\left[\frac{\bar{F}}{\bar{W}^{2/5}},\ \frac{G}{2}\left(\pi\bar{F}\right)^{1/2}\right] \qquad (5.5)$$

In the present results the dimensionless parameter (L) will be used to identify the isoviscous and piezoviscous lubrication regimes, where,

$$L = \frac{G}{2}\ (\pi\bar{F})^{1/2} \qquad (5.6)$$

5.3 Pressure Profiles

The pressure distributions are plotted in conjunction with the corresponding film shapes in Figures (5.1), (5.2) and (5.3). Each figure displays the change in pressure and film shape with the dimensionless central film thickness (H_o) as the cylinder approaches the plane surface under the influence of a constant externally applied load. The quantity $\left(L = \frac{G}{2}\ (\pi\bar{F})^{1/2}\right)$ is used as a parameter in all these representations. Three representative cases were considered, the values of the dimensionless parameter (L) employed in the present results being (L = 0.0) to represent the isoviscous lubrication regime and (L = 5,10) to represent the piezoviscous lubrication regime. All the physical data used in this study are given in Table (5.1).

Table (5.1) Physical Data

Physical Quantity		Case L=0.0	Case L = 5	Case L = 10
Load	(N/m)	15000	6535	26141
Cylinder Specifications				
Equivalent radius (R)	(m)	0.02	No	No
Effective elastic modulus (E')	(N/m^2)	$2.3x10^{11}$	change	change
Poisson's ratio (σ)	(-)	0.3		
Fluid Constants				
Atmospheric visocsity (η_o)	Pas	0.0411	0.0411	0.0411
Pressure-Viscosity coefficient (α)	(m^2/N)	-	$2.058x10^{-8}$	$2.058x10^{-8}$
Initial film thickness (H_o)	(-)	10^{-4}	10^{-4}	10^{-4}

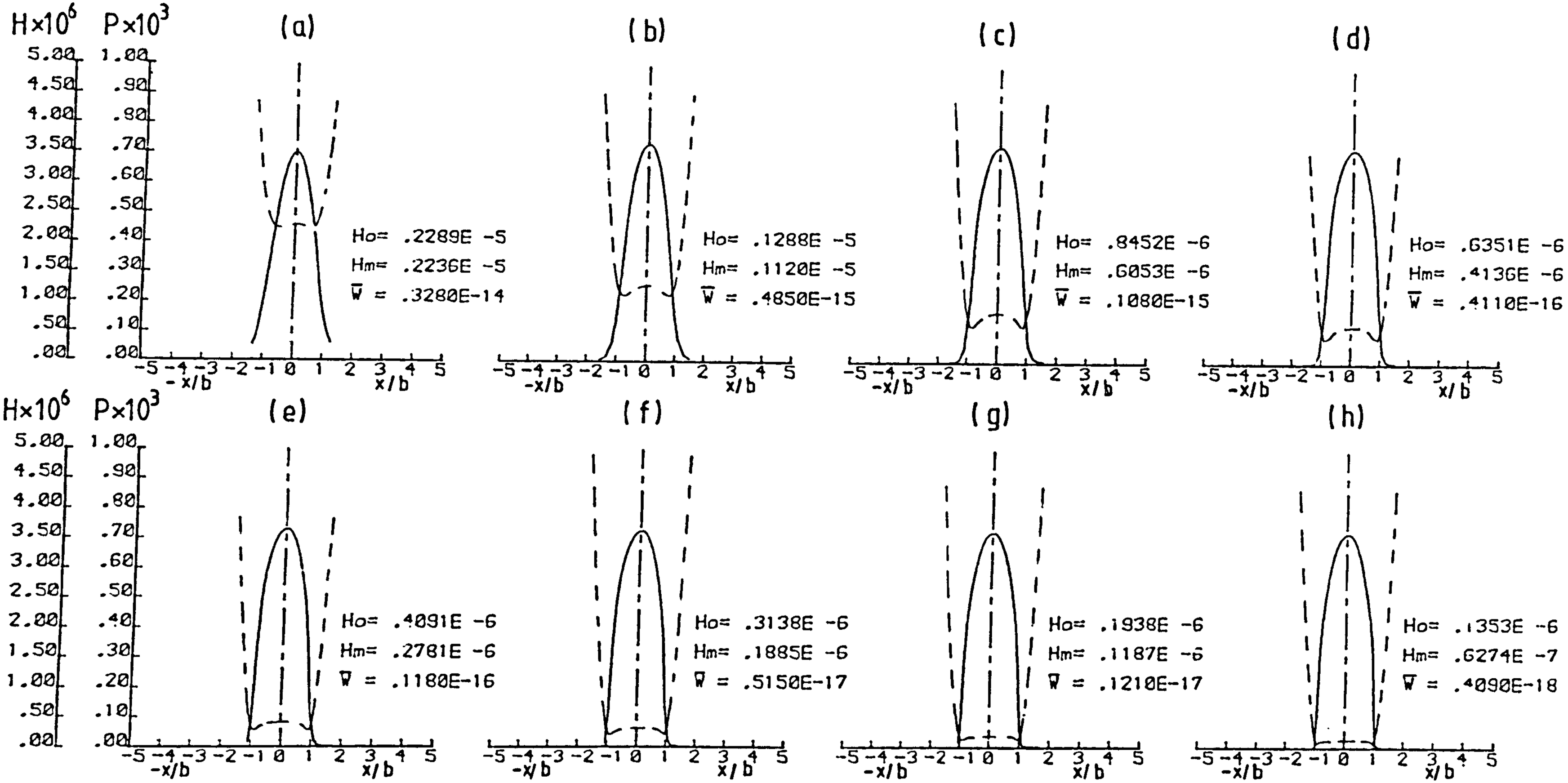

FIGURE(5 - 1) Pressure Distributions(——) and Film Shapes(- - -) for Elastic Cylinders With Squeeze Film Action Under the Influence of a Constant External Load in the Presence of an Isoviscous Fluid
(L=0.0)

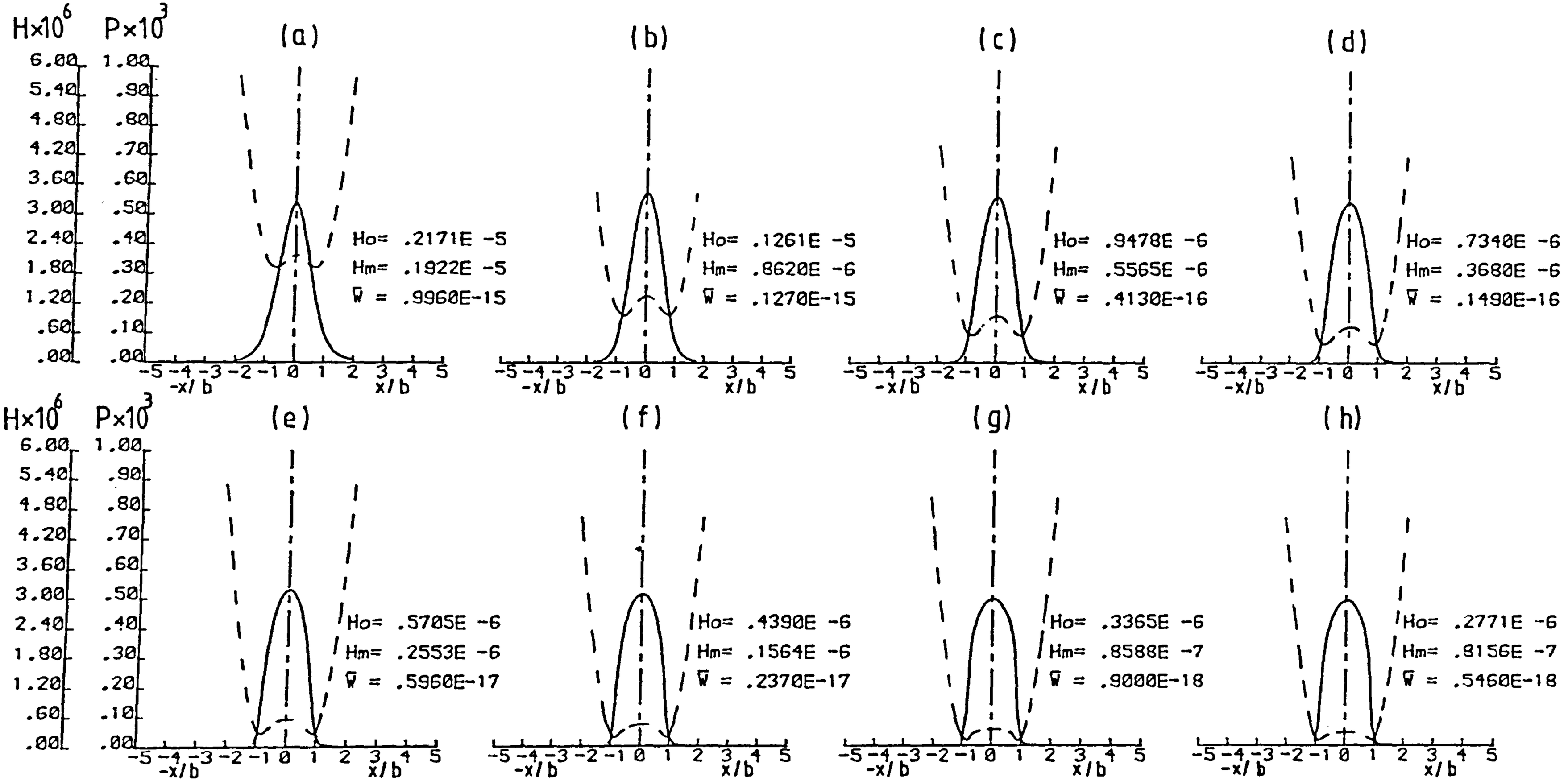

FIGURE(5 - 2) Pressure Distributions(———) and Film Shapes(– – –) for Elastic Cylinders With Squeeze Film Action Under the Influence of a Constant External Load in the Presence of a Piesoviscous Fluid
(L= 5)

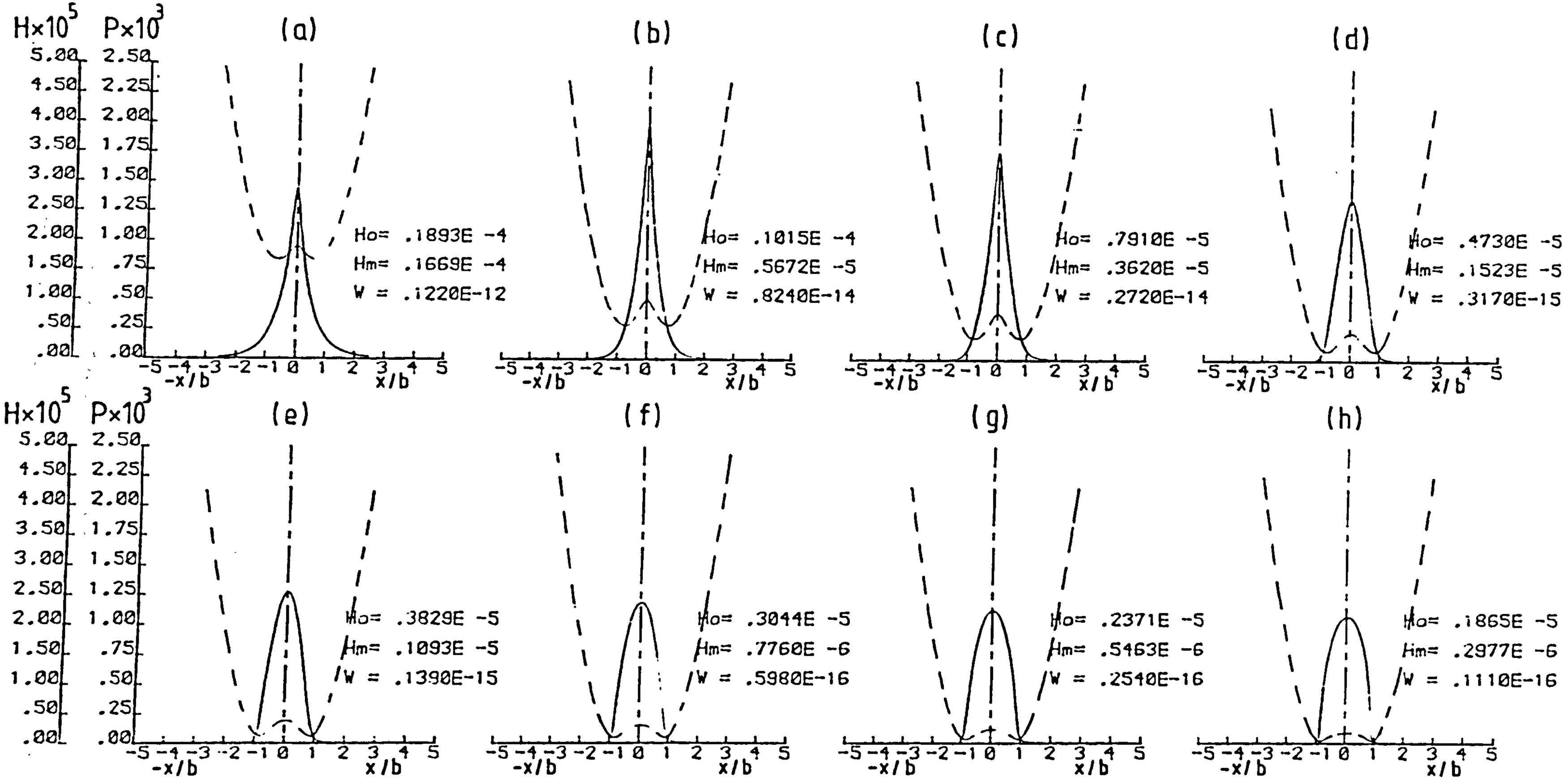

FIGURE(5 - 3) Pressure Distributions(——) and Film Shapes(— — —) for Elastic Cylinders With Squeeze Film Action Under the Influence of a Constant External Load in the Presence of a Piesoviscous Fluid
(L=10)

For the isoviscous lubrication case (L=0.0), Figure (5.1), the change in the form of the pressure curve as the dimensionless central film thickness (H_o) is decreased is clearly seen. As the dimensionless film thickness (H_o) is reduced, the pressure distribution converges to the Hertzian pressure distribution for dry contact corresponding to the load applied.

For the piezoviscous lubrication cases (L=5,10), Figures (5.2) and (5.3), the change in the pressure gradient near the centre of contact is quite different compared with the isoviscous case. Namely, at high dimensionless central film thickness the pressure gradient in the central region is far steeper than that shown in Figure (5.1) and a sharp pressure spike is produced at the centre. After the pressure spike reaches a certain maximum value the pressure gradient near the centre reverses its trend and begins to decrease. As the central film thickness (H_o) is further reduced the pressure spike is decreased and the pressure distribution converges towards the Hertzian pressure distribution for dry contact corresponding to the load applied.

Figure (5.4) is a plot of the maximum dimensionless pressure parameter $\left[\bar{P}_o \left(\frac{1}{\bar{F}}\right)^{1/2}\right]$ versus the dimensionless parameter $\left(\frac{H_o}{\bar{F}}\right)$. For the isoviscous lubrication case, (L=0.0), the central pressure gradually increases whilst decreasing the central film thickness and according to Herrebrugh's (1970) and Christensen's (1961) findings it will never exceed the Hertzian value of (0.41). On the other hand, for the piezoviscous lubrication case (L=5,10), the central pressure gradually increases with decreasing central film thickness, and then increases sharply to a maximum value. For

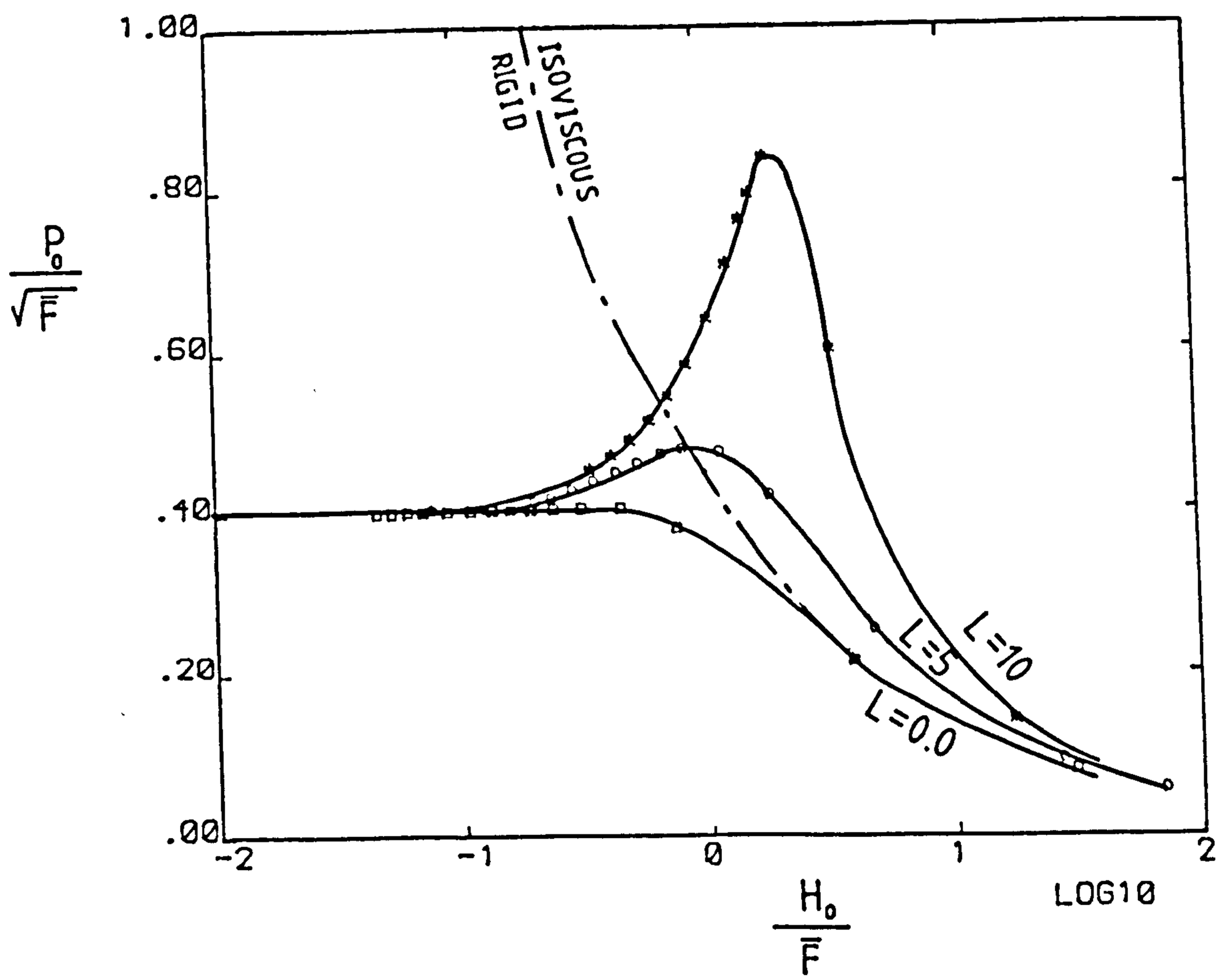

FIGURE(5 - 4) Variation of the Central Pressure for Elastic Cylinders With Squeeze Film Action in the Presence of Isoviscous(L = 0.0) and Piezoviscous(L = 5 , L = 10) Fluids.

a further decrease in the central film thickness the central pressure decreases rapidly and finally approaches the Hertzian value of (0.41), which is confirmation of Christensen's results. Furthermore, as (L) increases the maximum value of the dimensionless central pressure parameter $\left[P_o\left(\frac{1}{\bar{F}}\right)^{1/2}\right]$ is increased, e.g., the value predicted with (L=10) is twice the Hertzian value.

In connection with the above discussion, it can be noted that, when considering constant viscosity and rigid solids, the maximum pressure predicted is very high when the film thickness approaches zero. However the more elaborate theory taking account of elastic deformations has shown that the pressure remains finite and approaches the Hertzian value. When the most practical case of variable viscosity and elastic cylinders was considered, limited pressures in excess of the Hertzian pressure were generated in the oil film. This fact should be considered in the design of rolling element bearings where the contact stress levels are deemed to have a significant effect upon bearing life.

The central pressure results obtained for constant load in the presence of a piezoviscous fluid, ignoring the compressibility effect and the local deformation velocity, were compared with those of Lee and Cheng (1973) which considered both effects (Figures (5.5) and (5.6)). The central to Hertzian pressure ratio $\left(\frac{P_o}{P_{oh}}\right)$ is plotted against dimensionless central film thickness (H_o). Two values of the dimensionless load ($\bar{F}$) were used with the same value of the material parameter (G). The deviation was found to be about five percent (5%). That is, the pressure is only slightly influenced by ignoring the local deformation velocity and fluid

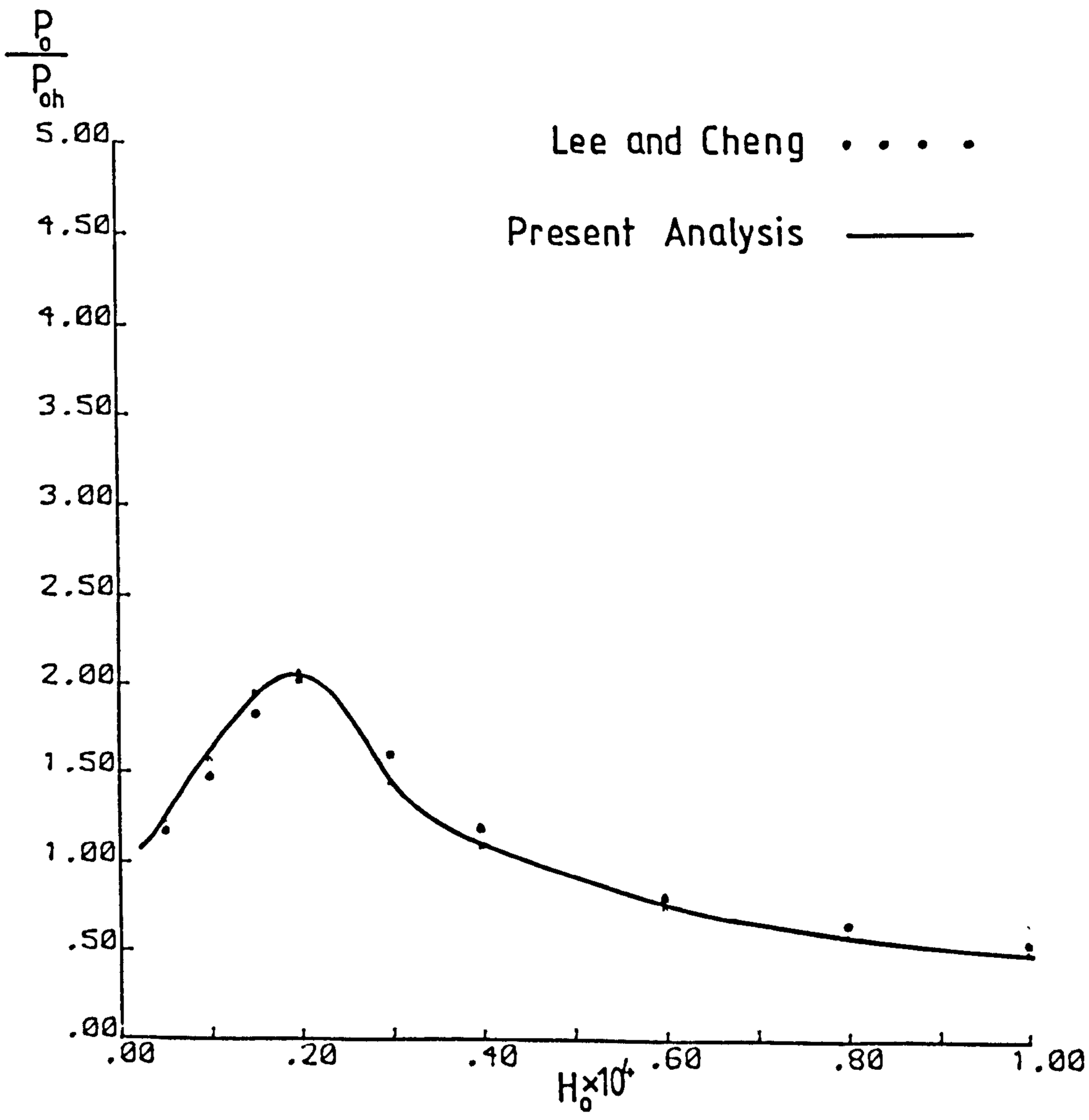

FIGURE(5 - 5) Comparison of the Central Pressure for Elastic Cylinders With Squeeze Film Action in the Presence of a Piezoviscous Fluid
$\bar{F}=10^{-5}$, $\theta=3180$

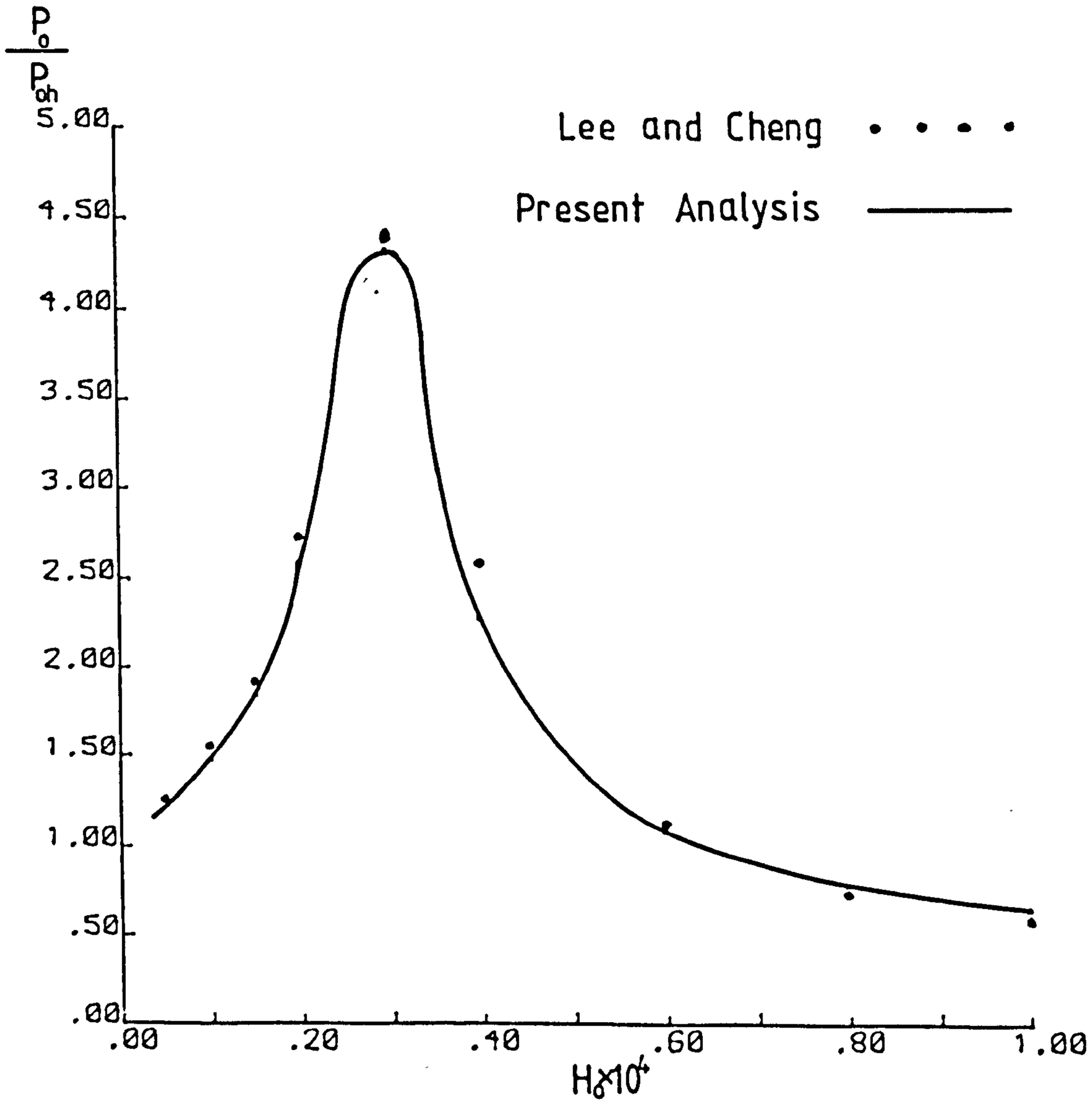

FIGURE(5 - 6) Comparison of the Central Pressure For Elastic Cylinders With Squeeze Film Action in the Presence of a Piezoviscous Fluid
$F = 1.25 \times 10^{-5}$, $\theta = 3180$

compressibility. However, it is recognized that the non-uniform velocity of approach assumption in elastohydrodynamic squeeze film problems may have serious effects on the solution at small separations. However, calculations in this region are extremely difficult and in situations where the combined effect of squeeze film and rolling is considered, such extremely small film thickness may not be of interest. In such cases it may be possible to proceed on the basis of the simple solution considering a uniform deformation velocity.

5.4 Film Thickness

The film thickness shapes are shown in conjunction with the corresponding pressure distributions in Figures (5.1), (5.2) and (5.3). The film shape is always symmetrical about the (z) axis. At an early stage of normal approach, an elastic dimple or pocket is formed at the centre of contact. As shown in Figures (5.7) and (5.8) the pocket depth increases sharply with decreasing central film thickness (H_o) until the maximum central pressure value occurs. For subsequent reductions of the central film thickness (H_o) the pocket depth decreases continuously. At the same time the region between the minimum film thickness and the centre line is gradually flattened. Eventually the film profile seems to approach the Hertzian shape for dry contact. In general the dimple becomes deeper and wider as the load increases and it is more pronounced in the piezoviscous than in the isoviscous case. The dimple width is approximately equal to the Hertzian contact width based on the same applied load. At high values of the dimensionless central film thickness (H_o) the minimum film thickness (H_m) is found at $\left(\frac{x}{b} = 0.0\right)$,

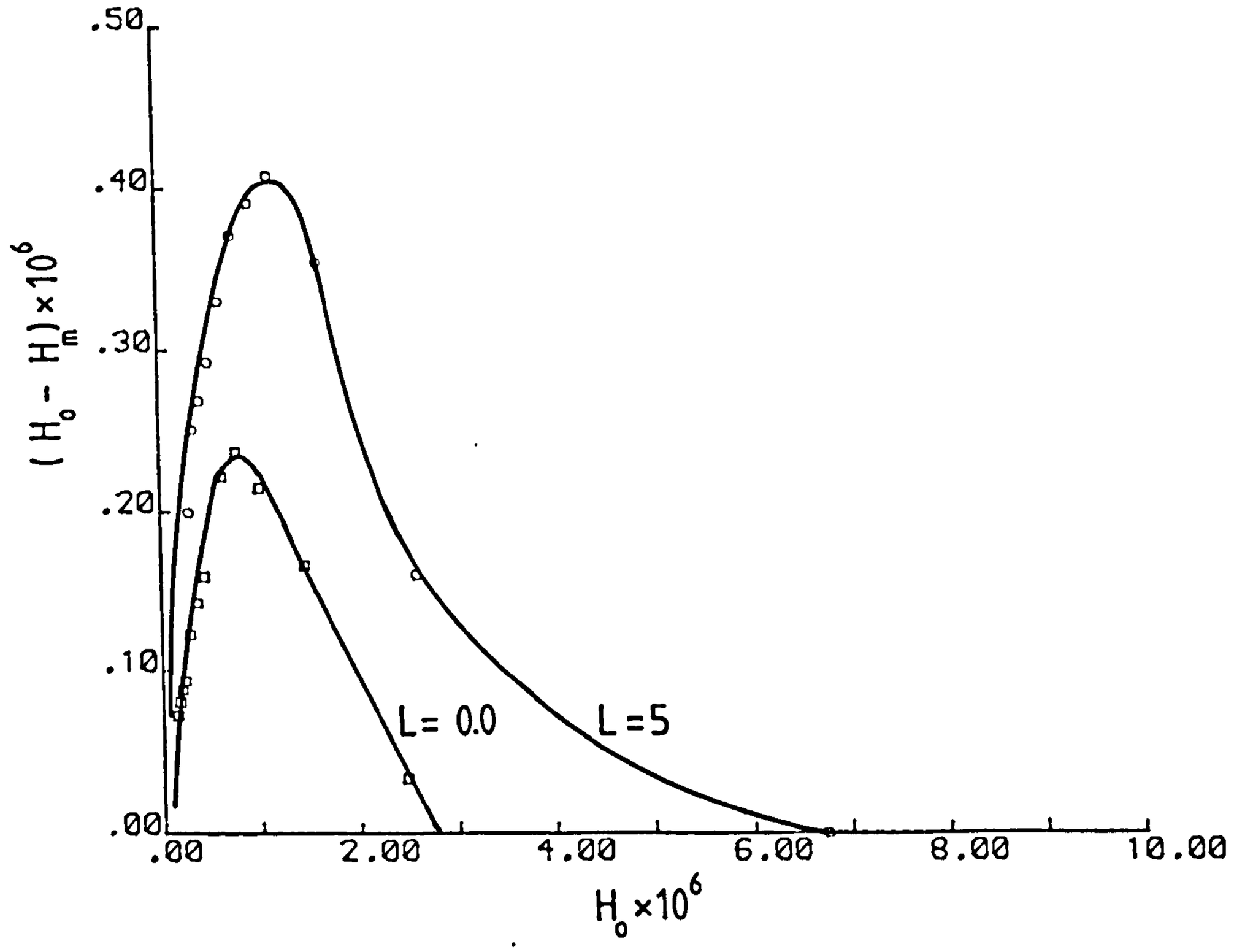

FIGURE(5 - 7) Variation of the Dimple Depth For Elastic Cylinders With Squeeze Film Action in the Presence of Isoviscous(L = 0.0) and Piezoviscous(L = 5) Fluids.

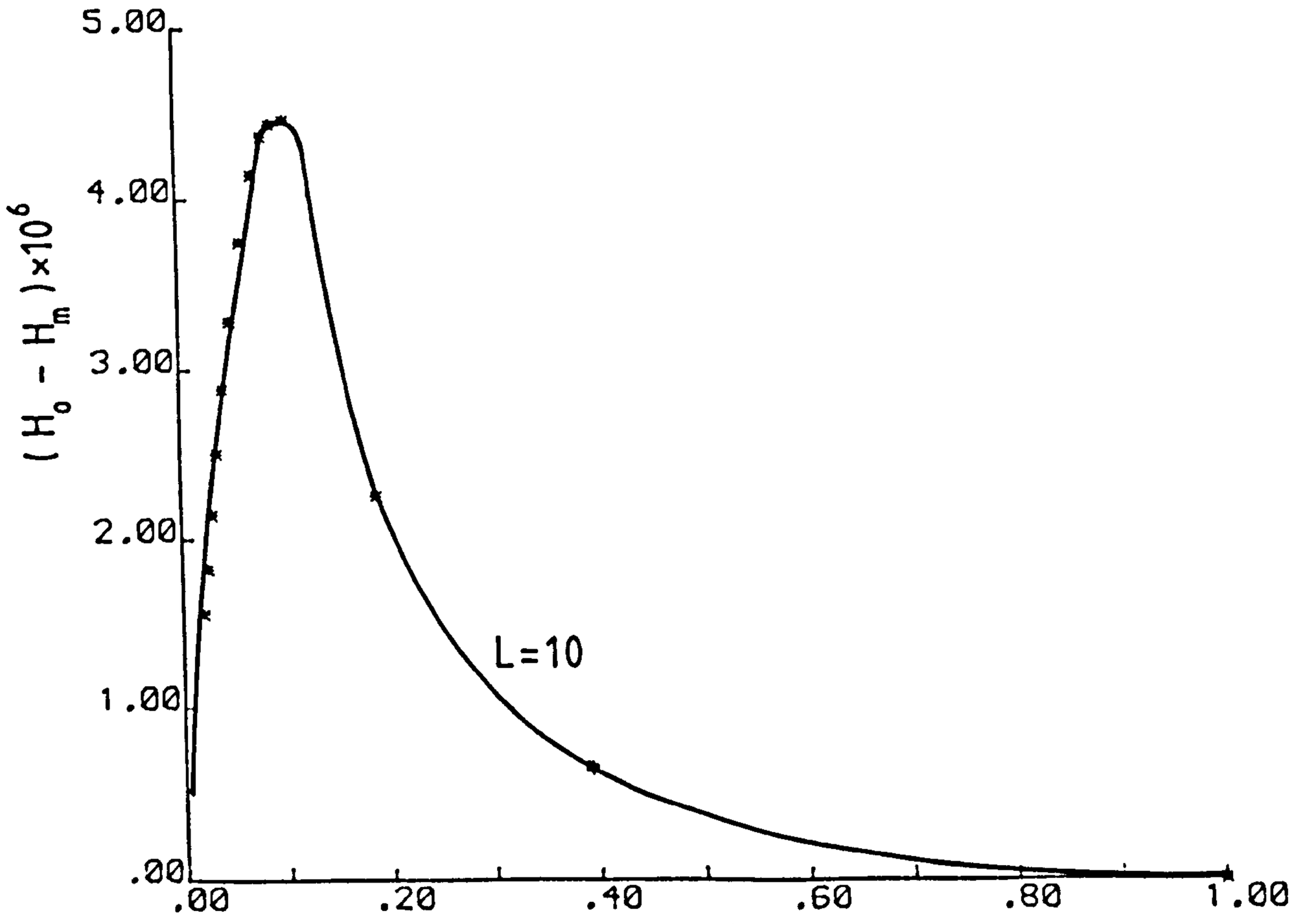

FIGURE(5 - 8) Variation of the Dimple Depth For Elastic Cylinders With Squeeze Film Action in the Presence of Piezoviscous Fluid

whereas at low values of (H_o) the minimum film thickness (H_m) is found close to $\left(\frac{x}{b} = 1, -1\right)$.

Due to lack of knowledge about the final stage of approach where solid-to-solid contact occurs, the formation of the dimple and the corresponding pressure distribution is still a subject of debate. Christensen arrived at a result which showed that the pressure and film thickness distributions approach the Hertzian case as a limit. Whereas, Lee and Cheng arrived at the conclusion that the pressure and film thickness distributions did not approach the Hertzian case in the limit but the entrapment of a pocket of lubricant occurred. Experiments indicate that entrapment takes place (Dowson and Jones (1967) and Gaman and Higginson (1974)), but theoretical studies cannot yet give a satisfactory explanation for perfectly smooth solids and Newtonian fluids.

Christensen defended his view by saying that the theory deals with a dynamic situation, i.e., the lubricant is flowing through the contact, and the general pressure and pressure gradient are connected with this flow. Entrapment, on the other hand, implies static conditions; no flow, and, for a Newtonian fluid, a constant pressure over the whole contact area. Such a distribution is not compatible with the maintenance of the central fluid pocket. It is therefore very difficult to see how the static entrapment situation can be the asymptotic limit of the elastohydrodynamic squeeze film motion. Now the Hertzian pressure distribution will elastically just remove the cylinder's curvature to make the contact zone flat and this is quite compatible with the elastohydrodynamic situation. To explain the discrepancy between the experiment and the theory, Christensen suggested that the lubricant may solidify

under the very high pressures existing in the final stage. In some circumstances pressure peak reaches quite high values, the boundary material yields and starts to flow at the centre of contact thereby producing a "plastic dimple".

Lee and Cheng acknowledged that the lubricant will not reach a uniform static pressure immediately after the entrapment. But the pressure and deformation profile will undergo extremely slow adjustment after the outer edge of the dimple makes contact such a condition is analogous to flow of an extremely viscous fluid inside an enclosed narrow gap with compliant walls.

With regard to the above discussion and the experimental evidence, it may be said that for real, rough surfaces and Newtonian fluids partial contact occurs at asperity contacts in the final stage of approach. The trapped lubricant is subjected to very high pressures, slow leakage will take place across the ring of apparent contact. After a long enough time the elastic indentation disappears and Hertzian contact conditions will be approached.

The minimum film thickness (H_m) is the most important quantity, with respect to the risk of metallic contact. The relationship between the parameters $\left(\frac{H_m}{H_o}\right)$ and $\left(\frac{H_o}{\bar{F}}\right)$ is shown in Figure (5.9). Under the same applied load, the deviation from the rigid-solid case $\left(\frac{H_m}{H_o} = 1\right)$ appears to start at a relatively larger film thickness in the presence of a piezoviscous fluid than that in the presence of an isoviscous fluid. Moreover, the pressure-dependent effect decreases the ratio $\left(\frac{H_m}{H_o}\right)$, thus a deeper dimple is produced.

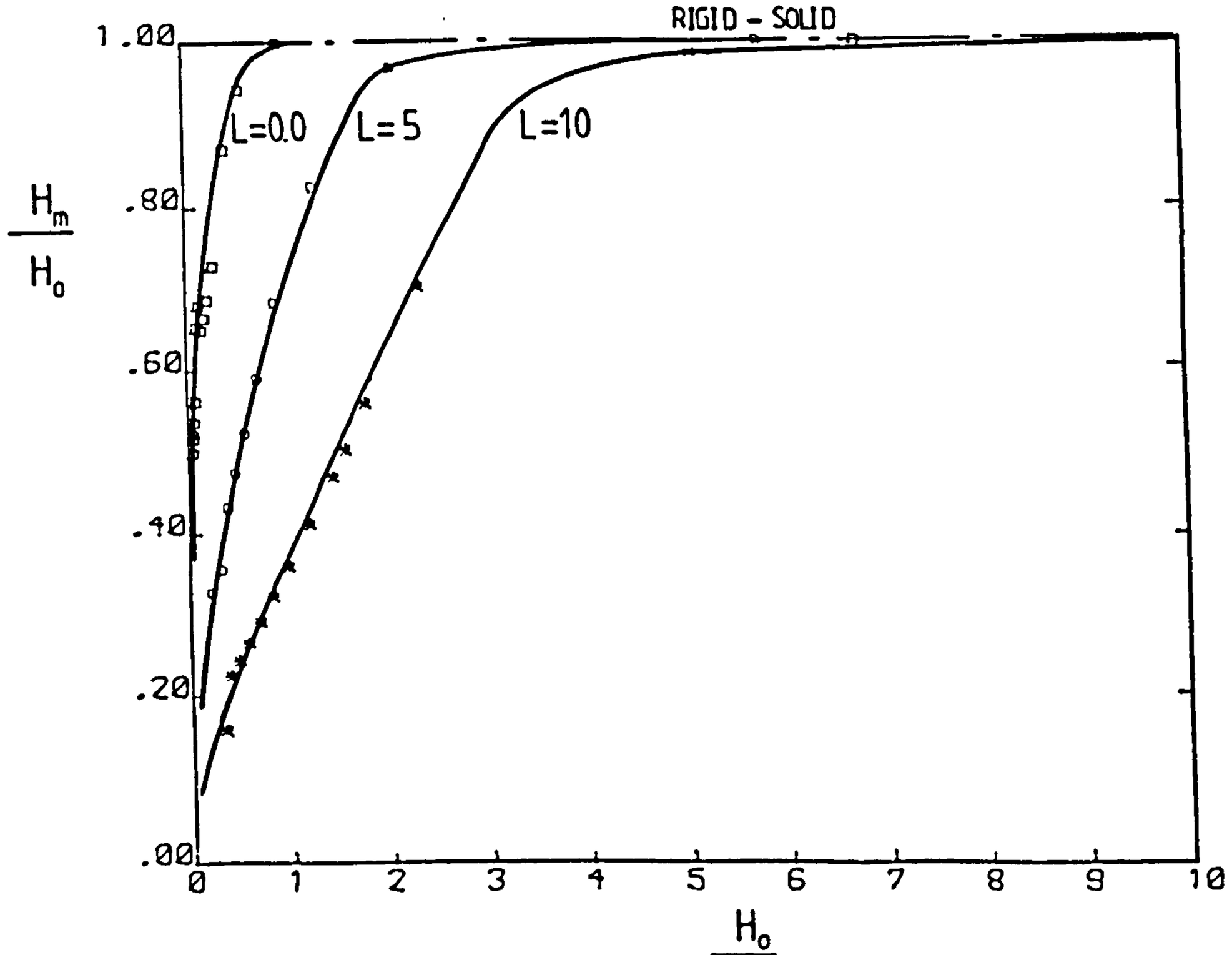

FIGURE(5 - 9) Variation of the Minimum Film Thickness for Elastic Cylinders With Squeeze Film Action in the Presence of Isoviscous(L=0.0) and Piezoviscous(L= 5 , L=10) Fluids.

5.5 Velocity of Approach

The variation of the dimensionless velocity of approach ($\bar{W}$) can be obtained from Figure (5.10). This figure represents the relationship between the dimensionless parameters $\left(\frac{H_o}{\bar{F}}\right)$ and $\left(\frac{\bar{W}}{\bar{F}^{5/2}}\right)$ at different values of the dimensionless parameter (L). It may be observed that, as the dimensionless parameter $\left(\frac{H_o}{\bar{F}}\right)$ is reduced, the dimensionless velocity of approach decreases. At the same applied load, the cylinder deceleration increases as the dimensionless parameter (L) increases. At high values of the dimensionless parameter $\left(\frac{H_o}{\bar{F}}\right)$ the solutions approach the rigid isoviscous case i.e., the asymptote,

$$\frac{H_o}{\bar{F}} = 5.62 \left(\frac{\bar{W}}{\bar{F}^{2/5}}\right)^{2/3}$$

Or, in terms of the physical quantities,

$$\frac{h_o}{R} = 5.62 \left(\frac{\eta_o W}{F}\right)^{2/3}$$

in which the equivalent modulus of elasticity (E') is not present.

Figure (5.11) represents the relationship between the dimensionless parameters $\left(\frac{H_o}{\bar{W}^{2/5}}\right)$ and $\left(\frac{\bar{F}}{\bar{W}^{2/5}}\right)$ according to the relationship (5.5). For low values of the load parameter $\left(\frac{\bar{F}}{\bar{W}^{2/5}}\right)$, relationship (5.5) approaches the asymptote,

$$\frac{H_o}{\bar{W}^{2/5}} = 5.62 \left(\frac{\bar{F}}{\bar{W}^{2/5}}\right)^{-2/3}$$

A very interesting feature of the functional relation (5.5), when the dimensionless parameter (L) is zero, is the fact that in the presence of an isoviscous fluid at the same film

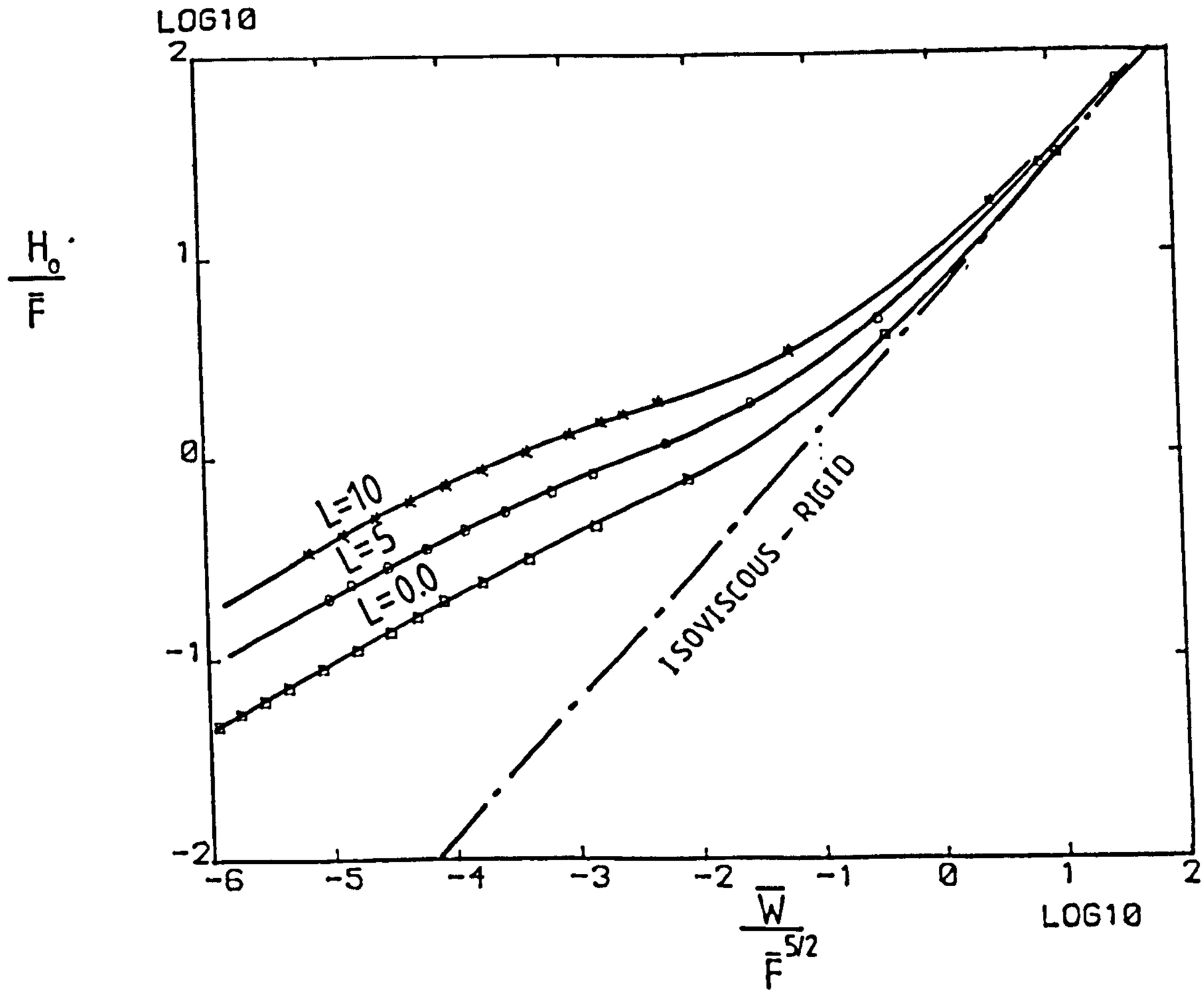

FIGURE(5 - 10) Variation of the Approach Velocity For Elastic Cylinders With Squeeze Film Action in the Presence of Isoviscous(L = 0.0) and Piezoviscous(L = 5 , L = 10) Fluids.

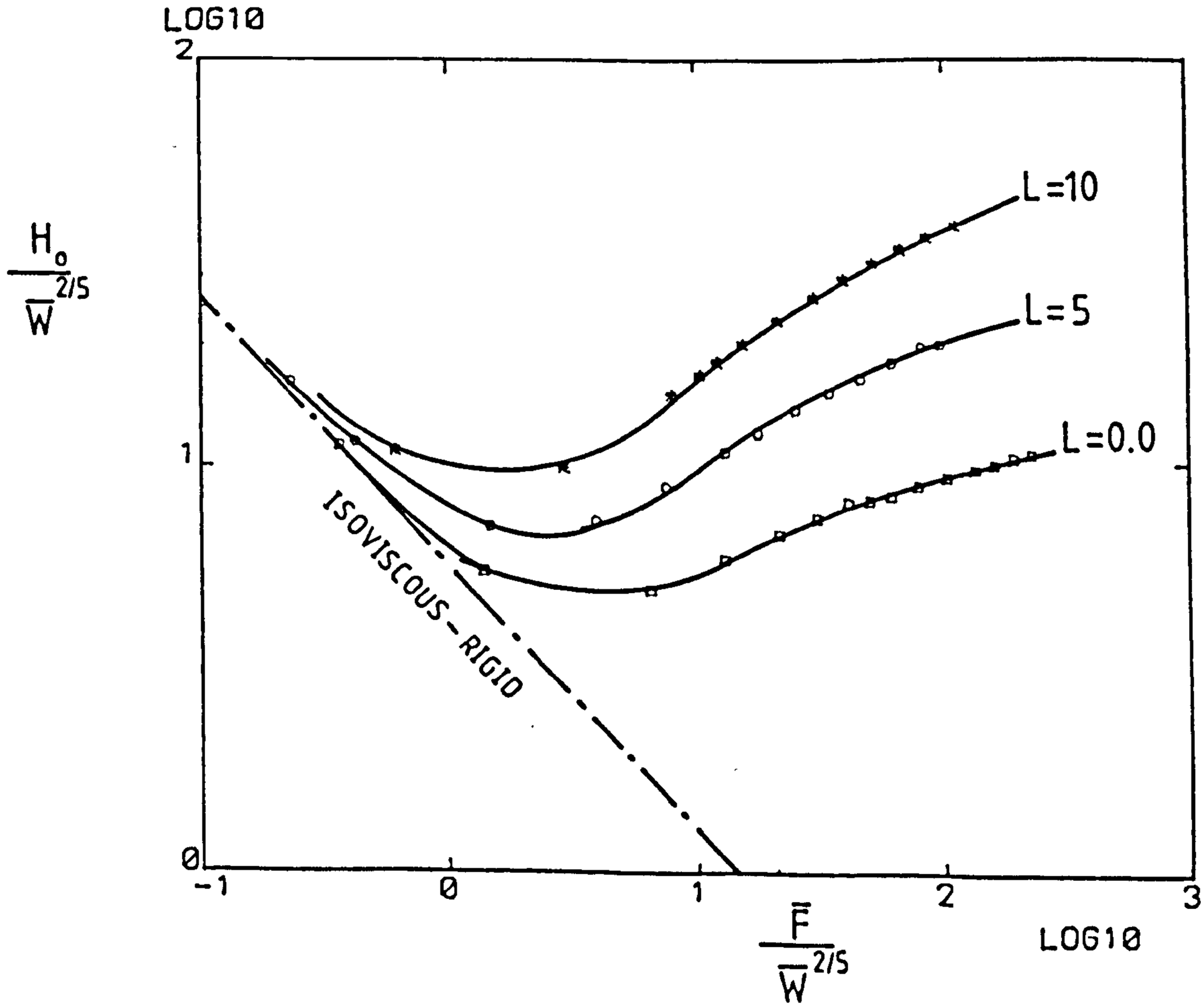

FIGURE(5 - 11) Bifurcation Phenomenon

thickness (H_o), the same velocity of approach (W) can be obtained by the application of two different loads. This is the bifurcation phenomenon that Herrebrugh observed and demonstrated mathematically in his solution for isoviscous lubrication via one single integral equation. this phenomenon can be explained by a "mental experiment" suggested by Christensen as follows. At constant (h_o), the velocity is varied by changing the load on the cylinders. At a small load the velocity of the mass centre of the cylinder will be small but so will the deformation velocity. In a repeat of the experiment with a large load the velocity of the mass-centre will be larger but so will the deformation velocity. The approach velocity being the difference between the absolute velocity of the rigid cylinder and the deformation velocity may still be small. It may in fact have the same value as in the first case.

With respect to the piezoviscous lubrication, it cannot be proved from the computation whether or not bifurcation might occur.

5.6 Concluding Remarks

The problem of the elastohydrodynamic squeeze film lubrication of line contacts has been investigated extensively in this chapter. The results have been evaluated for both isoviscous and piezoviscous fluids under prescribed loads. Graphical representations of pressure distributions and film shapes have been presented together at successive reductions of the central film thickness. The variation of the dimensionless minimum film thickness (H_m), velocity of approach ($\bar{W}$) and central film pressure (P_o) were included. The results described have been shown to

provide good agreement with results obtained by previous solutions.

From the analysis of the elastohydrodynamic squeeze film lubrication of line contacts the following conclusions may be drawn.

1. With constant viscosity, the maximum pressure in the film cannot exceed the Hertzian pressure corresponding to the applied load. With pressure dependent viscosity, however, the maximum film pressure can be very much larger than the corresponding Hertzian pressure.

2. For constant and variable viscosity solutions an elastic dimple is formed in the centre of the contact during the early stage of the normal approach. The depth of the dimple increases sharply with decreasing central film thickness (H_o) until the maximum central pressure value occurs. For subsequent reductions of the central film thickness the pocket depth decreases continuously. At the same time the region between the minimum film thickness and the centre line is gradually flattened. Subsequently the film profile and pressure distribution tend towards the Hertzian solutions for dry contact.

3. The effect of the local deformation velocity and the fluid compressibility upon the pressure may be ignored within the practical range of the minimum film thickness. However, it is recognized that the non-uniform velocity assumption may have greater significance at small separations. However, calculations in this region are extremely difficult.

4. In the presence of an isoviscous fluid, the same velocity of approach can be obtained by the application of two different loads at the same central film thickness. This is known as the bifurcation phenomenon.

CHAPTER 6

A THEORETICAL STUDY OF THE LUBRICATION OF RIGID CYLINDERS IN COMBINED ROLLING AND NORMAL MOTION

6.1 Introduction

The lubrication of rigid cylinders has attracted the attention of tribologists throughout this century because of its practical applications in the lubrication of lightly loaded rolling element bearings and involute spur gears. Theoretical solutions have been presented by several authors for rolling, rolling with sliding or normal approach (e.g. Martin (1916) and Christensen (1961)).

Sasaki et al (1962) presented a solution for the isothermal lubrication of rigid cylinders subjected to sinusoidal loading by using superposition of pressure curves generated by normal motion and entraining velocities. Appropriate boundary conditions for the film rupture in the exit were not satisfied. This solution was developed for a Bingham plastic which, at high speeds, would behave as a Newtonian-lubricant.

Vichard (1971) examined the phenomenon of viscous damping, both under hydrodynamic and elastohydrodynamic contact conditions. The principle governing variables, such as load, temperature, radius of curvature and speed, were varied in turn in a time-dependent manner and their effects were investigated. It was concluded that the damping phenomenon due to normal motion had a more substantial effect under elastohydrodynamic contact conditions than with rigid solids.

Dowson, Markho and Jones (1976) presented a general theoretical analysis of the hydrodynamic lubrication of rigid

cylinders by an isoviscous lubricant in combined rolling and normal motion. Results showed that normal motion significantly influenced the load-carrying capacity of the contact. The location of the film rupture boundary was also observed to have a significant effect upon the pressure distribution when the results were compared with the findings of Sasaki et al (1962). Moreover, it was concluded that when sinusoidal normal motion was superimposed upon 'entraining' motion, a substantial increase in the net load carrying capacity was obtained.

In the present chapter, the effect of squeeze film action due to normal motion combined with entraining action due to pure rolling has been investigated for rigid cylinders. The results were evaluated for both isoviscous and piezoviscous lubrication conditions under constant and sinusoidal normal loading.

Graphical representations of pressure distributions are presented for both normal approach and separation. The variation of the normal motion velocity and peak pressure at different values of the central film thickness are included. Moreover, the time history of the central film thickness under constant and sinusoidal normal loadings is introduced with discussion of the viscous damping phenomenon associated with the squeeze film action.

The results of this work for the isoviscous lubrication case have been compared with those developed by Vichard (1971) and Sasaki et al (1962) for sinusoidal loading. A good agreement was found.

The present investigation provides a proper foundation for the most practical case of the non-steady state elastohydrodynamic lubrication of line contacts considered later in Chapter (7). Further, the study of the piezoviscous lubrication of rigid cylinders in combined rolling and normal motion represents an extension of existing theories.

6.2 Dimensionless Parameters

The variables resulting from the theory of hydrodynamic lubrication of rigid cylinders by a piezoviscous lubricant in combined rolling and normal motion under sinusoidal loading are,

(R) effective radius of curvature, $\left[R = \frac{R_1 R_2}{R_1 + R_2}\right]$ (m)

(h_o) central film thickness (m)

(u) 'entraining' velocity (m/s)

(W) normal velocity of cylinder (in the direction (z)) (m/s)

($P_{iv,as}$) asymptotic isoviscous pressure obtained from Roelands (1966), $\left(\cong \frac{1}{\alpha}\right)$ (N/m^2)

(η_o) lubricant viscosity at atmospheric pressure ($N.s/m^2$)

(F_o) basic load of sinusoidal load (N/m)

(ω) time base (angular velocity of sinusoidal load) (s^{-1})

(f(t)) load function, (1 + a sinωt), dimensionless

(a) amplitude of sinusoidal load, dimensionless

(z) viscosity pressure index, a dimensionless constant

From the eleven variables mentioned above the following five dimensionless groups can be written:

(1) Dimensionless central film thickness parameter

$$H_o = \frac{h_o}{R}$$

(2) Dimensionless load parameter

$$\bar{F} = \frac{F}{u\eta_o}$$

(3) Dimensionless (normal/entraining) velocity parameter

$$\bar{q} = \frac{W}{u}$$

(4) Dimensionless parameter for pressure-viscosity dependency

$$\frac{\alpha\eta_o u}{R}$$

(5) Dimensionless damping parameter

$$D_p = \omega R \sqrt{\frac{\eta_o}{uF_o}}$$

It can be shown that a general solution for the hydrodynamic lubrication of rigid cylinders by a piezoviscous lubricant in combined rolling and normal motion under variable load depends upon four dimensionless groups only. These dimensionless groups consist mainly of the power products of the abovementioned dimensionless parameters. That is,

$$\pi_1 = H_o \bar{F} \tag{6.1}$$

$$\pi_2 = \frac{W}{u}\sqrt{\bar{F}} \tag{6.2}$$

$$\pi_3 = \frac{\alpha F^{3/2}}{R\sqrt{u\eta_o}} \tag{6.3}$$

$$\pi_4 = \omega R \sqrt{\frac{\eta_o}{u F_o}} \tag{6.4}$$

and the general solution of the problem is given by the relationship,

$$\pi_1 = \phi(\pi_2, \pi_3, \pi_4)$$

or

$$H_o\bar{F} = \phi\left(\frac{W}{u}\sqrt{\bar{F}},\ \frac{\alpha F^{3/2}}{R\sqrt{u\eta_o}},\ \omega R\sqrt{\frac{\eta_o}{u F_o}}\right) \tag{6.5}$$

In the case of constant applied external load the function (f(t)) is equal to unity. Moreover, the time base (ω) must be chosen as

$$\omega = \frac{1}{R}\sqrt{\frac{u F_o}{\eta_o}} \tag{6.6}$$

Thus the damping parameter (D_p) is equal to unity and the relationship (6.5) reduces to a simple one between three dimensionless groups. Therefore,

$$H_o\bar{F} = \phi\left[\frac{W}{u}\sqrt{\bar{F}},\ \frac{\alpha F^{3/2}}{R\sqrt{u\eta_o}}\right] \tag{6.7}$$

Consequently, it is seen that in the isoviscous case $\left[\frac{\alpha F^{3/2}}{R\sqrt{u\eta_o}} = 0\right]$ the two-dimensional functional relation (6.7) reduces to a simple relationship between two dimensionless groups.

In the present results the dimensionless parameter (L) will be used to identify the isoviscous and piezoviscous lubrication regimes, where,

$$\bar{L} = \frac{\alpha F^{3/2}}{R\sqrt{u\eta_o}} \tag{6.8}$$

the dimensionless pressure (P) is defined as $\left(\frac{pR}{u\,\eta_o}\right)$ and the dimensionless time is (ωt). The sinusoidal normal loading is

assumed to have the following form,

$$F = F_o (1 + a \sin \omega t) \qquad (6.9)$$

6.3 Pressure Profile Under Constant Load

The numerical results obtained for the dimensionless pressure parameter $\left[P(\bar{F})^{-3/2} = \frac{pR}{u\eta_o} \left(\frac{F}{u\eta_o} \right)^{-3/2} \right]$ distributions for normal approach, separation and pure rolling under constant load are illustrated in figures (6.1) and (6.2). five values of the dimensionless parameter $(H_o\bar{F})$ are used, that is, the two values $(H_o\bar{F} = 30, 15)$ to represent the normal approach case, the two values $(H_o\bar{F} = 1, 2)$ to represent the separation case and the value $(H_o\bar{F} =$ the pure rolling value) to represent the steady state case of pure rolling. The dimensionless quantity $\left(\bar{L} = \frac{\alpha F^{3/2}}{R\sqrt{u\eta_o}} \right)$ is used as a parameter in these figures to express the lubrication regime. Two representative cases were considered, the values of the dimensionless parameter $(\bar{L})$ employed in the present results being $(\bar{L} = 0.0)$ to represent the isoviscous lubrication regime, Figure (6.1), and $(\bar{L} = 5.2)$ to represent the piezoviscous lubrication regime, Figure (6.2). All the physical data used in this study are given in table (6.1).

It can be observed for both types of lubrication that when the value of the dimensionless parameter $(H_o\bar{F})$ is greater than the corresponding pure rolling value, the pressure distribution is less in magnitude than that of the pure rolling case. Further the maximum pressure location approaches the position of $\left(\frac{X}{\sqrt{2H_o}} = 0.0 \right)$, i.e., the position with pure squeeze film action. As the value of $(H_o\bar{F})$ is reduced towards its corresponding pure rolling value

Table (6.1) Physical Data for Constant Load

Calculations

Load (F) = 800 (N/m)

Entraining velocity (u) = 4.89×10^{-4} (m/s)

Effective radius (R) = 0.02 (m)

$\bar{L} = \frac{\alpha F^{3/2}}{R\sqrt{\eta_o u}}$	Steady State Film Thickness (H_{oR})	Starting Film Thickness (H_o)	Starting ($\bar{F}\ H_o$)
0	0.11962×10^{-6}	7.536×10^{-7}	30
		3.768×10^{-7}	15
		5.024×10^{-8}	2
		2.512×10^{-8}	1
5.2	0.16414×10^{-6}	7.536×10^{-7}	30
		3.768×10^{-7}	15
		5.024×10^{-8}	2
		2.512×10^{-8}	1

Pressure-viscosity coefficient (α) = 2.058×10^{-8} (m^2/N)

Time base (ω) = $\frac{1}{R}\sqrt{\frac{uF_o}{\eta_o}}$ = 154.2 (s^{-1})

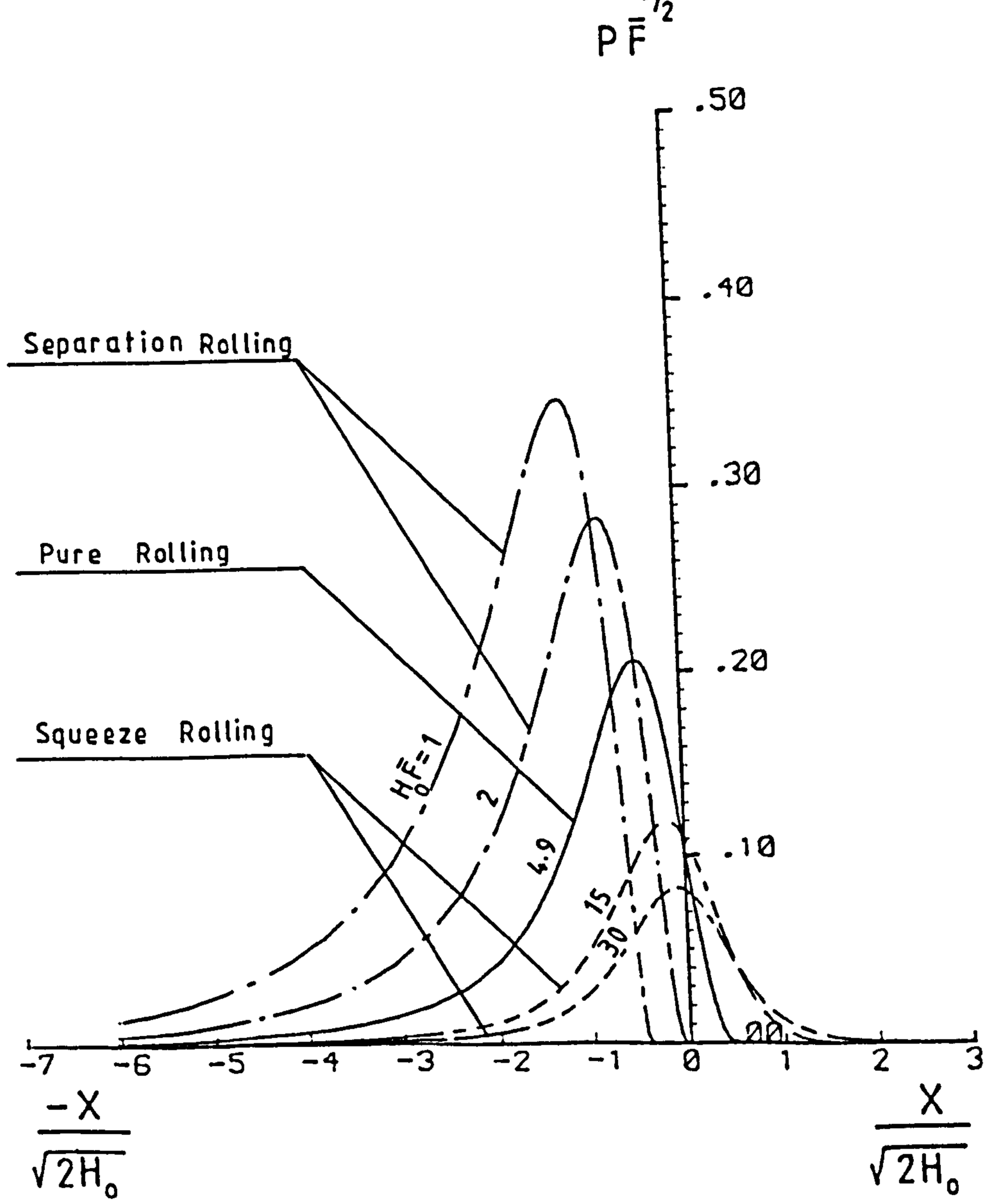

FIGURE(6 - 1) pressure Distribution For Rigid Cylinders in Combined Rolling and Normal Motion Under the Influence of a Constant Load in the Presence of an Isoviscous Fluid ($\bar{L}$= 0.0)

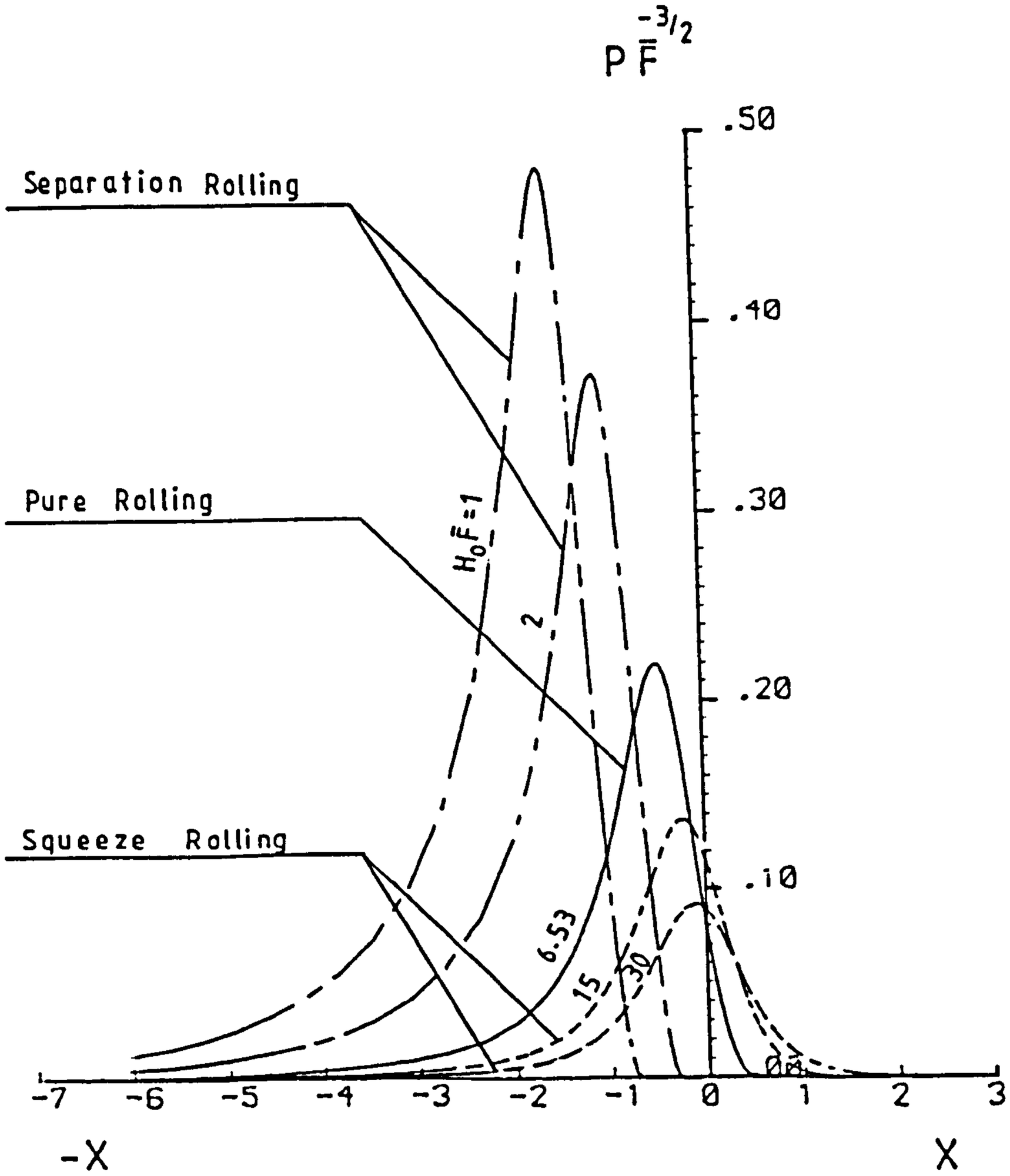

FIGURE(6 - 2) pressure Distribution for Rigid Cylinders in Combined Rolling and Normal Motion Under the Influence of a Constant Load in the Presence of a Piezoviscous Fluid ($\bar{L} = 5.2$)

'during normal approach', the position of oil film rupture in the divergent portion of the film gradually moves up-stream. When the value of $(H_o\bar{F})$ reaches its corresponding pure rolling value (e.g. for isoviscous lubrication according to Martin (1916), $H_o\bar{F} = 4.9$), the position of the film rupture and the position of maximum pressure are equi-distant (i.e. $\frac{X}{\sqrt{2H_o}} = 0.48, -0.48$ respectively) from the centre line $\left(\frac{X}{\sqrt{2H_o}} = 0.0\right)$.

At values of $(H_o\bar{F})$ less than that of the pure rolling value, the pressure magnitudes are much larger than those of pure rolling. The position of film rupture and the position of maximum pressure are in the convergent portion of the oil film. As the value of $(H_o\bar{F})$ is increased towards its corresponding pure rolling value 'during normal separation', the position of oil film rupture and the position of maximum pressure move down-stream gradually approaching their pure rolling positions.

In general with the same value of the dimensionless parameter $(H_o\bar{F})$, the pressure magnitude corresponding to isoviscous lubrication ($\bar{L} = 0.0$), Figure (6.1), is less than that of piezoviscous lubrication ($\bar{L} = 5.2$), Figure (6.2).

The variation of the peak pressure parameter $(P_k(\bar{F})^{-3/2})$ as a function of the dimensionless parameter $(H_o\bar{F})$ is shown in Figure (6.3), for the two values of the dimensionless parameter $(\bar{L})$, i.e., $(\bar{L} = 0.0, 5.2)$. Pressures of the order of twice the corresponding peak pressure in the steady state situation (pure rolling) are generated in the contact during 'normal separation'. In contrast, during 'normal approach', the peak pressure magnitudes never exceed

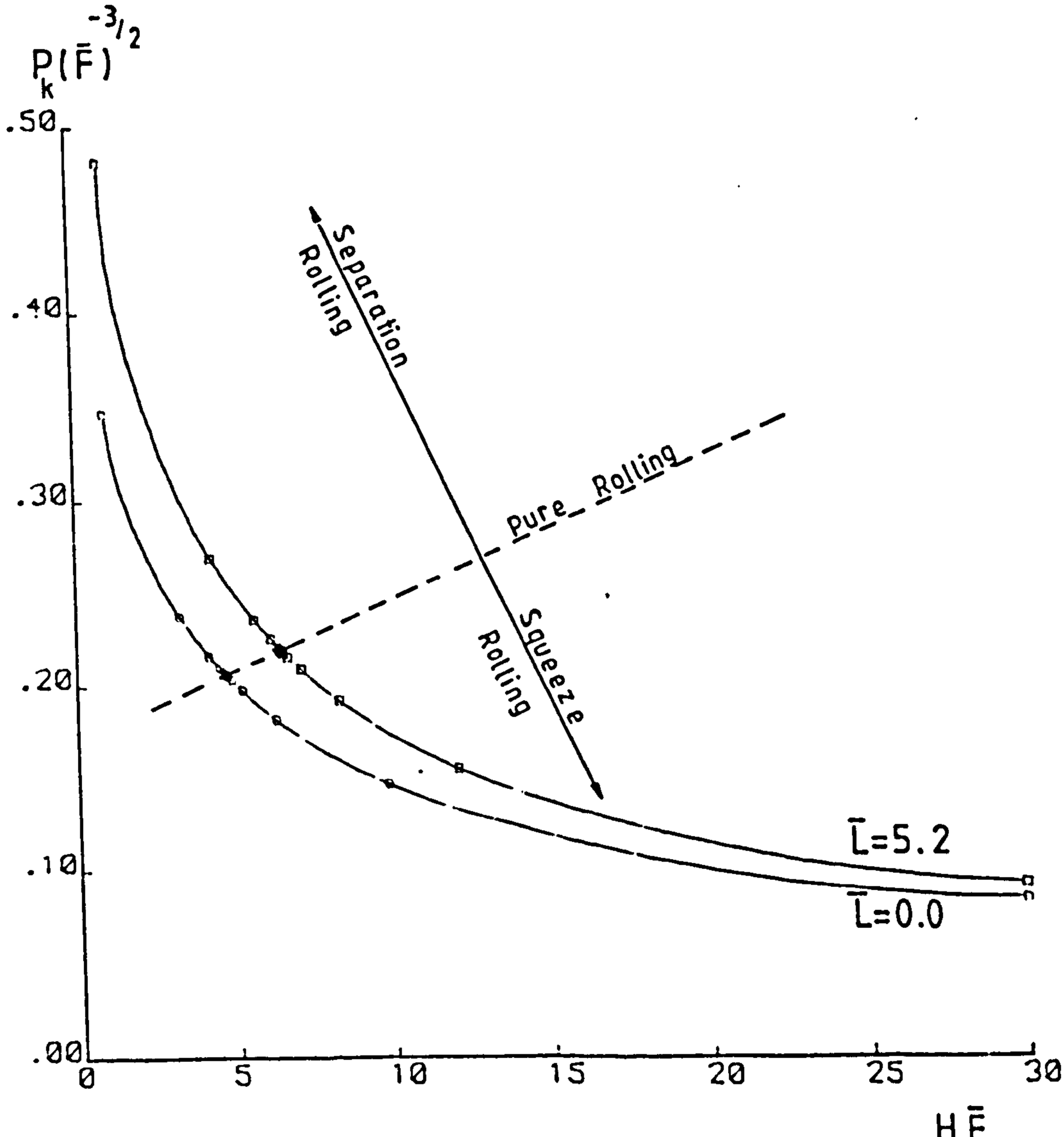

FIGURE(6 - 3) Variation of the Dimensionless Peak Pressure Parameter for Rigid Cylinders in Combined Rolling and Normal Motion Under the Influence of a Constant Load in the Presence of Isoviscous ($\bar{L}=0.0$) and Piezoviscous ($\bar{L}=5.2$) Fluids

the peak value of the steady state situation. Moreover, at the same value of $(H_o\bar{F})$ the peak pressure increases when the lubricant is taken to have pressure dependent viscosity.

6.4 Time History of Central Film Thickness Under Constant Load

A time history of the dimensionless central film thickness (H_o) when considering both isoviscous $(\bar{L} = 0.0)$ and piezoviscous $(\bar{L} = 5.2)$ lubrication is recorded in Figures (6.4) and (6.5) respectively. These figures display the variation of the dimensionless central film thickness parameter $(H_o\bar{F})$ with the dimensionless time (ωt), under a constant load, for both normal approach $(H_o\bar{F} = 30,15)$ and separation $(H_o\bar{F} = 1,2)$. It should be noted that the time base (ω) in this case is calculated by using equation (6.6) and has the value of $(154.2\ s^{-1})$.

For 'normal approach' the film thickness (H_o) decreases with the passage of time until it reaches the equilibrium at the pure rolling value (steady state condition). With 'separation' the trend is quite different, since the film thickness (H_o) increases with the passage of time until the equilibrium condition is reached.

The initial value of the dimensionless central film thickness parameter $(H_o\bar{F})$ and the dimensionless parameter $(\bar{L})$ have no significant effect on the time of damping (a time at the end of which (H_o) approaches its value of equilibrium within a range of five percent (5%)). The behaviour is determined by the time base (ω).

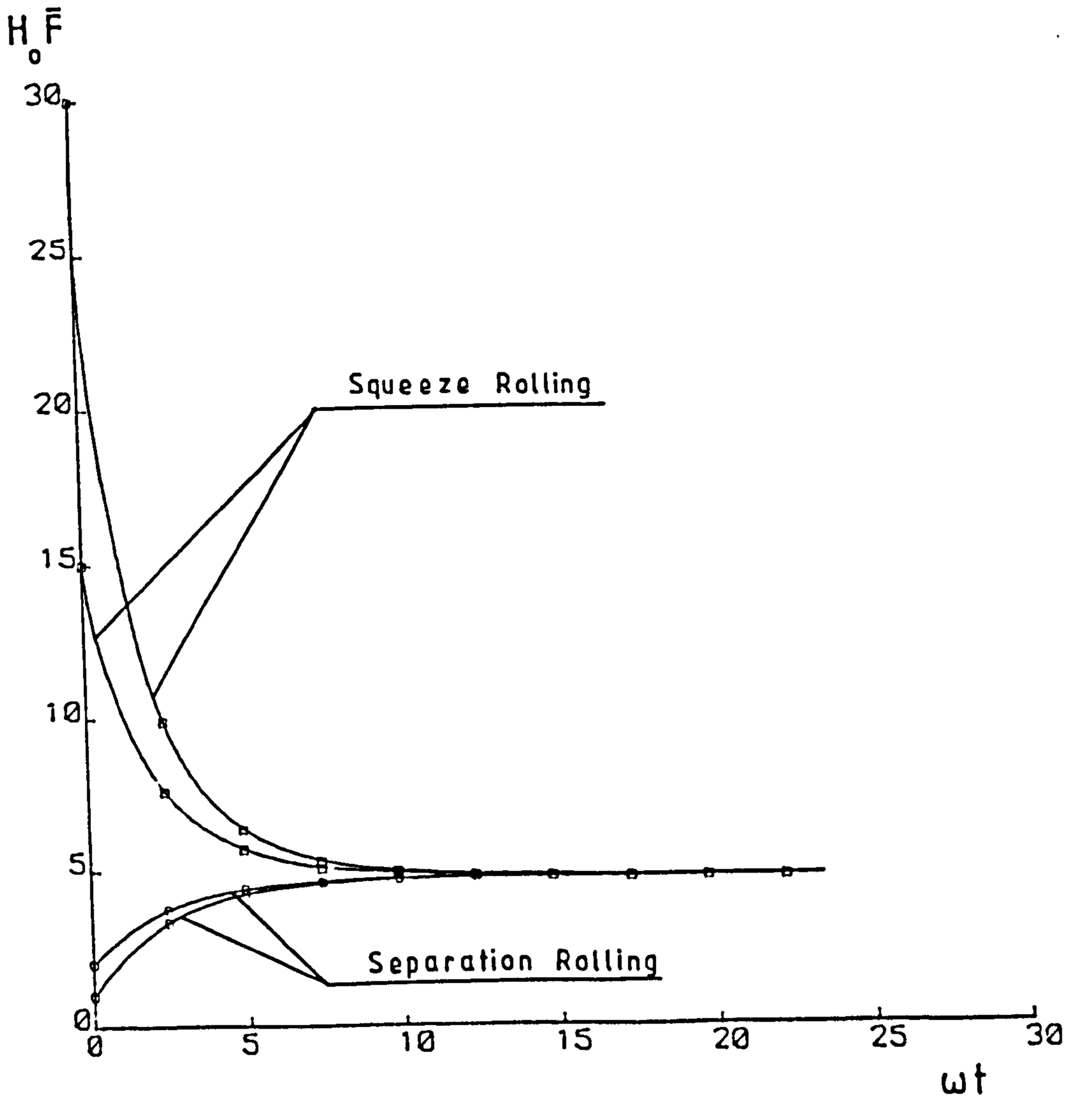

FIGURE(6 - 4) Time History of the Central Film Thickness for Rigid Cylinders in Combined Rolling and Normal Motion Under the Influence of a Constant Load in the Presence of an Isoviscous Fluid ($\bar{L}=0.0$)
($\omega=154.2\ s^{-1}$)

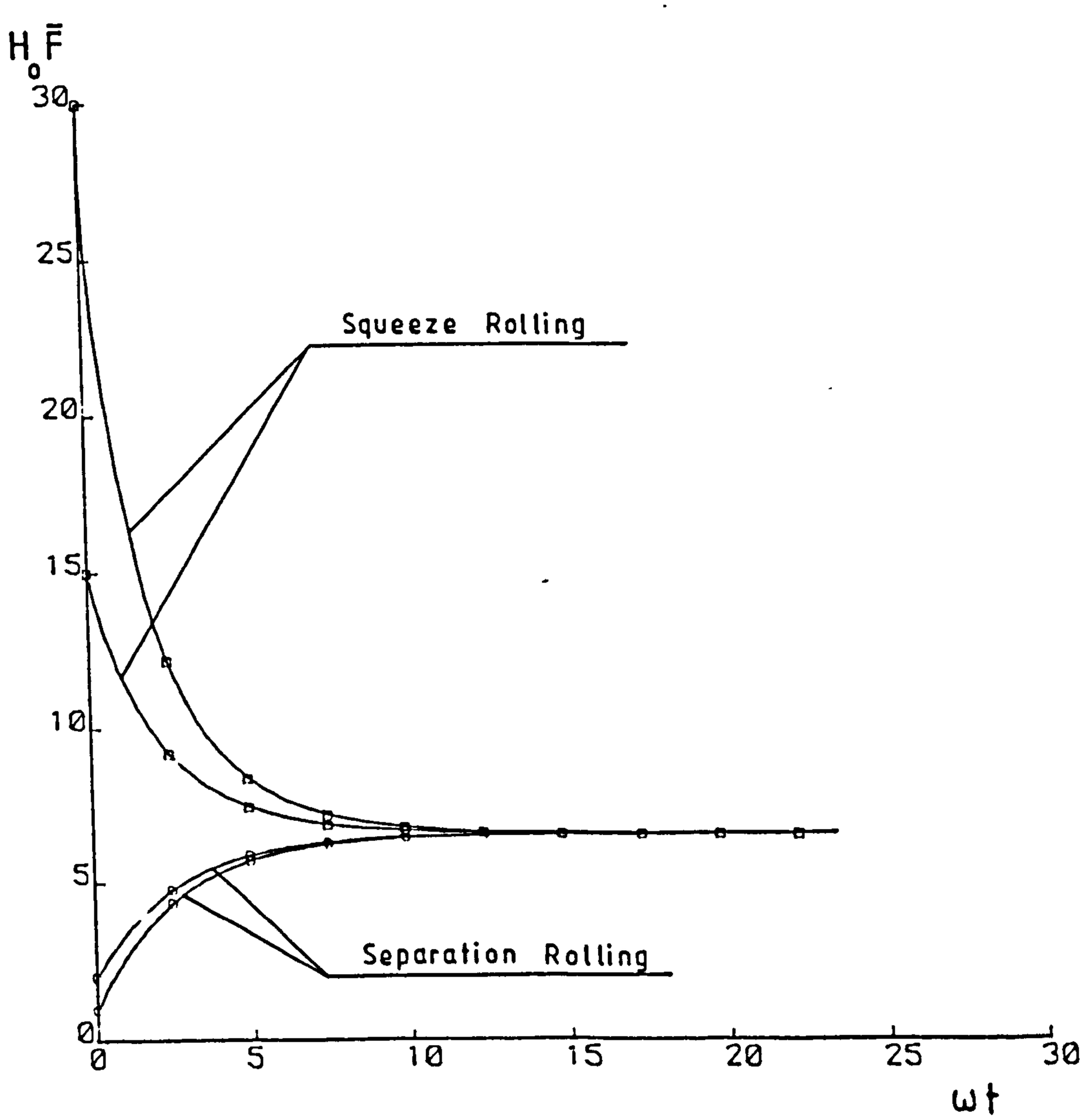

FIGURE(6 - 5) Time History of the Central Film Thickness for Rigid Cylinders in Combined Rolling and Normal Motion Under the Influence of a Constant Load in the Presence of a Piezoviscous Fluid ($\bar{L}=5.2$) ($\omega = 154.2\ s^{-1}$)

The motion is entirely similar to the motion of a one-degree-of-freedom vibratory system with viscous damping. Since the described motion is non-oscillatory the system is said to be overdamped.

The results for the isoviscous lubrication case ($\bar{L} = 0.0$) are in good agreement with the findings of Vichard (1971).

6.5 Normal Motion Velocity Under Constant Load

The variation of the velocity of the normal motion can be obtained from Figure (6.6). This figure represents the relationship between the dimensionless (normal/entraining) velocity parameter $\left(\frac{W}{u}\sqrt{\bar{F}}\right)$ and the dimensionless central film thickness parameter $(H_o\bar{F})$, under constant load, for both normal approach and separation. Two values of the dimensionless parameter $(\bar{L})$ are considered, the value $(\bar{L} = 0.0)$ to represent the isoviscous condition and the value $(\bar{L} = 5.2)$ to represent the piezoviscous condition.

It is clear that during 'normal approach' ($H_o\bar{F} > H_o\bar{F}$ (pure rolling)), as the dimensionless parameter $(H_o\bar{F})$ is reduced the velocity of approach decreases until a zero value is reached at the pure rolling condition. On the contrary, during 'normal separation' ($H_o\bar{F} < H_o\bar{F}$ (pure rolling)), as the dimensionless parameter $(H_o\bar{F})$ is increased, the velocity of separation decreases until reaching the zero value at the pure rolling condition.

Also, it can be seen that with the same applied load (F), entraining velocity (u) and the central film thickness (H_o) (points (A) and (B) on Figure 6.6)), the normal approach velocity (W) through the isoviscous fluid ($\bar{L} = 0.0$ & point (A)) is greater

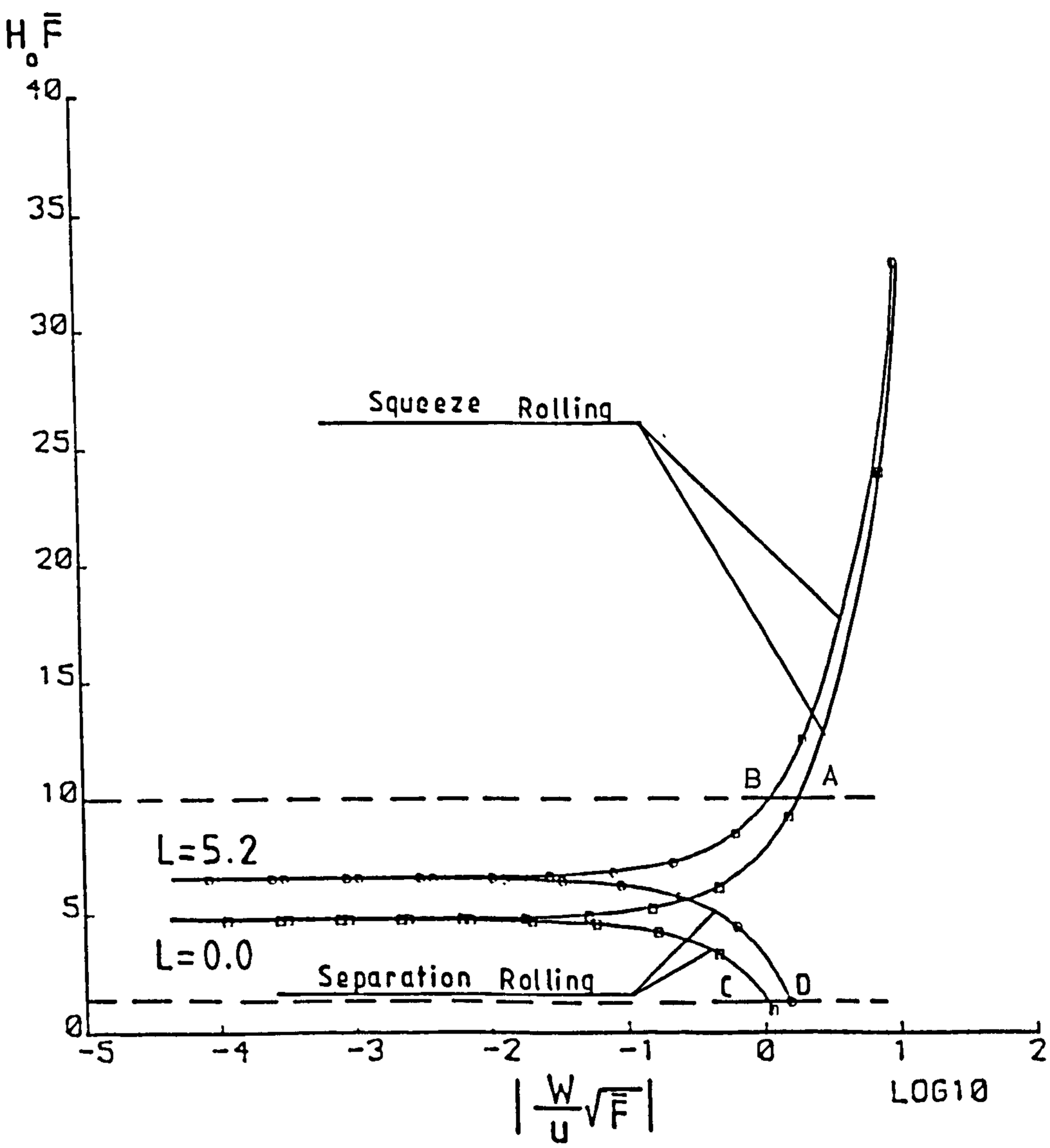

FIGURE(6 - 6) Variation of the Normal Motion Velocity for Rigid Cylinders in Combined Rolling and Normal Motion Under the Influence of a Constant Load in the Presence of Isoviscous ($\bar{L}=0.0$) and Piezoviscous ($\bar{L}=5.2$) Fluids

than that through the piezoviscous fluid ($\bar{L}$ = 5.2 & point (B)). Whereas, points (C) and (D) on Figure (6.6) show that under similar conditions, the normal separation velocity (W) through the isoviscous fluid ($\bar{L}$ = 0.0 & point (C)) is smaller than that through the piezoviscous fluid ($\bar{L}$ = 5.2 & point (D)).

6.6 Time History of Central Film Thickness Under Sinusoidal Normal Loading

The hydrodynamic lubrication response to sinusoidal loading of the form [$F(t) = F_o (1 + a \sin \omega t)$] is shown in Figures (6.7) to (6.12) and presented in Table (6.3). Each figure displays the variation of the dimensionless ratio $\left(\frac{H_o}{H_{oR}}\right)$ (i.e. the central film thickness $H_o(t)$/ the central film thickness (H_{oR}) of the pure rolling condition under the base load (F_o)) with the time (t). The hydrodynamic response of the isoviscous lubricant is plotted in conjunction with the corresponding response of the piezoviscous lubricant under the same loading condition. Two different amplitudes (a) of sinusoidal load of (0.5) and (0.25) were used. For the same force amplitude (a), three values of the dimensionless damping parameter (D_p) of (0.007), (0.64) and (1.3) were employed to study the viscous damping phenomenon associated with the squeeze-film action. The physical data for variable force calculations are shown in Table (6.2).

As shown in Figures (6.7) to (6.12), once the system is set into motion, it will initially undergo a non harmonic state of transient as well as to follow the frequency of the excitation. If the system possesses damping the part of the motion which is due to

Table (6.2) Physical Data for Variable Force

Calculations

$R = 0.02$ (m)

$\eta_o = 0.0411$ (P_{as}), $\alpha = 2.058 \times 10^{-8}$ (m^2/N)

Figure	Force Amplitude (a)	Basic Load (F_o) (N/m)	Entraining Velocity (u) (m/s)	Angular Velocity of Sinusoidal Load (ω) (s^{-1})	Damping Parameter (D_p)
6.7	0.5	10000	0.78	157	0.007
6.8	0.25	10000	0.78	157	0.007
6.9	0.5	1000	0.001	157	0.64
6.10	0.25	1000	0.001	157	0.64
6.11	0.5	800	0.0003	157	1.30
6.12	0.25	800	0.0003	157	1.30

The variable load function f(t) was assumed to take the following form,

$$F(t) = F_o (1 + a \sin \omega t)$$

Table (6.3)

Variation of Maximum Film Thickness, Minimum Film Thickness and Phase Angle With The Damping Parameter, Under Sinusoidal Loading, for Isoviscous and Piezoviscous Lubrication

Figure	Force Amplitude (a)	Maximum Film Thickness (m)	Minimum Film Thickness (m)	Pure Rolling Film Thickness Under (F_o) (h_{oR})$_{(m)}$	Ratio of Maximum Film Thickness to (h_{oR})	Ratio of Minimum Film Thickness to (h_{oR})	Phase Angle (ϕ) with Respect to the Load Cycle (degree)	Damping Parameter (D_p)	Lub. Regime
6.7	0.5	0.3036×10^{-4}	0.1011×10^{-4}	0.1575×10^{-4}	1.928	0.642	1.34	0.007	iso
		0.3476×10^{-4}	0.1816×10^{-4}	0.2156×10^{-4}	1.612	0.842	1.34	0.007	piezo
6.8	0.25	0.2024×10^{-4}	0.1213×10^{-4}	0.1517×10^{-4}	1.286	0.771	1.34	0.007	iso
		0.2569×10^{-4}	0.1937×10^{-4}	0.2156×10^{-4}	1.191	0.898	1.34	0.007	piezo
6.9	0.5	0.2635×10^{-6}	0.1616×10^{-6}	0.1953×10^{-6}	1.351	0.828	66.6	0.64	iso
		0.3288×10^{-6}	0.2457×10^{-6}	0.2661×10^{-6}	1.235	0.923	72.0	0.64	piezo
6.10	0.25	0.2214×10^{-6}	0.1748×10^{-6}	0.1953×10^{-6}	1.135	0.896	64.8	0.64	iso
		0.2889×10^{-6}	0.2523×10^{-6}	0.2661×10^{-6}	1.085	0.948	68.4	0.64	piezo
6.11	0.5	0.8856×10^{-7}	0.6820×10^{-7}	0.7340×10^{-7}	1.206	0.929	82.8	1.3	sio
		0.1230×10^{-6}	0.1079×10^{-6}	0.1099×10^{-6}	1.119	0.981	90.0	1.3	piezo
6.12	0.25	0.7917×10^{-7}	0.6979×10^{-7}	0.7340×10^{-7}	1.078	0.950	79.2	1.3	iso
		0.1134×10^{-6}	0.1068×10^{-6}	0.1099×10^{-6}	1.031	0.97	84.6	1.3	piezo

the transient motion will eventually die out. The part of the motion sustained by the sinusoidal excitation (steady state response) will persist as long as the excitation existed.

Ideally, in the absence of damping, when the applied force is decreasing, the film thickness should be increasing and vice versa. Therefore, when the force is a maximum the central film is a minimum as shown clearly in Figures (6.7) and (6.8) where the damping parameter (D_p) takes the value (0.007). However, the response as shown on Figures (6.9) to (6.12) for a higher damping condition does not follow this ideal pattern fully and exhibits different values of phase lag to the forcing cycle in the steady state condition. This lag is due to the increased influence of damping. Also, Figures (6.9) to (6.12) show that the transient regime vanishes after a few cycles and a steady state regime is then obtained.

Table (6.3) shows that, the phase difference (ϕ) approaches zero as (D_p) approaches zero and $\left(-\frac{\pi}{2}\right)$ as (D_p) approaches larger values ($D_p >> 0.05$). The amplitude of the force (a) has a little effect upon the phase difference (ϕ). Moreover, with the piezoviscous response the lag is somewhat larger than that of the isoviscous response under the same loading condition. This is mainly because of the presence of a larger damping force in the piezoviscous case.

In the steady-state condition, response fluctuations are considerably smaller in the piezoviscous case than those of the isoviscous case under the same loading condition. This indicates the higher load carrying capacity of the piezoviscous lubrication condition. For both isoviscous and piezoviscous lubrication a considerable

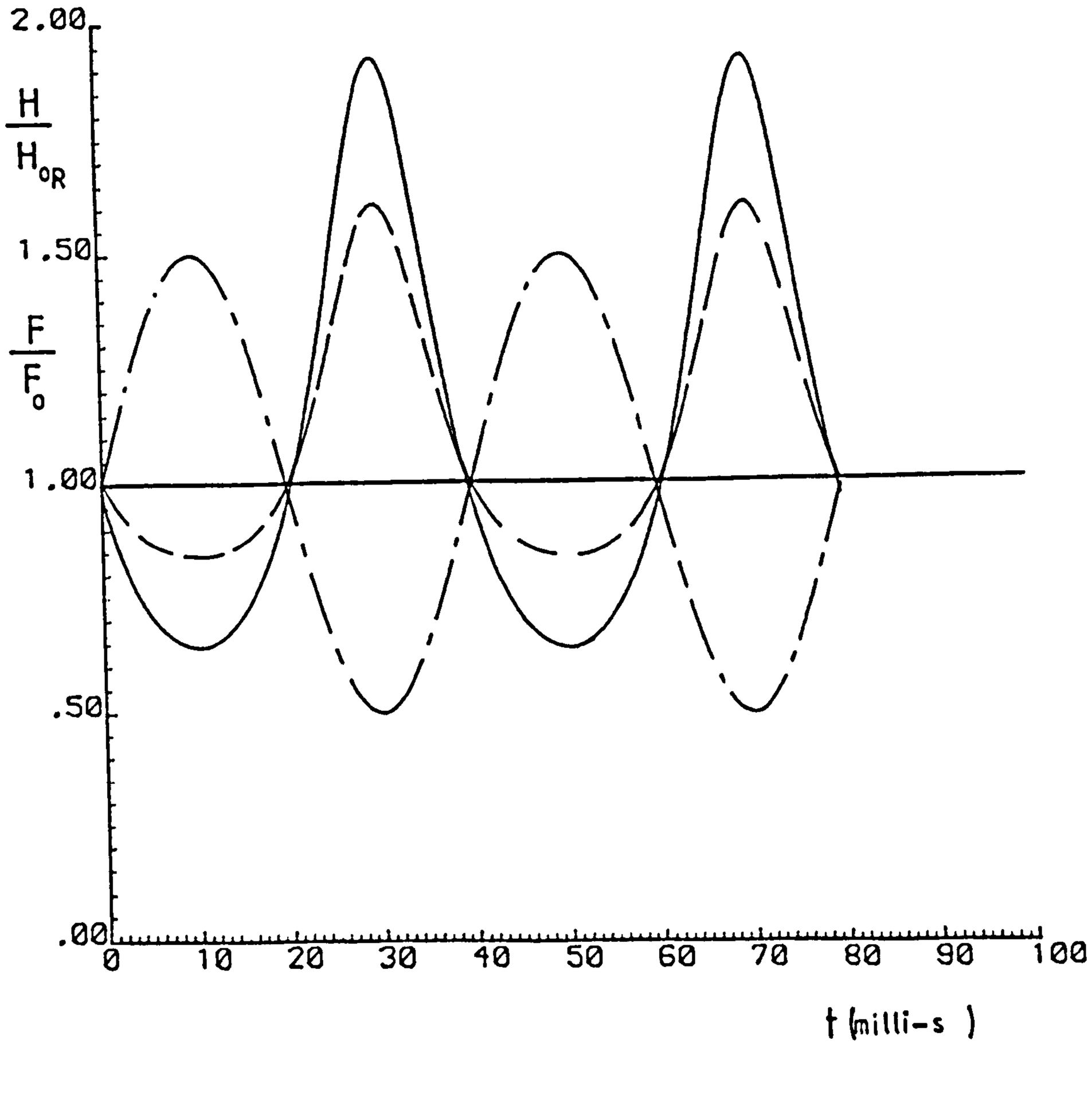

FIGURE(6 - 7) Time History of the Central Film Thickness for Rigid Cylinders in Combined Rolling and Normal Motion Under the Influence of a Sinusoidal Load (—·—) in the Presence of Isoviscous (———) and Piezoviscous (— — —) Fluids

($\alpha = 0.5$) ($D_p = 0.007$)

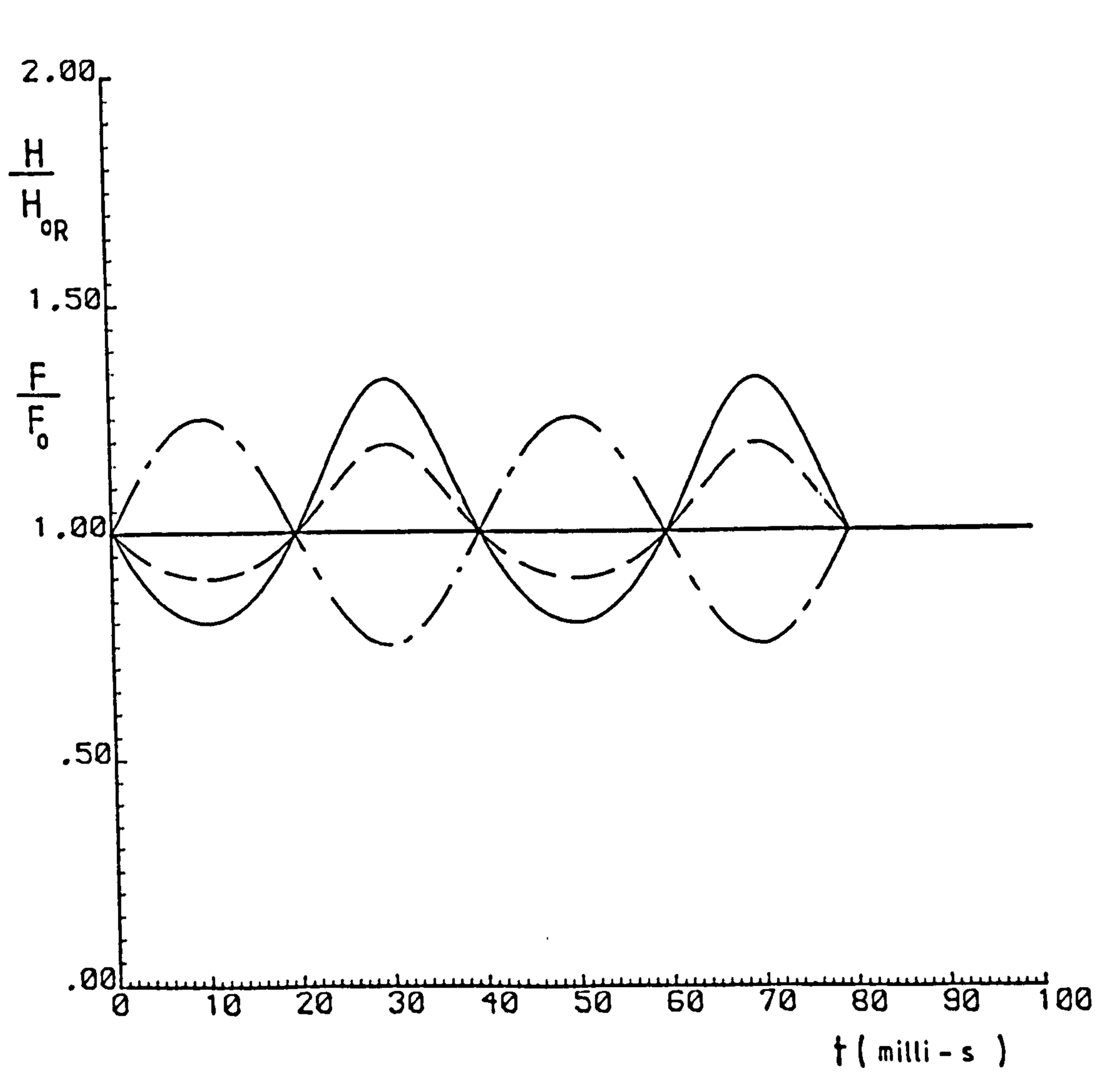

FIGURE(6 - 8) Time History of the Central Film Thickness for Rigid Cylinders in Combined Rolling and Normal Motion Under the Influence of a Sinusoidal Load (—·—) in the Presence of Isoviscous (———) and Piezoviscous (— — —) Fluids

($\alpha = 0.25$) ($D_p = 0.007$)

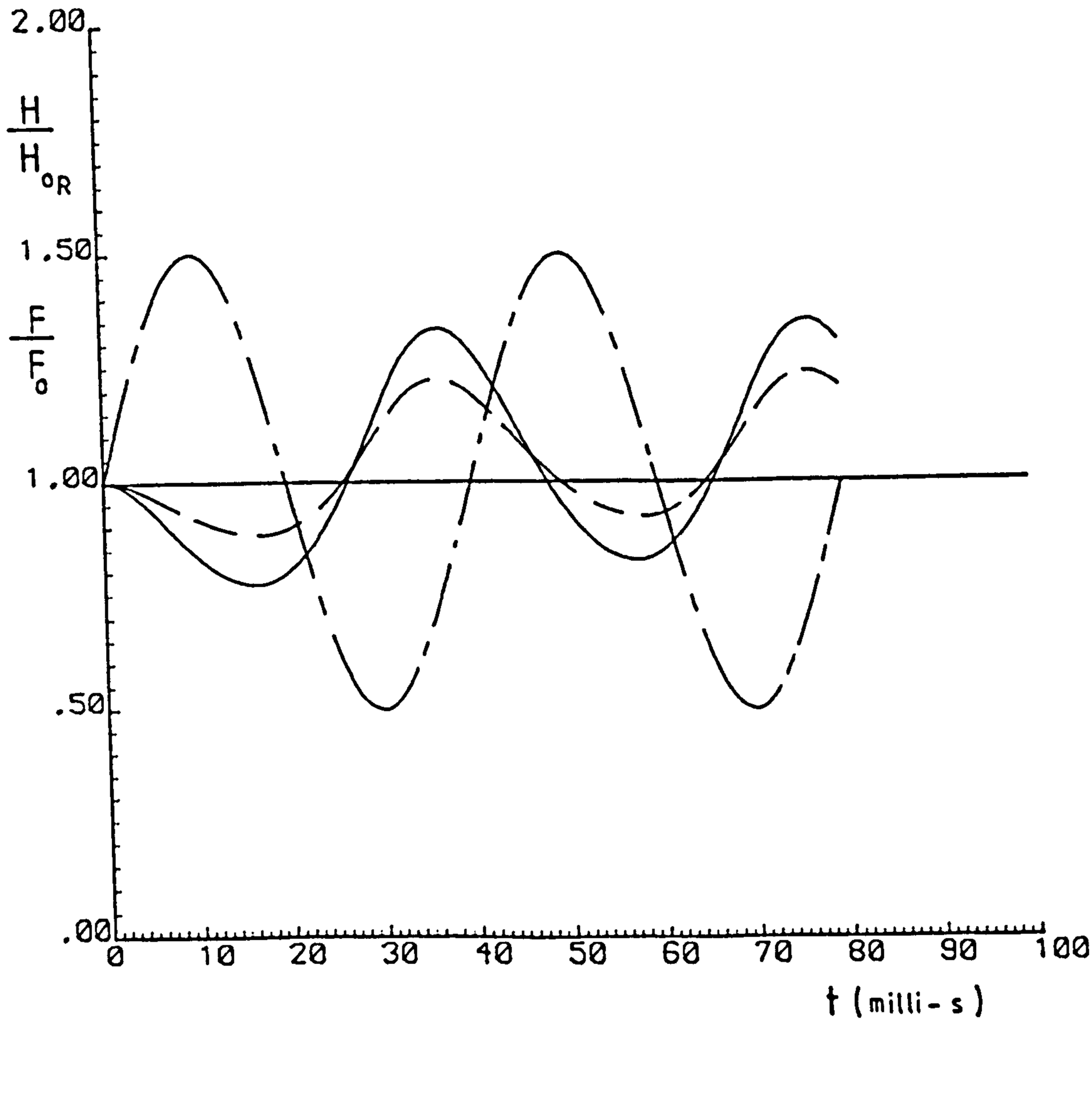

FIGURE(6 - 9) Time History of the Central Film Thickness for Rigid Cylinders in Combined Rolling and Normal Motion Under the Influence of a Sinusoidal Load (—·—) in the Presence of Isoviscous (———) and Piezoviscous (— — —) Fluids

($\alpha = 0.5$) ($D_p = 0.64$)

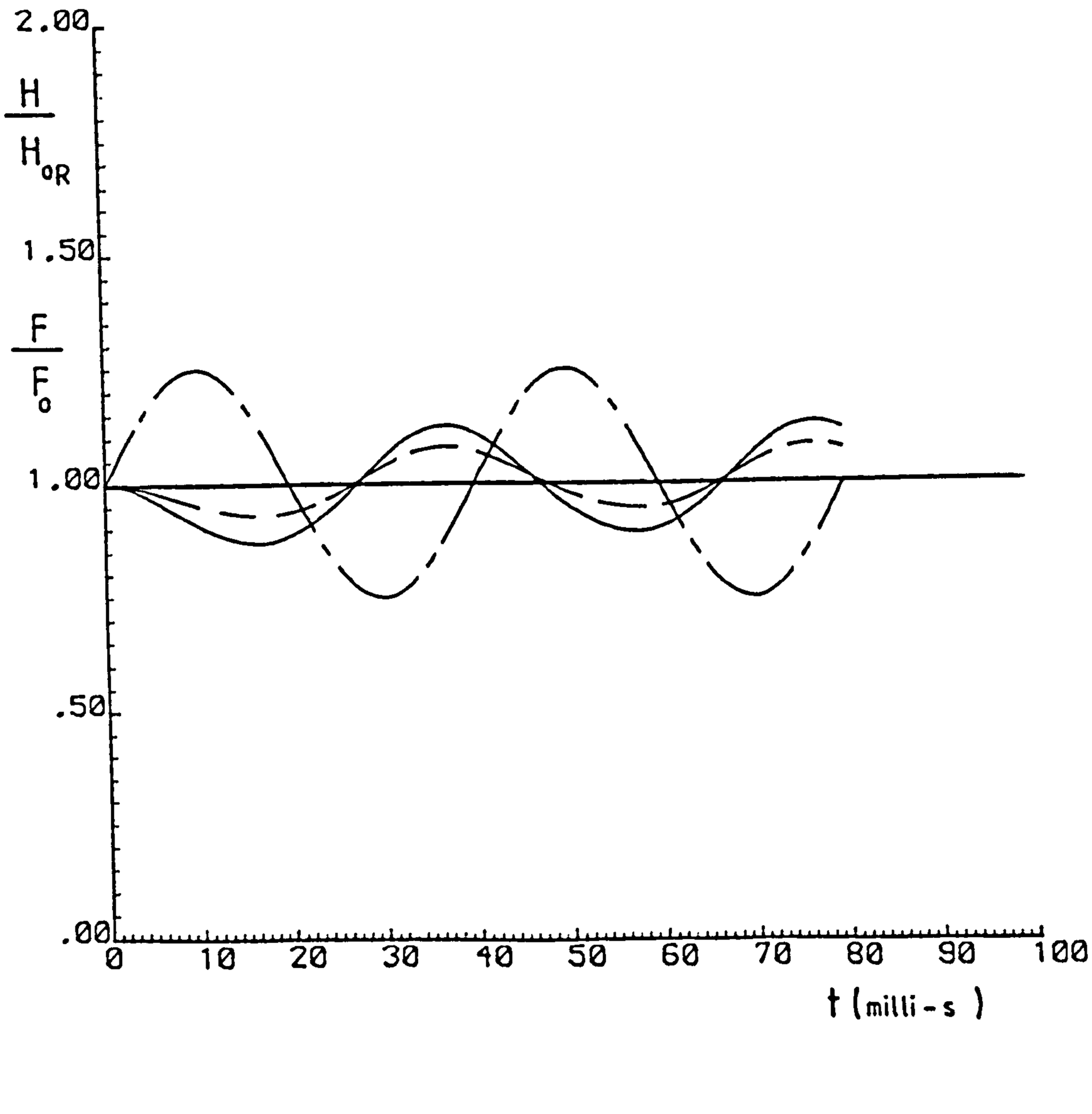

FIGURE(6 - 10) Time History of the Central Film Thickness for Rigid Cylinders in Combined Rolling and Normal Motion Under the Influence of a Sinusoidal Load (— · —) in the Presence of Isoviscous (———) and Piezoviscous (– — –) Fluids

($\alpha = 0.25$) ($D_p = 0.64$)

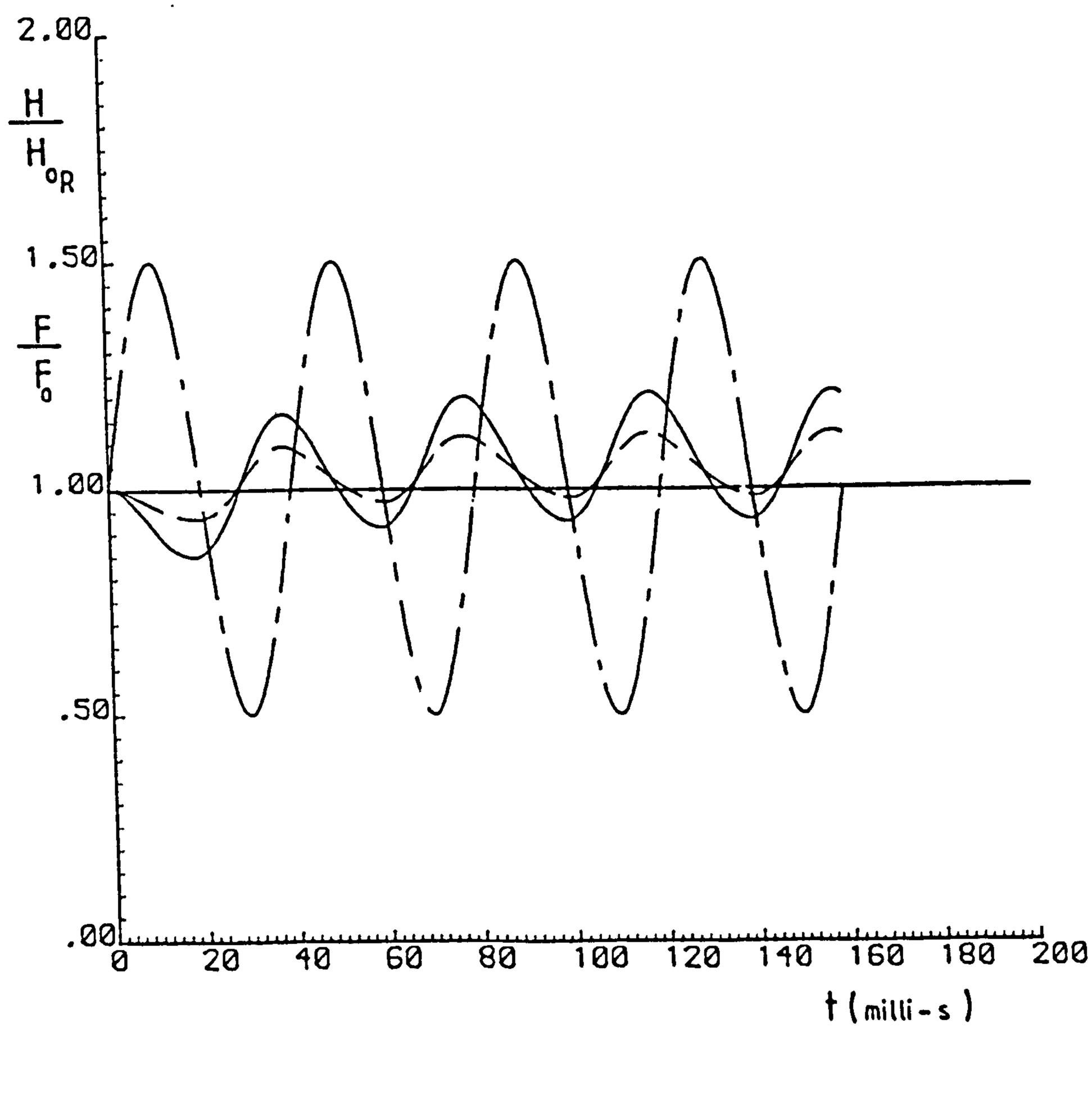

FIGURE(6 - 11) Time History of the Central Film Thickness for Rigid Cylinders in Combined Rolling and Normal Motion Under the Influence of a Sinusoidal Load (—·—) in the Presence of Isoviscous (———) and Piezoviscous (— — —) Fluids

($\alpha = 0.5$) ($D_p = 1.3$)

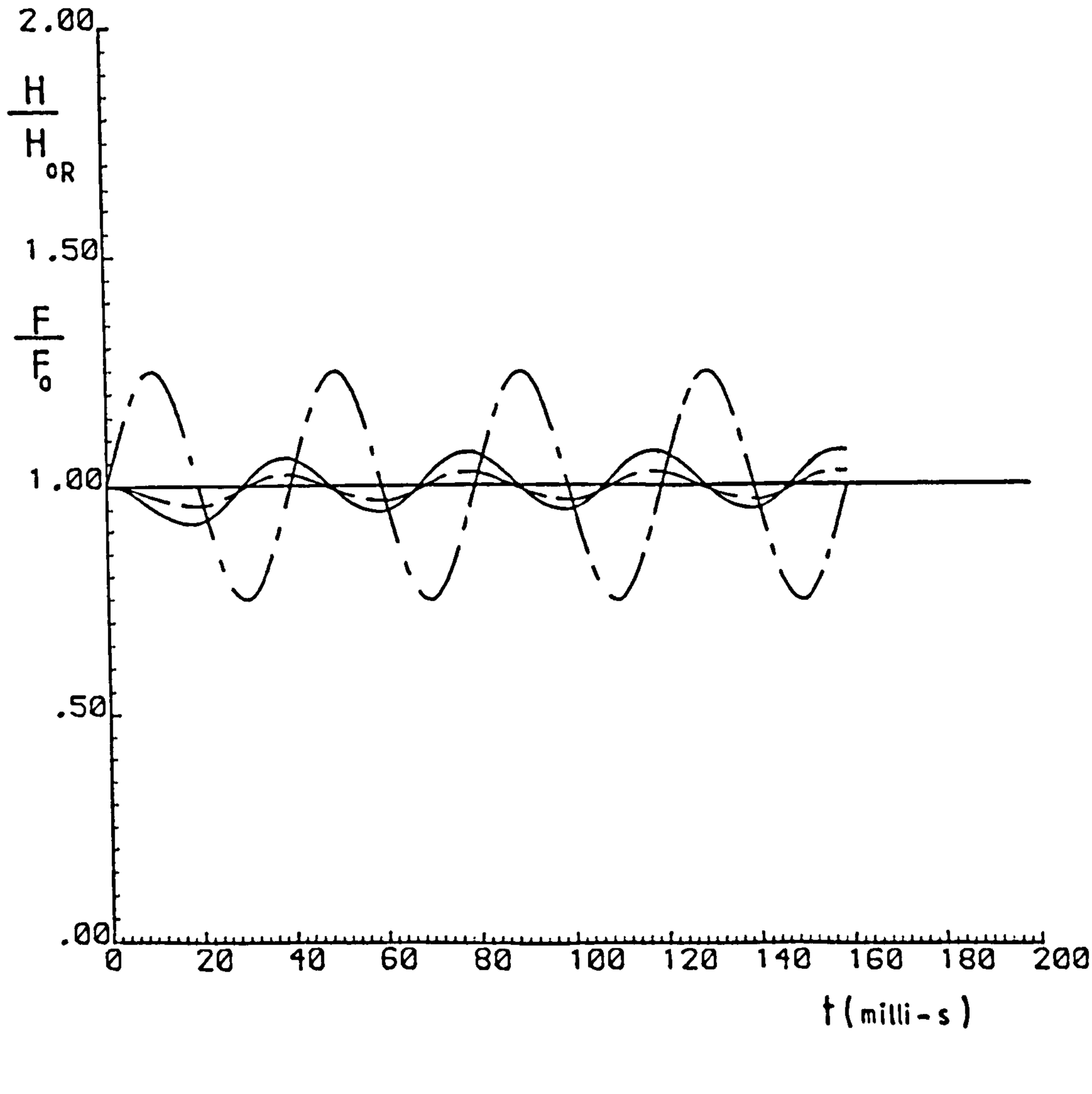

FIGURE(6 - 12) Time History of the Central Film Thickness for Rigid Cylinders in Combined Rolling and Normal Motion Under the Influence of a Sinusoidal Load (— ·—) in the Presence of Isoviscous (———) and Piezoviscous (— — —) Fluids

($\alpha = 0.25$) ($D_p = 1.3$)

reduction in the minimum film thickness may be obtained as the force amplitude increases. From Table (6.3) and Figures (6.7) and (6.8), a reduction in the minimum film thickness is obtained (about 16%) as the force amplitude (a) is increased from (0.25) to (0.5).

The results of the present work for various cases of isoviscous lubrication are compared with those of Sasaki et al (1962) and Vichard (1971) in Table (6.4), according to the following formulae,

Sasaki et al's formulae

$$F(t) = F_o (1 + a \sin \omega t) \tag{6.10}$$

$$\frac{H_o}{H_{oR}} = \frac{1}{[1 + a' \sin (\omega t - \phi)]^2} \tag{6.11}$$

$$a' = \frac{2a}{\left[\sqrt{16 + (3\pi\sqrt{2}\, D_p)}\right]^2} \tag{6.12}$$

$$\phi = \tan^{-1} \left(\frac{3\pi\sqrt{2}}{4} D_p\right) \tag{6.13}$$

Vichard's Formulae

$$F(t) = F_o (1 + a \sin \omega t) \tag{6.14}$$

$$\frac{H_o}{H_{oR}} = \frac{1}{[1 + a' \sin (\omega t - \phi)]} \tag{6.15}$$

$$\left.\begin{aligned} a' &= a && , \quad D_p < 0.05 \\ a' &= \frac{a}{1 + 2.25\, D_p^{1.64}} && , \quad 0.05 < D_p < 1 \\ a' &= 0.282\, D_p^{-0.954} && , \quad D_p > 1 \end{aligned}\right\} \tag{6.16}$$

Table (6.4) Comparison of the Present Analysis Results for Isoviscous Lubrication with the Previous Work of Sasaki et al (1962) and Vichard (1971)

Damping Parameter (Dp)	Force Amplitude (a)	Ratio of Maximum Film Thickness to the Pure Rolling Film Thickness (h_{oR}) under (F_o)					Ratio of Minimum Film Thickness to the Pure Rolling Film Thickness (h_{oR}) under (F_o)					Phase Angle (degree)		
		Present Work	Sasaki's		Vichard's		Present Analysis	Sasaki's		Vichard's		Present Analysis	Sasaki's	% error
			Ratio	% error	Ratio	% error		Ratio	% error	Ratio	% error			
0.007	0.5	1.928	1.777	8	2.00	3.7	0.642	0.640	0.3	0.666	3.8	1.34	1.33	0.75
0.007	0.25	1.286	1.306	1.5	1.333	3.6	0.771	0.790	2.5	0.800	3.7	1.34	1.33	0.75
0.64	0.5	1.351	1.251	7.4	1.316	2.6	0.828	0.817	1.3	0.806	2.6	66.6	64.9	2.6
0.64	0.25	1.135	1.115	1.7	1.136	0.1	0.896	0.901	0.64	0.892	0.45	64.4	64.9	0.8
1.30	0.5	1.206	1.122	7	1.221	0.1	0.929	0.896	3.5	0.901	3	82.8	77.0	7
1.30	0.25	1.078	1.058	1.8	1.058	-	0.950	0.946	0.4	0.947	0.3	79.2	77.0	2.8

Vichard did not present a formula for the phase angle (ϕ).

The deviation between the results of the present work and Vichard's formulae is somewhat smaller than that with Sasaki's formulae for the film thickness function as shown in Table (6.4). The phase angle results do, however, provide good agreement with Sasaki's formula (6.13).

6.7 Concluding Remarks

In this chapter, the effect of squeeze film action due to normal motion combined with 'entraining' action due to pure rolling has been investigated for the lubrication of rigid cylinders. The results were evaluated for both isoviscous and piezoviscous lubrication conditions under constant and sinusoidal normal loading. The variation of the normal motion velocity and peak pressure have been presented. The time histories of the central film thickness under constant and sinusoidal normal loadings were introduced with a discussion of the viscous damping phenomenon associated with the squeeze film action. The results with isoviscous lubrication, have been shown to provide good agreement with results obtained by previous authors.

The following conclusions were reached;

(i) Under Constant Load

1 - The 'normal approach' motion through an isoviscous fluid is faster than that through a piezoviscous fluid. The 'normal separation' motion through an isoviscous fluid is, however, slower than that through a piezoviscous fluid.

2 - Pressures of the order of twice the corresponding peak pressure in the steady state situation (pure rolling) can be generated in the contact during 'normal separation'. In contrast, during 'normal approach', the peak pressure magnitudes never exceed the peak value of the steady state situation. At the same central film thickness, speed and load, the pressure peak generated with a peizoviscous lubricant is larger than that generated with an isoviscous lubricant.

3 - The initial value of the central film thickness and the type of lubrication have no significant effect on the time of damping.

(ii) <u>Under Sinusoidal Loading</u>

1 - The effect of the squeeze-film is remarkable. This effect is entirely similar to a viscous damping phenomenon acting on a system which has one degree of freedom (the minimum film thickness). Its influence upon the flow is completely determined by the dimensionless damping parameter (D_p), where,

$$D_p = \omega R \sqrt{\frac{\eta_o}{u\ F_o}}$$

If the damping parameter (D_p) is less than (0.05) the squeeze effect is negligible (i.e. no damping). Hence, the relation between the minimum film thickness and the load may be described by the pure rolling relationship (e.g. for isoviscous lubrication the Martin's equation). If the damping parameter (D_p) is greater than (0.05) the squeeze effect is characterized by a damping of

oscillations generated by the variation of load. For large values of the damping parameter ($D_p >> 1$), the film does not follow the oscillations of load.

2 - In the steady-state condition, response fluctuations are considerably smaller in the piezoviscous case than those of the isoviscous case under the same loading condition. This indicates higher load carrying capacity with piezoviscous lubrication (i.e. the force amplitude (a) may be increased) than for isoviscous condition.

CHAPTER 7

A THEORETICAL STUDY OF THE LUBRICATION OF ELASTIC CYLINDERS IN COMBINED ROLLING AND NORMAL MOTION

7.1 Introduction

During the last two decades great progress has been reported in the understanding of the basic processes which are involved in the mechanism of elastohydrodynamic lubrication. Nominal line contacts occur between the races and the rollers in a cylindrical roller bearing, between a pair of involute gear teeth, and in the contact between a cam and its follower.

Most of the theoretical and experimental work on line contacts has been directed towards the determination of the minimum film thickness in rolling and rolling with sliding (e.g. Dowson and Higginson (1977)). Several investigations of the theory of elastohydrodynamic lubrication of line contacts in normal approach have been carried out (e.g. Christensen (1961))and the subject has been further discussed in Chapter (4).

The influence of combined 'entraining' and 'normal motion' upon elastohydrodynamic lubrication of line contacts has received little attention throughout the past years. Perhaps the most rigorous treatment of transient elastohydrodynamic lubrication was presented by Vichard (1971). The Grubin approximations were made for film shape and pressure distribution. The dynamic variations in load, entraining velocity and surface curvature were included in the analysis. The model was very simple, and hence it did not produce solutions which satisfied the elasticity and lubrication equations throughout the entire contact. Moreover, the characteristics of an elastohydrodynamic contact which were covered by Dowson and Higginson (1977) (e.g. the oil film restriction near the outlet and

the second pressure maximum of considerable height near the outlet end) did not emerge from the analysis. More recently, Wada and Tsukijihara (1981) presented a numerical solution to the elastohydrodynamic squeeze film problem of two rotating cylinders which simultaneously satisfied the governing elastic and hydrodynamic equations. Unfortunately the solutions were performed under constant centre pressure, exit film thickness and squeeze to entraining velocity ratio which did not correspond to any practical physical situation.

The present analysis makes the following advances over the previous elastohydrodynamic models and solutions schemes.

(a) It is a real transient analysis in which the full time histories of the system parameters are determined.

(b) Any specified load and load cycle can be accommodated.

(c) It utilizes a simple direct-iteration solution technique which simultaneously satisfies the governing elastic and hydrodynamic equations.

(d) It predicts all the characteristics of the elastohydrodynamic contact and the details of the pressure curve and oil film shape at different time intervals.

In the present chapter, the influence of squeeze film action due to normal motion combined with 'entraining' action due to pure rolling has been investigated for the case of the elastohydrodynamic lubrication of cylinders. The results were evaluated under constant and sinusoidal normal loading conditions. Graphical representations of pressure distributions and film shapes

are presented together for successive reductions of the central film thickness (H_o). The variation of the dimensionless minimum film thickness (H_m), velocity of approach ($\bar{W}$) and central pressure (P_o) under constant load are also included. Furthermore, the time history of the central film thickness (H_o) and the minimum film thickness (H_m) under constant and sinusoidal normal loadings are introduced with discussion of viscous damping associated with the squeeze film action.

7.2 Dimensionless Parameters

The variables resulting from the theory of elastohydrodynamic lubrication of cylinders in combined rolling and normal motion under sinusoidal loading are;

(R) effective radius of curvature, $\left[R = \frac{R_1 R_2}{R_1 + R_2}\right]$ (m)

(h) film thickness (m)

(u) 'entraining' velocity (m/s)

(W) normal velocity of cylinders (in the direction (z)) (m/s)

($P_{iv,as}$) asymptotic isoviscous pressure obtained from Roelands (1966), $\left(\simeq \frac{1}{\alpha}\right)$ (N/m^2)

(E') effective elastic modulus, $\left[\frac{2}{\frac{1-\sigma_1^2}{E_1} + \frac{1-\sigma_2^2}{E_2}}\right]$ (N/m^2)

(η_o) lubricant viscosity at atmospheric pressure ($N.s/m^2$)

(F_o) basic load of sinusoidal loading (N/m)

(ω) time base (angular velocity of sinusoidal load) (s^{-1})

(f(t)) load function, (1+a sin ωt), dimensionless

(a) amplitude of sinusoidal load, dimensionless

From the eleven variables mentioned above the following six dimensionless groups can be developed:

(1) Dimensionless film thickness

$$H = \frac{h}{R}$$

(2) Dimensionless load parameter

$$\bar{F} = \frac{F_o}{E'R}$$

(3) Dimensionless entraining velocity parameter

$$U = \frac{u\eta_o}{E'R}$$

(4) Dimensionless normal velocity parameter

$$\bar{W} = \frac{W\eta_o}{E'R}$$

(5) Dimensionless material parameter

$$G = \alpha E'$$

(6) Dimensionless damping parameter

$$D_e = \frac{\omega R}{u}\sqrt{\frac{F_o}{RE'}}$$

In the case of constant applied external load the function (f(t)) is equal to unity. Moreover, the time base (ω) must be chosen as:

$$\omega = \frac{u}{R\sqrt{\bar{F}}} \qquad (7.1)$$

Thus the dimensionless damping parameter (D_e) is equal to unity and the general solution depends upon the first five dimensionless groups only (i.e. H, $\bar{F}$, U, $\bar{W}$ and G).

In accordance with Vichard (1971), it was found that under sinusoidal loading the time histories of the minimum and central film thickness may be described completely by the dimensionless damping parameter (D_e) and the dimensionless entraining parameter (g_e), where,

$$g_e = \frac{\bar{F}_o^{3/2}}{GU} \tag{7.2}$$

In the present results the dimensionless pressure (P) is defined as $\left(\frac{p}{E'}\right)$, the dimensionless distance is $\left(X = \frac{x}{b}\right)$ and the dimensionless time is (ωt). The sinusoidal normal loading is assumed to have the following form,

$$F = F_o (1 + a \sin \omega t) \tag{7.3}$$

7.3 Pressure Profiles Under Constant Load

The pressure distributions, for constant load conditions involving both squeeze- film and entraining action, are plotted in conjunction with the corresponding film shapes in Figures (7.1), (7.2), (7.3) and (7.4). Each figure displays the change in pressure and film shape with the dimensionless central film thickness (H_o) as the cylinder approaches the plane surface under the influence of a constant externally applied load. All the physical data used in this study are given in Table (7.1)

The changes in the form of the pressure curve which occur as the dimensionless central film thickness (H_o) is decreased are clearly seen. At high values of the dimensionless central film

Table (7.1) Physical Data for Constant Load Calculations

Equivalent radius of curvature (R) = 0.02 (m)

Effective elastic modulus (E') = 2.3×10^{11} (N/m^2)

Poisson's ratio, (σ) = 0.3

Atmospheric viscosity, (η_o) = 0.0411 (Pas)

Pressure - Viscosity coefficient, (α) = 2.058×10^{-8} (m^2/N)

Physical Quantity	Case (1)	Case (2)	Case (3)	Rigid Isoviscous	Case (4)
Load (N/m)	15000	15000	10000	15000	30000
Entraining Velocity (u) (m/s)	0.01	0.05	0.01	0.01	0.1
Initial Film Thickness (H_o) (-)	0.12×10^{-4}	0.12×10^{-4}	0.12×10^{-4}	0.12×10^{-4}	0.3×10^{-4}
Dimensionless Load Parameter ($\bar{F}$)	3.26×10^{-6}	3.26×10^{-6}	2.174×10^{-6}	-	6.52×10^{-6}
Dimensionless Entraining Velocity Parameter (U)	8.93×10^{-14}	4.47×10^{-13}	8.93×10^{-14}	-	8.93×10^{-13}
Dimensionless Material Parameter (G)	4733	4733	4733	-	4733

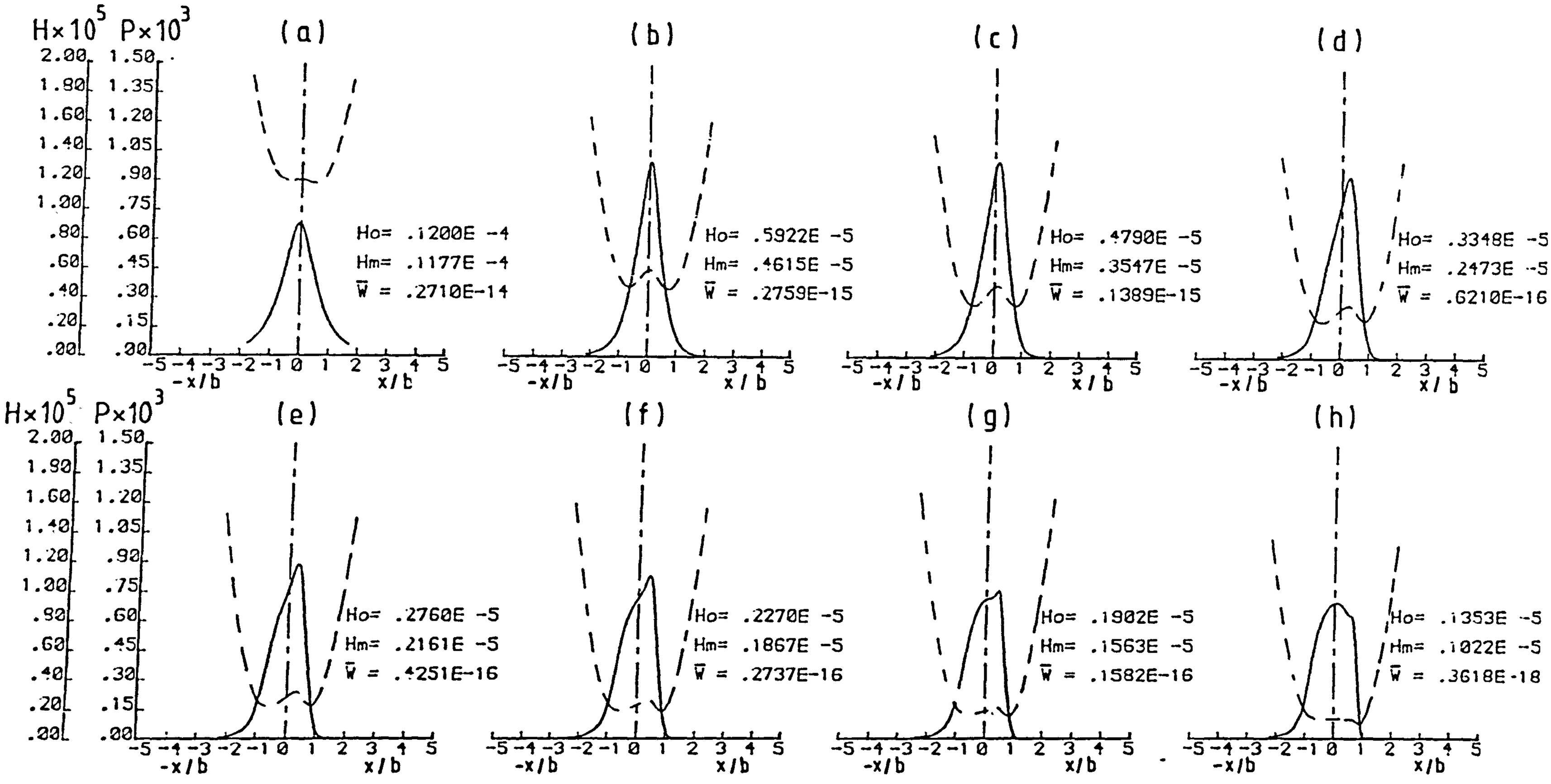

FIGURE(7 - 1) Pressure Distributions(——) and Film Shapes(— — —) for Elastic Cylinders in Combined Rolling and Squeeze Film Action Under the Influence of a Constant External Load in the Presence of a Piesoviscous Fluid

$\bar{F} = 3.26 \times 10^{-6}$ $\quad U = 8.93 \times 10^{-14}$ $\quad G = 4733$

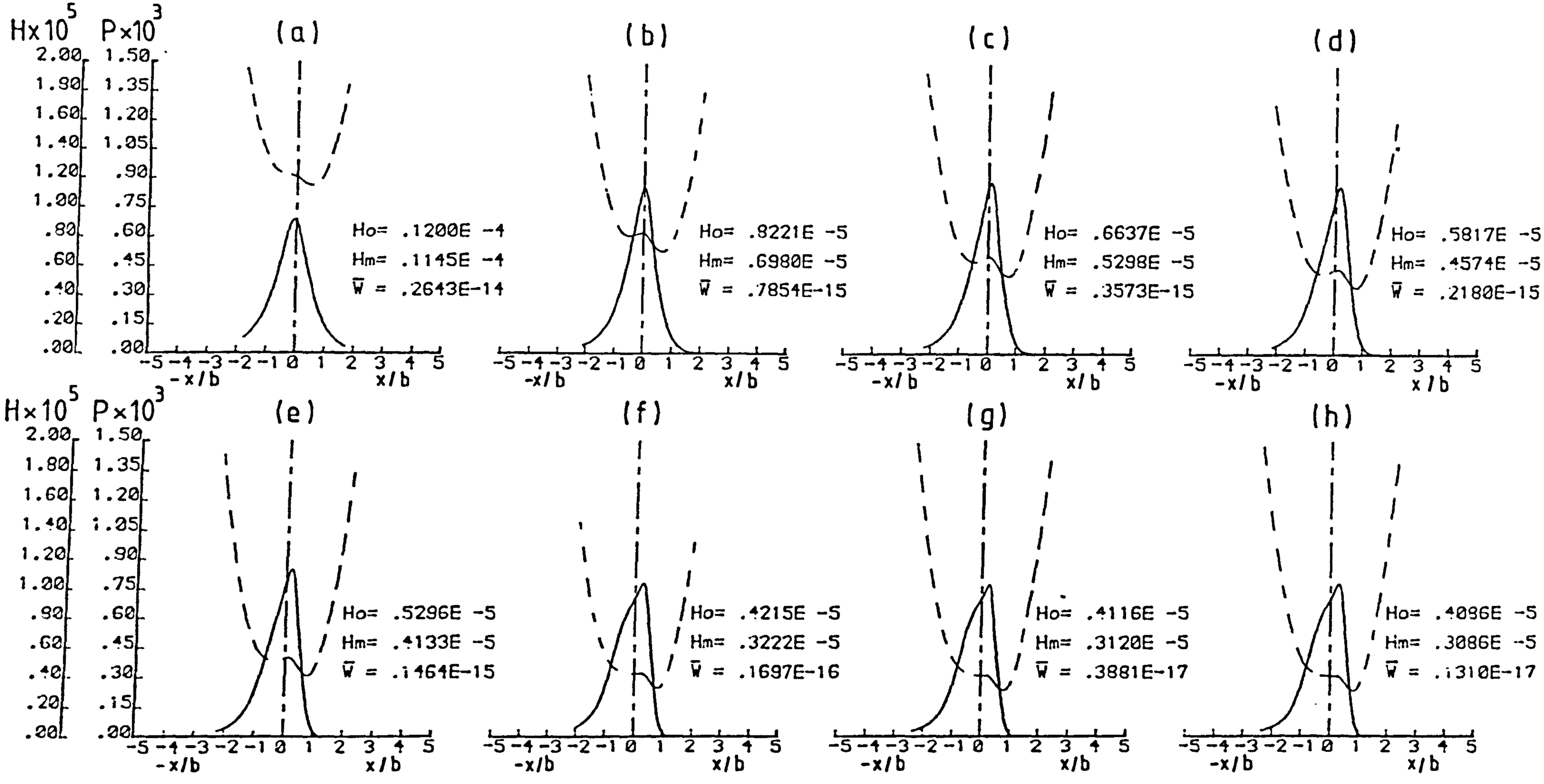

FIGURE(7 - 2) Pressure Distributions(——) and Film Shapes(— — —) for Elastic Cylinders in Combined Rolling and Squeeze Film Action Under the Influence of a Constant External Load in the Presence of a Piesoviscous Fluid

$\bar{F} = 3.26 \times 10^{-6}$ $U = 4.47 \times 10^{-13}$ $G = 4733$

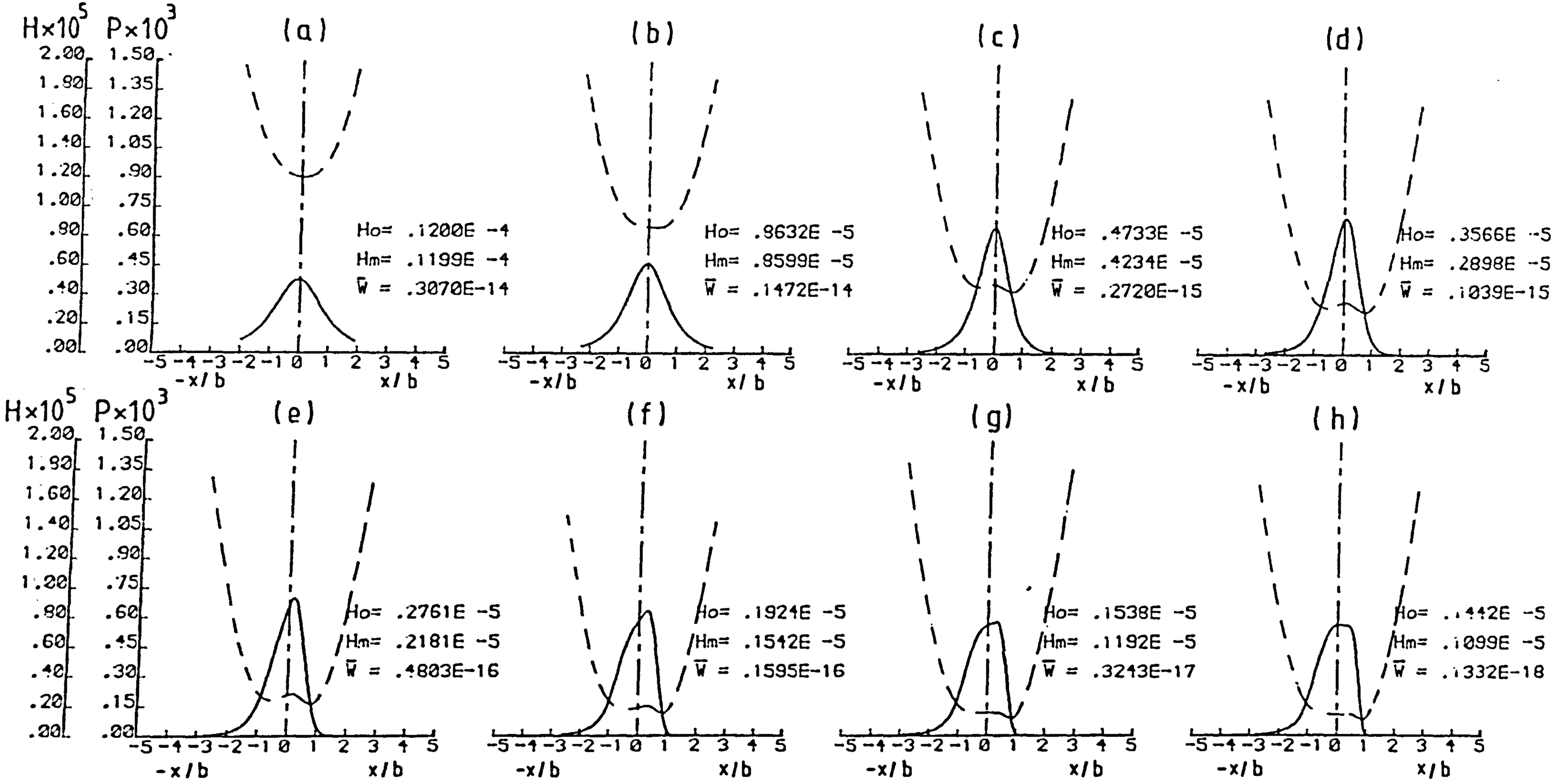

FIGURE(7 - 3) Pressure Distributions(——) and Film Shapes(— — —) for Elastic Cylinders in Combined Rolling and Squeeze Film Action Under the Influence of a Constant External Load in the Presence of a Piesoviscous Fluid

$\bar{F} = 2.17 \times 10^{-6}$ $U = 8.93 \times 10^{-14}$ $G = 4733$

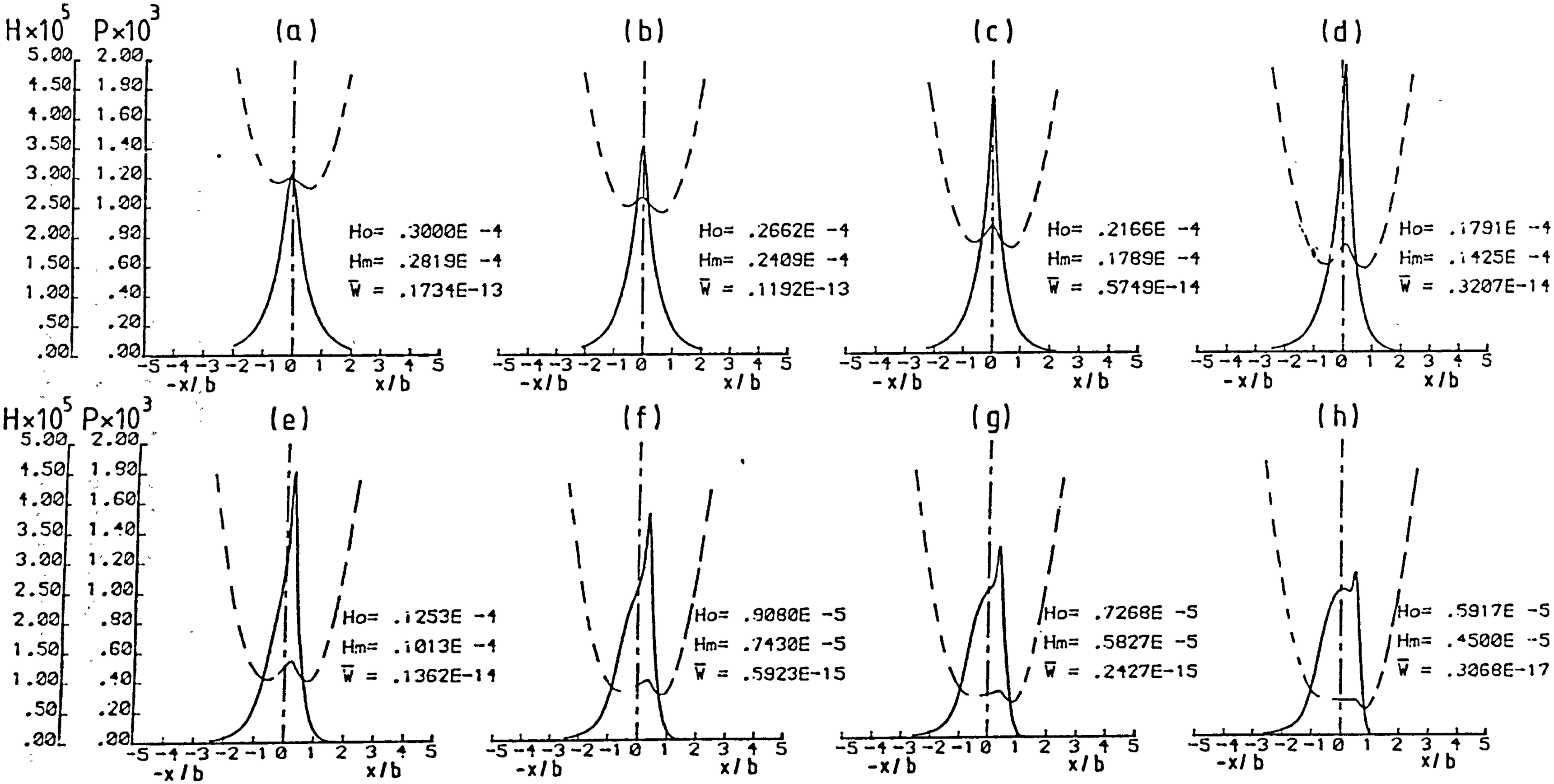

FIGURE(7 - 4) Pressure Distributions(——) and Film Shapes(- - -) for Elastic Cylinders in Combined Rolling and Squeeze Film Action Under the Influence of a Constant External Load in the Presence of a Piesoviscous Fluid

$\bar{F} = 6.52 \times 10^{-6}$ $U = 8.93 \times 10^{-13}$ $G = 4733$

thickness (greater than the corresponding pure rolling value), the pressure distribution is approximately symmetrical around the centre of contact, similar to the pure squeeze form and a sharp pressure spike is produced at the centre of the contact. As the central film thickness (H_o) is reduced the pressure spike increases until it reaches a certain maximum value. The position of oil film rupture in the divergent portion of the film gradually moves up-stream. The pressure spike moves from the centre towards the exit. When the value of (H_o) reaches its corresponding pure rolling value, the pressure distribution takes the well known pure rolling form of pressure distribution with all the characteristics of steady state elastohydrodynamic lubrication of line contacts (see Dowson and Higginson (1977)).

The effect of dimensinless entraining velocity parameter (U) upon the pressure distribution during normal approach may be obtained from Figure (7.1) and (7.2). The secondary pressure spike on the outlet side is particularly evident in the case of large values of (U), Figure (7.2).

The change in form of the pressure curve as the load is increased is shown in Figures (7.1) and (7.3). The movement towards a Hertzian pressure distribution with the larger value of ($\bar{F}$) is plain to see at the final stage of approach in Figure (7.1).

Figure (7.4) represents a particular case of higher dimensionless load and entraining velocity parameters. This figure was selected to express the well known characteristics of the elastohydrodynamic lubrication of line contacts, i.e. the near

Hertzian pressure distribution and the second pressure maximum of considerable height near the outlet end.

Figure (7.5) is a plot of the peak dimensionless pressure $\left(P_k = \frac{p_k}{E'}\right)$ versus the dimensionless central film thickness (H_o), two values of each of the dimensionless load parameter ($\bar{F}$) and the dimensionless entraining velocity parameter (U) were used. In general for elastohydrodynamic lubrication conditions, the peak pressure gradually increases with decreasing central film thickness, and reaches a maximum value. For further decrease in the central film thickness the peak pressure decreases rapidly and finally approaches the corresponding peak pressure value for the steady state situation (pure rolling). Furthermore, as (U) increases and ($\bar{F}$) decreases the dimensionless peak pressure is decreased.

It should be noted from the same figure that considering the condition for an isoviscous fluid and rigid solids, the trend of the peak pressure variation is quite different. Here, the peak pressure increases with decreasing (H_o) until it reaches a maximum value in the steady state situation.

It is possible now to distinguish between three different processes of lubrication in connection with the combined effect of 'entraining' and 'squeeze film' action in the non-steady state elastohydrodynamic lubrication of cylinders. At the earlier stage of motion when the central film thickness is large, the 'entraining' effect is relatively unimportant, and the pressure distribution is strongly influenced by the squeeze film effect. At a certain stage of motion both effects are important, hence a new pressure

1- $\bar{F} = 3.26\times10^{-6}$ $U = 8.93\times10^{-14}$

2- $= 3.26\times10^{-6}$ $= 4.47\times10^{-13}$

3- $= 2.17\times10^{-6}$ $= 8.93\times10^{-14}$

Rigid Solids - Isoviscous Fluid

Solution for Comparison With (1)

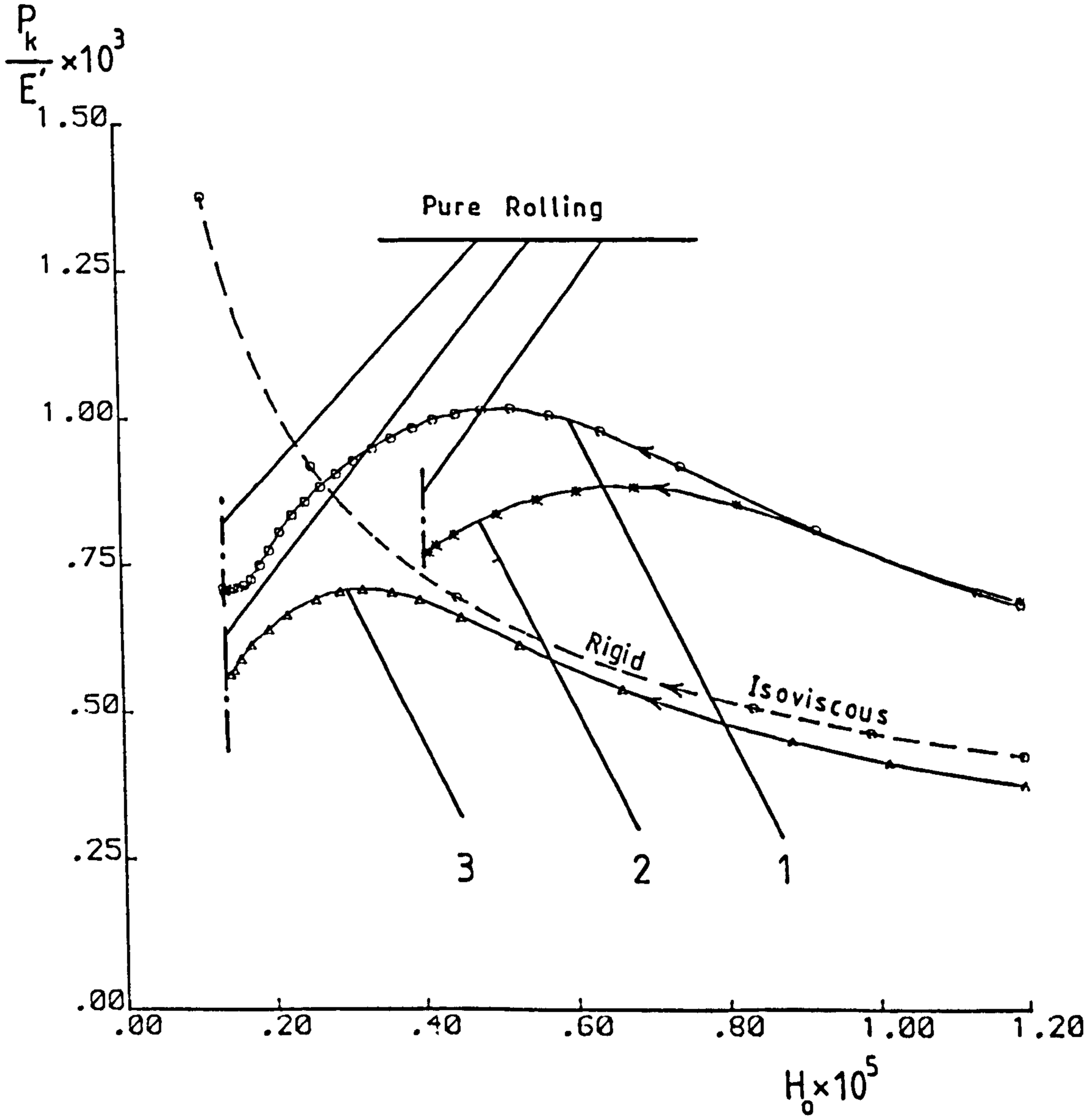

FIGURE(7 - 5) Variation of the dimensionless Peak Pressure for Elastic Cylinders in Combined Rolling and Squeeze Film Action Under the Influence of a Constant Load in the Presence of a Piezoviscous Fluid

G = 4733

distribtution is produced. This subsequent pressure distribution possesses both characteristics of the pressure distribution for pure squeeze film conditions and the pressure distribution for steady state conditions. As the central film thickness (H_o) approaches the steady state value the influence of the 'entraining' action takes over as the dominant effect.

7.4 Time Dependent Film Thickness Under Constant Load

The film shapes are shown in conjunction with the corresponding pressure distributions in Figures (7.1), (7.2), (7.3) and (7.4). At an early stage of normal approach, where the 'squeeze film' action is important, an elastic dimple or pocket is formed in the central region with two similar 'pips' on the inlet and outlet sides of the conjunction. The pocket depth increases sharply with decreasing central film thickness (H_o) until it reaches a maximum value as shown in Figure (7.6). For subsequent reductions of the central film thickness (H_o) the pocket depth decreases continuously. At the same time the 'pip' in the inlet region gradually disappears and the region between the inlet and the minimum film thickness on the outlet side is gradually flattened. Eventually the film profiles approach the well known shape for the steady state elastohydrodynamic lubrication condition (pure rolling). In general the dimple becomes deeper and occurs at higher central film thickness values as the dimensionless load parameter ($\bar{F}$) is increased. Sometimes, at high values of the dimensionless central film thickness (H_o), the minimum film thickness (H_m) may be found on the inlet side of the conjunction as shown in Figures (7.1 (d)) and (7.1 (e)). When the value of (H_o) approaches the pure rolling value the minimum film thickness (H_m) is found on the outlet side of the conjunction close to ($\frac{x}{b} = 1$).

1 - $\bar{F}$	$=3.26\times10^{-6}$	$U=8.93\times10^{-14}$
2 -	$=3.26\times10^{-6}$	$=4.47\times10^{-13}$
3 -	$=2.17\times10^{-6}$	$=8.93\times10^{-14}$

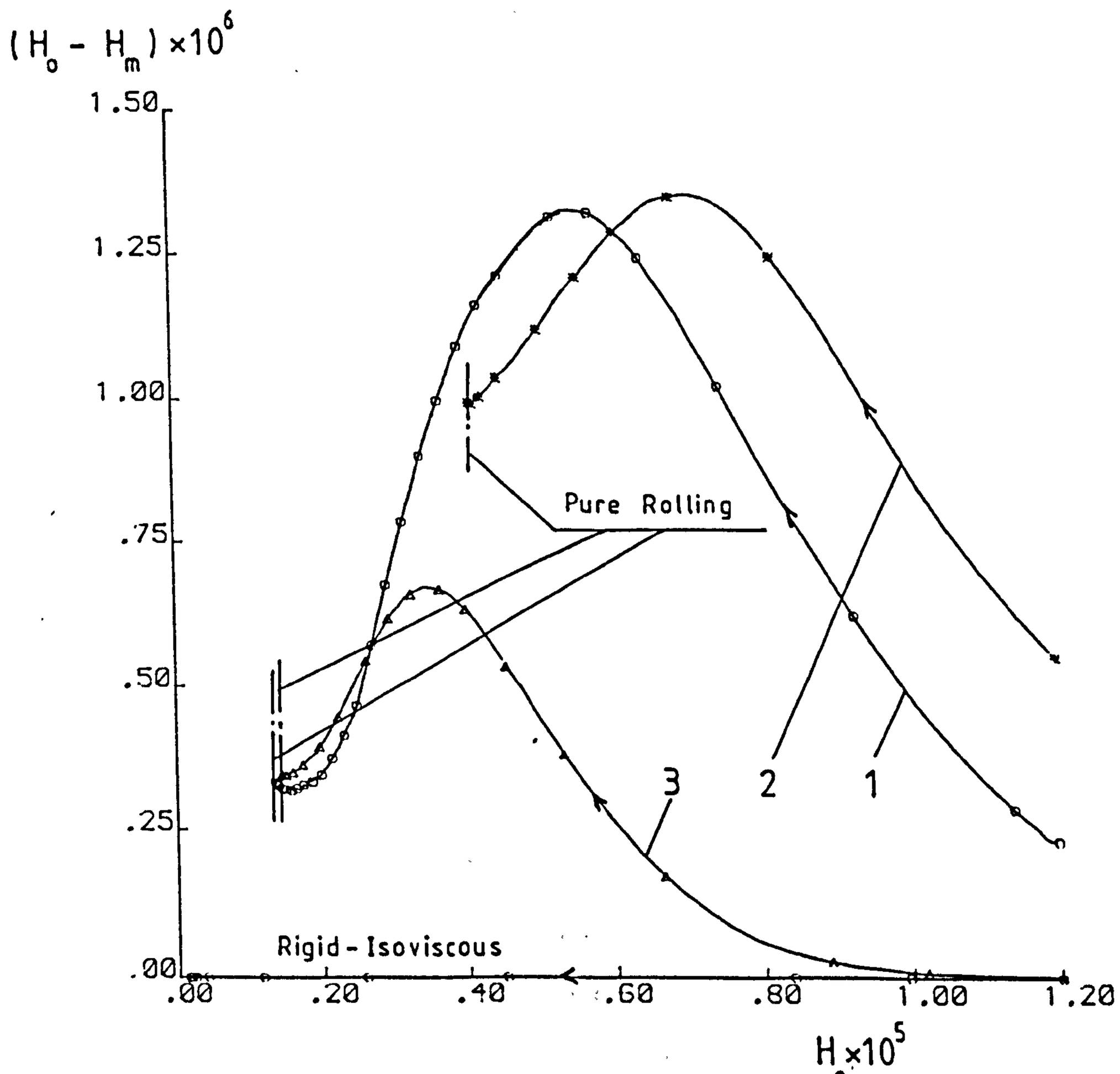

FIGURE(7 - 6) Variation of the Dimple Depth for Elastic Cylinders in Combined Rolling and Squeeze Film Action Under the Influence of a Constant Load in the Presence of a Piezoviscous Fluid

G = 4733

The minimum film thickness (H_m) is the most important quantity, with respect to the risk of metallic contact. The relationship between the parameter $\left(\frac{H_m}{H_o}\right)$ and the central film thickness (H_o) is shown in Figure (7.7). Moreover, the variation of the minimum film thickness (H_m) with the central film thickness (H_o) is given in Figure (7.8). Solutions are presented for different values of the constant dimensionless load parameter ($\bar{F}$) and the constant dimensionless entraining velocity parameter (U). It may be noticed from Figure (7.7) that the deviation from the isoviscous rigid-solids case $\left(\frac{H_m}{H_o} = 1\right)$ appears to start at a relatively larger film thickness as the dimensionless load parameter ($\bar{F}$) and entraining velocity parameter (U) are increased.

7.5 Velocity of Approach Under Constant Load

The variation of the dimensionless velocity of approach ($\bar{W}$) for specific conditions is displayed in Figure (7.9). This figure represents the relationship between the dimensionless velocity of approach parameter ($\bar{W}$) and the dimensionless central film thickness (H_o) at different values of the dimensionless load ($\bar{F}$) and the dimensionless entraining velocity parameter (U). As the dimensionless central film thickness (H_o) is reduced due to squeeze - film action the velocity of approach (W) decreases and approaches a zero value as the pure rolling condition is achieved.

It is evident that with the same applied load (F), entraining velocity (u) and central film thickness (H_o), the normal approach velocity (W) for an isoviscous fluid and rigid solids is much greater than that for a piezoviscous fluid and elastic solids.

1 - $\bar{F} = 3.26 \times 10^{-6}$ $U = 8.93 \times 10^{-14}$

2 - $= 3.26 \times 10^{-6}$ $= 4.47 \times 10^{-13}$

3 - $= 2.17 \times 10^{-6}$ $= 8.93 \times 10^{-14}$

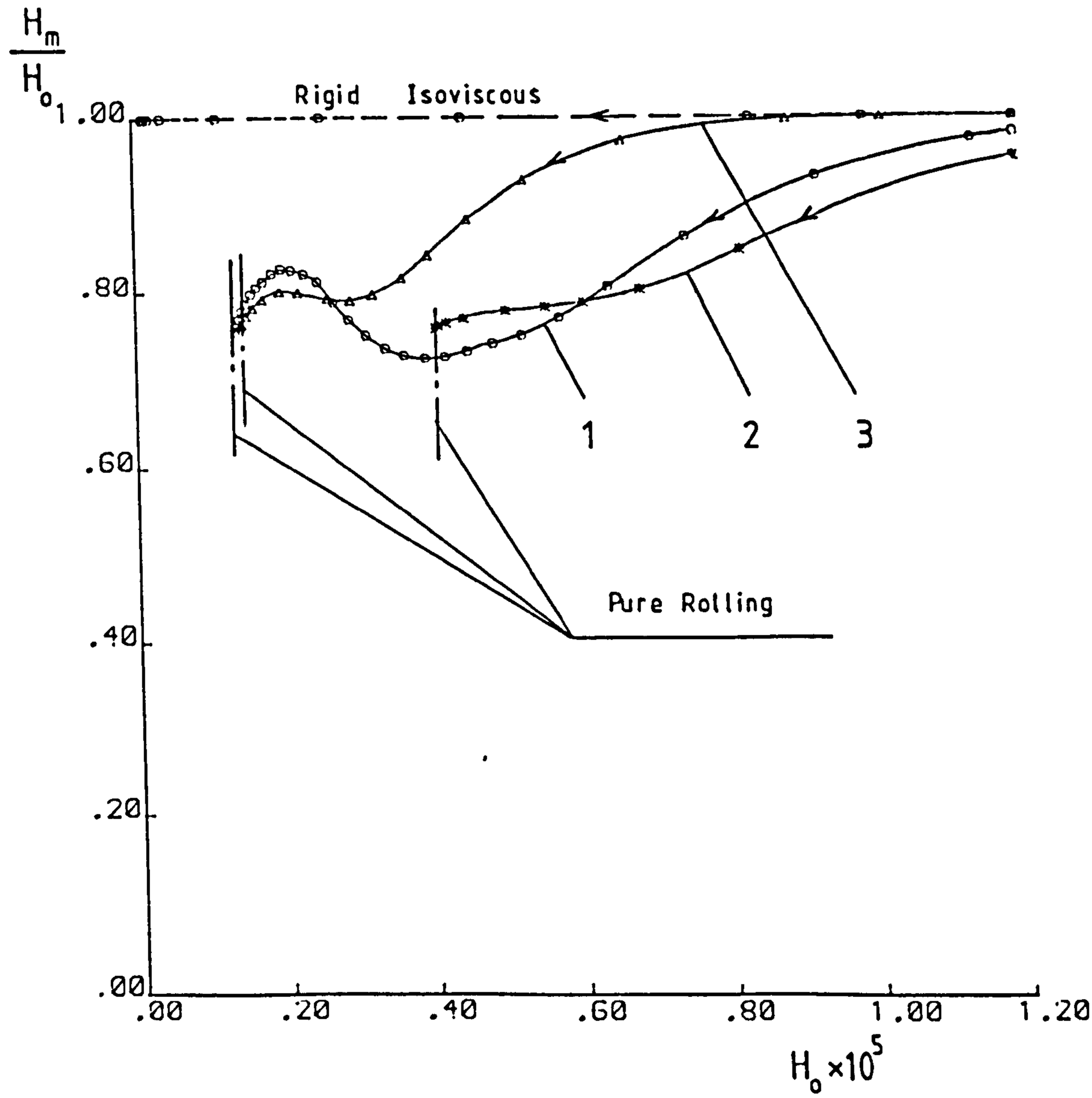

FIGURE(7 - 7) Variation of the Ratio (H_m / H_o) for Elastic Cylinders in Combined Rolling and Squeeze Film Action Under the Influence of a Constant Load in the Presence of a Piezoviscous Fluid

G = 4733

1 - $\bar{F}$	$=3.26\times10^{-6}$	$U=8.93\times10^{-14}$
2 -	$=3.26\times10^{-6}$	$=4.47\times10^{-13}$
3 -	$=2.17\times10^{-6}$	$=8.93\times10^{-14}$

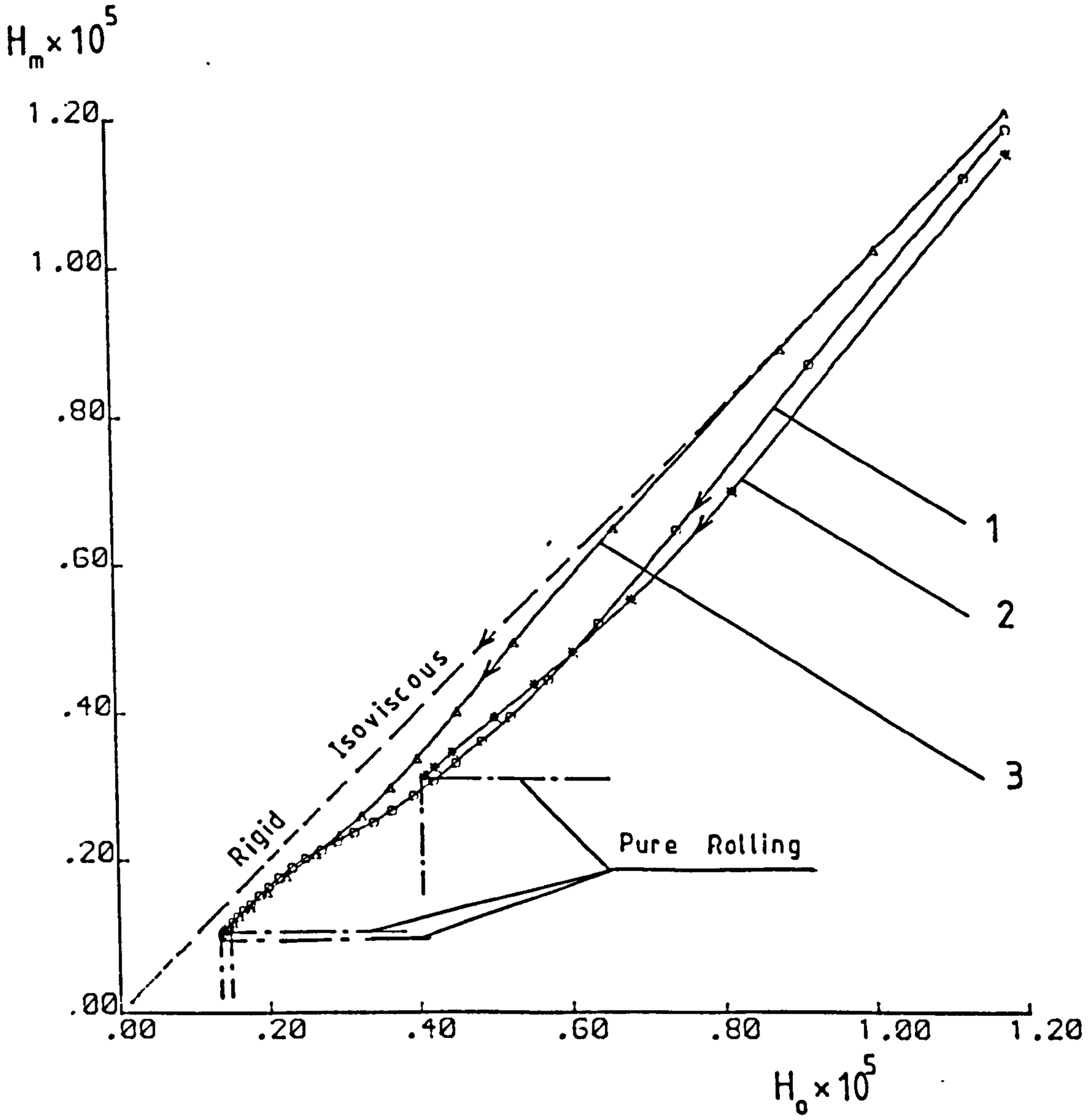

FIGURE(7 - 8) Variation of the Minimum Film Thickness for Elastic Cylinders in Combined Rolling and Squeeze Film Action Under the Influence of a Constant Load in the Presence of a Piezoviscous Fluid

G = 4733

1 - $\bar{F} = 3.26 \times 10^{-6}$ $U = 8.93 \times 10^{-14}$

2 - $= 3.26 \times 10^{-6}$ $= 4.47 \times 10^{-13}$

3 - $= 2.17 \times 10^{-6}$ $= 8.93 \times 10^{-14}$

Rigid Solids - Isoviscous Fluid

Solution for Comparison With (1)

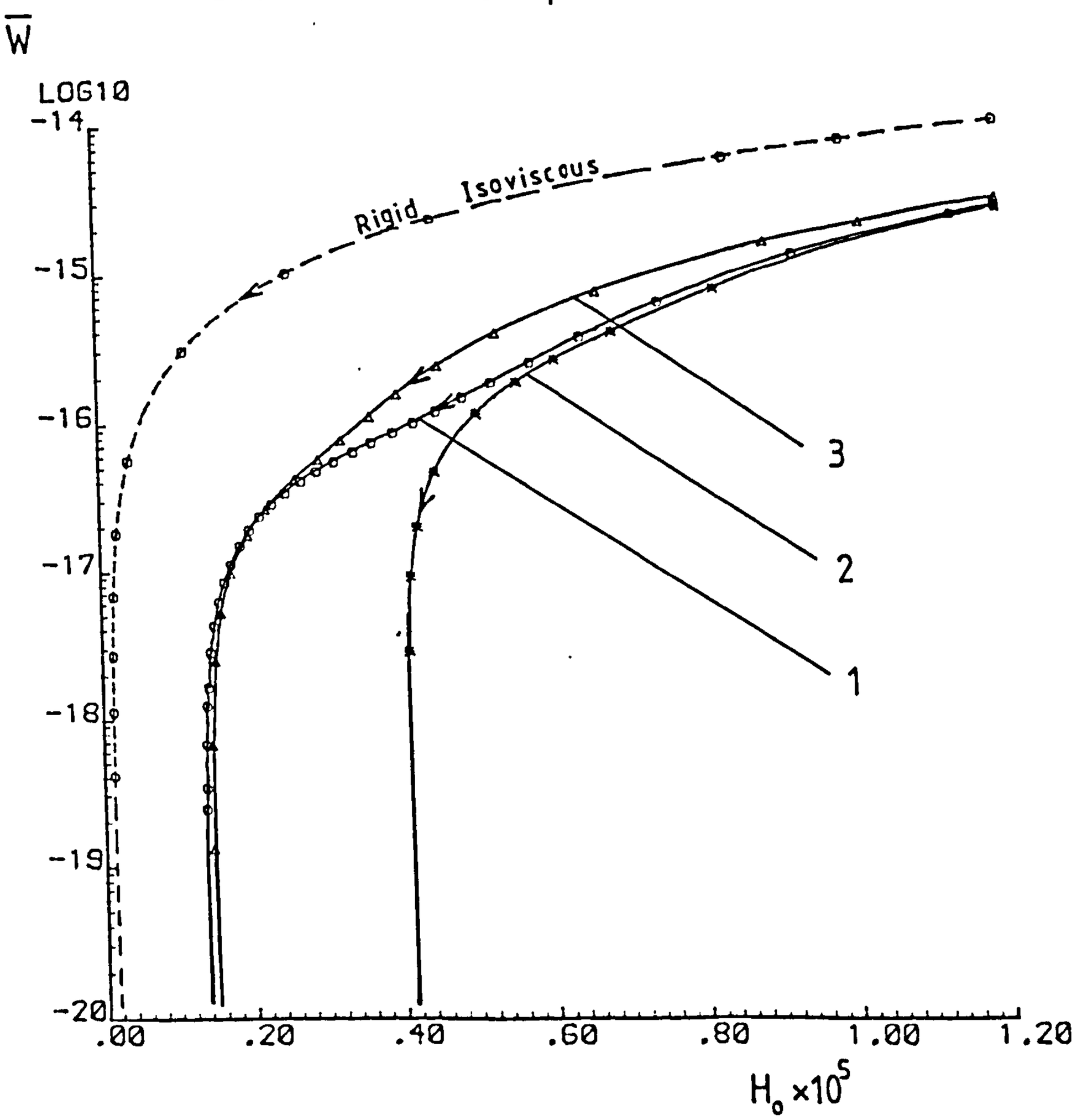

FIGURE(7 - 9) Variation of the Normal Approach Velocity for Elastic Cylinders in Combined Rolling and Squeeze Film Action Under the Influence of a Constant Load in the Presence of a Piezoviscous Fluid

G = 4733

For the same material parameter (G) and applied load parameter ($\bar{F}$), the normal approach velocity (W) decreases as the entraining parameter (U) increases.

The effect of elasticity under combined entraining and squeeze film action becomes more important as the dimensionless load parameter ($\bar{F}$) is increased for a given dimensionless entraining velocity parameter (U). Therefore, the velocity of normal approach (W), being the difference between the absolute velocity of the rigid body and the deformation velocity, is reduced when the dimensionless load parameter ($\bar{F}$) is increased.

7.6 Time History of Central and Minimum Film Thickness in Combined Squeeze-Film and Rolling Motion Under the Action of a Constant Load

Time histories of the dimensionless central film thickness (H_o) and the dimensionless minimum film thickness (H_m) are recorded in Figures (7.10) and (7.11) respectively for a number of specified conditions. These figures display the variation of the dimensionless central film thickness (H_o) and the dimensionless minimum film thickness (H_m) with time (t), under a constant load in combined entraining and squeeze film action. Two values of the dimensionless load ($\bar{F}$) and two values of the dimensionless entraining velocity parameter (U) were considered.

It is clear from Figure (7.10) that the central film thickness (H_o) decreases with the passage of time until it reaches equilibrium at the pure rolling or steady state condition. The total

1 - $\bar{F} = 3.26 \times 10^{-6}$ $U = 8.93 \times 10^{-14}$

2 - $= 3.26 \times 10^{-6}$ $= 4.47 \times 10^{-13}$

3 - $= 2.17 \times 10^{-6}$ $= 8.93 \times 10^{-14}$

Rigid Solids - Isoviscous Fluid

Solution for Comparison With(1)

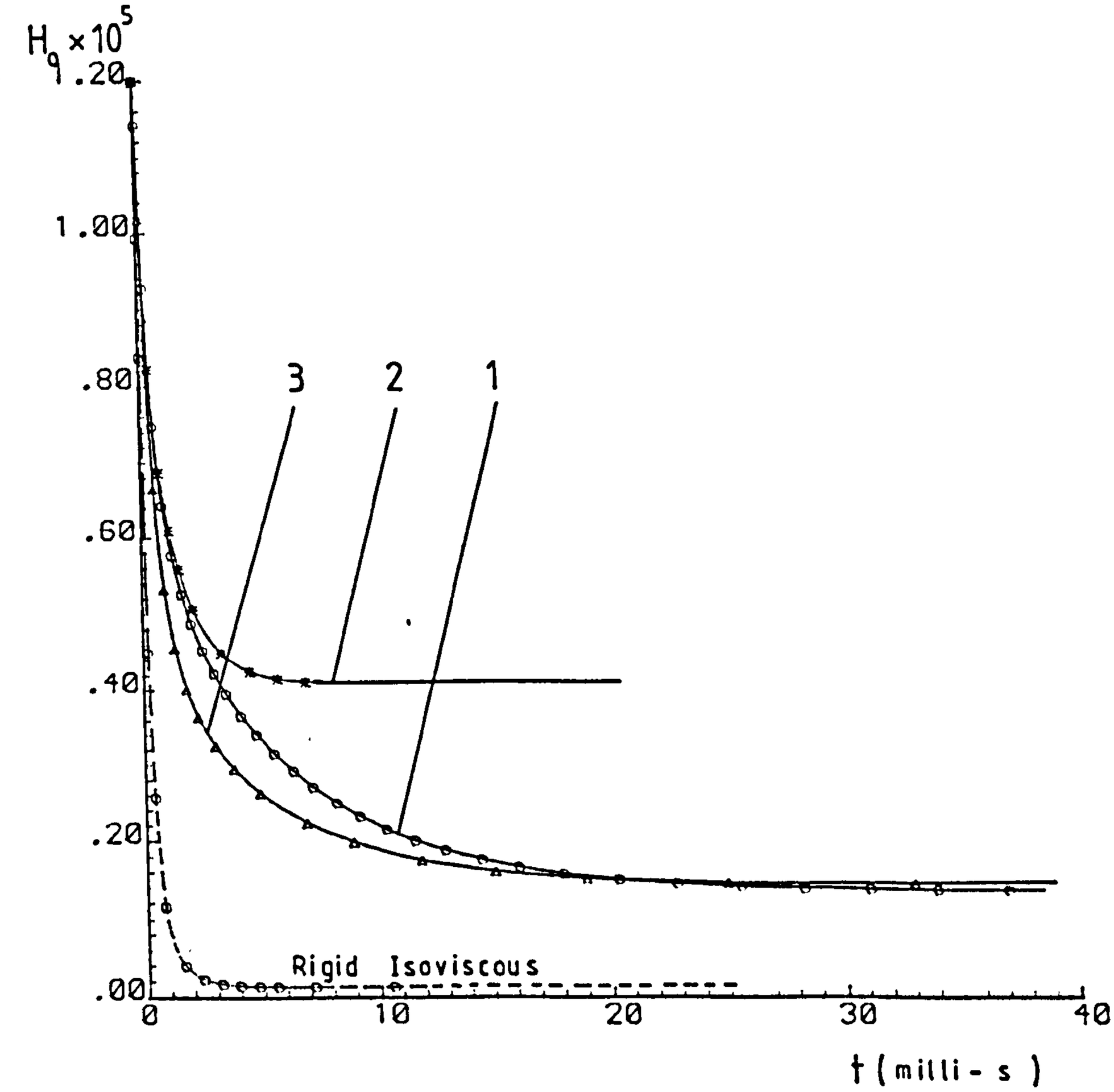

FIGURE(7 - 10) Time History of the Central Film Thickness for Elastic Cylinders in Combined Rolling and Squeeze Film Action Under the Influence of a Constant Load in the Presence of a Piezoviscous Fluid

G = 4733

1 - $\bar{F} = 3.26 \times 10^{-6}$ $U = 8.93 \times 10^{-14}$

2 - $= 3.26 \times 10^{-6}$ $= 4.47 \times 10^{-13}$

3 - $= 2.17 \times 10^{-6}$ $= 8.93 \times 10^{-14}$

Rigid Solids - Isoviscous Fluid

Solution for Comparison With(1)

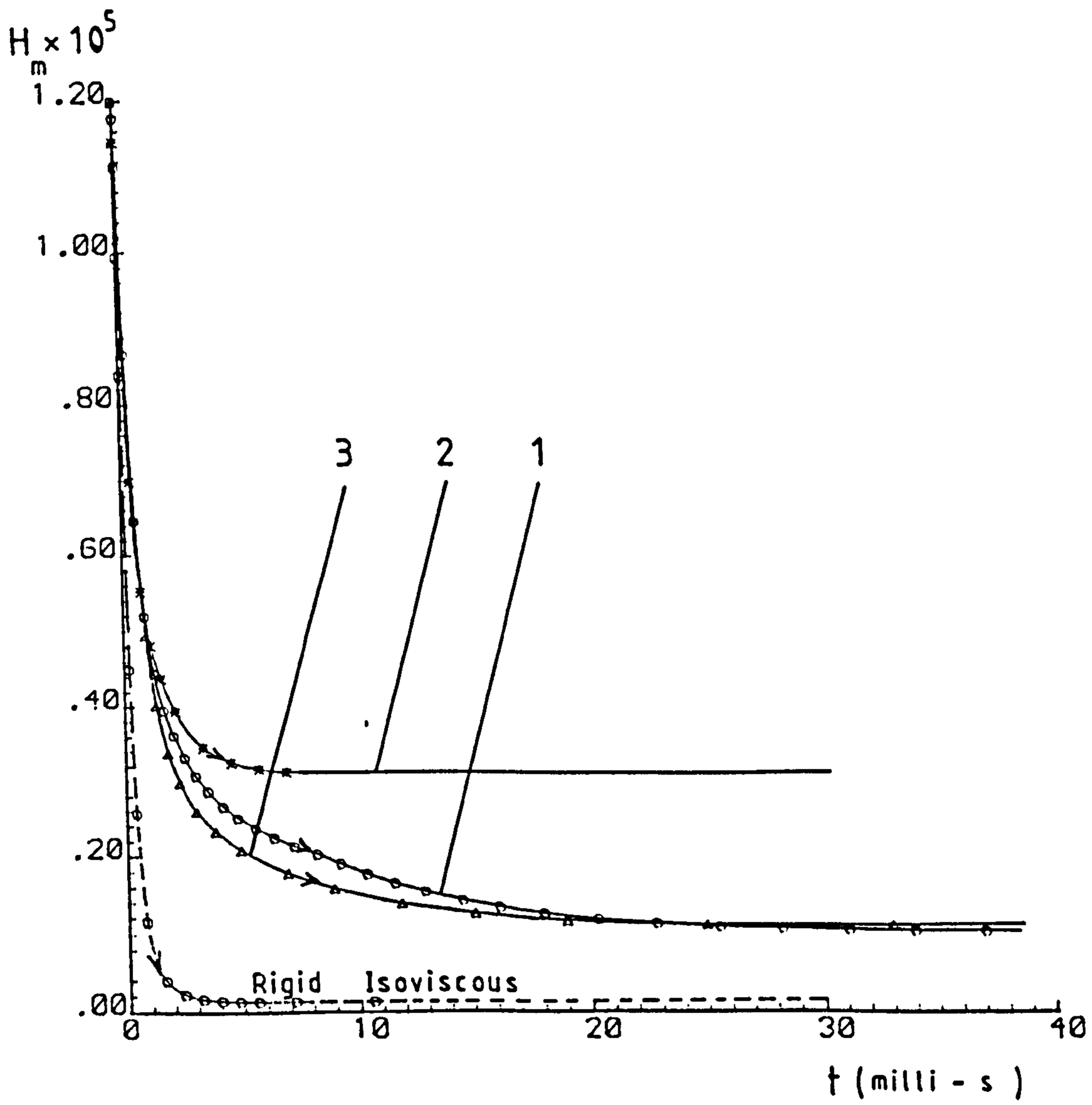

FIGURE(7 - 11) Time History of the Minimum Film Thickness for Elastic Cylinders in Combined Rolling and Squeeze Film Action Under the Influence of a Constant Load in the Presence of a Piezoviscous Fluid

G = 4733

time taken for (H_o) and (H_m) to approach their equilibrium values within a range of five percent (5%) increases as the dimensionless load ($\bar{F}$) increases and the entraining velocity parameter (U) decreases. Moreover, with the same applied load (F) and entraining velocity (u), the elastohydrodynamic system takes about <u>six</u> times longer to move to equilibrium than the hydrodynamic system (isoviscous and rigid solids). Hence, it seems that the elastic deformations of the surfaces bounding the flow emphasize transient effects.

Figure (7.11) shows that the behaviour of the minimum film thickness (H_m) is quite similar to the behaviour of the central film thickness (H_o) found in Figure (7.10).

7.7 Time History of Minimum Film Thickness Under Sinusoidal Normal Loading

An illustration of the elastohydrodynamic lubrication response of the minimum film thickness to sinusoidal loading of the form $\left[F(t) = F_o\ (1 + a \sin\omega t) \right]$ is shown in Figure (7.12) to (7.17). Each figure displays the variation of the dimensionless ratio $\left(\frac{H_m}{H_{mR}}\right)$ (i.e. the minimum film thickness $H_m(t)$/the minimum film thickness (H_{mR}) of the pure rolling condition for the base load (F_o)) with the dimensionless time (ωt). The influence of the different parameters of the system have been studied, i.e., the effect of the dimensionless damping parameter $\left(D_e = \frac{R}{u\sqrt{\bar{F}_o}}\right)$, the dimensionless entraining parameter $\left(g_e = \frac{\bar{F}_o^{3/2}}{GU}\right)$ and the amplitude of sinusoidal load (a). The physical data used in this study are shown in Table (7.2).

Table (7.2) Physical Data for Cyclic, Non-Steady State Force Calculations of Minimum Film Thickness

$R = 0.02$ (m) , $\eta_o = 0.0411$ (Pas) , $\alpha = 2.058 \times 10^{-8}$ (m^2/N)

Figure		Entraining Velocity (u) (m/s)	Basic Load(F_o) (N/m)	Force Amplitude (a)	Angular Velocity of Sinusoidal Load (ω) (s^{-1})	Damping Parameter (D_e)	Entraining Parameter (g_e)	$\bar{F}_o$	U	G
7.12	Case (1)	0.01	10000	0.5	15.7	0.046	7.56	0.217×10^{-5}	0.893×10^{-13}	4733
	Case (2)	0.01	10000	0.5	157	0.46	7.56	0.217×10^{-5}	0.893×10^{-13}	
	Case (3)	0.01	10000	0.5	314	0.92	7.56	0.217×10^{-5}	0.893×10^{-13}	
7.13	Case (1)	0.01	10000	0.5	314	0.92	7.56	0.217×10^{-5}	0.893×10^{-13}	
	Case (2)	0.004	6000	0.5	157	0.90	8.8	0.13×10^{-5}	0.357×10^{-13}	
7.14	Case (1)	0.01	10000	0.5	15.7	0.046	7.56	0.217×10^{-5}	0.893×10^{-13}	
	Case (2)	0.1	20000	0.5	157	0.066	2.1	0.43×10^{-5}	0.893×10^{-12}	
7.15	Case (1)	0.01	10000	0.5	157	0.46	7.56	0.217×10^{-5}	0.893×10^{-13}	
	Case (2)	0.01	10000	0.25	157	0.46	7.56	0.217×10^{-5}	0.893×10^{-13}	
7.16	Case (1)	0.1	20000	0.5	157	0.066	2.1	0.43×10^{-5}	0.893×10^{-12}	
	Case (2)	0.1	20000	0.25	157	0.066	2.1	0.43×10^{-5}	0.893×10^{-12}	
7.17	E.H.L.	0.01	10000	0.5	157	0.46	7.56	0.217×10^{-5}	0.893×10^{-13}	
	Rigid - Iso.	0.01	10000	0.5	157	-	-	-	-	

It is clear from the curves in Figures (7.12) to (7.16) that once the system has been set into motion it will initially undergo a non-harmonic transient following the frequency of the exitation. If the system possesses damping the part of the motion which is due to the transient motion will eventually die out. The part of the motion sustained by the sinusoidal exitation (steady state response) will persist as long as the exitation exists.

In the absence of damping the film thickness cycle would be in phase with the forcing (load) cycle. In this case the dimensionless minimum film thickness (H_m) would be a minimum when the force was a maximum. The curves of Figure (7.12) show that for a large range of the dimensionless damping parameter (D_e = 0.046, 0.46, 0.92), the damping is very important and the phase lag of the response to the forcing cycle in the steady state response varies with (D_e). When the damping parameter (D_e) takes the value (0.046) the damping effect is negligible and the response follows the forcing cycle quite closely. On the other hand, the response for a higher damping condition (D_e = 0.46, 0.92) do exhibit a phase lag.

Figures (7.13) and (7.14) show that the dimensionless entraining parameter (g_e) does not appear to have a drastic effect upon the amplitude of the minimum film thickness oscillations, and the damping is practically independent of (g_e).

The effect of the amplitude of the force (a) is shown in Figures (7.15) and (7.16). Two values of the dimensionless entraining parameter (g_e) were used; the high value being (g_e=7.56) and the lower value (g_e=2.1). A reduction in the minimum film

1- $D_e = 0.046$

2- $= 0.46$

3- $= 0.92$

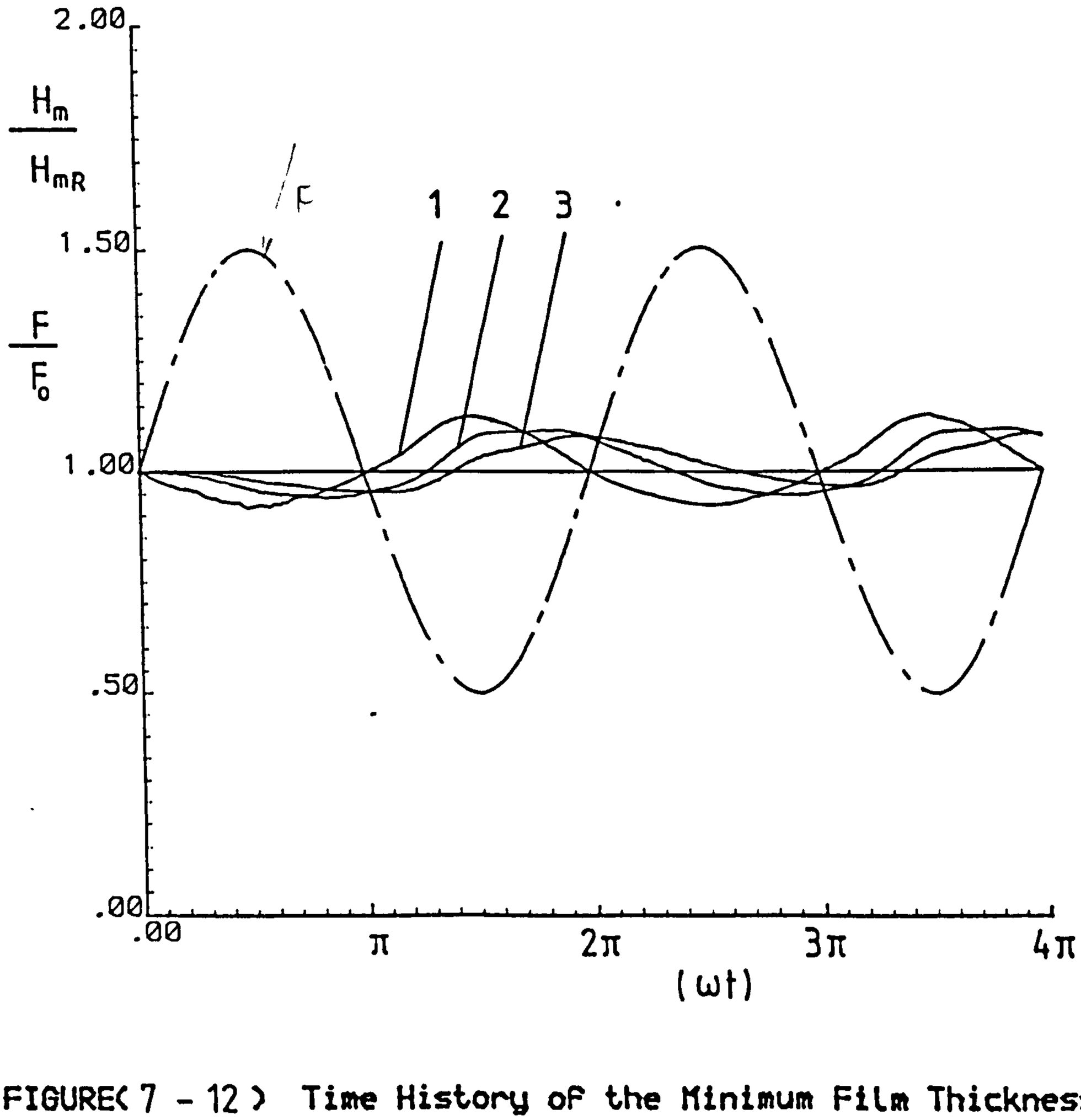

FIGURE(7 - 12) Time History of the Minimum Film Thickness for Elastic Cylinders in Combined Rolling and Normal Motion Under the Influence of a Sinusoidal Load (—·—) in the Presence of a Piezoviscous Fluid

$a = 0.5$ $g_e = 7.56$

$1 - g_e = 7.56$

$2 - \quad = 8.8$

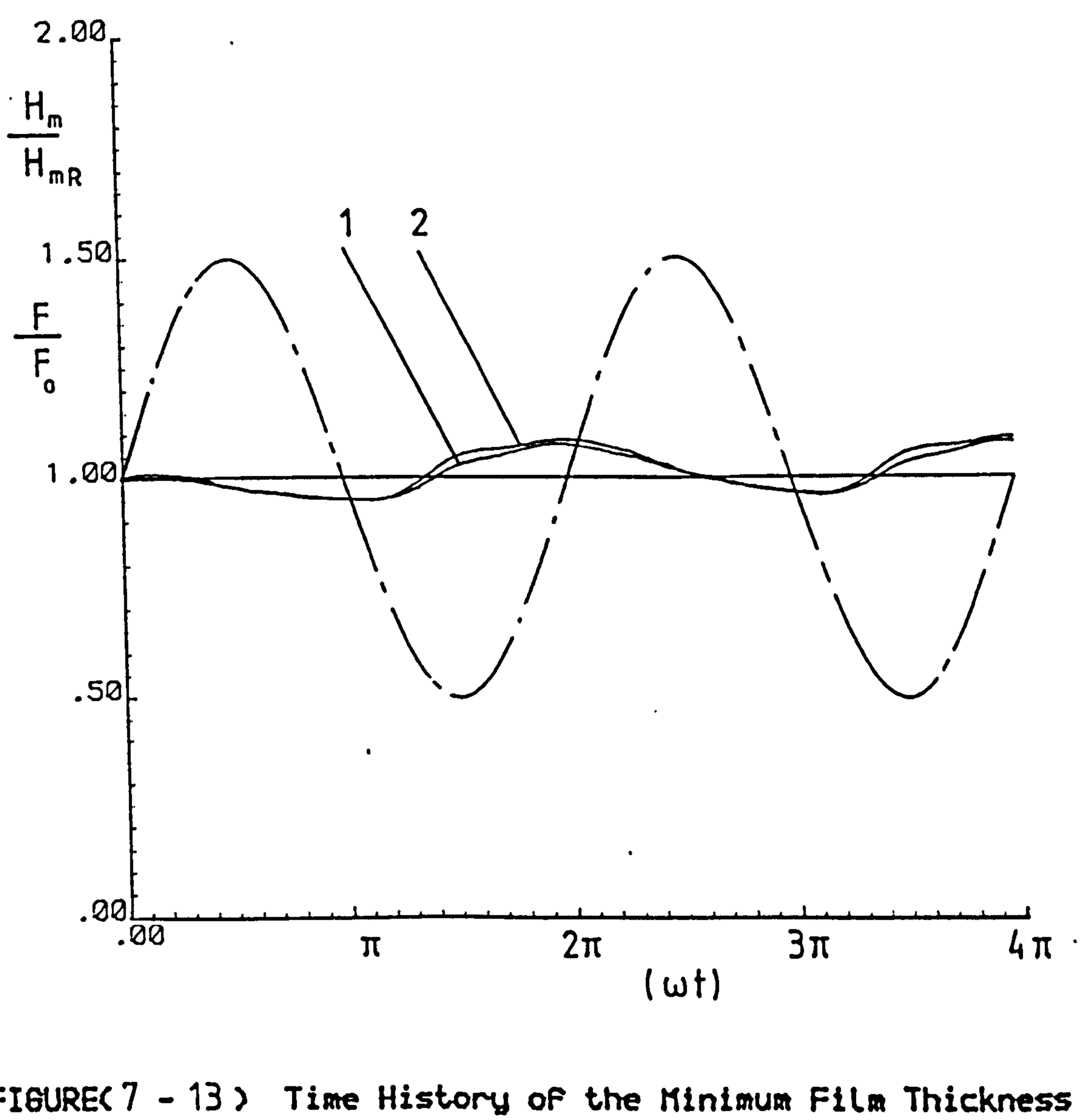

FIGURE(7 - 13) Time History of the Minimum Film Thickness for Elastic Cylinders in Combined Rolling and Normal Motion Under the Influence of a Sinusoidal Load (——-——) in the Presence of a Piezoviscous Fluid

$a = 0.5$ $\qquad$ $D_e = 0.9$

1 - g_e = 7.56

2 - = 2.1

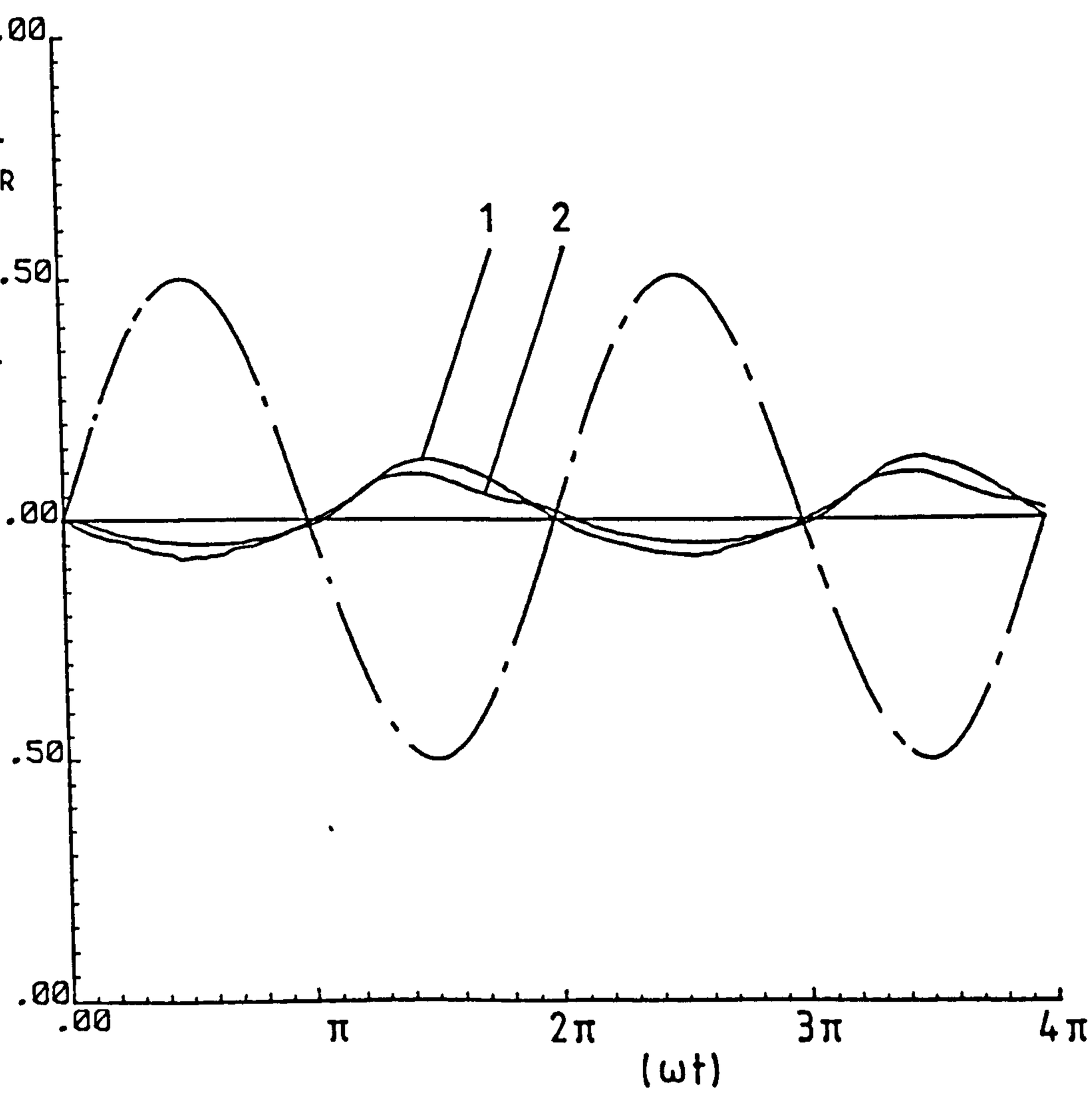

FIGURE(7 - 14) Time History of the Minimum Film Thickness for Elastic Cylinders in Combined Rolling and Normal Motion Under the Influence of a Sinusoidal Load (——-——) in the Presence of a Piezoviscous Fluid

$a = 0.5$ $D_e = 0.046, 0.066$

1- $\alpha = 0.5$

2- $= 0.25$

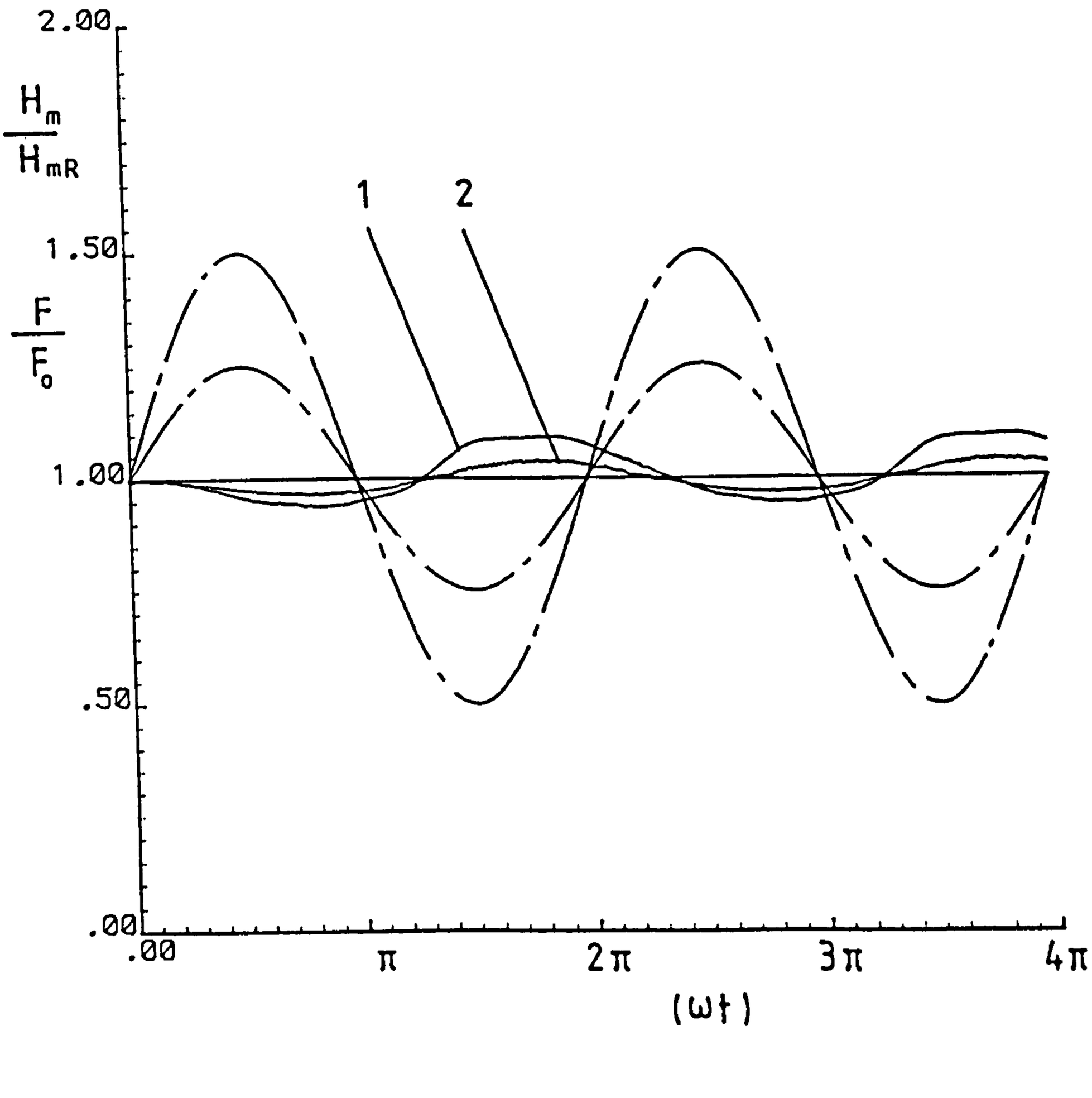

FIGURE(7 - 15) Time History of the Minimum Film Thickness for Elastic Cylinders in Combined Rolling and Normal Motion Under the Influence of a Sinusoidal Load (——-——) in the Presence of a Piezoviscous Fluid

$D_e = 0.46$ $g_e = 7.56$

1 - $\alpha = 0.5$

2 - $= 0.25$

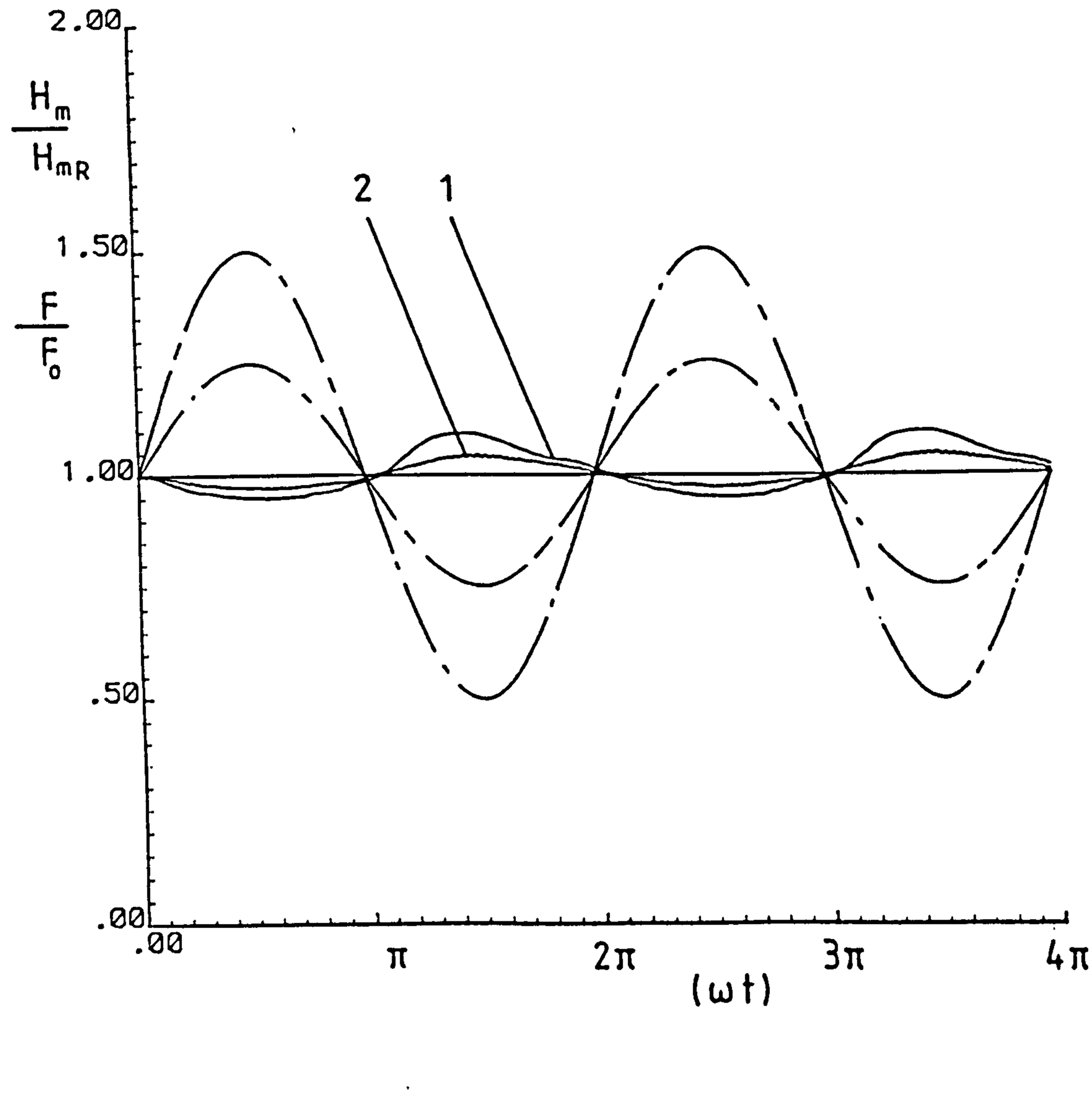

FIGURE(7 - 16) Time History of the Minimum Film Thickness For Elastic Cylinders in Combined Rolling and Normal Motion Under the Influence of a Sinusoidal Load (——-——) in the Presence of a Piezoviscous Fluid

$D_e = 0.066$ $g_e = 2.1$

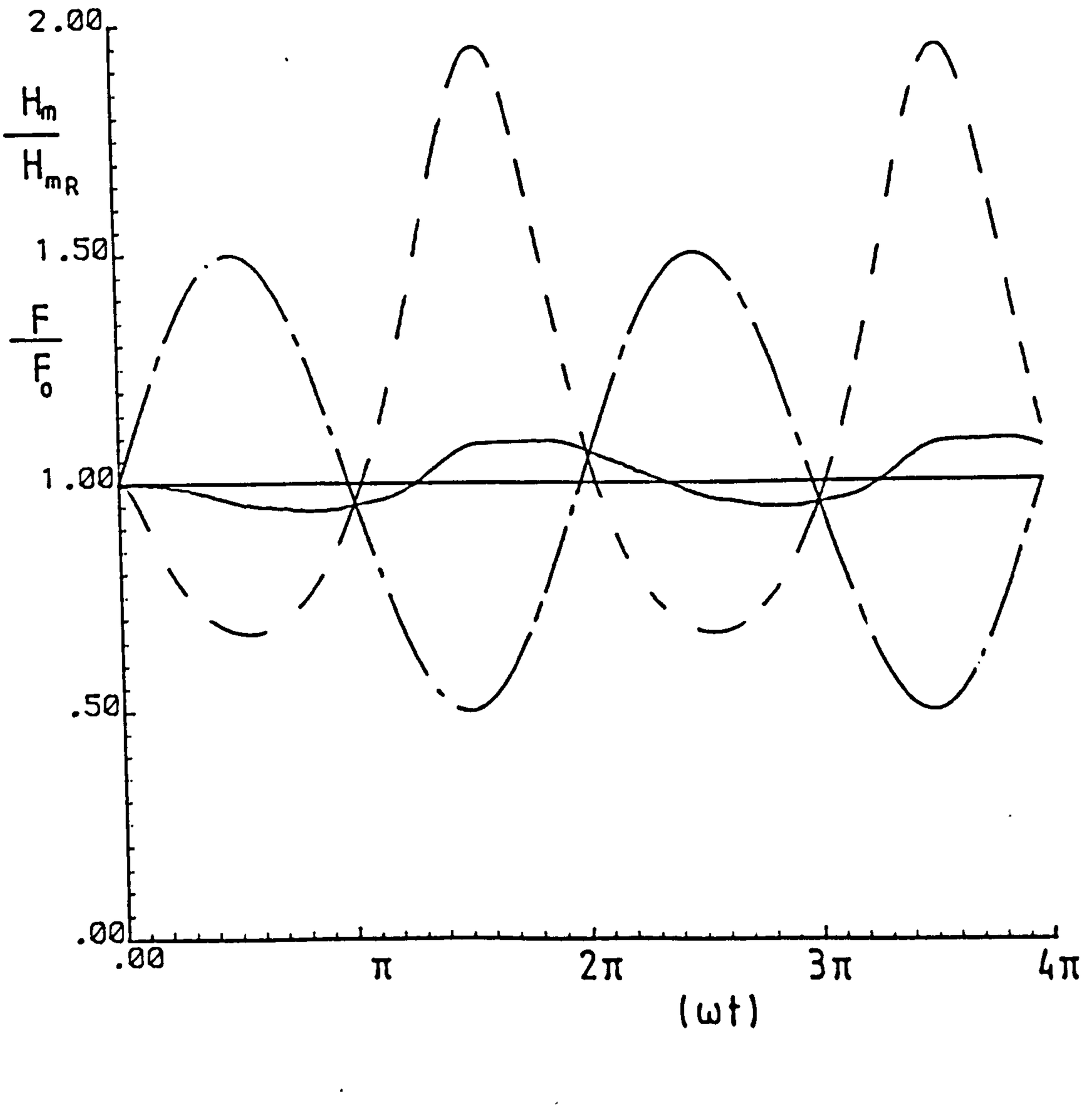

FIGURE(7 - 17) Comparison of Time History of the Minimum Film Thickness for Cylinders in Combined Rolling and Normal Motion Under the Influence of a Sinusoidal Load (— - —) With Elastohydrodynamic Theory (————) and Hydrodynamic Theory(— — —)

$a = 0.5$ $D_e = 0.46$ $g_e = 7.56$

thickness was obtained (about 2.1%) when the force amplitude (a) increased from (0.25) to (0.5). The apparent insensitivity shown by the lubricant to the applied load amplitude is a confirmation of the slight effect of the load on the minimum film thickness in elastohydrodynamic lubrication (see Dowson and Higginson (1977)). The same figures also show that the amplitude of the force (a) has little effect upon the damping.

The response of the minimum film thickness under both elastohydrodynamic and hydrodynamic (isoviscous and rigid - solids) conditions with the same loading [F(t)] and entraining velocity (u) are shown in Figure (7.17). It is clear that the elastohydrodynamic behaviour emphasizes the squeeze film effect so that the minimum film thickness is not very sensitive to the variation of the applied load. Hence, response fluctuations are considerably smaller with elastohydrodynamic conditions than under hydrodynamic conditions. Moreover, the damping effect due to normal motion is more pronounced for the elastohydrodynamic lubrication conditions.

7.8 Time History of Central Film Thickness Under Sinusoidal Normal Loading

The elastohydrodynamic lubrication response of the central film thickness to sinusoidal loading of the form [$F(t)=F_o(1+a\sin\omega t)$] is shown in Figures (7.18) to (7.23). Each figure displays the variation of the dimensionless ratio $\left(\frac{H_o}{H_{oR}}\right)$ (i.e. the central film thickness $H_o(t)$/the central film thickness (H_{oR}) of the pure rolling condition under the base load (F_o)) with the dimensionless time (ωt). The influence of the different parameters of the system upon central

film thickness has been studied, i.e., the effect of the dimensionless damping parameter $\left(D_e = \frac{\omega R}{u\sqrt{\bar{F}_o}}\right)$, the dimensionless entraining parameter $\left(g_e = \frac{\bar{F}_o^{3/2}}{GU}\right)$ and the amplitude of the sinusoidal load (a). The physical data used in this study are shown in Table (7.3).

Again, the curves of Figure (7.18) show that for a large range of the dimensionless parameter (D_e = 0.046, 0.46, 0.92), the damping is very important and the phase lag of the response to the forcing cycle in the steady state response varies with (D_e). On the other hand, Figures (7.19) and (7.20) show that the dimensionless entraining parameter (g_e) has an important effect upon the behaviour of the central film thickness response, particularly at low values of (g_e). At higher values of (g_e = 7.56, 8.8), figure (7.19), the behaviour of the central film thickness is quite similar to that of the minimum film thickness. Whereas, at low values (g_e), Figure (7.20), non-linear amplitude response characteristics may be observed as in the case when (g_e = 2.1). In this case the central film thickness shows a more complicated response to sinusoidal loading at small values of the dimensionless entraining parameter.

The effect of the amplitude of the force (a) is shown in Figures (7.21), (7.22) and (7.23). Three values of the dimensionless entraining parameter (g_e) were used, the high value (g_e = 8.8) and the two low values (g_e = 2.1, 0.95). At the higher value of the dimensionless entraining parameter (g_e = 8.8), Figure (7.21), the behaviour of central film thickness is quite similar to that for minimum film thickness. A reduction of about (2%) in the minimum value of the central film thickness throughout a complete forcing

Table (7.3) Physical Data for Cyclic, Non-Steady State Force Calculations of Central Film Thickness

$R = 0.02$ (m) , $\eta_o = 0.0411$ (Pas) , $\alpha = 2.058 \times 10^{-8}$ (m^2/N)

Figure		Entraining Velocity (u) (m/s)	Basic Load(F_o) (N/m)	Force Amplitude (a)	Angular Velocity of Sinusoidal Load (ω) (s^{-1})	Damping Parameter (D_e)	Entraining Parameter (g_e)	$\bar{F}_o$	U	G
7.18	Case (1)	0.01	10000	0.5	15.7	0.046	7.56	0.217×10^{-5}	0.893×10^{-13}	4733
	Case (2)	0.01	10000	0.5	15.7	0.46	7.56	0.217×10^{-5}	0.893×10^{-13}	
	Case (3)	0.01	10000	0.5	314	0.92	7.56	0.217×10^{-5}	0.893×10^{-13}	
7.19	Case (1)	0.01	10000	0.5	314	0.92	7.56	0.217×10^{-5}	0.893×10^{-13}	
	Case (2)	0.004	6000	0.5	157	0.90	8.8	0.13×10^{-5}	0.357×10^{-13}	
7.20	Case (1)	0.01	10000	0.5	15.7	0.046	7.56	0.217×10^{-5}	0.893×10^{-13}	
	Case (2)	0.1	20000	0.5	157	0.066	2.1	0.43×10^{-5}	0.893×10^{-12}	
7.21	Case (1)	0.004	6000	0.5	157	0.90	8.8	0.13×10^{-5}	0.357×10^{-13}	
	Case (2)	0.004	6000	0.25	157	0.90	8.8	0.13×10^{-5}	0.357×10^{-13}	
7.22	Case (1)	0.1	20000	0.5	157	0.066	2.1	0.43×10^{-5}	0.895×10^{-12}	
	Case (2)	0.1	20000	0.25	157	0.066	2.1	0.43×10^{-5}	0.895×10^{-12}	
7.23	Case (1)	0.5	34000	0.5	157	0.017	0.95	0.739×10^{-5}	0.446×10^{-11}	
	Case (2)	0.5	34000	0.25	157	0.017	0.95	0.739×10^{-5}	0.446×10^{-11}	

1 - $D_e = 0.046$

2 - $= 0.46$

3 - $= 0.92$

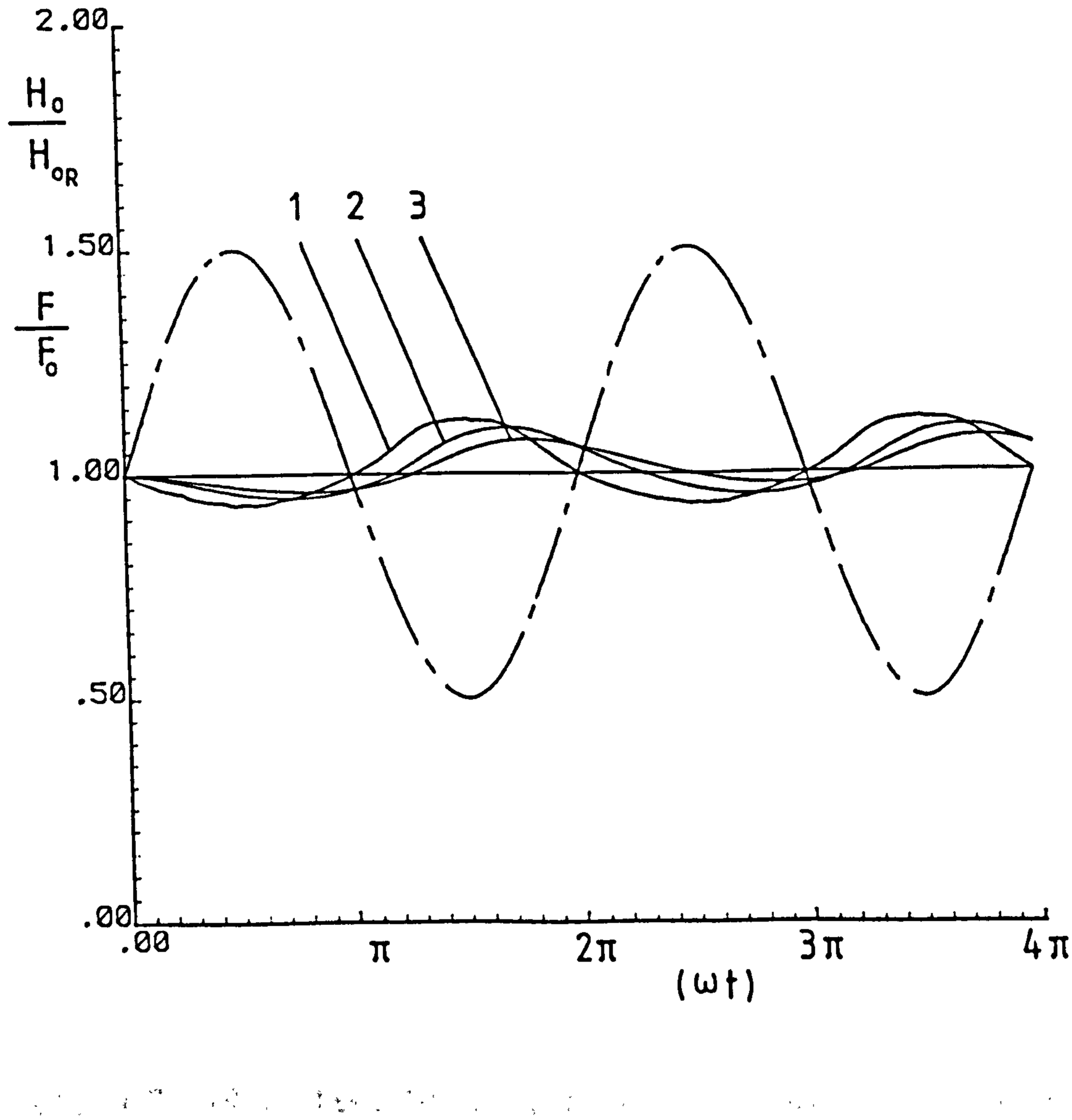

FIGURE(7 - 18) Time History of the Central Film Thickness for Elastic Cylinders in Combined Rolling and Normal Motion Under the Influence of a Sinusoidal Load (—— - ——) in the Presence of a Piezoviscous Fluid

$a = 0.5$ $g_e = 7.56$

1 - g_e = 7.56
2 - = 8.8

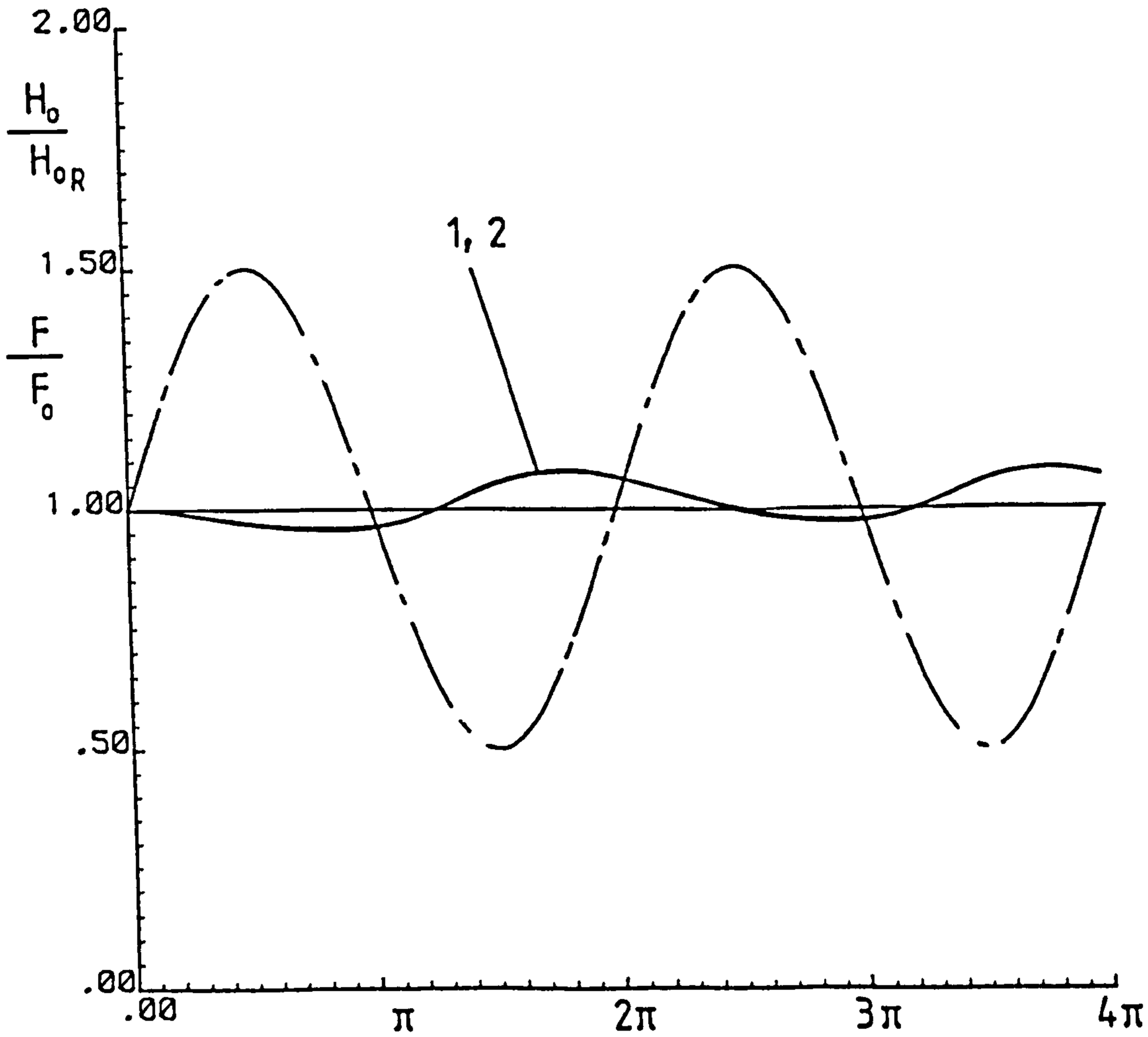

FIGURE(7 - 19) Time History of the Central Film Thickness for Elastic Cylinders in Combined Rolling and Normal Motion Under the Influence of a Sinusoidal Load (—— - ——) in the Presence of a Piezoviscous Fluid

α = 0.5 D_e = 0.9

1 - $g_e = 7.56$

2 - $= 2.1$

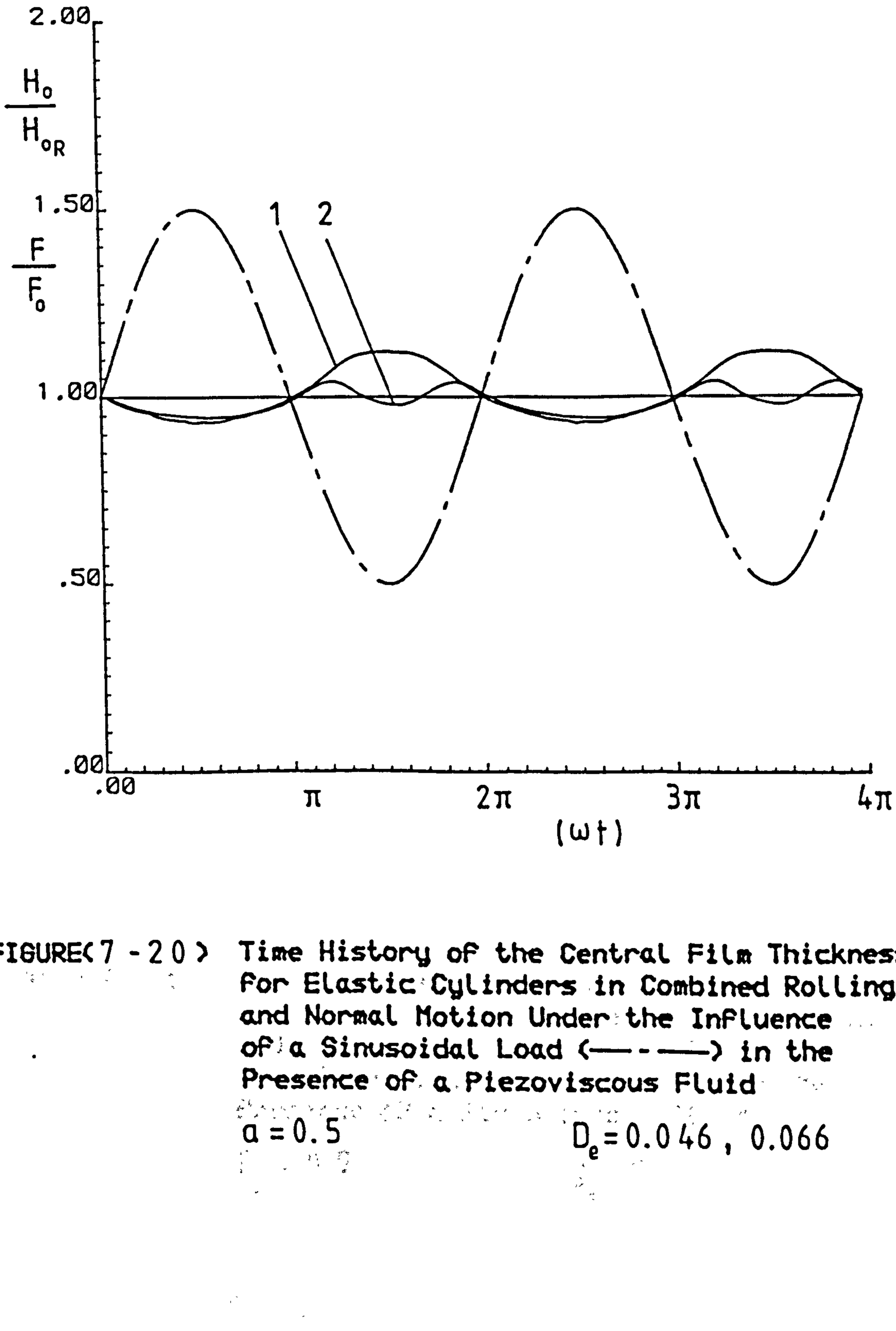

FIGURE(7 - 20) Time History of the Central Film Thickness for Elastic Cylinders in Combined Rolling and Normal Motion Under the Influence of a Sinusoidal Load (——-——) in the Presence of a Piezoviscous Fluid

$a = 0.5$ $D_e = 0.046, 0.066$

1 - a = 0.5

2 - = 0.25

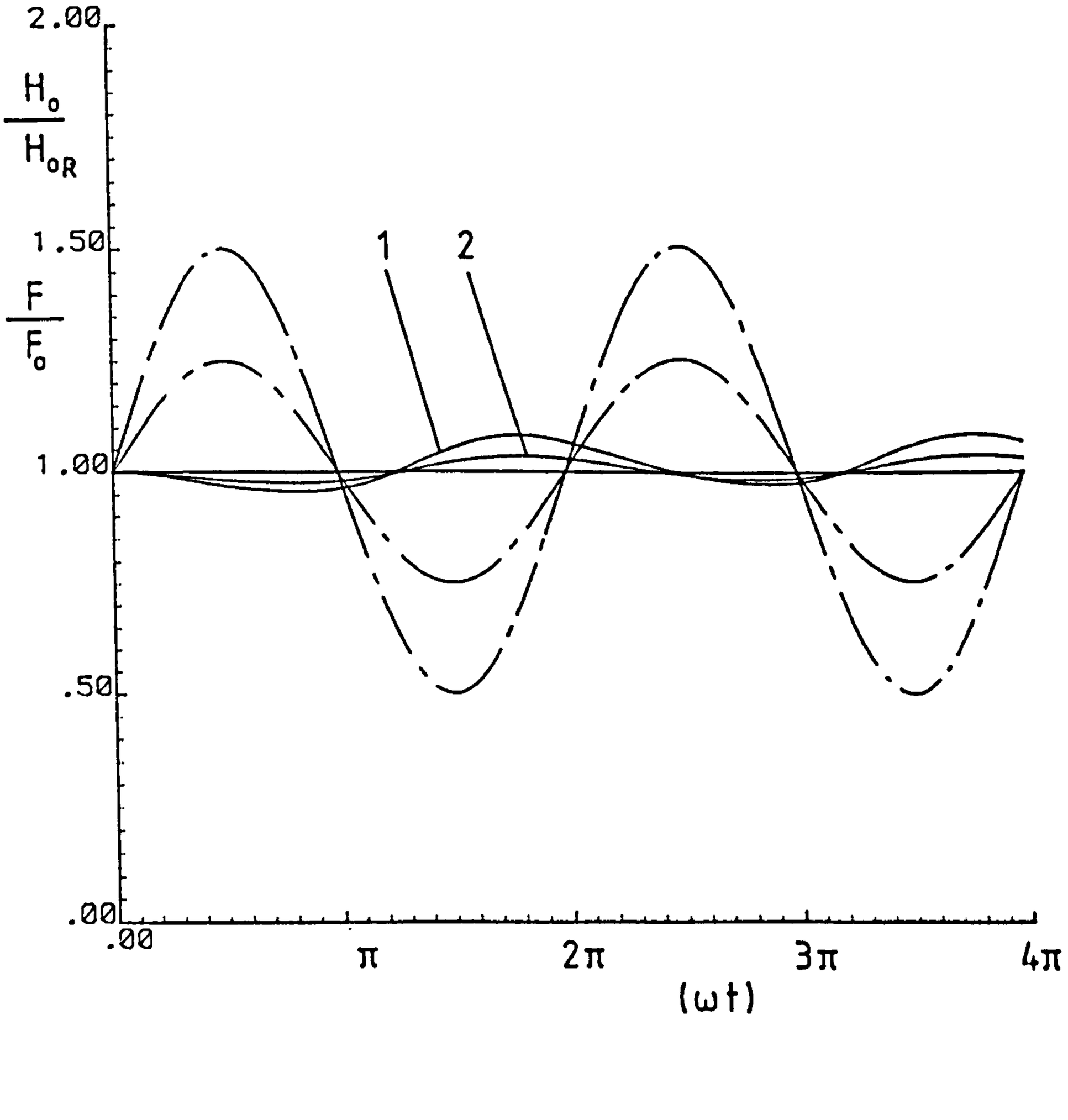

FIGURE(7 - 21) Time History of the Central Film Thickness for Elastic Cylinders in Combined Rolling and Normal Motion Under the Influence of a Sinusoidal Load (— · —) in the Presence of a Piezoviscous Fluid

$D_e = 0.9$ $g_e = 8.8$

1 - a = 0.5

2 - = 0.25

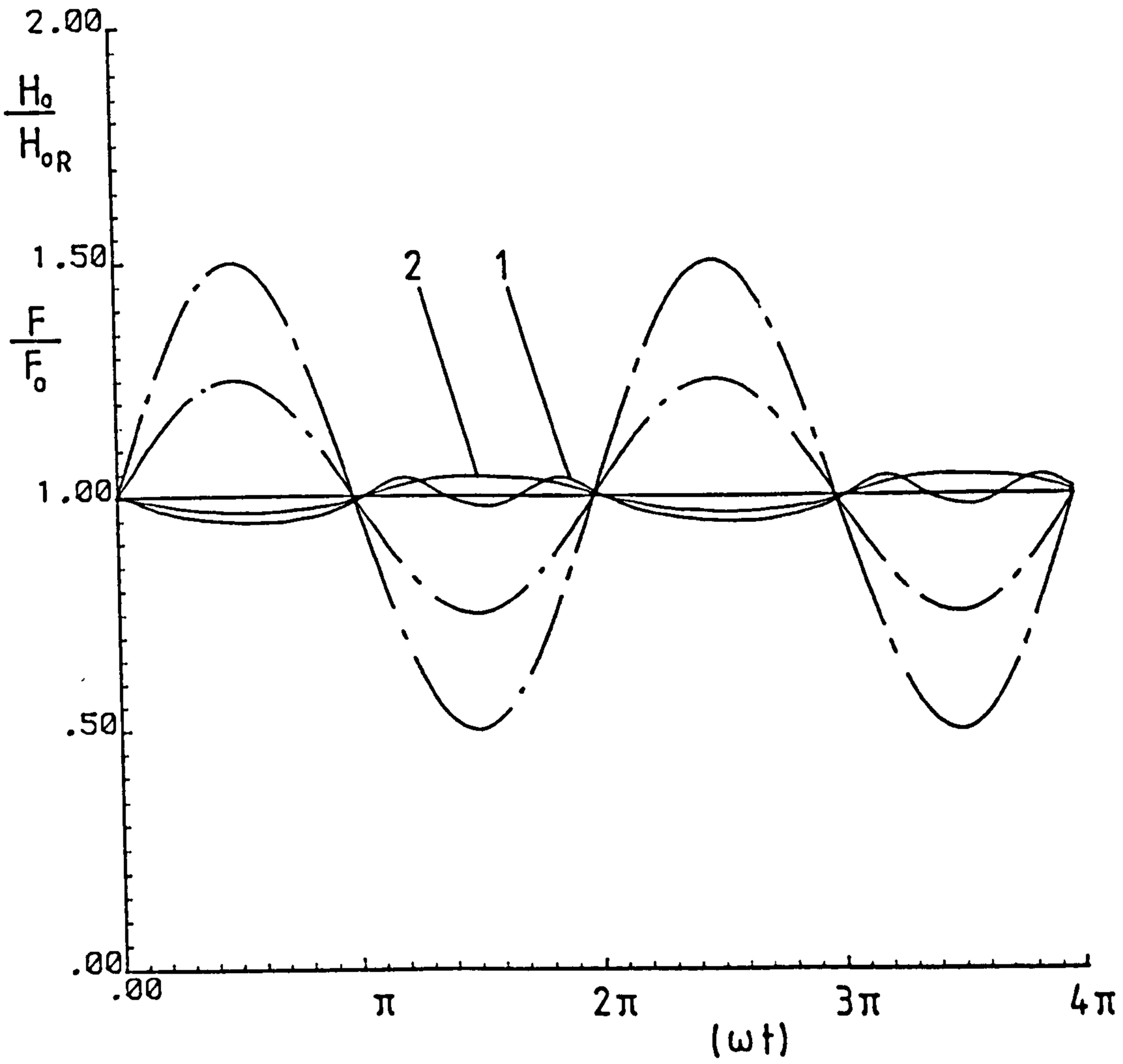

FIGURE(7 - 22) Time History of the Central Film Thickness for Elastic Cylinders in Combined Rolling and Normal Motion Under the Influence of a Sinusoidal Load (—— - ——) in the Presence of a Piezoviscous Fluid

$D_e = 0.066$ $g_e = 2.1$

1 - a = 0.5

2 - = 0.25

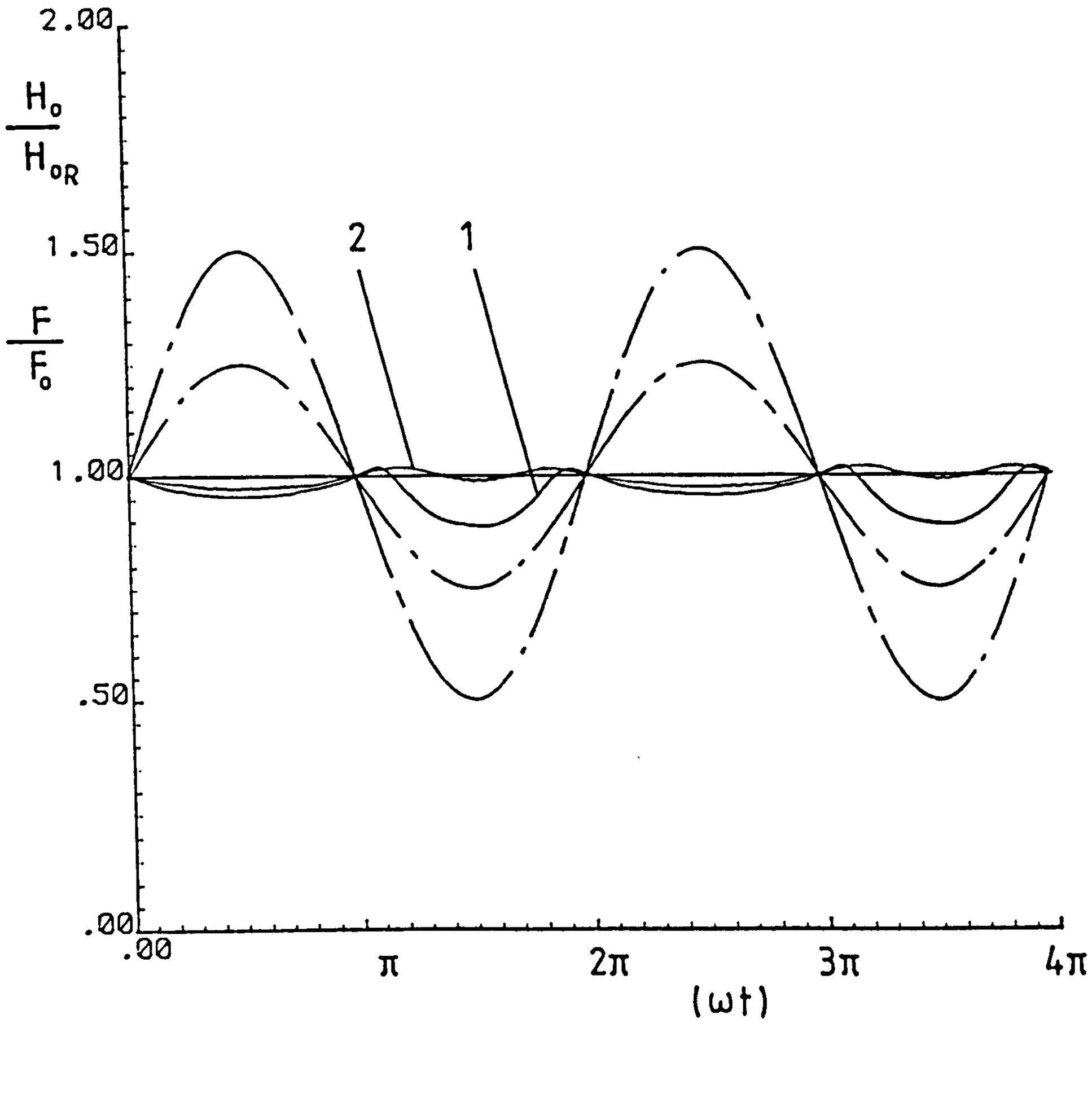

FIGURE(7 - 23) Time History of the Central Film Thickness for Elastic Cylinders in Combined Rolling and Normal Motion Under the Influence of a Sinusoidal Load (——-——) in the Presence of a Piezoviscous Fluid

$D_e = 0.017$ $g_e = 0.95$

cycle is obtained as the force amplitude is increased from (0.25) to (0.5). At the lower value of the dimensionless entraining parameter (g_e= 2.1), Figure (7.21), the non-linear amplitude response characteristics started to appear and no serious reduction in the minimum value of the central film thickness was obtained. At the lower value of the dimensionless entraining parameter (g_e=0.95), Figure (7.22), a reduction in the minimum value of the central film thickness of about (9%) was obtained as the force amplitude was increased from (0.25) to (0.5).

The elastohydrodynamic lubrication response to cyclic conditions becomes more stable as the value of the entraining parameter (g_e) is increased, because the pressure distribution and film shape in this case approach the Hertzian condition of dry contact. The presence of the Hertzian zone where the film shape is approximately constant gives an important stability to the system under cyclic conditions. On the other hand, at the low values of the entraining parameter (g_e), the film shape shows different forms ranging from the Hertzian to inclined shapes during the cycle. Hence, a more complicated response to cyclic conditions may be obtained, particularly with the central film thickness (H_o).

In the light of the cases considered, it may be observed that the central film thickness (H_o) behaviour in cyclic non-steady elastohydrodynamic lubrication is more complicated than that of the minimum film thickness. The response to a cyclic sinusoidal load is dependent to a great extent upon the damping parameter (D_e), the entraining parameter (g_e) and the amplitude of the load (a). Therefore, it would be difficult to anticipate with confidence the

variation of the central film thickness response under different circumstances. However, the minimum film thickness response might be readily predicted. Thus, the behaviour of dynamically loaded elastohydrodynamic line contact is probably better expressed in terms of the variation of minimum film thickness (H_m) for simplification and clarity.

7.9 Concluding Remarks

In this chapter, the influence of squeeze film action due to normal motion combined with 'entraining' action due to pure rolling has been investigated for the elastohydrodynamic lubrication of cylinders. The results were evaluated for specific conditions under constant and sinusoidal normal loading. Graphical representation of pressure distributions and film shapes have been presented together at successive reductions of the central film thickness (H_o). The variation of the dimensionless minimum film thickness (H_m), velocity of approach ($\bar{W}$) and peak pressure (P_k) under constant load have been included. Furthermore, the time histories of the central (H_o) and the minimum (H_m) film thickness under constant and sinusoidal normal loadings were introduced with a discussion of the viscous damping phenomenon associated with the squeeze film action.

The analysis presented makes the following advances over the previous elastohydrodynamic models and solutions schemes,

(a) It is a real transient analysis in which the full time histories of the system parameters are determined;

(b) Any specified load or load function can be accommodated;

(c) It utilizes a simple direct - iteration solution technique which simultaneously satisfies the governing elastic and hydrodynamic equations;

(d) It predicts all the characteristics of the elastohydrodynamic contact and the details of the pressure curve and oil film shape throughout the motion.

From the analysis of the influence of combined 'entraining' and 'normal motion' upon the elastohydrodynamic lubrication of line contacts the following conclusions may be drawn.

(i) <u>Under Constant Load</u>

1. Elastohydrodynamic lubrication of cylinders under the combined effect of 'entraining' and 'squeeze' film action may be divided into three different stages. In the early stage of motion, where the central film thickness is large, the 'entraining' effect is relatively unimportant, and the pressure and film shape are strongly influenced by the squeeze film effect. In the next stage, where both effects are important, new pressure distributions and film shapes are produced. These pressures and film shapes possess combined characteristics of the elastohydrodynamic lubrication of line contacts under pure rolling and pure squeeze film conditions. In the final stage, where the central film thickness (H_o) approaches the steady state value 'squeeze action' becomes unimportant, with the pressure distribution and film shapes being strongly influenced by the 'entraining action'. The results thus

possess all the characteristics of the steady state elastohydrodynamic lubrication phenomenon of line contacts.

2. The peak pressure gradually increases with decreasing film thickness, and reaches a maximum value. With a further decrease in the central film thickness, the peak pressure decreases rapidly and finally approaches the corresponding peak pressure value corresponding to the pure rolling situation. Furthermore, as the dimensionless entraining velocity parameter (U) increases and the dimensionless load parameter ($\bar{F}$) decreases the dimensionless peak pressure is increased.

3. In the early stages of normal approach, where the squeeze film action is more important than the entraining action, an elastic dimple or pocket is formed in the central region with approximately similar 'pips' on the inlet and outlet sides of the conjunction. The pocket depth increases sharply as the central film thickness (H_o) decreases until it reaches a maximum value. For subsequent reductions of the central film thickness (H_o) the pocket depth decreases continuously. At the same time the 'pip' at the inlet region disappears gradually and the region between the inlet and the minimum film thickness on the outlet side is gradually flattened. Eventually the film profile approaches the well known shape for steady state elastohydrodynamic lubrication conditions (pure rolling). The dimple becomes deeper and occurs at higher central film thicknesses as the dimensionless load ($\bar{F}$) is increased.

4. The squeeze-film time, determined by the time taken for (H_o) and (H_m) to approach their equilibrium values within a range of about five percent, increases as the dimensionless load ($\bar{F}$) increases and the entraining velocity parameter decreases. Moreover, with the same applied load (F) and entraining velocity (u), the elastohydrodynamic system takes about <u>six</u> times longer to establish equilibrium than the hydrodynamic system (isoviscous and rigid - solids). Hence, it seems that the elastic deformations of the surfaces bounding the conjunction emphasize transient effects.

(ii) <u>Under Sinusoidal Loading</u>

1. It was found that the squeeze film effect was more important under elastohydrodynamic than under hydrodynamic lubrications. The elastohydrodynamic behaviour emphasizes the squeeze effect so that the system is hardly affected by the variation of the system parameters. The general properties of the system are entirely similar to those of the hydrodynamic lubrication system.

The influence of the squeeze film effect upon the system at the position of the minimum film thickness (H_m) is completely determined by the dimensionless damping parameter (D_e), where,

$$D_e = \frac{\omega R}{u\sqrt{\bar{F}_o}}$$

If the damping parameter (D_e) is less than (0.05) the squeeze film effect is negligible (i.e. no damping). Hence,

under these conditions the relationship between the minimum film thickness and the load may be described by the pure rolling relationship introduced by Dowson and Higginson (1977). That is,

$$H_m = 1.6 \frac{G^{0.6} U^{0.7}}{[F_o (1+a \sin \omega t)]^{0.13}}$$

If the damping parameter (D_e) is greater than (0.05) the squeeze film effect is characterized by a damping of oscillations generated by the variation of load. For large values of the damping parameter ($D_e >> 1$), the film does not follow the oscillations of the load.

2. In cyclic non-steady elastohydrodynamic lubrication, the central film thickness response is more complicated than that of the minimum film thickness. It would be difficult to anticipate the variation of the central film thickness response under different circumstances, whereas, the minimum film thickness response might be readily predicted. Hence, the behaviour of dynamically loaded elastohydrodynamic line contacts is better expressed in terms of the variation of minimum film thickness.

3. In the cyclic loading condition, response fluctuations are considerably smaller under elastohydrodynamic than under hydrodynamic conditions with the same loading situations. This reflects the higher load carrying capacity under elastohydrodynamic lubrication conditions. Moreover, damping is more significant under elastohydrodynamic rather than hydrodynamic lubrication conditions.

CHAPTER 8

CONCLUSIONS AND SUGGESTIONS FOR FUTURE WORK

8.1 Introduction

The work described in this thesis has been concerned with the effects of squeeze-film action upon both hydrodynamically and elastohydrodynamically lubricated counterformal contact machine elements. This situation has not received wide spread attention previously. However, it has been increasingly recognized that squeeze film action plays an important role in preserving the lubricating film in many situations when the entraining velocity, which is responsible for hydrodynamic film formation under steady-state conditions (pure rolling), falls to zero at some stage in the cycle, as in synovial joints and reciprocating mechanisms.

The problem of squeeze-film lubrication for a point contact between rigid elliptical solids has been studied. A complete analytical solution for the problem has been developed considering both piezoviscous and isoviscous fluids.

A complete theoretical study of the elastohydrodynamic lubrication of line contacts with squeeze-film action and the combined effect of 'entraining' and squeeze film action, under the influence of constant and cyclic sinusoidal loads has been undertaken. Moreover, the influence of pressure on the physical properties of the lubricant has been incorporated in the solutions.

8.2 Analytical Solution for the Squeeze-Film Lubrication Problem for a Point Contact Between Rigid Ellipsoidal Solids

When two lubricated rigid ellipsoids approach each other along the line connecting their geometrical centres under an

external force, the lubricant between them is expelled by the squeeze-film action. A high pressure is generated in the lubricant due to the viscous resistance to motion of the fluid. The main object of the theoretical study presented in Chapter (2) was to determine the relationships between the load (F), normal velocity of approach (W) and time of approach (Δt) (the time required for the separation of the surfaces (h_o) to change by a specific amount (Δh_o)). The expressions developed for hydrodynamic lubrication with a pure squeeze film action considering an isoviscous fluid were,

$$W = \frac{Fh_o}{12\pi R^2 \eta_o} \sqrt{\frac{\delta}{1+\delta}}$$

and,

$$\Delta t = (t-t_1) = \frac{12\pi R^2 \eta_o}{F} \frac{1+\delta}{\sqrt{\delta}} \ln\left(\frac{h_{o1}}{h_o}\right)$$

The hydrodynamic lubrication behaviour in the presence of a piezoviscous fluids is characterized by the dimensionless velocity of approach ($\bar{\omega}$). Once ($\bar{\omega}$) attains its limiting value of $\left(\frac{1}{6}\right)$, an infinite pressure can be obtained at a finite film thickness, called the transitional film thickness $\left[h_{oT} = \frac{F.\alpha}{4\pi R \ln_2} \frac{\sqrt{\delta}}{1+\delta} \right]$, by the application of a finite load (F).

The squeeze film process with piezoviscous conditions under the influence of a constant load (F) may be divided into two distinct stages. Firstly the initial stage where the dimensionless velocity of approach ($\bar{\omega}$) is less than its limiting value of $\left\{\frac{1}{6}\right\}$, and secondly the final stage where the central pressure tends to infinity and the motion becomes independent of the applied load (F). The various expressions determined for each stage were as follows,

(a) - The Initial Stage ($h_o > h_{oT}$)

$$W = \frac{h_o^2}{2R\alpha\eta_o}\left[-1 + \sqrt{1 + \frac{\alpha F \sqrt{\delta}}{3\pi h_o R(1+\delta)}}\right]$$

and,

$$\Delta t = (t - t_1) = \frac{\alpha R\eta_o}{A} \ln\left[\frac{h_{o1} - A}{h_o - A}\right]$$

where,

$$A = \frac{\alpha F\sqrt{\delta}}{12\pi R(1+\delta)}$$

(b) - The Transitional Film Thickness ($h_o = h_{oT}$)

$$h_{oT} = \frac{F \cdot \alpha}{4\pi R \ 1n2} \quad \frac{\sqrt{\delta}}{(1+\delta)}$$

and,

$$W_T = \frac{h_{oT}^2}{6R\alpha\eta_o}$$

(c) - The Final Stage ($h_o < h_{oT}$)

$$W = \frac{h_o^2}{6R\alpha\eta_o}$$

and,

$$\Delta t = 6R\alpha\eta_o \left[\frac{1}{h_o} - \frac{1}{h_{o1}}\right]$$

When the theory developed was applied to a typical ball bearing example, it was found that pure squeeze-film lubrication alone was not sufficient to provide a continuous film of lubricant to separate the ball from the inner-race.

8.3 Numerical Solution for the Non-Steady State Elastohydrodynamic Lubrication of a Line Contact

The mathematical fomulation of the non-steady state elastohydrodynamic lubrication problem of line contacts was presented in Chapter (3). The equations constituting this particular type of lubrication problem are the one-dimensional Reynolds equation, coupled with the elasticity and load equations. These equations represent a non-linear integral-differential system which is very complicated and a full analytical solution has not yet been found. Hence, an approximate solution was found by using the finite-difference approximation method.

A procedure for the numerical solution of the complete isothermal transient elastohydrodynamic lubrication problem of line contacts, under the influence of constant and cyclic loads, has been presented in Chapter (4). This procedure called for the simultaneous solution of the Reynolds, elasticity and load equations at successive time steps. In the elasticity analysis the conjunction was divided into irregular areas with uniform pressures. In the numerical analysis of the Reynolds equation a pressure under-relaxation was introduced to obtain a satisfactory, converged, solution.

To solve the system of simultaneous linear equations resulting from the finite-difference and load equations in order to obtain the central velocity of approach (W_o) and the pressure distribution (P), the Gauss - Seidel iterative method was adopted initially. Considerable difficulty arose with respect to the

computational effort and convergence of the process. Therefore, a tri-diagonal matrix algorithm was used for the solution and found to be quicker and more accurate (a reduction in solution time by a factor of 30 was achieved). The only deficiency of the matrix solution method was that it required more computer fast storage space. The possibility of cavitation was recognized, especially as rolling action was considered, by the adoption of the Reynolds boundary condition in the divergent region. The location of the outlet boundary was determined by moving the exit position as required.

The numerical method presented is simple and efficient, but is only effective for moderate loads. As the load increases and the film thickness decreases, the convergence rate becomes progressively worse.

8.4 The Squeeze-Film Lubrication Problem for Elastic Cylinders

Squeeze-Film action occurs frequently in many machine components such as meshing gear teeth, journal bearings, cams and followers etc. The problem of elastohydrodynamic squeeze film lubrication of line contacts has been investigated extensively in Chapter (5). The present analysis makes the following advances over the previous elastohydrodynamic models and solutions:

(a) It is a real transient analysis in which the full time histories of the system parameters are determined;

(b) Any specified loading can be accommodated;

(c) It utilizes an elaborate direct-iteration solution technique capable of handling different types of

elastohydrodynamic lubrication problems, for example where there is an entraining action.

The results were evaluated for both isoviscous and piezoviscous fludis under prescribed loads. Graphical representations of pressure distributions and film shapes were presented together at successive reductions of the central film thickness. The variation of the dimensionless minimum film thickness (H_m), velocity of approach ($\bar{W}$) and central film pressure (P_o) were included. The results described have been shown to provide good agreement with results obtained by previous workers.

It was found that, with a piezoviscous fluid, the maximum pressure in the film can be very much larger than the Hertzian pressure corresponding to the applied load.

For isoviscous and piezoviscous lubrication conditions an elastic dimple is formed in the centre of the contact during the early stages of normal approach. The depth of the dimple increases sharply with decreasing central film thickness (H_o) until the maximum central pressure value is attained. The depth of the dimple decreases, as the central film thickness is further reduced and the film profile and pressure distribution converge to the Hertzian solution for dry contact.

Neither the local elastic deformation velocity nor the fluid compressibility have a significant effect upon the pressure within the range of the minimum film thickness considered. However, it is recognized that the non-uniform velocity of approach

assumption may have greater significance at small separations. However, calculations in this region are extremely difficult.

In the presence of an isoviscous fluid, the same velocity of approach can be obtained by the application of two different loads at the same central film thickness. This is known as the bifurcation phenomenon.

8.5 The Lubrication of Rigid Cylinders in Combined Rolling and Normal Motion

The analysis of lubrication of rigid cylinders has important practical applications in the lubrication of lightly loaded rolling-element bearings and involute spur gears. Most of the research activity in this field, however, has been concerned with steady running conditions, leaving a great deal to be undertaken on lubricated contacts subjected to non-steady state conditions. To provide an insight into the effect of squeeze film action due to normal motion combined with 'entraining' action due to pure rolling the study described in Chapter (6) was undertaken.

The results were evaluated for both isoviscous and piezoviscous lubrication conditions under constant and cyclic sinusoidal loading. The variation of the normal motion velocity and peak pressure with time have been presented. The time histories of the central film thickness under constant and sinusoidal normal loading were also investigated. The results for isoviscous lubrication were shown to provide good agreement with results obtained by previous authors.

Under constant load, it was found that pressures in excess of the corresponding peak pressure for the pure rolling condition can be generated when the film thickness was less than that of the pure rolling condition. The load carrying capacity with piezoviscous lubrication was higher than under the isoviscous condition.

Under cyclic sinusoidal loading the effect of squeeze-film action was remarkable. The effect is entirely similar to viscous damping phenomenon acting on a system which has one degree of freedom (the minimum film thickness). Its influence upon the system was completely determined by the dimensionless damping parameter (D_p), where,

$$Dp = \omega R \sqrt{\frac{\eta_o}{uF_o}}$$

If the damping parameter (D_p) is less than (0.05) the squeeze-film effect was negligible. Hence, the relation between the minimum film thickness and the load may be described by the pure rolling relationship.

The effect of the variation of viscosity with pressure was found to reduce the response fluctuations of the film thickness compared with the isoviscous case under the same loading conditions.

8.6 The Lubrication of Elastic Cylinders in Combined Rolling and Normal Motion

Contact between heavily loaded, lubricated nonconformal machine elements such as gear teeth and the rollers and tracks in a

roller bearing have been the subject of intensive research since the beginning of this century. Most of the theoretical and experimental work on line contacts has been concerned with steady state running conditions. However, within the range of practical situations, it has been recognized that such contacts are often subjected to cyclic variations of load and speed, and as a consequence a normal motion (squeeze action) is developed during operation. The study of the influence of combined 'entraining' and 'normal motion' upon elastohydrodynamic lubrication of line contacts has been presented in Chapter (7).

Some additional features of the present analysis over the previous elastohydrodynamic models are achieved. These include the prediction of all the characteristics of the elastohydrodynamic contact, i.e., the details of the pressure curve and oil film shape throughout the motion. Moreover, the numerical procedure considered the simultaneous solution of the elasticity and Reynolds equations.

Numerical results for line contacts, under moderate constant and sinusoidal loading conditions were obtained. Pressure distribution, film shapes and the variation of the system parameters have been presented in time sequence as the gap between the two cylinders changes. Moreover, the dynamic behaviour of the minimum and central film thickness subjected to constant and sinusoidal forcing were included. The viscous damping phenomenon associated with the squeeze-film action has also been discussed.

For a constant load it was found that the elastohydrodynamic lubrication of cylinders under the combined

effect of 'entraining' and 'squeeze' film action could be divided into three different stages. In the first stage, where the central film thickness is large, the lubrication process is strongly affected by squeeze-film action. For the second stage, both squeeze-film and entraining effects are important. In the final stage, the central film thickness approaches the steady state value and 'entraining' action takes over as the dominant effect.

Under constant load, pressures are much higher than those of pure rolling conditions can be generated at relatively large film thicknesses during 'normal approach'. In the early stage of normal approach, an elastic dimple or pocket is formed in the central region with approximately similar 'pips' on the inlet and outlet sides of the conjunction. The pocket depth increases sharply as the central film thickness decreases until it reaches a maximum value. For subsequent reductions of the central film thickness the pocket depth decreases continuously. At the same time the 'pip' at the inlet region gradually disappears. Eventually the film profile approaches the well-known shape for steady state elastohydrodynamic lubrication conditions in pure rolling.

Under constant load, and under the same conditions of applied load and entraining velocity, the elastohydrodynamic equilibrium takes about <u>six</u> times longer to establish than with the hydrodyanmic system (for isoviscous and rigid-solids). Therefore, it seems that the elastic deformations of the surfaces bounding the conjunctions emphasize transient effects.

Under cyclic sinusoidal loading the squeeze film effect was

more effective with elastohydrodynamic than with hydrodynamic lubrication conditions. The elastohydrodynamic behaviour emphasizes the beneficial effects of squeeze-film action so that the system is hardly affected by the variation of the parameters. The influence of the squeeze film upon the system at the position of the minimum film thickness is completely determined by the dimensionless damping parameter (D_e), where,

$$D_e = \frac{\omega R}{u} \sqrt{\bar{F}_o}$$

If the damping parameter (D_e) is less than (0.05) the squeeze film effect is negligible. Hence, the variation of the minimum film thickness with load is described by the following relationship,

$$H_m = 1.6 \frac{G^{0.6} U^{0.7}}{\left[F_o(1+a \sin\omega t) \right]^{0.13}}$$

With cyclic sinusoidal loading, it would be difficult to anticipate the variation of the central film thickness response, however, the minimum film thickness response may be more readily predicted. Hence the behaviour of dynamically loaded elastohydrodynamic line contacts is better expressed in terms of the variation of minimum film thickness.

8.7 SUGGESTIONS FOR FUTURE WORK

(1) The numerical procedure adopted in this thesis for the solution of non-steady state elastohydrodynamic lubrication problems of line contacts has been based on a straightforward iteration of the governing equations. However, this method failed to give convergent

solutions outside a limited range of medium loading conditions and relatively small film thickness. It would be of particular interest to investigate the convergence process of the programme to overcome these shortcomings in order to enable convergent solutions to be obtained under more practical conditions.

(2) The programme developed may find application in studies of the lubrication of line contacts whenever transient effects are of interest, e.g.,the lubrication of cams, spur gears, roller bearing and human joints.

(3) The results presented may be used to derive an empirical formula for the minimum film thickness in line contacts under non-steady state elastohydrodynamic lubrication.

(4) The development of the present analysis could be extended to include the study of thermal effects, the influence of surface roughness and the non-steady state lubrication of both finite line and point contacts.

(5) The general mathematical analysis for non-steady state lubrication developed in this thesis took account of the variation of the local deformation velocity throughout the contact. However, the results were obtained by assuming a uniform velocity distribution, since this reduces the computational effort without introducing serious errors.

REFERENCES

BARUS, C. (1893), 'Isotherms, Isopiestics, and Isometrics Relative to Viscosity'.
Am. J. Sci., Vol. 45, 87-96.

BIRD, R.B., STEWART, W.E. and LIGHTFOOT, E.N. (1960), 'Transport Phenomena'.
John Wiley & Sons.

BOWDEN, F.P. and TABOR, D. (1954), 'The Friction and Lubrication of Solids'.
Oxford, Clarendon Press.

BREWE, D.E., HAMROCK, B.J. and TAYLOR, C.M. (1979), 'Effect of Geometry on Hydrodynamic Film Thickness'.
Trans. A.S.M.E., J. Lubr. Technol., 101, No. 2, 231-239.

BROWNE, A.L., WICKER, D. and ROHDE, S.M. (1975), 'The Significance of Tread Element Flexibility to Thin Film Wet Traction'.
Tire Sci. and Technol., 3, 215-234.

BUSH, A.W. and SKINNER, P.H. (1984), 'The Effect of Surface Roughness in Elastohydrodynamic Lubrication'.
WEAR, Vol. 96, 2, 1984, 177-202.

CHANDRA, A. and ROGERS, R.J. (1983), 'The Normal Approach, Contact, and Rebound of Lubricated Cylinders'.
Trans A.S.M.E., J. Lubr. Technol., 105, No. 2, 271-279.

CHITTENDEN, R.J. (1984), Ph.D. Dissertation.
Dept. of Mech. Eng., Leeds University.

CHRISTENSEN, H. (1962), 'The Oil Film in a Closing Gap'.
Proc. R. Soc., London, A. 266, 312-328.

CHRISTENSEN, H. (1970), 'Elastohydrodynamic Theory of Spherical Bodies in Normal Approach'.
Trans A.S.M.E., J. Lubr. Technol, Series F, No. 1, Vol. 92, 145-154.

CONRY, T.F. (1981), 'An Analytical Solution for the Normal Load Carrying Capacity of Lightly Loaded Cylinders in Combined Rolling, Sliding and Normal Motion'.
Trans. A.S.M.E., J. Lubr. Technol., 103, No. 3, 467-468.

CONWAY, H.D. (1973), 'The Rate of Change of Film Thickness in the Elastohydrodynamic Squeeze-Film Process'.
Trans. A.S.M.E., J. Lubr. Technol., Series F, No. 3, Vol. 95, 391-393.

DOWSON, D. (1962), 'A Generalised Reynolds' Equation for Fluid-Film Lubrication'.
Int. J. Mech. Sci., 4, 159-170.

DOWSON, D. (1983), 'Non-Steady State Effects in Elasto-hydrodynamic Lubrication'.
Proceedings of an International Conference held at N.A.S.A. Lewis Research Centre, Cleveland, Ohio, April 18-21, 1983, 579-593.

DOWSON, D., DUNN, J.F. and TAYLOR, C.M. (1983), 'The Piezoviscous Fluid, Rigid Solid Regime of Lubrication'.
Proc. Inst. Mech. Engrs, 197(c), 43-51.

DOWSON, D. and HIGGINSON, G.R. (1959), 'Numerical Solution to the Elastohydrodynamic Problem'.
J. Mech. Eng. Sci., 1(1), 7-15.

DOWSON, D. and HIGGINSON, G.R. (1977), 'Elastohydrodynamic Lubrication. The Fundamentals of Roller and Gear Lubrication'.
Pergamon, Oxford.

DOWSON, D. and JONES, D.A. (1967), 'Entrapment Between Approaching Elastic Solids'.
Nature, 214, No. 5091, 947-948.

DOWSON, D. and JONES, D.A. (1968), 'Optical-Interference Method of Measurement of Time Dependent Elasto-hydrodynamic Film Profiles'.
Proc. Inst. Mech. Engrs., 182(3G), Report 3, 49-52.

DOWSON, D., MARKHO, P.H. and JONES, D.A. (1976), 'The Lubrication of Lightly Loaded Cylinders in Combined Rolling, Sliding, and Normal Motion. Part I: Theory'.
Trans A.S.M.E., J. Lubr. Technol., 98, No. 4, 509-516.

DOWSON, D., RUDDY, B.L. and ECONOMOU, P.N. (1983), 'The Elasto-hydrodynamic Lubrication of Piston Rings'.
Proc. R. Soc., London, A. 386, 409-430.

DOWSON, D. and TAYLOR, C.M. (1979), 'Cavitation in Bearings'.
Ann. Rev. Fluid Mech., 11, 35-66.

DUNN, J.F. (1983),Ph.D. Dissertation.
Dept. of Mech. Eng., Leeds University.

FINKIN, E.F. (1973), 'Experimental Investigation of Spherical Impact, Both Dry and With a Fluid Film'.
Trans. A.S.M.E., J. Lubr. Technol., Series F, No. 3, Vol. 95, 393-394.

GAMAN, I.G., HIGGINSON, G.R. and NORMAN, R. (1974), 'Fluid Entrapment by a Soft Surface Layer'.
Wear, 28 (1974), 345-352.

GOHOSH, M.K., HAMROCK, B.J. and BREWE, D. (1984), 'Hydrodynamic Lubrication of Rigid Nonconformal Contacts in Combined Rolling and Normal Motion'. Contributed by the Tribology Division of the A.S.M.E., for presentation at the ASME/ASLE Joint Lubrication Conference, San Diego, Calif., October 22-24, 1984.

GOULD, P. (1971), 'High-Pressure Spherical Squeeze Films'. Trans. A.S.M.E., J. Lubr. Technol., Series F, Vol. 91, 207-208.

HAI-TSING, Y., SHIAN-ZE, Z. and YU-SHIAN, H. (1983), 'The Computation of Unsteadily Loaded E.H.L. Film Thickness and Other Lubrication Parameter of Cam-Tappet Pairs of I.C. Engines and Analysis of Their Performance'. Proc. 10th Leeds-Lyon Symposium on Tribology, Eds. Dowson, D., Taylor, C.M., Godet, M. and Berthe, D., 171-181.

HAMROCK, B.J. (1976), Ph.D. Dissertation. Dept. of Mech. Eng., Leeds University.

HAMROCK, B.J. and DOWSON, D. (1976 (a)), 'Numerical Evaluation of Surface Deformation of Elastic Solids Subjected to Hertzian Contact Stress'. A.S.L.E. Trans., Vol. 19, No. 4, 279-286.

HAMROCK, B.J. and DOWSON, D. (1976 (b)), 'Isothermal Elastohydrodynamic Lubrication of Point Contacts, Part I - Theoretical Formulation'. Trans. A.S.M.E., J. Lubr. Technol., 98(2), 223-229.

HAMROCK, B.J. and DOWSON, D. (1981), 'Ball Bearing Lubrication - The Elastohydrodynamics of Elliptical Contacts'. John Wiley & Sons, New York.

HAMROCK, B.J. and JACOBSON, B.O. (1983), 'Elastohydrodynamic Lubrication of Rectangular Contacts'. N.A.S.A. Technical paper 2111.

HERREBRUGH, H. (1970), 'Elastohydrodynamic Squeeze Films Between Two Cylinders in Normal Approach'. Trans. A.S.M.E., J. Lubr. Technol, Series F, Vol. 92, No. 2, 292-302.

HIGGINSON, G.R. (1978), 'Squeeze Film Lubrication Between Compliant Solids'. Wear, 46 (1978), 387-395.

JAMES, N. and ETTLES, C.M.M. (1978), 'Solutions for the Normal Approach of an Axi-Symmetric Elasto-hydrodynamic Contact'. Proc. 5th Leeds-Lyon Symposium on Tribology, Eds. Dowson, D., Taylor, C.M., Godet, M. and Berthe, D., 47-59.

JOHNSON, K.L. (1970), 'Regimes of Elastohydrodynamic Lubrication'.
J. Mech. Eng. Sci., 12(1), 9-16.

KAPITZA, P. (1955), 'Hydrodynamic Theory of Lubrication During Rolling'.
Zh. Tekh. Fiz. 25(4), 747-762.

LEE, K.M. and CHENG, H.S. (1973), 'The Pressure and Deformation Profiles Between Two Normally Approaching Lubricated Cylinders'.
Trans. A.S.M.E., J. Lubr. Technol, Series F, Vol. 95, No. 3, 308-317.

LIN, Z.G. and MEDLEY, J.B. (1984), 'Transient Elastohydrodynamic Lubrication of Involute Spur Gears Under Isothermal Conditions'.
Wear, 95 (1984), 143-163.

MARKHO, P.H. (1972), Ph.D. Dissertation.
Dept. of Mech. Eng., Leeds University.

MARKHO, P.H. and DOWSON, D. (1976), 'The Lubrication of Lightly Loaded Cylinders in Combined Rolling, Sliding and Normal Motion. Part II: Experimental'.
Trans. A.S.M.E., J. Lubr. Technol., 98, No. 4, 517-523.

MARTIN, H.M. (1916), 'Lubrication of Gear Teeth'.
Engineering 102, 119-121.

McEWEN, E. (1952), 'The Effect of Variation of Viscosity with Pressure on the Load Carrying Capacity of Oil Films Between Gear Teeth'.
J. Inst. Petrol. 38, 646.

MEDLEY, J.B. and DOWSON, D. (1983), 'Lubrication of Elastic-Isoviscous Line Contacts Subject to Cyclic Time-Varying Loads and Entrainment Velocities'.
A.S.L.E. Trans., Vol. 27, No. 3, 243-251.

MOSTOFI, A. (1981), Ph.D. Dissertation.
Imperial College of Science and Technology, Mech. Eng. Dept., University of London.

PAUL, G.R. (1976), 'Time Dependent Viscosity Following a Pressure Rise Measured on an Impact Viscometer'.
A.S.L.E. Trans., Vol. 19, 17-22.

PAUL, G.R. and CAMERON, A. (1972), 'An Absolute High Pressure Impact Microviscometer Based on Refractive Index'.
Proc. R. Soc., London, A. 331, 171-184.

PRAKASH, J. (1984), 'On the Lubrication of Rough Rollers'.
Trans. A.S.M.E., Journal of Tribology, Vol. 106, No. 2, 211-217.

RAHNEJAT, H. (1984), Ph.D. Dissertation.
Imperial College of Science and Technology, Mech. Eng. Dept., University of London.

REYNOLDS, O. (1886), 'On the Theory of Lubrication and its Application to Mr. Beauchamp Tower's Experiments, including an experimental determination of the viscosity of olive oil'.
Philos. Trans. R. Soc. London, Ser. A. 177, 157-233.

ROBERTS, A.D. (1971), 'Squeeze Films Between Rubber and Glass'.
J. Phys. D: Appl. Phys., Vol. 4, 423-432.

ROELANDS, C.J.A. (1966), 'Correlation Aspects of the Viscosity-Pressure Relationship of Lubricating Oils'.
Druk V.R.B., Gronigen, Netherlands.

ROHDE, S.M. and OH, K.P. (1975), 'A Unified Treatment of Thick and Thin Film Elastohydrodynamic Problem by Using Higher Order Element Methods'.
Proc. R. Soc., London, A. 343, 315-331.

ROHDE, S.M., WICKER, D. and BROWNE, A.L. (1976), 'Dynamic Analysis of Elastohydrodynamic Squeeze Films'.
Trans A.S.M.E., J. Lubr. Technol, No. 3, 98, 401-408.

SASAKI, T., MORI, H. and OKINO, N. (1962), 'Fluid Lubrication Theory of Roller Bearings, Part I: Fluid Lubrication Theory for Two Rotating Cylinders in Contact'.
Trans. A.S.M.E., Journal of Basic Engineering, Series D, Vol. 84, No. 1, 166-174.

SIMON, V. (1981), 'Elastohydrodynamic Lubrication of Hypoid Gears'.
Trans. A.S.M.E. J. Mech. Design, Vol. 103, No. 1, 195-203.

STEINFÜHRER, G. (1980), 'Calculation of Film Thickness for Variable Velocity'.
Wear, 64 (1980), 195-200.

TIMOSHENKO, S. and GOODIER, J.N. (1951), 'Theory of Elasticity'.
2nd ed. McGraw Hill, New York.

VICHARD, J.P. (1971), 'Transient Effects in the Lubrication of Hertzian Contacts'.
J. Mech. Eng. Sci., 13, 173-189.

WADA, S. and TSUKIJIHARA, M. (1978), 'Elastohydrodynamic Lubrication of Squeeze Films (Part 1) Two Cylinders Lubricated with Grease'.
Bulletin of JSME, Vol. 21, No. 159, 1408-1415.

WADA, S. and TSUKIJIHARA, M. (1981 (a)), 'Elastohydrodynamic Squeeze Problem of Two Rotating Cylinders (Part 1, Newtonian Fluid').
Bulletin of the JSME, Vol. 24, No. 190, 737-742.

WADA, S. and TSUKIJIHARA, M. (1981 (b)), 'Elastohydrodynamic Squeeze Problem of Two Rotating Cylinders (Part 2, Bingham Solid').
Bulletin of the JSME, VOL. 24, NO. 192, 1072-1077.

WANG, K.L. and CHENG, H.S. (1981), 'A Numerical Solution to the Dynamic Load, Film Thickness and Surface Temperature in Spur Gears, Part I, Analysis, Part II, Results'.
J. Mech. Design, 103, 177-194.

APPENDIX A1

FORTRAN LISTING OF THE COMPUTER PROGRAM FOR THE NON-STEADY STATE ELASTOHYDRODYNAMIC ANALYSIS

```
C  LINE CONTACT PROGRAMME                                                FIL00020
C-----------------------                                                 FIL00030
      IMPLICIT REAL*8 (A-H,O-Z)                                          FIL00040
      COMMON/CASE/IDENSI,IVSCOS,IELAST,IAPVEL,HOO                        FIL00050
      COMMON/NODE/NI,NC,NXN,NCR,NIR,NX,MT                                FIL00060
      COMMON/LINE/XN,XNN,SBI,SBC,ZB                                      FIL00070
      COMMON/GEOM/PI,HO,RA,RB,R,Bl                                       FIL00080
      COMMON/VALS/P,GA,GB,XIA,XIB,EP,U,VW                                FIL00090
      COMMON/LUBR/Q1,Q2,Q5,Q6,Z                                          FIL00100
      COMMON/SOLN/PR(400),PRSV(400),H(400),S(400),W(400),PHI(400)        FIL00110
     * ,D1(400),D2(400),D3(400),Y(400),VS(400),DN(400)                   FIL00120
      COMMON/CONST/A(400),B(400),C(400),D(400),E(400)                    FIL00130
      COMMON/OMGA/OMGA1,OMGA2,OMGA3,HOC(80),DNP(400,1),HP(400,1)         FIL00140
      DIMENSION T(850),HT(850),WT(850),HMT(850),PMT(850),FT(850)         FIL00150
C                                                                        FIL00160
C IDENTITIES:                                                            FIL00170
C-----------                                                             FIL00180
C IDENSI  (IN SUBR. PROPER)=1    (VARIABLE DENSITY)                      FIL00190
C        (AND SUBR. CONST )=0    (CONSTANT DENSITY)                      FIL00200
C IVSCOS  (IN SUBR. PROPER)=1    (VARIABLE VISCOSITY)                    FIL00210
C                          =0    (CONSTANT VISCOSITY)                    FIL00220
C IELAST  (IN SUBR. ELAST) =1    (ELASTIC CYLINDER)                      FIL00230
C                          =0    (RIGID CYLINDER)                        FIL00240
C IAPVEL  (IN SUBR. CONST1)=1    (VARIABLE APP. VEL.)                    FIL00250
C                          =0    (CONSTANT APP. VEL.)                    FIL00260
C                                                                        FIL00270
      READ(5,*) IDENSI,IVSCOS,IELAST,IAPVEL,HOO,P1,JRUN,URF,SPEED        FIL00280
C MT= TO CONTROL THE FIREST AND SECONT STEP TO KEEP THE DENSITY AND       FIL00290
C     THE APP. VEL. CONSTANT                                             FIL00300
      MT=1                                                               FIL00310
C                                                                        FIL00320
                        KREAD=0                                          FIL00330
      CALL SETTIM                                                        FIL00340
6666                    CONTINUE                                         FIL00350
                        KREAD=KREAD+1                                    FIL00360
C VALUES:                                                                FIL00370
C--------                                                                FIL00380
C LOAD P=5.030023D2---------------                                       FIL00390
      GA=2.09300D11                                                      FIL00400
      GB=GA                                                              FIL00410
      XIA=0.3DO                                                          FIL00420
      XIB=XIA                                                            FIL00430
CCC   SPEED=0.000300DO ------------                                      FIL00440
C GEOMETRICAL DATA:                                                      FIL00450
C-----------------                                                       FIL00460
      PI=3.1415926DO                                                     FIL00470
      RA=0.04                                                            FIL00480
      RB=0.04                                                            FIL00490
      R =(RA*RB)/(RA+RB)                                                 FIL00500
      CALL TIME(IT,T,HT,HMT,PMT,WT,FT,DT,HOO,R,AMP,TAW,ITMAX,KREAD)      FIL00510
      RTIM=(T(IT)/TAW)*2.0*PI                                            FIL00520
      P=P1*(1.0+AMP*DSIN(RTIM))                                          FIL00530
      S2=(1.0DO-XIA**2)/GA+(1.0DO-XIB**2)/GB                             FIL00540
      EP=2.0/S2                                                          FIL00550
      B1=DSQRT(4.0*P*(S2/PI)*R)                                          FIL00560
      DEL=P*(S2/PI)*(2.0/3.0+DLOG(4.0*RA/B1)+DLOG(4.0*RB/B1))            FIL00570
C LUBRICANT DATA:                                                        FIL00580
C---------------
```

```
      VISE=0.631D-4                                                    FIL00590
      VISO=0.411D-1                                                    FIL00600
      Z=0.67D0                                                         FIL00610
      CVIS=EP/19609.5268D+4                                            FIL00620
      ELPHA=0.582744D-9                                                FIL00630
      BETA=1.68348D-9                                                  FIL00640
      Q1=VISE/VISO                                                     FIL00650
      Q2=CVIS                                                          FIL00660
      Q5=ELPHA*EP                                                      FIL00670
      Q6=BETA*EP                                                       FIL00680
      U=SPEED*VISO/(EP*R)                                              FIL00690
      UVW=VISO/(EP*R)                                                  FIL00700
C CREATION OF MESH:                                                    FIL00710
C------------------                                                    FIL00720
      ZB=(R/B1)*DSQRT(2.0*HOO*(82.0-1.0))                              FIL00730
      XN=ZB*B1                                                         FIL00740
      XNN=ZB                                                           FIL00750
      RI=.80                                                           FIL00760
      RC=1.0-RI                                                        FIL00770
      ZBI=RI*XNN                                                       FIL00780
      ZBC=RC*XNN                                                       FIL00790
      NI=20                                                            FIL00800
      NC=40                                                            FIL00810
      NXN=NI+NC+1                                                      FIL00820
      NCR=40                                                           FIL00830
      NIR=20                                                           FIL00840
      NX=NXN+NCR+NIR                                                   FIL00850
C NODAL STRUCTURE:                                                     FIL00860
C------------------                                                    FIL00870
      ANI=NI                                                           FIL00880
      ANC=NC+1                                                         FIL00890
      SBI=ZBI/(2.0*ANI-1.0)                                            FIL00900
      SBC=ZBC/(2.0*ANC-1.0)                                            FIL00910
C                                                                      FIL00920
      CALL DISTAN                                                      FIL00930
                        IF(IT.NE.1) GOTO 4244                          FIL00940
      CALL HERTZ                                                       FIL00950
4244                    CONTINUE                                       FIL00960
      DO 244 J=1,NX                                                    FIL00970
 244  PRSV(J)=PR(J)                                                    FIL00980
      IF(JRUN.NE.1) GOTO 899                                           FIL00990
                        JRUN=2                                         FIL01000
      DO 89 J=1,NX                                                     FIL01010
  89  READ(8,*)  YDUM,PR(J),HDUM,PRSV(J),JDUMM                         FIL01020
  899 CONTINUE                                                         FIL01030
C-----------------------X                                             FIL01040
      JCOUNT=0.0                                                       FIL01050
1999  CONTINUE                                                         FIL01060
      JCOUNT=JCOUNT+1                                                  FIL01070
      CPU=CPUTIM(X)                                                    FIL01080
      IF(CPU.GE.1785.00) GOTO 122                                      FIL01090
      WRITE(4,*)'CPU=',CPU                                             FIL01100
CC    WRITE(4,*) 'JCOUNT=',JCOUNT                                      FIL01110
      DO 299 J=1,NX                                                    FIL01120
      PR(J)=(PR(J)+(URF-1.)*PRSV(J))/URF                               FIL01130
299   PRSV(J)=PR(J)                                                    FIL01140
C-----------------------X                                             FIL01150
      CALL ELAST(NEGAT,HMIN)                                           FIL01160
```

```
      IF(NEGAT.EQ.1) GOTO 122                                          FIL01170
      CALL PROPER                                                      FIL01180
      CALL CONSTS(UVW)                                                 FIL01190
      CALL PLOAD(TSUMPR)                                               FIL01200
      CALL MAT(TSUMPR,R,B1,EP,P,VW,PMAX)                               FIL01210
C-----------------------X                                              FIL01220
      CALL TEST(JUMP,NX)                                               FIL01230
      IF(JUMP.NE.1) GOTO 1999                                          FIL01240
C-----------------------X                                              FIL01250
                        IF(IT.EQ.ITMAX) GOTO 122                       FIL01260
                        IF(IT.LT.ITMAX) GOTO 2992                      FIL01270
122   CONTINUE                                                         FIL01280
      DO 99  J=1,NX                                                    FIL01290
 99   WRITE(6,*) Y(J),PR(J),H(J),PRSV(J),J                             FIL01300
      WRITE(6,*) 'B1=',B1,'PO=',PO,'SB=',SB                            FIL01310
 12   FORMAT(6(2X,D10.3) ,I4 )                                         FIL01320
      WRITE(6,*) 'IDENSI=',IDENSI                                      FIL01330
      WRITE(6,*) 'IVSCOS=',IVSCOS                                      FIL01340
      WRITE(6,*) 'IELAST=',IELAST,'NEGAT=',NEGAT                       FIL01350
      WRITE(6,*) 'IAPVEL=',IAPVEL                                      FIL01360
      WRITE(6,*) 'HOO=',HOO                                            FIL01370
      WRITE(6,*) 'LOAD=',P                                             FIL01380
      WRITE(6,*) 'ZB=',ZB,'NI=',NI,'NC=',NC,'NCR=',NCR                 FIL01390
      WRITE(6,*)'RI=',RI                                               FIL01400
      WRITE(6,*)'U=',U                                                 FIL01410
      IF(JUMP.EQ.1) WRITE(6,*) 'CONVERGED SOL.******',' CPU=',CPU      FIL01420
2992                  CONTINUE                                         FIL01430
      WT(IT)=VW                                                        FIL01440
      HMT(IT)=HMIN                                                     FIL01450
      PMT(IT)=PMAX                                                     FIL01460
      FT(IT)=P                                                         FIL01470
                        IF(IT.EQ.ITMAX) GOTO 6665                      FIL01480
                        IF(IT.LT.ITMAX) IT=IT+1                        FIL01490
                        IF(IT.LE.ITMAX) GOTO 6666                      FIL01500
6665  DO 1001 I=1,IT                                                   FIL01510
1001  WRITE(10,72) I,T(I),HT(I),HMT(I),PMT(I),WT(I),FT(I)              FIL01520
72    FORMAT(I4,6(1X,E15.8))                                           FIL01530
      STOP                                                             FIL01540
      END                                                              FIL01550
C-----------------------------------------------------------------     FIL01560
C-----------------------------------------------------------------     FIL01570
      SUBROUTINE DISTAN                                                FIL01580
      IMPLICIT REAL*8(A-H,O-Z)                                         FIL01590
      COMMON/CASE/IDENSI,IVSCOS,IELAST,IAPVEL,HOO                      FIL01600
      COMMON/NODE/NI,NC,NXN,NCR,NIR,NX,MT                              FIL01610
      COMMON/LINE/XN,XNN,SBI,SBC,ZB                                    FIL01620
      COMMON/GEOM/PI,HO,RA,RB,R,B1                                     FIL01630
      COMMON/VALS/P,GA,GB,XIA,XIB,EP,U,VW                              FIL01640
      COMMON/LUBR/Q1,Q2,Q5,Q6,Z                                        FIL01650
      COMMON/SOLN/PR(400),PRSV(400),H(400),S(400),W(400),PHI(400)      FIL01660
     *,D1(400),D2(400),D3(400),Y(400),VS(400),DN(400)                  FIL01670
      COMMON/CONST/A(400),B(400),C(400),D(400),E(400)                  FIL01680
      COMMON/OMGA/OMGA1,OMGA2,OMGA3,HOC(80),DNP(400,1),HP(400,1)       FIL01690
      YD=0.0                                                           FIL01700
      DO 1 I=1,NX                                                      FIL01710
      Y(I)=YD                                                          FIL01720
      IF(I.LT.NI) THEN                                                 FIL01730
      YD=YD+SBI+SBI                                                    FIL01740
```

```
      ELSE IF(I.EQ.NI.OR.I.EQ.(NXN+NCR)) THEN                          FIL01750
      YD=YD+SBI+SBC                                                    FIL01760
      ELSE IF(I.LT.(NXN+NCR)) THEN                                     FIL01770
      YD=YD+SBC+SBC                                                    FIL01780
      ELSE                                                             FIL01790
      YD=YD+SBI+SBI                                                    FIL01800
      END IF                                                           FIL01810
1     CONTINUE                                                         FIL01820
      RETURN                                                           FIL01830
      END                                                              FIL01840
C-----------------------------------------------------------------     FIL01850
C-----------------------------------------------------------------     FIL01860
      SUBROUTINE HERTZ                                                 FIL01870
      IMPLICIT REAL*8 (A-H,O-Z)                                        FIL01880
      COMMON/CASE/IDENSI,IVSCOS,IELAST,IAPVEL,HOO                      FIL01890
      COMMON/NODE/NI,NC,NXN,NCR,NIR,NX,MT                              FIL01900
      COMMON/LINE/XN,XNN,SBI,SBC,ZB                                    FIL01910
      COMMON/GEOM/PI,HO,RA,RB,R,B1                                     FIL01920
      COMMON/VALS/P,GA,GB,XIA,XIB,EP,U,VW                              FIL01930
      COMMON/LUBR/Q1,Q2,Q5,Q6,Z                                        FIL01940
      COMMON/SOLN/PR(400),PRSV(400),H(400),S(400),W(400),PHI(400)      FIL01950
     * ,D1(400),D2(400),D3(400),Y(400),VS(40),DN(400)                  FIL01960
      COMMON/CONST/A(400),B(400),C(400),D(400),E(400)                  FIL01970
      COMMON/OMGA/OMGA1,OMGA2,OMGA3,HOC(80),DNP(400,1),HP(400,1)       FIL01980
      PO=(2.0*P)/(PI*B1)                                               FIL01990
      DO 1  J=1,NX                                                     FIL02000
      X=Y(J)                                                           FIL02010
      S20=(1.0-(X-XNN)**2)                                             FIL02020
      IF(S20.LT.0.0D0.OR.S20.EQ.0.0D0)  GOTO 3                         FIL02030
      PR(J)=PO*DSQRT(S20)/EP                                           FIL02040
CCC   GOTO 1----------------------                                     FIL02050
3     PR(J)=0.0D0                                                      FIL02060
1     CONTINUE                                                         FIL02070
      RETURN                                                           FIL02080
      END                                                              FIL02090
C-----------------------------------------------------------------     FIL02100
C-----------------------------------------------------------------     FIL02110
      SUBROUTINE ELAST(NEGAT,HMIN)                                     FIL02120
      IMPLICIT REAL*8 (A-H,O-Z)                                        FIL02130
      COMMON/CASE/IDENSI,IVSCOS,IELAST,IAPVEL,HOO                      FIL02140
      COMMON/NODE/NI,NC,NXN,NCR,NIR,NX,MT                              FIL02150
      COMMON/LINE/XN,XNN,SBI,SBC,ZB                                    FIL02160
      COMMON/GEOM/PI,HO,RA,RB,R,B1                                     FIL02170
      COMMON/VALS/P,GA,GB,XIA,XIB,EP,U,VW                              FIL02180
      COMMON/LUBR/Q1,Q2,Q5,Q6,Z                                        FIL02190
      COMMON/SOLN/PR(400),PRSV(400),H(400),S(400),W(400),PHI(400)      FIL02200
     * ,D1(400),D2(400),D3(400),Y(400),VS(400),DN(400)                 FIL02210
      COMMON/CONST/A(400),B(400),C(400),D(400),E(400)                  FIL02220
      COMMON/OMGA/OMGA1,OMGA2,OMGA3,HOC(80),DNP(400,1),HP(400,1)       FIL02230
      HMIN=1.0D0                                                       FIL02240
      NEGAT=0.0                                                        FIL02250
      IF(IELAST.EQ.0) GOTO 90                                          FIL02260
      DO 7  I=1,NX                                                     FIL02270
      SUM1=0.0D0                                                       FIL02280
4     DO 8  J=1,NX                                                     FIL02290
      X=DABS(Y(I)-Y(J))                                                FIL02300
C-----------------                                                     FIL02310
      IF(J.LE.NI) THEN                                                 FIL02320
```

```
       SB=SBI                                                          FIL02330
      ELSE IF(J.LE.(NXN+NCR)) THEN                                     FIL02340
       SB=SBC                                                          FIL02350
      ELSE                                                             FIL02360
       SB=SBI                                                          FIL02370
      END IF                                                           FIL02380
C-----------------                                                     FIL02390
      S3=X-SB                                                         FIL02400
      S33=S3**2                                                       FIL02410
      S4=X+SB                                                         FIL02420
      S44=S4**2                                                       FIL02430
      S5=DLOG(B1)                                                     FIL02440
      D1(J)=S3*DLOG(S33)-S4*DLOG(S44)+4.0*SB*(1.0-S5)                 FIL02450
      SUM1=SUM1+PR(J)*D1(J)                                           FIL02460
 8    CONTINUE                                                        FIL02470
      W(I)=SUM1*(2.0*B1)/PI                                           FIL02480
 7    CONTINUE                                                        FIL02490
 90   DO 9 J=1,NX                                                     FIL02500
      S(J)=0.5*(B1/R)**2*(Y(J)-XNN)*(Y(J)-XNN)                        FIL02510
      DW=(W(J)-W(NXN))/R                                              FIL02520
      IF(IELAST.EQ.0) DW=0.0                                          FIL02530
      H(J)=HOO+S(J)+DW                                                FIL02540
      NJ=J                                                            FIL02550
      IF(H(J).LT.0.0) GOTO 55                                         FIL02560
      IF(H(J).GT.HMIN) GOTO 99                                        FIL02570
      HMIN=H(J)                                                       FIL02580
 99   PHI(J)=PR(J)*(H(J)**1.5)                                        FIL02590
 9    CONTINUE                                                        FIL02600
 55   IF(H(NJ).LT.0.0) NEGAT=1                                        FIL02610
      RETURN                                                          FIL02620
      END                                                             FIL02630
      SUBROUTINE CONSTS(UVW)                                          FIL02640
      IMPLICIT REAL*8(A-H,O-Z)                                        FIL02650
      COMMON/CASE/IDENSI,IVSCOS,IELAST,IAPVEL,HOO                     FIL02660
      COMMON/NODE/NI,NC,NXN,NCR,NIR,NX,MT                             FIL02670
      COMMON/LINE/XN,XNN,SBI,SBC,ZB                                   FIL02680
      COMMON/GEOM/PI,HO,RA,RB,R,B1                                    FIL02690
      COMMON/VALS/P,GA,GB,XIA,XIB,EP,U,VW                             FIL02700
      COMMON/LUBR/Q1,Q2,Q5,Q6,Z                                       FIL02710
      COMMON/SOLN/PR(400),PRSV(400),H(400),S(400),W(400),PHI(400)     FIL02720
     *,D1(400),D2(400),D3(400),Y(400),VS(400),DN(400)                 FIL02730
      COMMON/CONST/A(400),B(400),C(400),D(400),E(400)                 FIL02740
      COMMON/OMGA/OMGA1,OMGA2,OMGA3,HOC(80),DNP(400,1),HP(400,1)      FIL02750
C-------------------------------------------------------------------- FIL02760
C  CALCULATIONS OF THE DIFFERANT VALUES OF OMEGA & RETAINING OF THE    FIL02770
C   PREVIOUS VALUES OF DNSITY AND VISCOSITY AS DHP( ),HP(( ).          FIL02780
C-------------------------------------------------------------------- FIL02790
C      MT=TIME STEP INDEX (FROM THE MAIN PROGRAMME)                    FIL02800
       M=MT                                                           FIL02810
       HOC(M)=H(NXN)                                                  FIL02820
       DO 300 J=1,NX                                                  FIL02830
       DNP(J,M)=DN(J)                                                 FIL02840
       HP(J,M)=H(J)                                                   FIL02850
 300   CONTINUE                                                       FIL02860
C---AVOIDING THE CALCULATIONS OF OMEGA AT STEP 1&2 BY USING MT        FIL02870
       IF(MT.LT.3) GOTO 100                                           FIL02880
       HO1=HOC(M)-HOC(M-1)                                            FIL02890
       HO2=HOC(M-1)-HOC(M-2)                                          FIL02900
```

```
      HO3=HOC(M-2)-HOC(M)                                              FIL02910
      OMGA1=HO1/(-HO2*HO3)                                             FIL02920
      OMGA2=-HO3/(-HO1*HO2)                                            FIL02930
      OMGA3=(-HO3+HO1)/(-HO3*HO1)                                      FIL02940
100   CONTINUE                                                         FIL02950
      DO 200 J=2,NX-1                                                  FIL02960
       IF(J.LT.NI) THEN                                                FIL02970
       X1=SBI+SBI                                                      FIL02980
       X2=X1                                                           FIL02990
       ELSE IF(J.EQ.NI) THEN                                           FIL03000
       X1=SBI+SBI                                                      FIL03010
       X2=SBI+SBC                                                      FIL03020
       ELSE IF(J.EQ.(NI+1)) THEN                                       FIL03030
       X1=SBI+SBC                                                      FIL03040
       X2=SBC+SBC                                                      FIL03050
       ELSE IF(J.LT.(NXN+NCR)) THEN                                    FIL03060
       X1=SBC+SBC                                                      FIL03070
       X2=X1                                                           FIL03080
       ELSE IF(J.EQ.(NXN+NCR)) THEN                                    FIL03090
       X1=SBC+SBC                                                      FIL03100
       X2=SBC+SBI                                                      FIL03110
       ELSE IF(J.EQ.(NXN+NCR+1)) THEN                                  FIL03120
       X1=SBC+SBI                                                      FIL03130
       X2=SBI+SBI                                                      FIL03140
       ELSE                                                            FIL03150
       X1=SBI+SBI                                                      FIL03160
       X2=X1                                                           FIL03170
       END IF                                                          FIL03180
      X11=X1*X1                                                        FIL03190
      X22=X2*X2                                                        FIL03200
      X12=X1*X2                                                        FIL03210
      X12T=X1+X2                                                       FIL03220
      X12D=X1-X2                                                       FIL03230
      X12ST=X11+X22                                                    FIL03240
      X12SD=X11-X22                                                    FIL03250
      X12TS=X12T*X12T                                                  FIL03260
      X12DS=X12D*X12D                                                  FIL03270
C                                                                      FIL03280
      CO=1.0/(X12*X12T)**2                                             FIL03290
      C4=12.0*(B1/R)**2                                                FIL03300
      C5=R/(B1*X12*X12T)                                               FIL03310
C                                                                      FIL03320
      V1=DN(J+1)*H(J)**1.5/VS(J+1)                                     FIL03330
      V2=DN(J)*H(J)**1.5/VS(J)                                         FIL03340
      V3=DN(J-1)*H(J)**1.5/VS(J-1)                                     FIL03350
C-------------                                                         FIL03360
      V4=DN(J+1)*DSQRT(H(J+1))/VS(J+1)                                 FIL03370
      V5=DN(J)*DSQRT(H(J))/VS(J)                                       FIL03380
      V6=DN(J-1)*DSQRT(H(J-1))/VS(J-1)                                 FIL03390
C-------------                                                         FIL03400
C-------------                                                         FIL03410
      V41=DN(J+1)*H(J+1)*X11                                           FIL03420
      V42=DN(J)*H(J)*X12SD                                             FIL03430
      V43=DN(J-1)*H(J-1)*X22                                           FIL03440
C-------------                                                         FIL03450
C-------------                                                         FIL03460
      O4=C4*U*(C5*(V41-V42-V43))                                       FIL03470
C-------------                                                         FIL03480
```

```
C VARIABLES DEPENDING ON BEFORE PREVIOUS , PREVIOUS AND CURRENT STEPS   FIL03490
C-------------------------------------------------------------------   FIL03500
      IF(MT.LT.3) GOTO 205                                             FIL03510
      V51=(OMGA1*DNP(J,(M-2))+OMGA2*DNP(J,(M-1))+OMGA3*DN(J))          FIL03520
      V52=(OMGA1*HP(J,(M-2))+OMGA2*HP(J,(M-1))+OMGA3*H(J))             FIL03530
 205  IF(IAPVEL.EQ.0) V52=1.0                                          FIL03540
      IF(IDENSI.EQ.0) V51=0.0                                          FIL03550
C                                                                      FIL03560
      O5=C4*UVW*(V51*H(J)+V52*DN(J))                                   FIL03570
C=====================================================================FIL03580
C CALCULATIONS OF THE DIFFERENT VARIABLES OF FINITE DIFF. EQU.         FIL03590
C---------------------------------------------------------------------FIL03600
       A(J)=CO*(V1*(X11+2.0*X12)*X11-V2*X11*X12SD+V3*X12*X12)          FIL03610
       C(J)=CO*(V1*X11*X22+V2*X22*X12SD+V3*X22*X2*(2.0*X1+X2))         FIL03620
       C1=CO*(-V1*X11*X12TS+V2*X12SD*X12SD-V3*X12TS*X22)               FIL03630
       C2=-1.5*CO*(V4*(H(J+1)*(X11+2.0*X12)-H(J)*X12TS+H(J-1)*X22)*X11 FIL03640
     *-V5*(H(J+1)*X11-H(J)*X12SD-H(J-1)*X22)*X12SD                     FIL03650
     *-V6*(H(J)*X12TS-H(J-1)*X2*(2.0*X1+X2)-H(J+1)*X11)*X22)           FIL03660
       B(J)=(C1+C2)                                                    FIL03670
       D(J)=O5                                                         FIL03680
       E(J)=O4                                                         FIL03690
C---------------------------------------------------------------------FIL03700
CCCCC WRITE(6,66) X1,X2,A(J),B(J),C(J),D(J),E(J),J                     FIL03710
 200  CONTINUE                                                         FIL03720
 66   FORMAT(7(1X,E10.3),I3)                                           FIL03730
      RETURN                                                           FIL03740
      END                                                              FIL03750
C---------------------------------------------------------------------FIL03760
C---------------------------------------------------------------------FIL03770
      SUBROUTINE PROPER                                                FIL03780
      IMPLICIT REAL*8(A-H;O-Z)                                         FIL03790
      COMMON/CASE/IDENSI,IVSCOS,IELAST,IAPVEL,HOO                      FIL03800
      COMMON/NODE/NI,NC,NXN,NCR,NIR,NX,MT                              FIL03810
      COMMON/LINE/XN,XNN,SBI,SBC,ZB                                    FIL03820
      COMMON/GEOM/PI,HO,RA,RB,R,B1                                     FIL03830
      COMMON/VALS/P,GA,GB,XIA,XIB,EP,U,VW                              FIL03840
      COMMON/LUBR/Q1,Q2,Q5,Q6,Z                                        FIL03850
      COMMON/SOLN/PR(400),PRSV(400),H(400),S(400),W(400),PHI(400)      FIL03860
     *,D1(400),D2(400),D3(400),Y(400),VS(400),DN(400)                  FIL03870
      COMMON/CONST/A(400),B(400),C(400),D(400),E(400)                  FIL03880
      COMMON/OMGA/OMGA1,OMGA2,OMGA3,HOC(80),DNP(400,1),HP(400,1)       FIL03890
C---------------------------------------------------------------------FIL03900
C CALCULATIONS OF THE VISCOSITY AND DENSITY                            FIL03910
C---------------------------------------------------------------------FIL03920
      DO 10 J=1,NX                                                     FIL03930
      DN(J)=1.0+(Q5*PR(J))/(1.0+Q6*PR(J))                              FIL03940
      IF(IVSCOS.EQ.0) GOTO 9                                           FIL03950
      VS(J)=Q1**(1.0-(1.0+PR(J)*Q2)**Z)                                FIL03960
CVIS  VS(J)=DEXP(PR(J)*2.3D11*2.058D-8)                                FIL03970
 9    IF(IDENSI.EQ.0) DN(J)=1.0                                        FIL03980
      IF(IVSCOS.EQ.0) VS(J)=1.0                                        FIL03990
 10   CONTINUE                                                         FIL04000
      RETURN                                                           FIL04010
      END                                                              FIL04020
C---------------------------------------------------------------------FIL04030
C---------------------------------------------------------------------FIL04040
       SUBROUTINE TEST(JUMP,NX)                                        FIL04050
       IMPLICIT REAL*8 (A-H,O-Z)                                       FIL04060
```

```
      COMMON/SOLN/PR(400),PRSV(400),H(400),S(400),W(400),PHI(400)      FIL04070
     * ,D1(400),D2(400),D3(400),Y(400),VS(400),DN(400)                 FIL04080
      JUMP=0.0                                                         FIL04090
      SUM=0.0                                                          FIL04100
      SUMP1=0.0                                                        FIL04110
      DO 30 J=2,NX-1                                                   FIL04120
      DIF=DABS(PR(J)-PRSV(J))                                          FIL04130
      SUMP1=PR(J)+SUMP1                                                FIL04140
30    SUM=SUM+DIF                                                      FIL04150
      SUM=SUM/SUMP1                                                    FIL04160
      WRITE(4,*)'TEST=',SUM                                            FIL04170
      IF(SUM.LE.0.5D-2)  JUMP=1                                        FIL04180
      IF(JUMP.EQ.1) WRITE(4,*) 'CONVRGED SOLUTION**********'           FIL04190
      RETURN                                                           FIL04200
      END                                                              FIL04210
CTTTTTTTTTTTTTTTTTTTTTTTTTTTTTTTTTTTTTTTTTTTTTTTTTTTTTTTTTTTTTTTTTTTT FIL04220
      SUBROUTINE TIME(IT,T,HT,HMT,PMT,WT,FT,DT,HOO,R,AMP,TAW,ITMAX,    FIL04230
     *KREAD)                                                           FIL04240
      IMPLICIT REAL*8 (A-H,O-Z)                                        FIL04250
      DIMENSION T(850),HT(850),WT(850),HMT(850),PMT(850),FT(850)       FIL04260
                IF(KREAD.EQ.1) READ(5,*) IT,DT,AMP,TAW,ITMAX           FIL04270
      IF(IT.EQ.1) THEN                                                 FIL04280
      T(1)=0.0                                                         FIL04290
      HT(1)=HOO                                                        FIL04300
      ELSE                                                             FIL04310
                IF(KREAD.GT.1) GOTO 72                                 FIL04320
      DO 1 I=1,IT-1                                                    FIL04330
1     READ(9,71) KI,T(I),HT(I),HMT(I),PMT(I),WT(I),FT(I)               FIL04340
71    FORMAT(I4,6(1X,E15.8))                                           FIL04350
72    I=IT                                                             FIL04360
      HT(I)=HT(I-1)-WT(I-1)*DT/R                                       FIL04370
      T(I)=T(I-1)+DT                                                   FIL04380
      HOO=HT(I)                                                        FIL04390
      END IF                                                           FIL04400
      RETURN                                                           FIL04410
      END                                                              FIL04420
CMMMMMMMMMMMMMMMMMMMMMMMMMMMMMMMMMMMMMMMMMMMMMMMMMMMMMMMMMMMMMMMMMMM FIL04430
      SUBROUTINE MAT(TSUMPR,R,B1,EP,P,VW,PMAX)                         FIL04440
      IMPLICIT REAL*8 (A-H,O-Z)                                        FIL04450
      COMMON/NODE/NI,NC,NXN,NCR,NIR,NX,MT                              FIL04460
      COMMON/LINE/XN,XNN,SBI,SBC,ZB                                    FIL04470
      COMMON/CONST/A(400),B(400),C(400),D(400),E(400)                  FIL04480
      COMMON/SOLN/PR(400),PRSV(400),H(400),S(400),W(400),PHI(400)      FIL04490
     * ,D1(400),D2(400),D3(400),Y(400),VS(400),DN(400)                 FIL04500
      DIMENSION AMAT(180,180),BMAT(180),SOLMAT(180),AAMAT(180,180)     FIL04510
     * ,WKS1(180),WKS2(180)                                            FIL04520
C                                                                      FIL04530
7771                    CONTINUE                                       FIL04540
      PNOND=P/(EP*B1)                                                  FIL04550
      AMAT(1,1)=B(2)                                                   FIL04560
      AMAT(1,2)=A(2)                                                   FIL04570
      DO 10 I=3,NX-2                                                   FIL04580
10    AMAT(1,I)=0.0D0                                                  FIL04590
      AMAT(1,NX-1)=D(2)                                                FIL04600
C                                                                      FIL04610
      DO 200 J=2,NX-2                                                  FIL04620
      DO 100 I=1,NX-2                                                  FIL04630
      IF(I.EQ.J-1) AMAT(J,I)=C(J+1)                                    FIL04640
```

```
      IF(I.EQ.J)    AMAT(J,I)=B(J+1)                                        FIL04650
      IF(I.EQ.J+1) AMAT(J,I)=A(J+1)                                         FIL04660
      IF(I.LT.J-1) AMAT(J,I)=0.0D0                                          FIL04670
      IF(I.GT.J+1.AND.I.LT.NX-1) AMAT(J,I)=0.0D0                            FIL04680
 100  CONTINUE                                                              FIL04690
 200  CONTINUE                                                              FIL04700
C                                                                          FIL04710
      DO 20 J=1,NX-2                                                        FIL04720
 20   AMAT(J,NX-1)=D(J+1)                                                   FIL04730
      AMAT(NX-1,NX-1)=0.0D0                                                 FIL04740
C                                                                          FIL04750
      DO 30 I=1,NI-2                                                        FIL04760
 30   AMAT(NX-1,I)=(SBI+SBI)/H(I+1)**1.5                                    FIL04770
      AMAT(NX-1,NI-1)=(0.5*(SBI+SBI)+0.5*(SBI+SBC))/H(NI)**1.5              FIL04780
      AMAT(NX-1,NI)=(0.5*(SBI+SBC)+0.5*(SBC+SBC))/H(NI+1)**1.5              FIL04790
      DO 40 I=NI+1,NXN+NCR-2                                                FIL04800
 40   AMAT(NX-1,I)=(SBC+SBC)/H(I+1)**1.5                                    FIL04810
      AMAT(NX-1,NXN+NCR-1)=(0.5*(SBC+SBC)+0.5*(SBC+SBI))/H(NXN+NCR)**       FIL04820
     $1.5                                                                  FIL04830
      AMAT(NX-1,NXN+NCR)=(0.5*(SBC+SBI)+0.5*(SBI+SBI))/H(NXN+NCR+1)**       FIL04840
     $1.5                                                                  FIL04850
      DO 50 I=NXN+NCR+1,NX-2                                                FIL04860
 50   AMAT(NX-1,I)=(SBI+SBI)/H(I+1)**1.5                                    FIL04870
      AMAT(NX-1,NX-1)=0.0D0                                                 FIL04880
C                                                                          FIL04890
C ELEMENTS OF MATRIX B                                                     FIL04900
C--------------------                                                      FIL04910
      DO 60 J=1,NX-2                                                        FIL04920
 60   BMAT(J)=E(J+1)                                                        FIL04930
      BMAT(NX-1)=PNOND                                                      FIL04940
                        IF(KNA.EQ.1) GOTO 7772                             FIL04950
      IA=180                                                                FIL04960
      NA=NX-1                                                               FIL04970
                        NEXET=NA                                           FIL04980
 888                    CONTINUE                                           FIL04990
      IAA=180                                                               FIL05000
      IFAIL=1                                                               FIL05010
C                                                                          FIL05020
      CALL F04ATF(AMAT,IA,BMAT,NA,SOLMAT,AAMAT,IAA,WKS1,WKS2,IFAIL)         FIL05030
C                                                                          FIL05040
      PHI(1)=0.0D0                                                          FIL05050
      PHI(NX)=0.0D0                                                         FIL05060
                        PNEGAT=0.0                                         FIL05070
      DO 70 J=1,NA-1                                                        FIL05080
      PHI(J+1)=SOLMAT(J)                                                    FIL05090
      PR(J+1)=PHI(J+1)/H(J+1)**1.5                                          FIL05100
                        IF(PR(J+1).LT.PNEGAT) THEN                         FIL05110
                        PNEGAT=PR(J+1)                                     FIL05120
                        NEXET=J                                            FIL05130
                        END IF                                             FIL05140
 70   CONTINUE                                                              FIL05150
                        KNA=0.0                                            FIL05160
                        DO 71 J=NEXET+1,NX                                 FIL05170
 71                     PR(J)=0.0D0                                        FIL05180
                        DO 72 J=1,NX                                       FIL05190
                        IF(PR(J).LT.0.0D0) THEN                            FIL05200
                        KNA=1                                              FIL05210
                        GOTO 777                                           FIL05220
```

```
                    END IF                                                  FIL05230
72                  CONTINUE                                                FIL05240
777                 IF(KNA.EQ.1) GOTO 7771                                  FIL05250
7772                IF(KNA.EQ.1) THEN                                       FIL05260
                    DO 61 J=1,NEXET-1                                       FIL05270
61                  AMAT(J,NEXET)=AMAT(J,NX-1)                              FIL05280
                    DO 62 I=1,NEXET-1                                       FIL05290
62                  AMAT(NEXET,I)=AMAT(NX-1,I)                              FIL05300
                    AMAT(NEXET,NEXET)=AMAT(NX-1,NX-1)                       FIL05310
                    BMAT(NEXET)=BMAT(NX-1)                                  FIL05320
                    NA=NEXET                                                FIL05330
CCCCCCC             WRITE(4,*) '1 VW=',VW,'1 PCEN=',PR(NXN)                 FIL05340
                    GOTO 888                                                FIL05350
                    END IF                                                  FIL05360
      PR(1)=0.0D0                                                           FIL05370
      PR(NX)=0.0D0                                                          FIL05380
      VW=SOLMAT(NA)                                                         FIL05390
C-------------------------                                                  FIL05400
C SELECTION OF MAX PRESSURE                                                 FIL05410
      PMAX=0.0                                                              FIL05420
      DO 707 J=1,NX                                                         FIL05430
      IF(PR(J).GT.PMAX) PMAX=PR(J)                                          FIL05440
 707  CONTINUE                                                              FIL05450
C-------------------------                                                  FIL05460
CCC   WRITE(4,*) 'VW=',VW,'PCEN=',PR(NXN)                                   FIL05470
      RETURN                                                                FIL05480
      END                                                                   FIL05490
CLLLLLLLLLLLLLLLLLLLLLLLLLLLLLLLLLLLLLLLLLLLLLLLLLLLLLLLLLLLLLLLLLLLLLLL  - FIL05500
      SUBROUTINE PLOAD(TSUMPR)                                              FIL05510
      IMPLICIT REAL*8 (A-H,O-Z)                                             FIL05520
      COMMON/SOLN/ PR(400),PRSV(400),H(400),S(400),W(400),PHI(400)          FIL05530
     *,D1(400),D2(400),D3(400),Y(400),VS(400),DN(400)                       FIL05540
      COMMON/NODE/NI,NC,NXN,NCR,NIR,NX,MT                                   FIL05550
      COMMON/LINE/XN,XNN,SBI,SBC,ZB                                         FIL05560
      TSUM10=0.0D0                                                          FIL05570
      DO 200 J=2,NI-1                                                       FIL05580
 200  TSUM10=TSUM10+2.0*PR(J)                                               FIL05590
      TSUM1=0.5*(SBI+SBI)*(PR(NI)+TSUM10)                                   FIL05600
      TSUM2=0.5*(SBI+SBC)*(PR(NI)+PR(NI+1))                                 FIL05610
      TSUM30=0.0D0                                                          FIL05620
      DO 300 J=NI+2,NXN+NCR-1                                               FIL05630
 300  TSUM30=TSUM30+2.0*PR(J)                                               FIL05640
      TSUM3=0.5*(SBC+SBC)*(PR(NI+1)+PR(NXN+NCR)+TSUM30)                     FIL05650
      TSUM4=0.5*(SBC+SBI)*(PR(NXN+NCR)+PR(NXN+NCR+1))                       FIL05660
      TSUM50=0.0D0                                                          FIL05670
      IF((NXN+NCR+2).GT.(NX-1)) GOTO 500                                    FIL05680
      DO 400 J=NXN+NCR+2,NX-1                                               FIL05690
400   TSUM50=TSUM50+2.0*PR(J)                                               FIL05700
500   TSUM5=0.5*(SBI+SBI)*(PR(NXN+NCR+1)+TSUM50)                            FIL05710
      TSUMPR=TSUM1+TSUM2+TSUM3+TSUM4+TSUM5                                  FIL05720
      RETURN                                                                FIL05730
      END                                                                   FIL05740
```

APPENDIX A2

FINITE DIFFERENCE REPRESENTATIONS FOR A VARIABLE MESH

The finite difference representations have been developed for the dummy variable (ψ) and for the mesh shown in Figure (A2-1).

At the three consecutive nodal points $(X_{i-1,j})$, $(X_{i,j})$, $(X_{i+1,j})$, a function of (X) such as (ψ) can be represented by a parabola, where

$$\psi = AX^2 + BX + C \tag{A2.1}$$

This expression gives values of the function at the three points aforementioned. Thus,

$$\psi_{i-1,j} = A(X_{i-1,j})^2 + B(X_{i-1,j}) + C \tag{A2.2}$$

$$\psi_{i,j} = A(X_{i,j})^2 + B(X_{i,j}) + C \tag{A2.3}$$

$$\psi_{i+1,j} = A(X_{i+1,j})^2 + B(X_{i+1,j}) + C \tag{A2.4}$$

From Figure (A2.1) it follows that,

$$X_{i,j} = X_{i-1,j} + \alpha_1 \tag{A2.5}$$

$$X_{i+1,j} = X_{i-1,j} + (\alpha_1 + \alpha_2) \tag{A2.6}$$

Substituting equation (A2.5) into equation (A2.3) and subtracting equation (A2.2) from equation (A2.3) gives

$$\psi_{i,j} - \psi_{i-1,j} = A\left[2\alpha_1(X_{i-1,j}) + \alpha_1^2\right] + B\alpha_1 \tag{A2.7}$$

Substituting equation (A2.6) into equation (A2.4) and subtracting equation (A2.2) from equation (A2.4) gives

$$\psi_{i+1,j} - \psi_{i-1,j} = A\left[2(\alpha_1+\alpha_2)\,(X_{i-1,j}) + (\alpha_1+\alpha_2)^2 + B\,(\alpha_1+\alpha_2)\right] \tag{A2.8}$$

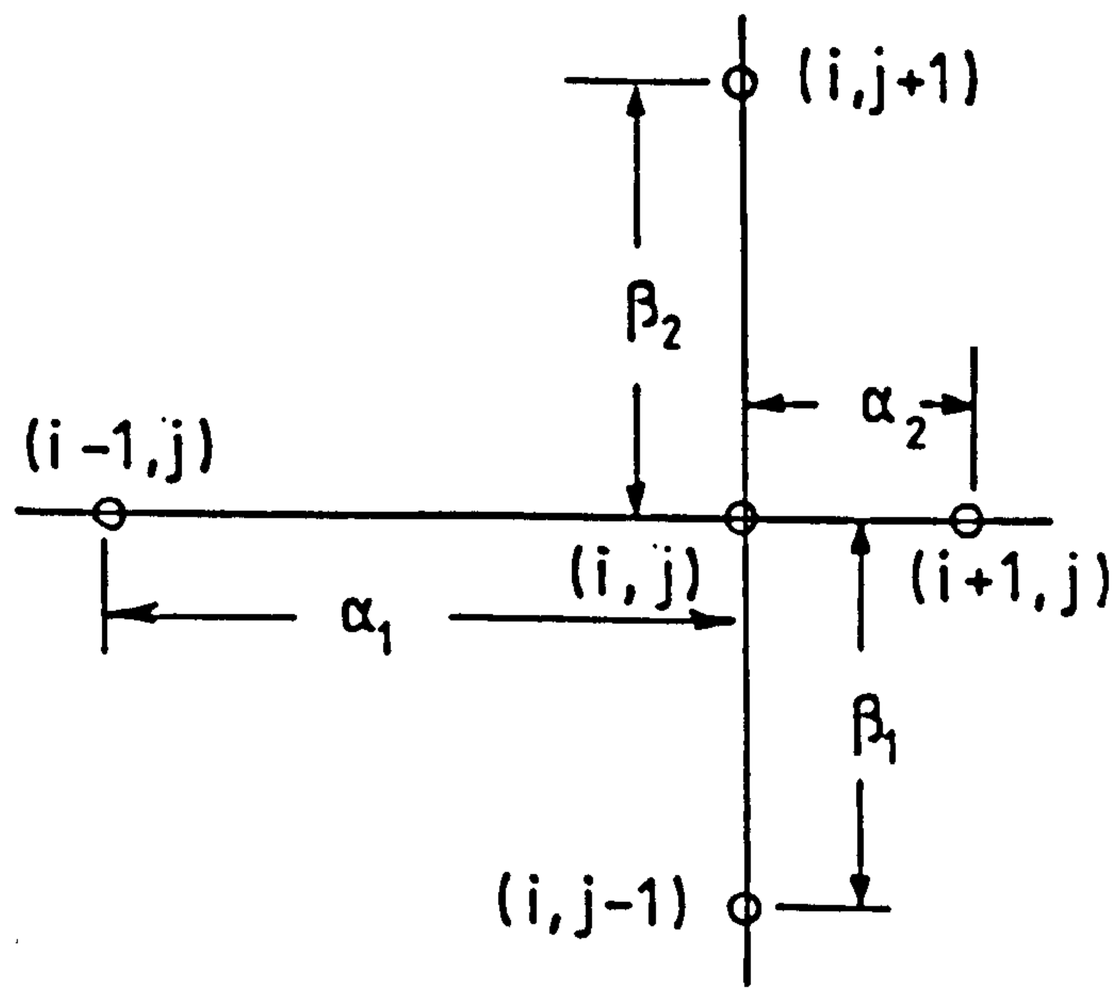

FIGURE (A2-1) Mesh Used In Numerical Analysis

From these two equations (A2.7) and (A2.8) the constants (A) and (B) can be obtained, giving,

$$A = \frac{\alpha_1(\psi_{i+1,j} - \psi_{i-1,j}) - (\alpha_1+\alpha_2)\ (\psi_{i,j} - \psi_{i-1,j})}{\alpha_1\ (\alpha_1+\alpha_2)^2 - \alpha_1^2\ (\alpha_1+\alpha_2)} \qquad \text{(A2.9)}$$

and

$$B = \frac{(\alpha_1+\alpha_2)^2\ (\psi_{i,j} - \psi_{i-1,j}) - \alpha_1^2\ (\psi_{i+1,j} - \psi_{i-1,j})}{\alpha_1\ (\alpha_1+\alpha_2)^2 - \alpha_1^2\ (\alpha_1+\alpha_2)}$$

$$- 2A\ X_{i-1,j} \qquad \text{(A2.10)}$$

substituting (A) and (B) back into equation (A2.3) yields,

$$C = \psi_{i,j} - AX_{i,j} - B\ X_{i,j}$$

although this is not required.

The following derivatives can be written using equations (A2.9) and (A2.10)

$$\left.\frac{\partial\psi}{\partial X}\right)_{i-1,j} = 2A\ X_{i-1,j} + B$$

$$= \frac{(\alpha_1+\alpha_2)^2\ (\psi_{i,j} - \psi_{i-1,j}) - \alpha_1^2\ (\psi_{i+1,j} - \psi_{i-1,j})}{\alpha_1\ (\alpha_1+\alpha_2)^2 - \alpha_1^2\ (\alpha_1+\alpha_2)} \qquad \text{(A2.11)}$$

$$\left.\frac{\partial\psi}{\partial X}\right)_{i,j} = 2A\ X_{i,j} + B = 2A\ (X_{i-1,j} + \alpha_1) + B$$

$$= \frac{(\alpha_1+\alpha_2)^2\ (\psi_{i,j} - \psi_{i-1,j}) - \alpha_1^2\ (\psi_{i+1,j} - \psi_{i-1,j})}{\alpha_1(\alpha_1+\alpha_2)^2 - \alpha_1^2\ (\alpha_1 +\alpha_2)}$$

$$+ 2\alpha_1 \left[\frac{\alpha_1(\psi_{i+1,j} - \psi_{i-1,j}) - (\alpha_1+\alpha_2)(\psi_{i,j} - \psi_{i,-1,j})}{\alpha_1(\alpha_1+\alpha_2)^2 - \alpha_1^2\ (\alpha_1+\alpha_2)}\right] \qquad \text{(A2.12)}$$

$$\left.\frac{\partial\psi}{\partial X}\right)_{i+1,j} = \frac{(\alpha_1+\alpha_2)^2\ (\psi_{i,j} - \psi_{i-1,j}) - \alpha_1^2(\psi_{i+1,j} - \psi_{i-1,j})}{\alpha_1\ (\alpha_1+\alpha_2)^2 - \alpha_1^2\ (\alpha_1+\alpha_2)}$$

$$+ 2(\alpha_1+\alpha_2)\left[\frac{\alpha_1\ (\psi_{i+1,j} - \psi_{i-1,j}) - (\alpha_1+\alpha_2)(\psi_{i,j} - \psi_{i-1,j})}{\alpha_1\ (\alpha_1+\alpha_2)^2 - \alpha_1^2\ (\alpha_1+\alpha_2)}\right] \qquad \text{(A2.13)}$$

$$\left.\frac{\partial^2\psi}{\partial X^2}\right)_{i-1,j} = \left.\frac{\partial^2\psi}{\partial X^2}\right)_{i,j} = \left.\frac{\partial^2\psi}{\partial X^2}\right)_{i+1,j} = 2A$$

$$= 2\left[\frac{\alpha_1\ (\psi_{i+1,j} - \psi_{i-1,j}) - (\alpha_1+\alpha_2)\ (\psi_{i,j} - \psi_{i-1,j})}{\alpha_1\ (\alpha_1+\alpha_2)^2 - \alpha_1^2\ (\alpha_1+\alpha_2)}\right] \qquad \text{(A2.14)}$$